CENTRALE LILLE

THÈSE

Présentée en vue d'obtenir le grade de

DOCTEUR

En

Spécialité : Informatique

Par

Tifaout ALMEFTAH

DOCTORAT DELIVRE PAR CENTRALE LILLE

Titre de la thèse :

Algorithmes d'optimisation avancés pour les tests groupés

Advanced optimization algorithms for group testing

Soutenue le 10 Décembre 2025 devant le jury d'examen :

Président	M. Lucas LÉTOCART	Professeur, Université Sorbonne Paris Nord, France
Rapportrice	Mme. Sourour ELLOUMI	Professeure, ENSTA Paris, France
Examinateur	M. Boris DETIENNE	Maître de conférences, Université de Bordeaux, France
Examinateur	M. Yannick KERGOSIEN	Maître de conférences, Université de Tours, France
Invité	M. Vincent SOBANSKI	PU-PH, Université de Lille, France
Directeur de thèse	M. Frédéric SEMET	Professeur, Centrale Lille, France
Co-directrice de thèse	Mme. Martine LABBÉ	Professeure, Université Libre de Bruxelles, Belgique
Co-encadrant de thèse	M. Diego CATTARUZZA	Maître de conférences, Université d'Udine, Italie

Thèse préparée au Centre de Recherche en Informatique, Signal et Automatique de Lille
CRIStAL - UMR CNRS 9189 et au Centre Inria de l'Université de Lille - Centrale Lille
École Doctorale MADIS 631

Un souvenir d'il y a vingt ans...

Maîtresse : Et toi ma fille, comment t'appelles-tu ? Et quel âge as-tu ?
Moi : Je m'appelle Tifaout et j'ai huit ans.
Maîtresse : Que fait ton père ?
Moi : Je me rappelle qu'il m'a dit qu'il est technicien en informatique. Mais je ne sais pas ce qu'il fait exactement.
Maîtresse : Ah d'accord, et il a fait quoi comme études ?
Moi : Je ne sais pas, il a sûrement fait toutes les études qu'il fallait... Il est très intelligent !
Maîtresse : Tu veux dire un doctorat ?
Moi : C'est quoi un doctorat ?
Maîtresse : C'est le plus haut diplôme qu'on peut acquérir à l'université.
Moi : Waouh ! Mon père doit avoir ça.
Maîtresse : Et toi, ma fille, tu veux faire quoi quand tu seras grande ?
Moi : Je veux un doctorat, tout comme mon père !

à mon père chéri,
enfant, je croyais que tu avais,
le plus grand diplôme au monde.
Aujourd'hui,
c'est moi qui le reçois,
c'est à toi que je le dois,
et à ma mère chérie que je le dédie.

Acknowledgments

This Ph.D. journey has been intense, enriching, and full of growth. It was also, in many ways, a deeply human adventure. None of it would have been possible without the support, guidance, and presence of exceptional people, and I would like to express my sincere gratitude to all of you.

First and foremost, I warmly thank my supervisors, Martine Labbé, Frédéric Semet, and Diego Cattaruzza, for your trust, generosity, patience, and constant support. Thank you for challenging me, guiding me when needed, and also for giving me the freedom to explore and grow as a researcher. This topic was unfamiliar to all of us at the beginning, and we navigated it through many trials and ideas—formulations, valid inequalities, Benders decomposition, and beyond—in search of what could work best. Even if most of these explorations do not appear in this manuscript, they shaped my learning and the path that led to the results presented here. Thank you for standing by me through the difficult moments; I truly felt supported.

I would like to warmly thank the members of my jury—Sourour Elloumi, Lucas Létocart, Boris Detienne, Yannick Kergosien, and Vincent Sobanski—for accepting to evaluate my work, for the time you dedicated to reading and discussing it, and for the quality of your feedback. The defence was an intense and memorable experience, made rigorous and encouraging by your questions, comments, and kindness. I was particularly touched by the sincere recognition and the positive energy that emerged from our discussions. Thank you as well for making the trip to Lille to be part of this important moment.

I am grateful to the medical and research teams at Lille University Hospital for the collaboration on the ANA screening project. It has been a privilege to connect this research with a real large-scale screening initiative in autoimmune diseases. Special thanks to Vincent Sobanski and his team at CHU de Lille for their trust and for the opportunity to learn from you while applying these methods to an important public health topic.

I am deeply grateful to the INOCS team and to the Centre Inria de l'Université de Lille for the inspiring research environment, the rich scientific exchanges, and the strong human values that made these years so meaningful. Thank you to all the researchers, engineers, administrative staff, security guards, maintenance workers, and everyone I have crossed paths with for the warm welcome and daily kindness. A special thank you also goes to the Inria Communication Service for trusting me with scientific popularization

initiatives, especially those aimed at young girls. These collaborations taught me a lot and brought encounters and friendships that I will always cherish.

To my colleagues and friends, thank you for the laughter, the long chats, the encouragement, and for being there in the busiest moments (the order does not import, sometimes): Wenjiao, Mesut, Salma, Mathis, Adrien, Nathan, Maxime, Kaba, Hélène, Luis S, Luis R, Matteo, Pablo, Juan Pablo, Nathalia, Gaël, Francesco, Barbara, Yue, Luce, Paul, Pamela, Maryam, Ikram, Yuan, Arnaud, Mathieu, Daniel, Antoine, Manon, Magda, Maxime, Simon, Raphaël, Alice, Moad, Belkis, Siham, Sihem, and many others. I may not be able to list everyone—the years and the Ph.D. did take some brain effort—but please know that you are all in my heart, and that many of you have become close friends.

I would like to thank Duane Graves for sharing his experience in group testing during the COVID-19 crisis at the very beginning of my Ph.D., and Vincent Vandavelle for verifying some statistical derivations in my performance measures calculations.

A very special thank you to Dr. Arrivé Jirard, Pascale, Stéphanie, Yassine, Riyad, Brigitte, and Dr. Warin, whose support and kindness helped me through difficult times during this Ph.D. Your support and expertise gave me strength when I needed it most.

I would also like to thank all my teachers and professors, from elementary school to my Master's degree, who shaped my curiosity and my academic path. A special thank you to Anass Nagih and Imed Kacem, who introduced me to Operations Research and Optimization—a field I felt naturally drawn to long before I knew it had a name. I also want to thank Mohamed Lemzoud; you were the best mathematics teacher I ever had.

Special thanks to Édouard—you literally saved my life. Without you this Ph.D. would not have been finished or have been carried by someone else. Thanks to you, I now know how to swim and can save others by myself!

To my cherished parents, thank you for your infinite love and sacrifices. You did everything possible to educate me and give me the strength to pursue my dreams. To my family—Souad, Badr, Shahrazad, Hassan, Adam, Aya, my grand-parents, uncles and aunts—thank you for your presence and your prayers. I also deeply thank Soumaya, Saad, and Nelya, all my friends near and far who supported me, and my in-laws, Khalti Laaziza, Ammi Mohamed, Amine, Fatima, Achraf, Halima, Ikram, Mahlo, for their kindness and support. I dedicate this work to the memory of Khalti Laaziza, who prayed for me; now I pray for her mercy.

Finally, I express my deepest thanks to my dear husband, Habib. Your love, care, patience, and daily support carried me through every step of this Ph.D. My life switched to the best the first time we fell in love!

Dear mama & baba, this accomplishment is as much yours as it is mine.

Contents

Acknowledgments iii

Table of Contents v

List of Figures viii

List of Tables xi

Introduction 1

1 Literature Review 9

2 Mathematical Formulations for Risk-based Non-adaptive Two-Dimensional Group Testing with Equal Group Size 17

2.1 Problem Description 18

2.2 Statistical Framework and Performance Measures 25

2.2.1 Adapting Performance Measures for Heterogeneous Populations . 26

2.2.1.1 False negative classification 27

2.2.1.2 False positive classification 27

2.2.1.3 Expected number of tests 27

2.2.2 Contributions of Groups to Performance Measures 28

2.2.2.1 Contribution of a group to the false negative classification 28

2.2.2.2 Contribution of a group to the false positive classification 29

2.2.2.3 Contribution of a group to the expected number of tests 30

2.2.3 Selected Performance Measure 31

2.3 Mathematical Formulations 31

2.3.1 Mixed Integer Nonlinear Formulation 31

2.3.2 Strengthening F^3_{MINLP} with Symmetry Breaking Constraints . . . 35

2.3.3 An Extended Formulation 36

2.4 Heuristics 37

2.4.1 Construction Heuristic 38

2.4.2 Swap-based Local Search 38

2.4.3 Iterative Ejection Cycles Local Search . . . 39
2.4.4 Gradient Design and Spiral Design from McMahan *et al.* (2012b) for Square Matrix-based Group Testing . . . 43
2.4.5 Three Variants of The Construction Heuristic . . . 44
2.5 Computational Experiments . . . 44
2.5.1 Instance Generation . . . 45
2.5.2 Local Search: Comparison of $\mathcal{LS}_{IEC}$ to $\mathcal{LS}_{PS}$ . . . 46
2.5.3 Comparison of the Five Heuristics to the best-known Solutions . . . 50
2.5.4 Empirical comparison of F^{3}_{MINLP}, $F^{\text{SYM}}_{\text{MINLP}}$ and $F^{\text{EXT}}_{\text{MINLP}}$ . . . 50
2.5.4.1 Some Properties of best-known Solutions . . . 53
2.6 Conclusion and Future Work . . . 53

3 A Branch-and-Price Algorithm for Risk-based Non-adaptive Two-Dimensional Group Testing with Equal Group Size 57
3.1 Enhanced Extended Formulation . . . 58
3.1.1 Linearization of $F^{\text{EXT}}_{\text{MINLP}}$ . . . 58
3.1.2 An Alternative Extended Formulation . . . 59
3.1.3 Comparison of the Formulations . . . 61
3.2 Simultaneous Column-and-Row Generation . . . 63
3.2.1 Restricted Master Problem . . . 63
3.2.2 Pricing Problem . . . 64
3.2.3 Solution Methods for the Pricing Problem . . . 67
3.2.3.1 A Nonlinear Formulation for the PP . . . 67
3.2.3.2 Exact Labeling Algorithm for the PP . . . 69
3.2.3.3 Heuristics Based on the Exact Labeling Algorithm . . . 71
3.2.4 Initialization of $RMP(\bar{\mathcal{K}})$ . . . 72
3.2.5 Lagrangian Lower Bound . . . 73
3.2.6 Simultaneous Column-and-Row Generation Overview . . . 76
3.3 Branch-and-Price Algorithm . . . 78
3.3.1 Branching Rules . . . 78
3.3.1.1 Highest Fractional Variable Branching Rules . . . 78
3.3.1.2 Ryan and Foster Branching Rule . . . 79
3.3.2 Primal Heuristic . . . 80
3.3.3 Branch-and-Price Algorithm Overview . . . 81
3.4 Computational Experiments . . . 82
3.4.1 Instance Description . . . 83
3.4.2 Empirical Comparison of $F^{\text{EXT}}_{\text{RLT}}$ and $F^{\text{EXT}}_{\text{MINLP}}$ . . . 83
3.4.3 Evaluation of the Exact Pricing Algorithms . . . 83
3.4.4 Evaluation of the Branching Rules . . . 86

3.4.5 Some Properties of Best Known Solutions 89
3.5 Conclusion and Perspectives 89

4 Risk-based Non-adaptive Two-Dimensional Group Testing with multiplex Antinuclear Antibody assays: Application for Rare Autoimmune Disease Prevention 93
4.1 Background and Motivation 94
4.2 Problem Description 96
4.3 Computational Experiments 98
4.3.1 Instance Generation 98
4.3.2 Experiment Design 102
4.3.3 Results 103
4.4 Conclusion and Perspectives 106

Conclusions and Perspectives 109

References 113

Appendix 119

Résumé étendu en français 197

List of Figures

1 Example of Dorfman group testing with $N = 10$ and groups of 5 samples each. 1
2 Example of adaptive group testing process with $N = 100$ 4
3 Example of non-adaptive two-dimensional group testing process with $N = 100$, and column and row groups of 10 samples each. 5
4 Structure of the thesis. 7

2.1 Matrix-like design for $G = 2L$. 21
2.2 Complete graph K_G for $G = L+1$, where vertices are groups $G_1, G_2, \ldots, G_G$, and edges represent individuals. 23
2.3 Example for $G = 2L$ with $N = 9$, $L = 3$ 23
2.4 Example for $N = 12, L = 3$ with $G > 2L$. Phase 1 fills rows horizontally, Phase 2 distributes individuals vertically, and final groups are shown. 23
2.5 Example for $N = 18, L = 4$ with $L \nmid N$. Phase 1 fills rows horizontally, Phase 2 completes the incomplete group, and final groups are shown. 24
2.6 Example for $N = 20$, $L = 5$, and $G = 8$: The first $L = 5$ groups (G_1 to G_5) contain $L - k = 2$ empty positions, followed by transposed elements from G_6, G_7, and G_8. The last $k = 3$ groups are filled horizontally. The remaining $L(L-k)$ occurrences of individuals form a smaller subproblem, solved recursively with $N' = \frac{L(L-k)}{2}$, $G' = L$, and $L' = L - k$, based on the cases of G' relative to L'. In this example, $N' = 5$, $G' = 5$, and $L' = 2$, corresponding to the case $G' > 2L'$. 24
2.7 Illustration of the different configurations for individuals i and j. 39
2.8 Two ejection cycles in a feasible solution with $N = 9$ and $L = 3$. 40
2.9 Solution properties in optimal solution or best incumbent by varying (Se, Sp) 54

3.1 Illustration of the constraint (3.16). If G_l is selected in the solution, one group G_{k_i} intersecting with G_l in i must also be selected in the solution $\forall i \in G_l$. 60
3.2 Solution properties in optimal or best incumbent solutions by varying (Se, Sp) for $N \in \{12, 16, 25, 36\}$. 90

3.3 Solution properties in optimal or best incumbent solutions by varying (Se, Sp) for $N \in \{49, 64, 81, 100\}$. 91

4.1 ANA Testing Process: Immunofluorescence followed by Specific Testing for Positive Samples 95

4.2 Expected gain in the number of tests compared to individual testing, for each dataset and configuration (N, L). The gain is computed as $\left(1 - \frac{\mathbb{E}[T(S)]}{N}\right) \times 100$. 104

List of Tables

1.1 Group Testing Studies with Realistic Assumptions: Considerations and Optimization Techniques . . . 10

2.1 A solution that always satisfies ((i)-(iii)) . . . 20
2.2 Notation for MINLP formulations. . . . 32
2.3 Notation for the extended formulation. . . . 37
2.4 Characteristics of the instances including sensitivity and specificity. . . . 45
2.5 Average relative gaps and improvement ratios of $\mathcal{LS}_{PS}$ and $\mathcal{LS}_{IEC}$ by (Se, Sp, N) for each heuristic. . . . 47
2.6 Explanation of headings in Tables 2.7 and 2.8 . . . 48
2.7 Aggregated characteristics of iterations in $\mathcal{LS}_{IEC}$ for each heuristic. . . . 49
2.8 Aggregated First Time Optimal Solution Found per Iteration in $\mathcal{LS}_{IEC}$. 51
2.9 Comparison of heuristics with Relative Gap (%). . . . 52
2.10 Column headings. . . . 52
2.11 Aggregated performance comparison of formulations by N . . . 52

3.1 Characteristics of the instances including sensitivity and specificity. . . . 83
3.2 Aggregated performance comparison of extended formulations by N . . . 83
3.3 Comparison of $\texttt{CRG-EXT}_{\texttt{LAB}}$ and $\texttt{CRG-EXT}_{\texttt{GUR}}$ when $Se = Sp = 0.95$ with Instance $ID = 1$. . . . 84
3.4 Performance of $\texttt{CRG-EXT}_{\texttt{LAB}}$ when $Se = Sp = 0.95$ with Instance $ID = 1$. . 85
3.5 Tested configurations of Algorithm 5. . . . 86
3.6 Aggregated comparison of the three branching rules. . . . 87
3.7 Aggregated final results with BP-HFY. . . . 88

4.1 Sensitivities and specificities of Bioplex Assay for various ANA antibodies and their associated pathologies. . . . 99
4.2 Distribution of antinuclear antibody positive frequency in male and female participants at different ages adapted from (Guo *et al.*, 2014). . . . 99
4.3 Numbers of ANA-specific antibodies in positive sera: breakdown by sex and by age group adapted from (Guo *et al.*, 2014). . . . 100

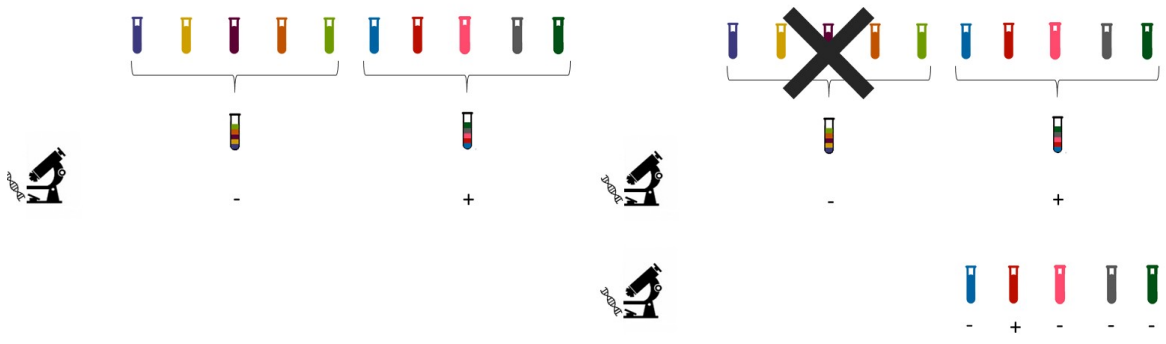
4.4 Number of positive individuals for each ANA by age group, distinguishing females (F) and males (M), adapted from (Hayashi *et al.*, 2008). 101
4.5 Prevalences of ANA specificities by sex and age group (in $[0, 1]$) computed from Guo *et al.* (2014). 102
4.6 Probability of being positive for each ANA by age group and sex (in $[0, 1]$) computed from Hayashi *et al.* (2008). 103
4.7 Proportion (in %) by age group and sex from Table 4.2. 103
4.8 Proportion (in %) by age group and sex from Table 4.4. 103
4.9 Results of the simultaneous column-and-row generation on the root node 106
4.50 Comparison of Branching Rules for N=36, L=3, Instance ID = 1 120
4.51 Comparison of Branching Rules for N=36, L=4, Instance ID = 1 121
4.52 Comparison of Branching Rules for N=36, L=6, Instance ID = 1 122
4.53 Comparison of Branching Rules for N=36, L=3, Instance ID = 2 123
4.54 Comparison of Branching Rules for N=36, L=4, Instance ID = 2 124
4.55 Comparison of Branching Rules for N=36, L=6, Instance ID = 2 125
4.56 Comparison of Branching Rules for N=36, L=3, Instance ID = 3 126
4.57 Comparison of Branching Rules for N=36, L=4, Instance ID = 3 127
4.58 Comparison of Branching Rules for N=36, L=6, Instance ID = 3 128
4.59 Comparison of Branching Rules for N=36, L=3, Instance ID = 4 129
4.60 Comparison of Branching Rules for N=36, L=4, Instance ID = 4 130
4.61 Comparison of Branching Rules for N=36, L=6, Instance ID = 4 131
4.62 Comparison of Branching Rules for N=36, L=3, Instance ID = 5 132
4.63 Comparison of Branching Rules for N=36, L=4, Instance ID = 5 133
4.64 Comparison of Branching Rules for N=36, L=6, Instance ID = 5 134
4.70 Comparison of Branching Rules for N=81, L=3, Instance ID = 1 135
4.71 Comparison of Branching Rules for N=81, L=3, Instance ID = 2 136
4.72 Comparison of Branching Rules for N=81, L=3, Instance ID = 3 137
4.73 Comparison of Branching Rules for N=81, L=3, Instance ID = 4 138
4.74 Comparison of Branching Rules for N=81, L=3, Instance ID = 5 139
4.75 Comparison of Branching Rules for N=100, L=4, Instance ID = 1 140
4.76 Comparison of Branching Rules for N=100, L=4, Instance ID = 2 141
4.77 Comparison of Branching Rules for N=100, L=4, Instance ID = 3 142
4.78 Comparison of Branching Rules for N=100, L=4, Instance ID = 4 143
4.79 Comparison of Branching Rules for N=100, L=4, Instance ID = 5 144
4.10 Performance Comparison of the Formulations for $N = 6$ 146
4.11 Performance Comparison of the Formulations for $N = 9$ 147
4.12 Performance Comparison of the Formulations for $N = 10$ 148
4.13 Performance Comparison of the Formulations for $N = 12$ 149
4.14 Comparison of heuristics for N = 6, L = 3 150

4.15 Comparison of heuristics for N = 9, L = 3 151
4.16 Comparison of heuristics for N = 10, L = 4 152
4.17 Comparison of heuristics for N = 12, L = 3 153
4.18 Comparison of heuristics for N = 12, L = 4 154
4.19 All possible groups of size $L = 3$ for $N = 6$ and their C_k, D_{kl} values, with $Se = Sp = 0.95$ and $\mathbf{p} = (0.01, 0.02, 0.03, 0.04, 0.05, 0.06)$. 155
4.20 Comparison of Branching Rules for N=6, Instance ID = 1 156
4.21 Comparison of Branching Rules for N=6, Instance ID = 2 157
4.22 Comparison of Branching Rules for N=6, Instance ID = 3 158
4.23 Comparison of Branching Rules for N=6, Instance ID = 4 159
4.24 Comparison of Branching Rules for N=6, Instance ID = 5 160
4.25 Comparison of Branching Rules for N=9, Instance ID = 1 161
4.26 Comparison of Branching Rules for N=9, Instance ID = 2 162
4.27 Comparison of Branching Rules for N=9, Instance ID = 3 163
4.28 Comparison of Branching Rules for N=9, Instance ID = 4 164
4.29 Comparison of Branching Rules for N=9, Instance ID = 5 165
4.30 Comparison of Branching Rules for N=10, Instance ID = 1 166
4.31 Comparison of Branching Rules for N=10, Instance ID = 2 167
4.32 Comparison of Branching Rules for N=10, Instance ID = 3 168
4.33 Comparison of Branching Rules for N=10, Instance ID = 4 169
4.34 Comparison of Branching Rules for N=10, Instance ID = 5 170
4.35 Comparison of Branching Rules for N=12, Instance ID = 1 171
4.36 Comparison of Branching Rules for N=12, Instance ID = 2 172
4.37 Comparison of Branching Rules for N=12, Instance ID = 3 173
4.38 Comparison of Branching Rules for N=12, Instance ID = 4 174
4.39 Comparison of Branching Rules for N=12, Instance ID = 5 175
4.40 Comparison of Branching Rules for N=16, Instance ID = 1 176
4.41 Comparison of Branching Rules for N=16, Instance ID = 2 177
4.42 Comparison of Branching Rules for N=16, Instance ID = 3 178
4.43 Comparison of Branching Rules for N=16, Instance ID = 4 179
4.44 Comparison of Branching Rules for N=16, Instance ID = 5 180
4.45 Comparison of Branching Rules for N=25, Instance ID = 1 181
4.46 Comparison of Branching Rules for N=25, Instance ID = 2 182
4.47 Comparison of Branching Rules for N=25, Instance ID = 3 183
4.48 Comparison of Branching Rules for N=25, Instance ID = 4 184
4.49 Comparison of Branching Rules for N=25, Instance ID = 5 185
4.65 Comparison of Branching Rules for N=64, Instance ID = 1 186
4.66 Comparison of Branching Rules for N=64, Instance ID = 2 187
4.67 Comparison of Branching Rules for N=64, Instance ID = 3 188

4.68 Comparison of Branching Rules for N=64, Instance ID = 4 189
4.69 Comparison of Branching Rules for N=64, Instance ID = 5 190
4.80 Performance Comparison of the Formulations for $N = 6$ 191
4.81 Performance Comparison of the Formulations for $N = 9$ 192
4.82 Performance Comparison of the Formulations for $N = 10$ 193
4.83 Performance Comparison of the Formulations for $N = 12, L = 3$ 194
4.84 Performance Comparison of the Formulations for $N = 12, L = 4$ 195

Introduction

Group testing, a concept introduced by Dorfman (1943), revolutionized mass screening methods. It offers a highly efficient approach for detecting diseases within large scale populations where the probability of positivity for a disease, or prevalence, is low. Initially developed to screen U.S. Army recruits for syphilis during the Second World War, group testing involves pooling individual samples and testing them collectively. Concretely, this method combines specimens from multiple individuals in groups. If a group tests negative, all its members are considered negative. In case of a positive result, at least one in the group is positive, and the individuals are retested individually to determine which ones are positive. Figure 1 illustrates the Dorfman testing procedure: a population of $N = 10$ individuals is divided into two groups of 5 pooled samples each (Figure 1a). The first group tests negative, while the second tests positive and its individuals are retested individually to identify the positives (Figure 1b). In total, only 7 tests are performed to screen 10 individuals, saving 3 tests compared to individual testing–a gain of 30%. This methodology significantly conserves resources by reducing the number of tests needed. This saving allows for an increase in the number of daily tests without increasing the allocated resources. This method thus optimizes existing capacities and extends the efficiency of screening, responding more dynamically to public health challenges.



(a) Making and testing groups (b) Testing the positive group

Figure 1: Example of Dorfman group testing with $N = 10$ and groups of 5 samples each.

Group testing has been extensively applied in public health for infectious disease control, including screening for sexually transmitted diseases (STDs) such as Chlamydia

(Aprahamian *et al.*, 2019), blood donation screening for HIV and hepatitis B virus (HBV) (Weusten *et al.*, 2011), and influenza mass surveillance (Hourfar *et al.*, 2007). It is also utilized in wastewater surveillance for SARS-CoV-2 detection and outbreak prevention (Colosi *et al.*, 2021). Beyond infectious diseases, group testing has been applied in food safety, such as Salmonella detection in table eggs (Pasquali *et al.*, 2014), drug discovery (Kainkaryam & Woolf, 2009), and DNA sequencing (Pevzner & Lipshutz, 1994). Additionally, group testing is used in industry and telecommunications for quality control (Sobel & Groll, 1959), software testing (Blass & Gurevich, 2002), and early detection of network anomalies (Bui *et al.*, 2013).

While group testing marked a critical advancement, it operated initially under unrealistic assumptions, including a perfect test (no misclassification error), a homogeneous population (the same probability of positivity for all individuals), and an infinite population. Of course, reality does not follow this mathematical setting. A misclassification error could characterize a test. Indeed, a test has an imperfect sensitivity (true positive probability, that is, the capacity of the test to detect true positive individuals) and an imperfect specificity (true negative probability, that is, the capacity of the test to detect true negative individuals). In other words, a test can incorrectly classify a true negative individual as positive and a true positive individual as negative. The latter configuration can have disastrous outcomes, such as a truly disease-positive patient spreading the illness if not separated and/or not treated with the correct therapy. However, the configuration where a true negative individual is classified as positive could result in waste in its overall form.

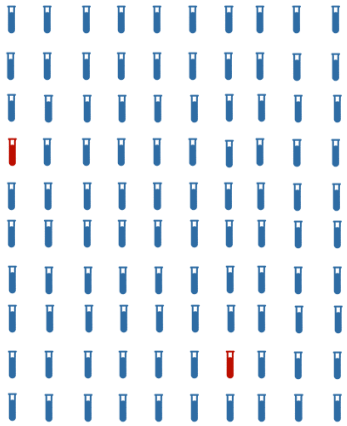
The population to be screened is heterogeneous, meaning that each and every individual has a probability of testing positive due to potential risk factors that can vary from one individual to another. Naturally, in a realistic scenario, the population consists of a known number of individuals for screening at each time period. Moreover, in group testing, an important assumption is that there is enough material in the collected sample to be equally participating in a group or more and for a confirmatory test if necessary.

An additional important consideration in group testing design is the dilution effect. Indeed, forming very large size groups may worsen the test inability to detect one positive individual among multiple other negative individuals. This issue has been addressed in the literature by either mathematical formulations of the sensitivity and specificity of the tests as a function of the individuals pooled in the group or by limiting the size of the groups. For example, Yelin *et al.* (2020) demonstrates the possibility of identifying a SARS-CoV-2 positive case within a combined sample from a group of up to 32 or even 64 individuals, given specific conditions are met. Conversely, Ben-Ami *et al.* (2020) recommend that the optimal number of individuals in a group for effective testing is 8 to guarantee the reliability of the group test.

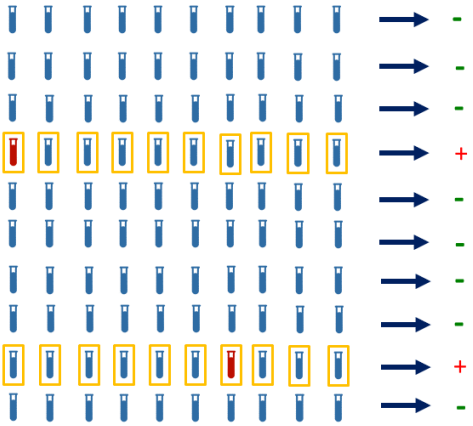
Thus, the goal of group testing design is to determine how to group the individuals for optimal screening. This includes deciding on the size of the groups and their composition. Consequently, the central problem for a realistic group testing policy can be formulated as follows: for a given heterogeneous population of N individuals with known risks of positivity, an imperfect test with a sensitivity and a specificity, form groups of individuals (computing the number, the size and the assignment of the individuals to the groups) so as to classify the population into positive and negative individuals with the minimal expected number of tests and the maximal accuracy in terms of misclassification error.

The past decades have known considerable research and studies since the groundbreaking works of Dorfman in 1943. In the remaining, we refer to Dorfman scheme as the conventional scheme in which groups of samples are formed in the first step and tests are conducted on these groups, and individual testing is performed in the second step whenever a test on a group is positive. Indeed, some studies have proposed a multi-stage group testing strategy, in which, rather than testing positive groups individually, subgroups of positive groups are formed and the negative subgroups are discarded to reduce the number of tests. We refer the reader to Daniel *et al.* (2021) for a comprehensive survey on multi-stage group testing. Adaptive group testing is the name given to this method of creating groups. In this design, the groups for the next step are created based on the results of tests conducted on the groups of the current step. Figure 2 illustrates an example of adaptive group testing with $N = 100$ individuals, including two positive cases. In the first step, we form 10 groups of 10 individuals each and test them. Two groups test positive. At this point, one option would be to retest all 20 individuals from these two groups individually, resulting in a total of 30 tests (10 group tests + 2×10 individual tests). However, as shown in the figure, a more efficient alternative consists of creating smaller subgroups within each positive group and testing them. Only the positive subgroups are then retested individually. This approach reduces the total number of tests to 24 over three steps, saving 6 tests compared to direct individual retesting.

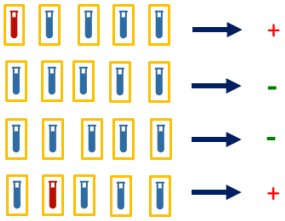
When compared to the Dorfman technique, adaptive group testing offers for considerably more cost savings. However, in practice, this design may not be reliable. On the one hand, it may lengthen the time it takes to receive results even further which may not be feasible in a variety of situations where quick outcomes are required. Furthermore, group testing requires the use of specialized technological equipment and materials to create the groups and conduct the tests. As a result, one should optimize the use of this expensive infrastructure. On the other hand, a constraint on the divisibility of samples (that is the maximum number of times a sample can be divided, or in other words, the maximum number of tests the sample can belong to) limits the number of stages in an adaptive approach. That is why, generally speaking, Dorfman testing has been the most used scheme for its simplicity.



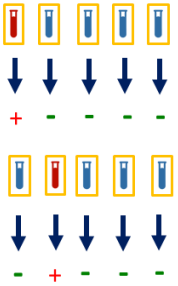
(a) 100 samples with 2 positives



(b) Testing groups



(c) Testing subgroups

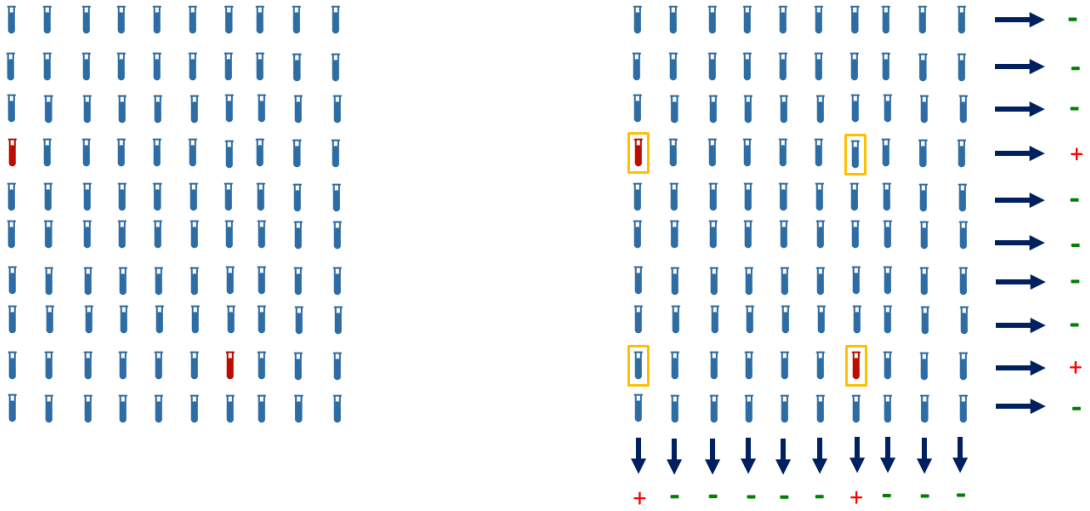


(d) Individual Testing

Figure 2: Example of adaptive group testing process with $N = 100$

To address this limitation, the works of Phatarfod & Sudbury (1994) have introduced array testing and have suggested a single-round group testing where individuals belong to two different groups. In this approach, individuals are assigned to a matrix. The individuals in the same row (column) represent a group. In settings with perfect tests, the suspicious positive individuals would only appear in the intersection of positive rows and positive columns. Phatarfod & Sudbury (1994) research gave rise to a new family of approaches called non-adaptive group testing. Figure 3 shows a non-adaptive two-dimensional group testing strategy for $N = 100$ individuals arranged in a 10×10 matrix. Each row and each column form a group, leading to 20 group tests in the first step. Individuals who lie at the intersection of positive rows and positive columns are considered suspicious and are retested individually. In the example, 4 individuals are retested in the second step, totaling 24 tests. Although this strategy requires more group tests at the

beginning, it is a practical investment that allows for fewer steps and targets directly the suspicious individuals, leading to a more efficient overall process.



(a) 100 samples with 2 positives

(b) Testing column and row groups

Figure 3: Example of non-adaptive two-dimensional group testing process with $N = 100$, and column and row groups of 10 samples each.

Problematic

This non-adaptive group testing method, though efficient in parallelization, highlighted challenges with test perfection assumptions. To the best of our knowledge, no work on exact methods for non-adaptive two-dimensional group testing with a heterogeneous population has been reported. Existing algorithms in the literature often rely on unrealistic assumptions such as population homogeneity or perfect tests, and are primarily heuristic. Our research aims to fill this significant gap by proposing and exactly solving a general model for two-dimensional group testing design with a finite heterogeneous population and imperfect tests. This model also incorporates bounded equal-sized groups to avoid the dilution effect, where group sizes cannot go beyond values based on clinical studies for the disease being tested.

Contributions

This thesis introduces novel advancements in risk-based group testing, specifically focusing on developing mathematical models and algorithms for non-adaptive two-dimensional group testing with equal group sizes. The main contributions are summarized as follows:

1. We developed a generalized risk-based non-adaptive two-dimensional group testing model where all groups are of equal size. This generalizes the array testing (square-based) into a more generalized form. The model includes the definition of eligible group sizes and statistical performance measures for evaluating the testing designs.

2. We proposed integer mathematical models for the group testing problem, accompanied by algorithms to construct feasible solutions and local search methods to improve them. Additionally, we evaluated existing heuristics from the matrix-based group testing literature, providing a framework to measure their performance in this new context.

3. We proposed a tighter extended formulation, supported by mathematical proofs, and developed methods to solve its linear relaxation using simultaneous column-and-row generation. This formulation tackles the challenge of correctly estimating missing dual variables. Since the simultaneous column-and-row generation procedure does not always converge (i.e., the master problem is not necessarily solved to optimality), we compute a Lagrangian lower bound on the relaxation to provide a valid bound. Algorithms were developed to solve the complex pricing problem, and a Branch-and-Price algorithm was designed to handle large-scale instances effectively.

4. In collaboration with Lille University Hospital, we adapted the developed approaches to consider multiple prevalences per individual based on positivity to several antinuclear antibodies. This application, which focuses on prevention strategies for rare autoimmune diseases, not only demonstrates the practical impact of the proposed models and methods but also inspires hope for their potential in public health contexts.

Thesis Outline

The thesis is organized as a narrative that guides the reader step by step. The chapters are intended to be read in the order presented, with each chapter building on the previous ones. Note that Chapter 4 is an extension of the problem studied and builds on Chapter 2 and Chapter 3. We refer the reader to Figure 4 for a comprehensive view of the structure of the thesis. Hereafter, a summary of the key points of each chapter.

Chapter 1 In this chapter, we provide a non exhaustive literature review on solving group testing design with Combinatorial Optimization. This chapter establishes the foundation for the problem we study in subsequent chapters, highlighting the gaps in existing methods and the motivation for our work.

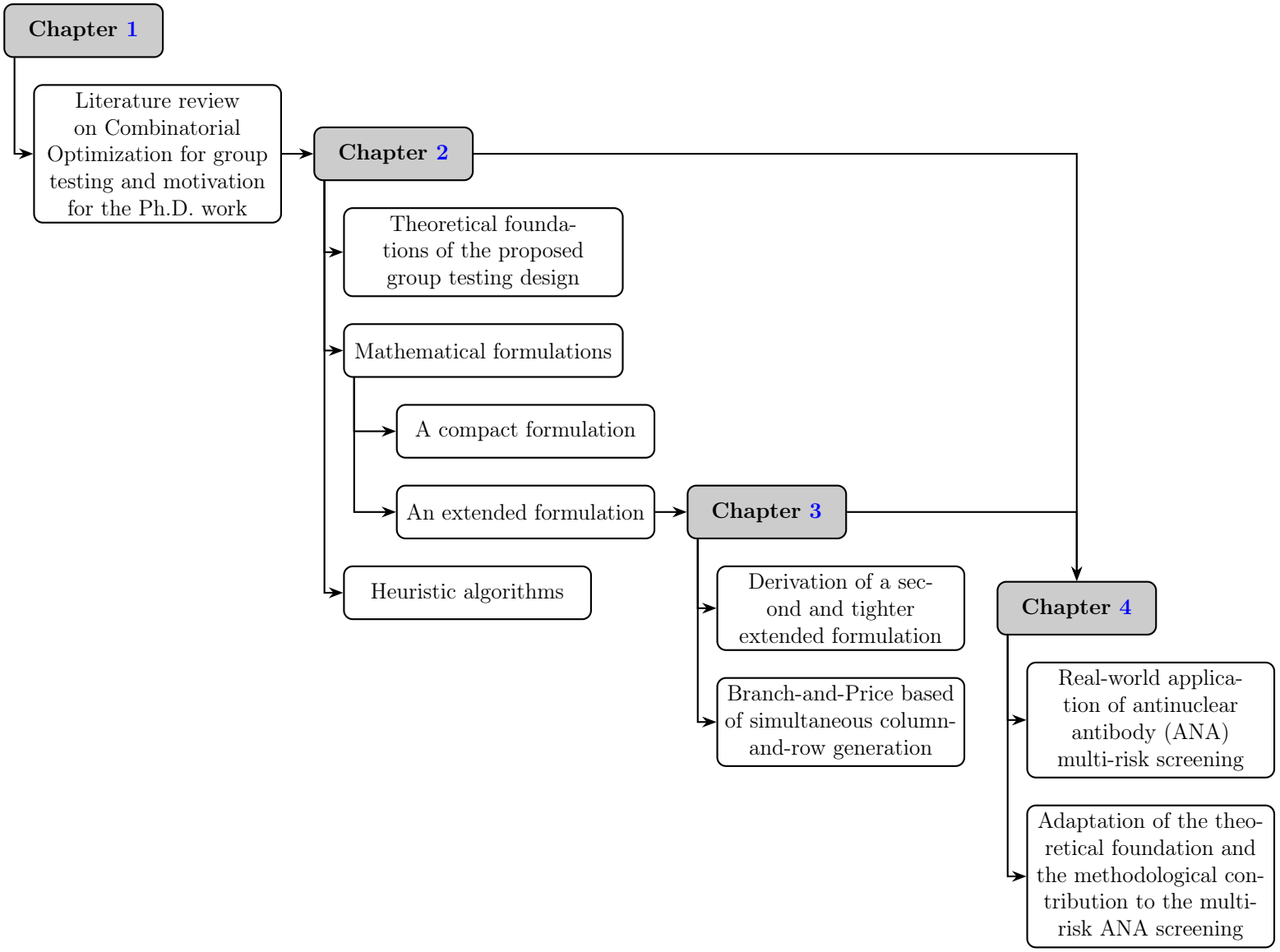


Figure 4: Structure of the thesis.

Chapter 2 Here, we define the two-dimensional group testing problem with groups of equal size, which has not been studied in the literature. We develop mathematical models and propose constructive and improving heuristic algorithms to solve the problem. This chapter forms the basis for further algorithmic developments in later chapters.

Chapter 3 Building on the extended mathematical model from Chapter 2, this chapter introduces a tighter extended formulation to improve the computational efficiency of solving the studied group testing problem. We propose a Branch-and-Price algorithm, leveraging the extended model to handle larger instances more efficiently. The chapter includes a detailed explanation of the simultaneous column-and-row generation, including the pricing problem, its resolution, and the use of accelerating strategies.

Chapter 4 This chapter presents a collaboration with the Lille University Hospital, where we apply our theoretical models and algorithms to a real-world case study. The application focuses on rare disease prevention in the Hauts-de-France region. We discuss how the methods developed in previous chapters can be adapted to the practical settings of public health planning and analyze the outcomes of applying these approaches to real data.

Conclusions and Perspectives This conclusion provides a summary of the main contributions of the Ph.D. research, including the theoretical developments, the design and performance of the proposed algorithms, and their practical relevance. It also acknowledges the limitations encountered, particularly in terms of algorithmic scalability. Finally, it outlines potential directions for future research including potential extensions of studied problem.

Chapter 1

Literature Review

The existing literature on group testing is extensive; however, it is mainly focused on statistics, bio-medicine, biochemistry, and related fields. Only a few studies consider the problem from a Combinatorial Optimization perspective. Given the vast amount of literature, this chapter aims to provide an overview rather than an exhaustive survey of the topic. We emphasize how our research is aligned with the most pertinent works. This chapter focuses on works that address the group testing design problem within the context of Combinatorial Optimization. Moreover, we restrict our literature review to works that deal with realistic assumptions, namely, a heterogeneous population and an imperfect test. A selection of the most relevant articles is summarized in Table 1.1, highlighting for each study the practical considerations addressed and the optimization techniques employed.

The problem of one-dimensional risk-based group testing under realistic assumptions has been studied in the work of Aprahamian *et al.* (2019). The authors formulated the problem with two mathematical models. One where the objective is to minimize a convex combination of the expected number of false negatives, false positives, and the number of tests. The second one is where the objective is to minimize the misclassification error under a budget constraint. They proved an important theorem that defines the properties of the optimal solution. This theorem enabled the authors to formulate the problem using a constrained shortest path model. In a setting where only the false negatives are minimized without a budget constraint, the problem reduces to a shortest path problem for which they proposed a polynomial algorithm to solve it. This contrasts with the conjecture by McMahan *et al.* (2012a) that the problem was NP-hard. Their research on Chlamydia demonstrated the high efficiency of risk-based models. Additionally, Almeftah *et al.* (2020) implemented an ad-hoc algorithm based on labelling using SARS-CoV-2 screening data, showing the benefits of group testing in large-scale screening.

Aprahamian *et al.* (2018) suggest and study a three-tier adaptive risk-based array pooling strategy that takes into account inaccuracies in the tests, the pooling effect's dilution, and the individuals' risk profiles. Tier 1 tests all row pools; if at least one row

Table 1.1: Group Testing Studies with Realistic Assumptions: Considerations and Optimization Techniques

Design	Reference	Considerations	Optimization Techniques
Adaptive	Lin *et al.* (2024c)	Proactive/reactive mass screening	Mixed-integer nonlinear programming
	Lin *et al.* (2024a)	Proactive targeted screening, limited budget, multiple tests	Multi-dimensional fractional knapsack
	Lin *et al.* (2024b)	Proactive targeted screening, limited budget	Nonconvex MIP, fractional knapsack
	El Hajj *et al.* (2022a)	Limited budget, heterogeneity, coverage vs. harm	Mathematical programming
	Aprahamian & El-Amine (2022)	Multiple tests	Mathematical programming, network flow
	El Hajj *et al.* (2022b)	Multiple variant/panel genetic screening	Mathematical programming
	Bish *et al.* (2021)	Robust group size, risk stratification	Mathematical programming
	Almeftah *et al.* (2020)	Minimize errors/tests, limited group size	Labeling algorithm
	Aprahamian *et al.* (2020a)	Multiple tests, risk uncertainty	Mathematical programming
	Aprahamian *et al.* (2020b)	Risk uncertainty, error minimization	Mathematical programming
	Aprahamian *et al.* (2019)	Error/test minimization	Mathematical programming, shortest path reduction
	Aprahamian *et al.* (2018)	Three-tier design, error minimization	Mathematical programming
Non-Adaptive	McMahan *et al.* (2012a)	Square/rectangular matrix, error minimization	Heuristics
	This Ph.D. research	Equal group size, generic 2D design, Error/test minimization	Mixed-integer nonlinear programming, Branch-and-Price, local search

pool's test result is positive, testing moves to Tier 2. Tier 2 limits the testing matrix to only include individuals in positive-testing rows (this minimizes dilution in Tier 2), and all column pools of the reduced testing matrix are tested. Tier 3 individuals are individually tested and categorized based on the outcome of their individual test, if they are located at the intersection of a positive-testing row and a positive-testing column. All other individuals are categorized as negative.

The past few years have seen considerable research and studies since the groundbreaking works of Aprahamian *et al.* (2019). The following works address the group testing problem while considering more realistic features.

Aprahamian *et al.* (2020b) focuses on designing static group testing schemes, where the group sizes and subject assignments are determined once and remain fixed for all future testing rounds. This means that once the scheme is set, it does not adapt to changing conditions or information, which makes implementation simpler and less costly compared to dynamic protocols. In contrast, dynamic protocols adjust group sizes and assignments at each testing round, based on updated risk assessments, making them more responsive but also more complex to manage operationally. A significant challenge here is determining the probability that an individual is positive, which complicates the design of efficient group testing strategies. Estimating these uncertain risks while ensuring the scheme remains effective adds complexity. The authors model this problem as a network flow problem, where evaluating performance measures (like misclassification error) requires the computation of high-dimensional integrals, which is computationally demanding. They developed analytical tools to drastically simplify these calculations, making it feasible to solve realistic-sized problems to optimality. Their approach significantly reduces the computational burden, providing practical methods for efficient static group testing under uncertain conditions.

Aprahamian *et al.* (2020a) focus on designing optimal group testing strategies that are robust to uncertain prevalence rates, which makes the problem more challenging compared to traditional deterministic approaches. They address the Dorfman group testing scheme, which involves testing groups of specimens initially and then retesting individuals if the group tests positive. A key motivation is to develop a robust approach that works effectively under uncertain and dynamically changing disease prevalence, which is common in public health scenarios such as disease outbreaks. The authors model this problem using a regret-based robust optimization framework. In contrast to deterministic models where the prevalence rate is known, they consider the realistic case of uncertain prevalence rates, which significantly increases complexity. The problem is modeled as an optimization problem with a min-max regret objective, to minimize the worst-case deviation from an optimal solution, given the uncertainty in prevalence. The formulation requires evaluating complex integrals to calculate performance measures, which is computationally challenging. However, thanks to the structural properties established in their

work, the authors provide exact closed-form solutions for the deterministic case and tools to simplify the robust model calculations, enabling feasible implementation even in complex, real-world settings. This robust approach results in testing schemes that are both cost-effective and less sensitive to variations in prevalence, providing practical benefits for public health screening under uncertainty. In an application to SARS-CoV-2 study, Bish *et al.* (2021), the authors consider a robust method to determine optimal pool sizes for different risk groups, even under uncertain conditions. The authors tackle the robustness by considering different possible scenarios of prevalence, each representing a potential realization of the infection rate. To make the pooled testing approach adaptive, they use a sequential design. In each testing period, the prevalence rate is updated based on data from previous testing periods. This means that at the start of each new testing period, they update the pool sizes by calculating a new estimate for the prevalence, using data from all past periods. This sequential updating ensures that the pooling design adapts to changing conditions, making it more efficient and effective over time. Their method demonstrated significant reductions in the number of tests required, showing how robust pooling can be used to expand testing capacity even when resources are limited.

El Hajj *et al.* (2022a) addresse the problem of optimal screening of heterogeneous populations under limited testing resources, focusing on COVID-19 as a case study. The motivation is to maximize testing coverage and minimize potential harm caused by undetected infections, especially when testing resources are scarce. The authors consider multiple attributes for the population, such as positivity risk and potential harm, which makes the decision of whom to test more complex. They propose a testing strategy that partitions the population into those to be tested individually, those for pooled testing, and those not tested.

The problem is modeled as a complex combinatorial optimization problem, specifically a constrained multivariate set partitioning problem. To make it tractable, the authors reformulate it as a network flow problem. By leveraging the structure of this problem, they develop an exact polynomial-time algorithm for maximizing coverage and propose an effective heuristic for minimizing harm. Their work highlights the substantial benefits of considering multiple dimensions of heterogeneity and provides practical tools for efficient resource allocation in disease screening.

Aprahamian & El-Amine (2022) consider the availability of multiple tests in which the decision problem accounts also for the decision of which test to use for which group and whether the population cannot be screened fully is an optimal solution. They provide an exact polynomial algorithm to solve the problem.

Lin *et al.* (2024a), Lin *et al.* (2024c) and Lin *et al.* (2024b) address the challenging problem of designing effective mass screening strategies under complex and realistic conditions where resources are limited. Their motivation lies in the need to control disease outbreaks effectively, especially when there are not enough testing resources available

to screen an entire population. To address this, they propose targeted mass screening, which involves prioritizing specific sub-populations for testing based on their risk profiles, instead of attempting to test everyone. This approach is aimed at maximizing the efficiency and accuracy of testing while operating under a limited budget.

The authors focus on combining proactive and reactive screening strategies. Proactive screening targets individuals who may not show symptoms but are at high risk due to factors like their occupation or underlying health conditions. Reactive screening, on the other hand, involves testing symptomatic individuals to confirm their infection. The challenge is how to allocate a limited testing budget effectively between these two approaches while also considering the diversity within the population, often termed as heterogeneous sub-populations. These sub-populations may vary in terms of their exposure risks, prevalence of the disease, and other characteristics.

The decision problem for targeted mass screening is to identify which sub-populations should be tested and how the testing should be carried out–whether individually or through group testing. To solve this, the authors use optimization-based frameworks that model these decisions mathematically. They incorporate both individual testing and Dorfman group testing. The objective is to allocate testing in a way that minimizes misclassifications while considering the limited testing capacity.

In terms of solutions, the authors found that the complexity of obtaining an optimal solution varies depending on the specific problem settings. The problems considered in these three studies are modeled using various types of optimization approaches, each depending on the complexity of the setting. The individual testing models are formulated as fractional knapsack problems, where the optimal solutions can be obtained using a greedy algorithm due to the clear structure of how testing capacity should be allocated across sub-populations based on risk levels. However, when it comes to incorporating group testing, the problem becomes more complex, involving non-linear relationships and discrete choices that transform it into a mixed-integer nonlinear program. This type of model incorporates decisions on both which sub-populations to target and how to design group sizes for testing. Due to the complexity introduced by these non-linear and discrete factors, exact solutions are not computationally feasible in all cases. Therefore, the authors propose efficient heuristic approaches to solve these problems, aiming to find good quality solutions within reasonable timeframes. These heuristics leverage the underlying properties of the problem, focusing on efficient allocation strategies that approximate optimal outcomes while managing the practical constraints of limited testing resources.

The literature on optimal one-dimensional group testing has been extensively studied, incorporating more and more realistic features and important operational considerations, especially in infectious disease contexts. These features include targeted mass screening, limited testing budgets, population multidimensionality, and robustness against uncertainties. However, two-dimensional group testing has not received similar attention

regarding the establishment of optimal methods. Despite the potential benefits of two-dimensional approaches, particularly since the introduction of non-adaptive array blood testing, there has been a lack of focus on understanding and optimizing these designs for complex, realistic scenarios. This gap calls for further research to establish optimal strategies for two-dimensional group testing, especially in the context of infectious disease screening.

Indeed, the introduction of array testing by Phatarfod & Sudbury (1994) and its implications for single-round testing processes underscored the potential for parallelization and thus for substantial time and resource savings. However, the existing state of the art on non-adaptive group testing mainly focuses on homogeneous populations. In this setting, the problem is simplified, and there is no need to assign individuals to groups. Typically, the main decision in these cases is deciding the dimensions of the testing matrix, whether it is square with $n \times n$ matrix where $n = \sqrt{N}$ or rectangular with $m \times q$ matrix where $m \times q = N$. On the other hand, research on individual assignments in non-adaptive group testing for heterogeneous populations is scarce, underscoring the need for our research. The work of McMahan *et al.* (2012b) addressed these limitations by introducing risk-based heuristics (gradient and spiral designs) that consider individual heterogeneity under imperfect tests. The limited existing literature uses heuristics and needs more research that incorporates optimal assignment solutions under a realistic setting of group testing.

The work of Hudgens & Kim (2011) proved that some values of group size will never be optimal when used in square based two-dimensional group testing when compared to individual testing. Moreover, the authors proved the interval for individual risk positivity to the binary characteristic to screen within which two-dimensional square group testing is more efficient than individual testing. Although their research considers a homogeneous population, their results give insights on the group sizes and the values of risk positivity when two-dimensional group testing is to be used.

Three-dimensional group testing has also been explored, with the work of Kim & Hudgens (2009) providing insights into the efficiency of three-dimensional designs compared to lower dimensions. Their findings suggest that higher-dimensional group testing can offer greater efficiency in certain contexts. For a detailed description of a hypercube algorithm considering higher-dimensional group testing (e.g., three-dimensional) for a homogeneous population in the context of SARS-CoV-2, see Mutesa *et al.* (2021).

However, in this study, we focus on two-dimensional group testing due to its relative simplicity of application compared to three-dimensional methods, which tend to be more complex in terms of practical implementation. Even though two-dimensional group testing itself is more challenging to apply compared to one-dimensional approaches, it offers a balance between complexity and efficiency. And more importantly, we study the problem design of a risk-based non-adaptive two-dimensional group testing for a heterogeneous

population with imperfect test and consideration of dilution effect. The following chapter (Chapter 2) tackles this problem by proposing mathematical formulations and solution methods. Beyond that, it also addresses additional aspects of this challenging problem.

Chapter 2

Mathematical Formulations for Risk-based Non-adaptive Two-Dimensional Group Testing with Equal Group Size

In this chapter, we tackle a challenge in two-dimensional group testing where we group individuals into equal-sized groups. This method makes it easier for laboratories to work with their available resources and equipment on groups of the same size. Our main focus is on creating these groups in such a way that we minimize errors in identifying who has a disease and reduce the number of tests needed. This is particularly complex due to the heterogeneous nature of the population, where individuals have different probabilities of being disease-positive, and the inherent imperfections of diagnostic tests. This research aims to fill a significant gap: finding an effective method for organizing these groups, taking into account the varying risk of disease among individuals and the limitations of the tests.

Specifically, we show that two-dimensional group testing is much more flexible than it might first appear. Initially inspired by the layout of tray wells, as dictated by the requirements of instruments like PCR (The Polymerase Chain Reaction (Mullis, 1994)) machines, it turns out that the structure of these wells is not a limitation at all. Whether a well contains a sample from an individual or a mixture of samples from several individuals does not affect the testing process. This understanding emphasizes the method's adaptability, allowing for a broader range of applications in mass screening without being tied to the conventional matrix setup.

In this chapter, we present several key contributions. First, we define a generalized design for Two-Dimensional Group Testing with Equal Group sizes (2D-GTEG) and provide the eligible values of group sizes that satisfy this design. This generalization moves beyond the traditional row/column concept in matrix designs, focusing solely on

defining groups of the same size. Such flexibility enables decision-makers, like medical laboratories, to choose group sizes that best match their operational constraints, such as staff capacity and available equipment. Second, we derive expressions for performance measures, including the expected number of false negatives, false positives, and tests following our design. These formulas are crucial for evaluating solutions. We then propose mathematical programs and develop algorithms to construct feasible solutions, along with local search methods to improve them. When the population to screen allows for a square matrix group testing design, we demonstrate the effectiveness of the proposed heuristics against the existing heuristics and evaluate their performance against exact methods by conducting studies on random data sets. This enables us to compare the performance of the heuristics relative to optimal or best-known solutions.

This chapter is organized as follows. Section 2.1 defines the problem and describes the novelty of our design. In Section 2.2, extended and derived statistical performance measures are presented. We propose in Section 2.3 our mathematical programs to formulate the problem. Section 2.4 describes heuristics used to solve the studied problem. Section 2.5 presents the results of applying our methods to random datasets. Finally, Section 2.6 discusses the implications of our findings and suggests directions for future research.

2.1 Problem Description

Let us denote by $\mathcal{I} = \{1, 2, \ldots, N\}$ the set of individuals to be tested, with their corresponding known probabilities of being disease-positive (prevalences) $\mathbf{p} = \{p^1, p^2, \ldots, p^N\}$. We assume the individuals are independent. We consider an imperfect test, where the result of the test on an individual or group is denoted by $\tau(\cdot) \in \{0, 1\}$, with $\tau(\cdot) = 1$ indicating a positive test result and $\tau(\cdot) = 0$ indicating a negative test result. The true status of an individual or group is represented by $(\cdot)^+$ for true positivity and $(\cdot)^-$ for true negativity.

The sensitivity of the test, $Se = P(\tau(\cdot) = 1 \mid (\cdot)^+)$, represents the probability of detecting a true-positive result, and the specificity, $Sp = P(\tau(\cdot) = 0 \mid (\cdot)^-)$, represents the probability of correctly identifying a true-negative result. We assume $Se, Sp \in [0, 1]$ with $Se + Sp - 1 \in [0, 1]$, indicating the possibility of misclassification errors. In other words, the test may incorrectly classify a true-negative as positive or a true-positive as negative. Furthermore, the sensitivity and specificity are assumed to be identical for both individual testing (e.g., confirmatory testing) and group testing.

We consider the dilution effect (a positive individual may not be detected when diluted in a large group of negative samples) through a group size L that cannot exceed a derived value from a clinical study on the disease under investigation.

Furthermore, we consider non-adaptive two-dimensional group testing with an `AND` scheme (Habtesllassie *et al.*, 2015). Here, by non-adaptive, we mean that all tests are

designed in advance and do not depend on the outcomes of previous tests. And by `AND` scheme we mean that an individual in the intersection of two groups is retested individually only if both intersecting groups test positive.

Given the set of individuals $\mathcal{I}$ and the set of groups $\mathcal{G} = \{1, 2, \ldots, G\}$, the problem studied is to form groups $G_k, k \in \mathcal{G}$ where:

(i) Each individual i exactly belongs to two distinct groups G_k and G_l

(ii) Each two groups G_k and G_l share at most one individual i.

(iii) Each group contains exactly L individuals.

(iv) The misclassification error and expected number of tests are minimized.

Remark 2.1. *Since each individual has to be part of two groups and two groups intersect at most once, it follows that* $G = \frac{2N}{L}$.

In the literature, two-dimensional tests are designed on a population of N individuals, where the groups are represented under a matrix $n \times m$ with $n \times m = N$. Note that if $m = n$, the population fits a square matrix. Each individual is then at the intersection of a row and a column, which represents a restricted subspace of all possible two-dimensional configurations.

To overcome this limitation, some studies have explored more flexible designs based on the *magnitude of overlapping* among groups. This magnitude refers to how much the groups intersect with each other in terms of shared individuals. Two extreme cases are generally considered. In a *minimal overlapping* configuration, the number of pairs of groups sharing one individual in common is minimized, resulting in a larger number of group pairs that share no individuals at all. In contrast, *maximal overlapping* refers to a design where each pair of groups shares exactly one individual in common, thereby maximizing the overlap among the groups.

The study by Xiong *et al.* (2019) introduced this concept of overlapping magnitude to analyze and improve matrix pooling designs. They demonstrated that the efficiency of matrix pooling is closely related to the degree of overlap between groups. Their proposed design achieves maximal overlapping, where each pair of groups intersects in exactly one individual. They show that the new design outperforms matrix pooling in efficiency while retaining the pooling sensitivity and specificity.

In this chapter we propose a generalization of the two-dimensional design of group testing that goes beyond a simple matrix representation. One of the most important questions we raise concerns the values of eligible group size L for which the conditions ((i)–(iii)) are satisfied. We show that, through Proposition 2.2, for the same population of N individuals, there are potentially several group sizes for which a two-dimensional group testing design is possible, from the minimal overlapping setting to the maximal

overlapping setting. This allows the decision-maker (medical analysis laboratory) to choose the group size that suits the laboratory's staff and equipment.

Proposition 2.2. *For $N > 2$, an integer L satisfies ((i))–((iii)) if and only if $L \mid 2N$ and $2 \leq L \leq \left\lfloor \frac{4N}{1+\sqrt{1+8N}} \right\rfloor$.*

Proof. $\Rightarrow$ If a solution satisfies conditions ((i))–((iii)), then we must have $L \mid 2N$ and $2 \leq L \leq \left\lfloor \frac{4N}{1+\sqrt{1+8N}} \right\rfloor$.

Given the condition that every individual belongs to exactly two groups it follows that $G \times L = 2N$. Thus L must divide $2N$.

Table 2.1: A solution that always satisfies ((i)-(iii))

G_1	$\{ 1, 2\}$
G_2	$\{ 2, 3\}$
G_3	$\{ 3, 4\}$
$\ldots$	$\ldots$
G_{N-1}	$\{ N-1, N\}$
G_N	$\{ N, 1\}$

It is obvious that L has to be greater than or equal to 2. Otherwise each individual would be tested alone. Please note that when $L = 2$, $G = N$ and a feasible solution in this setting is given in Table 2.1. Note that this solution corresponds with the minimal overlapping among groups. It is left to determine the maximal value of L that is eligible. To this end please note that the maximal value of L corresponds to the minimal value of G. In fact, the number of groups G is minimal when the overlapping satisfying (ii) is maximal. That is, each pair of groups shares exactly one individual i. This means that the number of pairs of groups is equal to the number of individuals in the population as each intersection of two groups represents one individual, which can be mathematically expressed as $\binom{G}{2} = \frac{G(G-1)}{2} = N$. Leading to the second order equation $G^2 - G - 2N = 0$. The only meaningful root is $G = \frac{1+\sqrt{1+8N}}{2}$. Which leads to the inequality $\frac{1+\sqrt{1+8N}}{2} \leq G \leq N$. Consequently, we obtain the interval for the final values of L which can be found in the proposition.

$\Leftarrow$ Given a value of $N > 2$, assume L is an integer such that $2 \leq L \leq \lfloor \frac{4N}{1+\sqrt{1+8N}} \rfloor$ and $L \mid 2N$. We show that we can construct a solution satisfying conditions ((i))–((iii)).

We proceed by splitting into sub-cases according to the value of L. Let $G = \frac{2N}{L}$. There are three cases: $G = 2L$, $G > 2L$ or $G < 2L$.

Case $G = 2L$ This corresponds to $L = \sqrt{N}$. We arrange the individuals in a matrix-like design. The first L groups $(G_1, \ldots, G_L)$ are filled row-wise with consecutive blocks of size L. The remaining L groups of size L $(G_{L+1}, \ldots, G_{2L})$ are filled column-wise (vertical filling). This ensures that each individual appears twice and every pair of groups intersects

in at most one individual. Figure 2.1 illustrates the filling and Figure 2.3 gives an example for $N = 9$, $L = 3$.

G_1	1	2	$\dots$	L
G_2	$L+1$	$L+2$	$\dots$	$2L$
$\vdots$	$\vdots$	$\vdots$	$\ddots$	$\vdots$
G_L	$(L-1)L+1$	$\dots$		L^2
G_{L+1}	1	$L+1$	$\dots$	$(L-1)L+1$
$\vdots$	$\vdots$	$\vdots$	$\ddots$	$\vdots$
G_{2L}	L	$2L$	$\dots$	L^2

Figure 2.1: Matrix-like design for $G = 2L$.

Case $G > 2L$

In this case, the number of groups $G = \frac{2N}{L} > 2L$. We distinguish between the two sub-cases depending whether $L \mid N$ or not.

Sub-case $G > 2L$**,** $L \mid N$ Let $M = \frac{N}{L}$ denotes the number of groups required to fully cover the individuals in the first phase. The construction proceeds as follows:

- **Phase 1: Horizontal Placement.** Place the N individuals row by row across the first M groups $G_1, G_2, \dots, G_M$, such that each group contains exactly L individuals: For each group G_g ($g \in \{1, \dots, M\}$), assign $\{(g-1)L+1, (g-1)L+2, \dots, gL\}$ to G_g.

- **Phase 2: Vertical Sinusoidal Placement.** Construct the remaining M groups $G_{M+1}, G_{M+2}, \dots, G_{2M}$ by scanning vertically through the first M groups (since $L < M$) in a sinusoidal pattern: First, collect the first L individuals of the first L groups $G_1, G_2, \dots, G_L$ and place them in G_{M+1}. Then, collect the next L individuals (either from the next L groups $G_{L+1}, G_{L+2}, \dots$ or by switching to the second individual of the first L groups) and place them in G_{M+2}. Continue this process, alternating between rows and switching groups as needed. Figure 2.4 illustrates the whole process for $L \mid N$ for $N = 12$, $L = 3$.

Sub-case $G > 2L$**,** $L \nmid N$ Let $M = \lfloor \frac{N}{L} \rfloor$ and note that there will be an incomplete group G_{M+1}, which contains only $e < L$ individuals. The construction proceeds as follows:

- **Phase 1: Horizontal Placement.** Place N individuals row by row across the first M groups $G_1, G_2, \dots, G_M$, ensuring that each group contains exactly L individuals. The last group G_{M+1} will contain $e < L$ individuals.

- **Phase 2: Completion and Sinusoidal Placement.** Start by completing the incomplete group G_{M+1}. To do this, scan vertically through the first M groups

$G_1, G_2, \ldots, G_M$, collecting individuals that have not yet been placed in G_{M+1}. After completing G_{M+1}, construct the remaining groups $G_{M+2}, G_{M+3}, \ldots, G_{\frac{2N}{L}}$ by following the sinusoidal scanning approach: Start with the L individuals already placed in the first L groups $G_1, G_2, \ldots, G_L$ and place them in G_{M+2}. Continue by collecting the next L individuals (avoiding the $L - e$ individuals we placed in Phase 2 in group G_{M+1}) and assign them to G_{M+3}, proceeding similarly until all remaining groups are filled. Figure 2.5 illustrates the whole process for $L \nmid N$ for $N = 18$, $L = 4$.

Case $G < 2L$ We first prove that $G > L$. To satisfy the conditions (i)-(iii), when placing the first L individuals in group G_1, these L individuals cannot appear together in any subsequent group $G_2, G_3, \ldots$. Hence, we need at least $L + 1$ groups. Thus, the number of groups $G = \frac{2N}{L} = L + k$, where $1 \leq k \leq L - 1$. In the following, we describe the construction algorithm for $k = 1$ and $k \geq 2$.

Sub-case $k = 1$**.** When $k = 1$, we construct a complete graph K_G where the vertices represent the groups $G_1, \ldots, G_{L+1}$, and each edge corresponds to an individual as $N = \frac{L(L+1)}{2} = \binom{L+1}{2}$. As such, each individual appears in two distinct groups (once for each endpoint of the edge), groups intersect in exactly one individual (shared edge between two vertices) and each group contains exactly L individuals.

Sub-case $2 \leq k \leq L - 1$**.** Here, $2N = G \cdot L = (L + k) \cdot L = 2kL + L(L - k)$. As such, it follows that $N = kL + \frac{L(L-k)}{2}$. The solution is constructed in three steps. First, we fill the last k horizontal groups. Note that $G < 2L$ implies that $N < L^2$ and thus $kL < N$. Hence, we place the first kL individuals sequentially across the last k groups $G_{L+1}, G_{L+2}, \ldots, G_{L+k}$, such that each group contains exactly L individuals. Second, use the transpose of the last k groups to place individuals in the first L groups $G_1, \ldots, G_L$. Specifically, take the first column of individuals from $G_{L+1}, G_{L+2}, \ldots, G_{L+k}$ and place them in G_1. Repeat for the second column: place its individuals in G_2, and so on until all kL individuals are placed in the first L groups. After this step, we have accounted for $2kL$ occurrences. Third, the remaining $L(L - k)$ occurrences are handled as follows. If $k = L-1$, exactly L occurrences of the individuals remain, which are placed vertically in the first column of the L groups. Otherwise, $2 \leq k \leq L-2$, this corresponds to a smaller recursive problem with $G' = L, \quad L' = L - k$, where the problem is solved recursively using the appropriate case ($G' = 2L'$ or $G' > 2L'$ or $G' < 2L'$) based on the new values of G' and L'. Figure 2.6 illustrates the process when $G < 2L$ with $2 \leq k \leq L - 2$ for $N = 20$, $L = 5$.

Conclusion The construction algorithm described in this proof guarantees the existence and the construction of a feasible solution given N and $L|2N$ and in the interval in all cases ($G = 2L$, $G > 2L$, $G < 2L$). This proof completes the sufficiency of the proposed values of L in the interval.

□

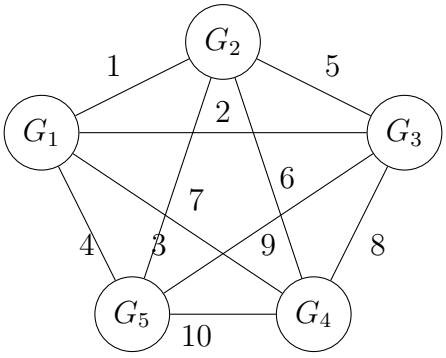
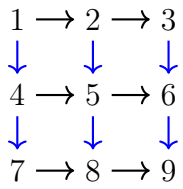


Figure 2.2: Complete graph K_G for $G = L + 1$, where vertices are groups $G_1, G_2, \ldots, G_G$, and edges represent individuals.

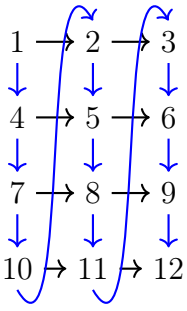


(a) Phase 1 in black Phase 2 in blue.

G_1	1, 2, 3
G_2	4, 5, 6
G_3	7, 8, 9
G_4	1, 4, 7
G_5	2, 5, 8
G_6	3, 6, 9

(b) Result.

Figure 2.3: Example for $G = 2L$ with $N = 9$, $L = 3$



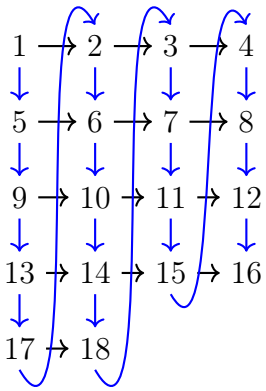
(a) Phase 1 (horizontal, black arrows) and Phase 2 (vertical, blue arrows).

G_1	1, 2, 3
G_2	4, 5, 6
G_3	7, 8, 9
G_4	10, 11, 12
G_5	1, 4, 7
G_6	10, 2, 5
G_7	8, 11, 3
G_8	6, 9, 12

(b) Resulting groups.

Figure 2.4: Example for $N = 12, L = 3$ with $G > 2L$. Phase 1 fills rows horizontally, Phase 2 distributes individuals vertically, and final groups are shown.

Example Let $N = 36$. Thanks to Proposition 2.2, we can determine all the possible

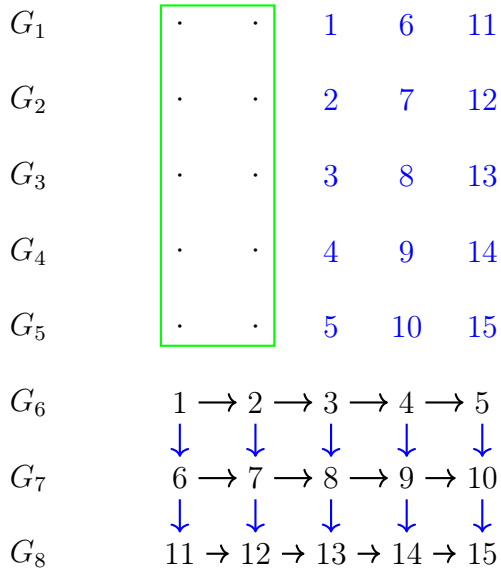


(a) Phase 1 and Phase 2 filling.

G_1	1, 2, 3, 4
G_2	5, 6, 7, 8
G_3	9, 10, 11, 12
G_4	13, 14, 15, 16
G_5	17, 18, 1, 5
G_6	9, 13, 17, 2
G_7	6, 10, 14, 18
G_8	3, 7, 11, 15
G_9	4, 8, 12, 16

(b) Resulting groups.

Figure 2.5: Example for $N = 18, L = 4$ with $L \nmid N$. Phase 1 fills rows horizontally, Phase 2 completes the incomplete group, and final groups are shown.



(a) Phase 1 in black and Phase 2 recursive.

G_1	16	17	1	6	11
G_2	18	19	2	7	12
G_3	20	16	3	8	13
G_4	18	20	4	9	14
G_5	17	19	5	10	15
G_6	1	2	3	4	5
G_7	6	7	8	9	10
G_8	11	12	13	14	15

(b) Result.

Figure 2.6: Example for $N = 20$, $L = 5$, and $G = 8$: The first $L = 5$ groups (G_1 to G_5) contain $L - k = 2$ empty positions, followed by transposed elements from G_6, G_7, and G_8. The last $k = 3$ groups are filled horizontally. The remaining $L(L-k)$ occurrences of individuals form a smaller subproblem, solved recursively with $N' = \frac{L(L-k)}{2}$, $G' = L$, and $L' = L - k$, based on the cases of G' relative to L'. In this example, $N' = 5$, $G' = 5$, and $L' = 2$, corresponding to the case $G' > 2L'$.

values of L. The integer values in the interval $[2, \lfloor \frac{4N}{1+\sqrt{1+8N}} \rfloor = 8]$ are $\{2, 3, 4, 5, 6, 7, 8\}$. Since L divides $2N = 72$, 5 has to be discarded. Consequently, $L \in \{2, 3, 4, 6, 7, 8\}$.

Remark 2.3. *Note that when the only possible value of L is 2, non-adaptive two-*

dimensional group testing with equal group size is clearly not interesting since it implicates forming $G = N$ groups of size $L = 2$. One-dimensional (Dorfman) group testing may be a better option in this case.

Remark 2.4. *Note that if the size of $N \geq 3$ of the population to screen is a prime number, then the only valid value of L is 2, and by Remark 2.3, the proposed design is not interesting. To overcome this situation, one may add one single artificial individual $N + 1$ with prevalence $p^{N+1} = 0$ and the design becomes applicable.*

Remark 2.5. *If one wants to verify if a feasible solution can be represented in an equivalent square matrix solution with rows and columns when $L = \sqrt{N}$, it can be verified by solving the square matrix layout check problem F_{SQUARE} described in the Appendix 4.4.*

In order to formally describe the problem we study in this chapter let us introduce the following notation. Let $\mathcal{S}$ be the set of all solutions that satisfy conditions ((i)-(iii)). Given $S \in \mathcal{S}$, let $\mathbb{E}[FN(S)]$ be the expected number of false negatives, $\mathbb{E}[FP(S)]$ be the expected number of false positives and $\mathbb{E}[T(S)]$ be the expected number of tests for S.

The optimization problem can then be formulated as follows:

$$\min_{S \in \mathcal{S}} \quad \lambda_1 \mathbb{E}[FN(S)] + \lambda_2 \mathbb{E}[FP(S)] + (1 - \lambda_1 - \lambda_2)\mathbb{E}[T(S)] \tag{2.1}$$

where λ_1, λ_2 and $(1 - \lambda_1 - \lambda_2)$ with $\lambda_1, \lambda_2 \in [0, 1]$ and $\lambda_1 + \lambda_2 \leq 1$ are the weights assigned to the expected number of false negatives, false positives, and tests, respectively. The decision-maker can choose to optimize any convex combination of $\mathbb{E}[\mathrm{FN}(S)]$, $\mathbb{E}[\mathrm{FP}(S)]$, and $\mathbb{E}[T(S)]$ by appropriately setting the values of λ_1 and λ_2. The decision problem (2.1) looks over all the feasible solutions satisfying ((i)-(iii)), for the optimal solution with the minimal linear combination of the misclassification error and the expected number of tests. The decision maker can then choose to optimize any convex combination of the $\mathbb{E}[FN(S)]$, $\mathbb{E}[FP(S)]$ and $\mathbb{E}[T(S)]$.

2.2 Statistical Framework and Performance Measures

The formulation (2.1) provided earlier is a combinatorial model. The evaluation of a solution in group testing relies on well-defined performance measures, such as the expected number of false positives, false negatives, and the total number of tests. These measures provide a statistical basis for assessing the quality of a solution. In this section, we adapt performance measures from the literature, originally developed for homogeneous populations, to address the challenges of heterogeneous populations. Additionally, we compute the contributions of individual groups and overlapping pairs of groups to these performance measures. These calculations are necessary for formulating the optimization problem in later sections.

2.2.1 Adapting Performance Measures for Heterogeneous Populations

Performance measures for group testing problems, such as those presented in Habtesllassie *et al.* (2015), are traditionally derived under the assumption of a homogeneous population. However, in our problem, individuals have heterogeneous probabilities of being disease-positive, requiring modifications to these measures. This subsection details how we adapt the definitions of false positives, false negatives, and the number of tests to reflect the heterogeneity of the population. These adaptations form the foundation for evaluating solutions in the context of our problem.

Given a feasible solution $S = \{G_1, G_2, \cdots, G_{|S|}\}$, the misclassification test outcomes for our configuration (`AND` scheme) occur in the subsequent setting. A true positive individual $i \in \mathcal{I}$ belonging to the distinct groups G_k and G_l, is classified as false negative if the test outcome on G_k is negative or the test outcome on G_l is negative. A true negative individual i belonging to the distinct groups G_k and G_l, is classified as false positive if the test outcome on G_k is positive, and the test outcome on G_l is positive, and the individual confirmatory test outcome on i is positive. A group G_k is positive means that either it is true positive (it contains at least one positive individual) or it is a false positive (all the individuals in the group are true negative but the test on the group turns out to be positive due to test errors).

Let G_k^+ and G_k^- denote the events that the group G_k contains at least one truly positive individual or only truly negative individuals, respectively. Similarly, i^+ (respectively i^-) denotes that individual i is truly positive (respectively negative). Based on Habtesllassie *et al.* (2015), the probability $P(\tau(G_k) = 1)$ that the test outcome on group G_k is positive can be written as follows.

$$\begin{aligned} P(\tau(G_k) = 1) &= P(\tau(G_k) = 1 \mid G_k^-) \cdot P(G_k^-) + P(\tau(G_k) = 1 \mid G_k^+) \cdot P(G_k^+) \\ &= (1 - Sp) \prod_{i \in G_k} (1 - p^i) + Se(1 - \prod_{i \in G_k} (1 - p^i)) \\ &= Se - (Se + Sp - 1) \prod_{i \in G_k} (1 - p^i) \end{aligned} \tag{2.2}$$

Hereafter, based on Habtesllassie *et al.* (2015), we compute the false negative and false positive classifications as well as the expected number of tests for the studied design for a feasible solution S. In what follows, let G_k and G_l the two groups to which individual i belongs, such that $G_k \cap G_l = \{i\}$. Let $FN(i)$ and $FP(i)$ denote the indicator random variables, respectively corresponding to the false-negative classification and false positive classification of individual i. Let $T(i)$ denotes the indicator random variable corresponding to the number of tests performed for individual i.

2.2.1.1 False negative classification

For a given individual i within a solution S, we are given

$$\begin{aligned}\mathbb{E}[FN(i)] &= P(i^+) - P(i^+ \cap (\tau(G_k) = 1 \cap \tau(G_l) = 1) \cap \tau(i) = 1) \\ &= P(i^+) - P(\tau(G_k) = 1 \mid i^+)P(\tau(G_l) = 1 \mid i^+)P(\tau(i) = 1 \mid i^+)P(i^+) \\ &= p^i(1 - Se^3)\end{aligned} \tag{2.3}$$

Consequently, the expected number of false negatives $\mathbb{E}[FN(S)]$ for S is given by $\mathbb{E}[FN(S)] = \sum_{i \in \mathcal{I}} \mathbb{E}[FN(i)]$.

Remark 2.6. *Here, the expected number of false negatives $\mathbb{E}[FN(S)]$ depends solely on the set of individuals being tested and remains constant irrespective of how the groups are formed in the two-dimensional group testing configuration.*

2.2.1.2 False positive classification

For a given individual i within a solution S, we have

$$\begin{aligned}\mathbb{E}[FP(i)] &= P(i^- \cap (\tau(G_k) = 1 \cap \tau(G_l) = 1) \cap \tau(i) = 1) \\ &= P(i^-)P(\tau(G_k) = 1|i^-)P(\tau(G_l) = 1|i^-)P(\tau(i) = 1|i^-) \\ &= (1 - p^i)(1 - Sp)\left(Se - (Se + Sp - 1)\prod_{j \in G_k, j \neq i}(1 - p^j)\right) \\ &\quad \left(Se - (Se + Sp - 1)\prod_{h \in G_l, h \neq i}(1 - p^h)\right)\end{aligned} \tag{2.4}$$

Consequently, the expected number of false positives $\mathbb{E}[FP(S)]$ for S is given by $\mathbb{E}[FP(S)] = \sum_{i \in \mathcal{I}} \mathbb{E}[FP(i)]$.

2.2.1.3 Expected number of tests

The total expected number of tests is the sum of the initial group tests and the expected number of individual retests. Recall that an individual i at the intersection of G_k and G_l is retested if both groups G_k and G_l test positive. We then have

$$
\begin{aligned}
\mathbb{E}[T(i)] &= P(\tau(G_k) = 1 \cap \tau(G_l) = 1) \\
&= P(\tau(G_k) = 1|i^+)P(\tau(G_l) = 1|i^+)P(i^+) \\
&+ P(\tau(G_k) = 1|i^-)P(\tau(G_l) = 1|i^-)P(i^-) \\
&= Se^2 p^i + (1 - p^i) \left(Se - (Se + Sp - 1) \prod_{j \in G_k, j \neq i} (1 - p^j) \right) \\
&\quad \left(Se - (Se + Sp - 1) \prod_{h \in G_l, h \neq i} (1 - p^h) \right) \\
&= Se^2 p^i + \frac{\mathbb{E}[FP(i)]}{1 - Sp}
\end{aligned}
\tag{2.5}
$$

Consequently, the expected number of tests for a feasible solution S is:

$$
\mathbb{E}[T(S)] = \sum_{i \in \mathcal{I}} \mathbb{E}[T(i)] = G + \sum_{i \in \mathcal{I}} p^i Se^2 + \frac{\mathbb{E}[FP(S)]}{1 - Sp} \tag{2.6}
$$

Remark 2.7. *The expected number of tests $\mathbb{E}[T(S)]$ is a function of the expected number of false positives $\mathbb{E}[FP(S)]$. By definition, it is equal to the number G of groups initially tested, plus the number of tests conducted in the second stage, which depends on the number of positive results, including both true positives and false positives.*

The adapted performance measures describe the overall behavior of a solution S. To formulate our optimization problem, however, we need a finer granularity: the contributions of each group and each pair of overlapping groups to the performance measures. The next section derives explicit expressions for the contributions of groups and overlapping pairs of groups to $\mathbb{E}[FN(S)]$, $\mathbb{E}[FP(S)]$ and $\mathbb{E}[T(S)]$.

2.2.2 Contributions of Groups to Performance Measures

Let respectively $\mathbb{E}[FN(G_k)]$, $\mathbb{E}[FP(G_k)]$ and $\mathbb{E}[T(G_k)]$ be the contribution of group G_k in false negative misclassification, false positive misclassification and expected number of tests of S. Let respectively $\mathbb{E}[FP((G_k, G_l))]$ and $\mathbb{E}[T((G_k, G_l))]$ be the contribution of an intersecting pair of groups (G_k, G_l) in false positive misclassification and in expected number of tests of a feasible solution S. The following derives the expressions of these contributions.

2.2.2.1 Contribution of a group to the false negative classification

Given a group $G_k, k \in \mathcal{G}$, we compute the contribution $\mathbb{E}[FN(G_k)]$ of this group in the expected number of false negatives $\mathbb{E}[FN(S)]$.

As each individual $i \in \mathcal{I}$ will belong, in a solution, to two groups G_k and G_l, we can write the contribution $\mathbb{E}[FN(G_k)]$ as:

$$\mathbb{E}[FN(G_k)] = \frac{(1 - Se^3)}{2} \sum_{i \in G_k} p^i \tag{2.7}$$

Thus, the expected number of false negatives for a solution S is:

$$\mathbb{E}[FN(S)] = \sum_{k \in \mathcal{G}} \mathbb{E}[FN(G_k)] \tag{2.8}$$

2.2.2.2 Contribution of a group to the false positive classification

Let G_k and G_l be the two groups such that $G_k \cap G_l = \{i\}$. The expected number of false positives is as follows.

$$\begin{aligned}
\mathbb{E}[FP(S)] &= \sum_{i \in \mathcal{I}} \mathbb{E}[FP(i)] \\
&= \sum_{i \in \mathcal{I}} (1 - p^i)(1 - Sp) \left(Se - (Se + Sp - 1) \prod_{j \in G_k, j \neq i} (1 - p^j) \right) \\
&\quad \left(Se - (Se + Sp - 1) \prod_{h \in G_l, h \neq i} (1 - p^h) \right) \\
&= \underbrace{\sum_{i \in \mathcal{I}} (1 - Sp) Se^2 (1 - p^i)}_{\mathcal{A}} \\
&\underbrace{- \sum_{i \in \mathcal{I}} (1 - Sp) Se (Se + Sp - 1) \prod_{j \in G_k} (1 - p^j)}_{\mathcal{B}} \\
&\underbrace{- \sum_{i \in \mathcal{I}} (1 - Sp) Se (Se + Sp - 1) \prod_{h \in G_l} (1 - p^h)}_{\mathcal{C}} \\
&\underbrace{+ \sum_{i \in \mathcal{I}} (1 - Sp)(Se + Sp - 1)^2 (1 - p^i) \prod_{j \in G_k, j \neq i} (1 - p^j) \prod_{h \in G_l, h \neq i} (1 - p^h)}_{\mathcal{D}}
\end{aligned} \tag{2.9}$$

The terms $\mathcal{A}$, $\mathcal{B}$, and $\mathcal{C}$ directly correspond to the contributions of individual groups G_k to the expected number of false positives ($\mathbb{E}[FP(S)]$), whereas term $\mathcal{D}$ accounts for the interaction between pairs of overlapping groups (G_k, G_l). This distinction allows us to deduce the impact of each group and pair of groups on the overall false positive rate, guiding the optimization process under the provided constraints.

Knowing that each individual i will occur, in a solution, in two groups G_k, G_l, then we can write the following expressions:

$$\sum_{i\in\mathcal{I}}(1-Sp)Se^2(1-p^i) = \frac{(1-Sp)Se^2}{2}\sum_{k\in\mathcal{G}}\sum_{i\in G_k}(1-p^i) \tag{2.10}$$

In a group G_k, the term $(1-Sp)Se(Se+Sp-1)\prod_{j\in G_k}(1-p^j)$ will occur as many times as L. Thus, we know that each group G_k will contribute with its coefficient $\prod_{i\in G_k}(1-p^i)$ once for each individual i such that $i \in G_k$, in the expression of $\mathbb{E}[FP(S)]$.

$$\begin{aligned}\mathcal{B}+\mathcal{C} &= -\sum_{i\in\mathcal{I}}(1-Sp)Se(Se+Sp-1)\prod_{j\in G_k}(1-p^j)\\ &\quad -\sum_{i\in\mathcal{I}}(1-Sp)Se(Se+Sp-1)\prod_{h\in G_l}(1-p^h)\\ &= -L(1-Sp)Se(Se+Sp-1)\sum_{k\in\mathcal{G}}\prod_{i\in G_k}(1-p^i)\end{aligned} \tag{2.11}$$

Consequently, we can derive for each group G_k its corresponding contribution $\mathbb{E}[FP(G_k)]$ to the expected number of false positives $\mathbb{E}[FP(S)]$ as follows.

$$\mathbb{E}[FP(G_k)] = \frac{(1-Sp)Se^2}{2}\sum_{i\in G_k}(1-p^i) - L(1-Sp)Se(Se+Sp-1)\prod_{i\in G_k}(1-p^i) \tag{2.12}$$

Now, for each pair of groups (G_k, G_l), intersecting in one individual i, we have:

$$\begin{aligned}\mathbb{E}[FP((G_k,G_l))] &= (1-Sp)(Se+Sp-1)^2(1-p^i)\\ &\quad \prod_{j\in G_k, j\neq i}(1-p^j)\prod_{h\in G_l, h\neq i}(1-p^h)\end{aligned} \tag{2.13}$$

Hence, we can write the expected number of false positives for a feasible solution S as

$$\mathbb{E}[FP(S)] = \sum_{k\in\mathcal{G}}\mathbb{E}[FP(G_k)] + \sum_{k,l\in\mathcal{G},|G_k\cap G_l|=1}\mathbb{E}[FP((G_k,G_l))] \tag{2.14}$$

2.2.2.3 Contribution of a group to the expected number of tests

From (2.6) together with (2.14), we can derive $\mathbb{E}[T(G_k)]$ and $\mathbb{E}[T((G_k,G_l))]$ as follows.

$$\mathbb{E}[T(G_k)] = 1 + \frac{Se^2}{2}\sum_{i\in G_k}p^i + \frac{1}{1-Sp}\mathbb{E}[FP(G_k)] \tag{2.15}$$

$$\mathbb{E}[T((G_k,G_l))] = \frac{\mathbb{E}[FP((G_k,G_l))]}{1-Sp} \tag{2.16}$$

Thus, we can write the expected number of tests for a feasible solution S as

$$\mathbb{E}[T(S)] = \sum_{k \in \mathcal{G}} \mathbb{E}[T(G_k))] + \sum_{k,l \in \mathcal{G}, |G_k \cap G_l| = 1} \mathbb{E}[T((G_k, G_l))] \tag{2.17}$$

2.2.3 Selected Performance Measure

Based on Remarks 2.6 and 2.7, we focus in the remainder of this chapter on minimizing solely in (2.1) the expected number of false positives $\mathbb{E}[FP(S)]$ thus setting $\lambda_2 = 1$.

Readability constants. In the remainder of the manuscript, the expression of $\mathbb{E}[FP(S)]$ and the proposed optimization formulations repeatedly involve the same coefficients depending only on the test characteristics (Se, Sp) and the group size L. For readability, we introduce the following shorthand constants once for all:

$$Q := \frac{(1 - Sp)\, Se^2}{2}, \qquad R := L(1-Sp)\, Se(Se+Sp-1), \qquad U := (1-Sp)(Se+Sp-1)^2. \tag{2.18}$$

Coefficients Q and R are respectively involved in the *sum term* and the *product term* of $\mathbb{E}[FP(G_k)]$ for each group G_k in a feasible solution S, whereas U is involved in the *interaction term* $\mathbb{E}[FP((G_k, G_l))]$ associated with any intersecting pair (G_k, G_l) in S. Using Q, R, and U allows us to keep subsequent mathematical expressions compact without changing the underlying models.

2.3 Mathematical Formulations

Having established the statistical performance measures derived in the previous section, we now develop mathematical formulations for the problem. We will start with a mixed integer nonlinear formulation, enhance it with symmetry-breaking constraints, and then present an extended formulation.

2.3.1 Mixed Integer Nonlinear Formulation

The overall notation used for the formulation is summarized in Table 2.2. This table includes the sets, variables, and parameters used in our mixed integer nonlinear programming (MINLP) formulations. The sets $\mathcal{I}$ and $\mathcal{G}$ define the individuals to be screened and the groups to be formed, respectively. The parameters include the size of the groups L, the population's disease-positive probabilities $\mathbf{p}$, the sensitivity of the test Se and the specificity of the test Sp. The formulation $\mathrm{F}^1_{\mathrm{MINLP}}$ make use of binary variables z_{ik}, $i \in \mathcal{I}, k \in \mathcal{G}$ that equal 1 if individual i belongs to a specific group G_k, 0 otherwise.

Table 2.2: Notation for MINLP formulations.

Sets	$\mathcal{I}$	the set of individuals to screen
	$\mathcal{G}$	the set of groups to make, $\mathcal{G} = \{1, 2, \ldots, G\}$
Variables	$z_{ik} = \begin{cases} 1, & \text{if individual } i \text{ is in group } G_k,\ k \in \mathcal{G} \\ 0, & \text{otherwise} \end{cases}$	
Parameters	L	the size of groups
	$\mathbf{p}$	the population's known probabilities of being disease-positive
	Se	the sensitivity of the test
	Sp	the specificity of the test

$$
\begin{aligned}
[\mathrm{F}^1_{\mathrm{MINLP}}] \quad \min & \sum_{k\in\mathcal{G}} \left[Q \sum_{i\in\mathcal{I}} (1-p^i)\, z_{ik} - R \prod_{i\in\mathcal{I}} (1 - p^i z_{ik}) \right] + \\
& U \sum_{k\in\mathcal{G}} \sum_{l\in\mathcal{G}:l>k} \left[\sum_{i\in\mathcal{I}} (1-p^i) z_{ik} z_{il} \prod_{j\in\mathcal{I}\setminus\{i\}} \left(1 - p^j z_{jk}\right) \prod_{h\in\mathcal{I}\setminus\{i\}} \left(1 - p^h z_{hl}\right) \right] && (2.19) \\
\text{s.t.} & \sum_{k\in\mathcal{G}} z_{ik} = 2 \quad \forall i \in \mathcal{I} && (2.20) \\
& \sum_{i\in\mathcal{I}} z_{ik} z_{il} \le 1 \quad \forall k, l \in \mathcal{G}, l > k && (2.21) \\
& \sum_{i\in\mathcal{I}} z_{ik} = L \quad \forall k \in \mathcal{G} && (2.22) \\
& z_{ik} \in \{0, 1\} \quad \forall i \in \mathcal{I}, \forall k \in \mathcal{G} && (2.23)
\end{aligned}
$$

The objective function (2.19) minimizes the expected number of false positives $\mathbb{E}[FP(S)]$ derived in Section 2.2.2 (see (2.12)–(2.14)), using the shorthand coefficients defined in (2.18). It is written as the sum of (i) contributions of individual groups and (ii) interaction contributions due to pairs of intersecting groups. A key point is that the assignment variable z_{ik} activates or deactivates the factor $(1 - p^i)$ depending on whether individual i belongs to group G_k. In the sum term $\sum_{i\in\mathcal{I}}(1-p^i)z_{ik}$, z_{ik} acts as a selector: the contribution is 0 when $z_{ik} = 0$ and equals $(1 - p^i)$ when $z_{ik} = 1$, so $(1 - p^i)$ is counted if and only if $i \in G_k$. In the product term $\prod_{i\in\mathcal{I}}(1 - p^i z_{ik})$, the same mechanism ensures that non-assigned individuals contribute a neutral factor 1 (when $z_{ik} = 0$) while assigned individuals contribute the intended factor $(1 - p^i)$ (when $z_{ik} = 1$); equivalently, $\prod_{i\in\mathcal{I}}(1 - p^i z_{ik}) = \prod_{i\in G_k}(1 - p^i)$.

Constraints (2.20) impose that each individual belongs to exactly two groups. Con-

straints (2.21) impose that each pair of groups (G_k, G_l) with $l > k$ contains at most one individual in common. Constraints (2.22) impose that each group G_k contains exactly L individuals. Finally, constraints (2.23) are the integrality constraints for variables z_{ik}.

Remark 2.8. *In formulation F^1_{MINLP}, the number of decision variables z_{ik} is given by $G \times N$, where $G = \frac{2N}{L}$ is the number of groups in a feasible solution. For fixed N, this number decreases as the group size L increases. Conversely, the number of possible groups of size L, given by $\binom{N}{L}$, increases with L.*

The formulation $\mathrm{F}^1_{\mathrm{MINLP}}$ is a nonconvex integer nonlinear program for which solving to global optimality is generally known to be difficult (Burer & Letchford, 2012). Note that the objective function is highly nonlinear because it contains multilinear products such as $\prod_{i\in\mathcal{I}}(1-p^i z_{ik})$. When expanded, these terms define a multilinear (pseudo-Boolean) polynomial of degree up to N in the assignment variables. However, due to constraint (2.22), each group contains exactly L individuals in any feasible solution, so only up to L factors are active. We next reformulate these products into quadratic expressions in order to rely on a commercial solver for quadratic optimization such as for example Gurobi Optimization, LLC (2024).

First let us rewrite the product as follows.

$$\prod_{i\in\mathcal{I}}(1-p^i z_{ik}) = \left(\prod_{i=1}^{j-1}(1-p^i z_{ik})\right)\left(\prod_{i=j}^{N}(1-p^i z_{ik})\right). \tag{2.24}$$

For a fixed individual number j in the natural order given by the population $\mathcal{I}$, we can notice that the product $\prod_{i=1}^{N}(1-p^i z_{ik})$ can be seen as the product of the terms $1-p^i z_{ik}$ of the individuals numbered from 1 to $j-1$, multiplied by the product of the terms $1-p^i z_{ik}$ of the individuals numbered from j to N.

As such, using *sequential quadratization in polynomial optimization* (Anthony *et al.*, 2017; Elloumi & Verchère, 2023), let us introduce the continuous variable h_{jk} which computes the term $\prod_{i=1}^{j}(1-p^i z_{ik})$ for the group G_k. Note that $h_{jk} = h_{j-1,k}(1-p_j)z_{jk} = h_{j-1,k} - p_j h_{j-1,k} z_{jk}$ as a consequence of (2.24). Let us introduce the continuous variable $f^k_{i-1,i} = h_{i-1,k} z_{ik}$ for each $i \in \mathcal{I}\setminus\{1\}$.

$$f^k_{i-1,i} \le h_{i-1,k} \quad \forall k \in \mathcal{G}, \forall i \in \mathcal{I}\setminus\{1\} \tag{2.25}$$

$$f^k_{i-1,i} \le z_{ik} \quad \forall k \in \mathcal{G}, \forall i \in \mathcal{I}\setminus\{1\} \tag{2.26}$$

$$f^k_{i-1,i} \ge h_{i-1,k} - (1-z_{ik}) \quad \forall k \in \mathcal{G}, \forall i \in \mathcal{I}\setminus\{1\} \tag{2.27}$$

$$f^k_{i-1,i} \in [0,1] \quad \forall k \in \mathcal{G}, \forall i \in \mathcal{I}\setminus\{1\} \tag{2.28}$$

Consequently, and because variables$h$ are bounded by 1, we have the following con-

straints to compute h_{jk}.

$$h_{1k} = 1 - p^1 z_{1k} \tag{2.29}$$
$$h_{jk} = h_{j-1,k} - p^j f^k_{j,j-1} \quad \forall j \in \mathcal{I} \setminus \{1\} \tag{2.30}$$
$$h_{jk} \in [0,1] \quad \forall i \in \mathcal{I} \tag{2.31}$$

And in the objective function, we substitute $\prod_{i\in\mathcal{I}}(1-p^i z_{ik})$ by h_{Nk}. The formulation becomes then:

$$\begin{aligned}[\mathrm{F}^2_{\mathrm{MINLP}}]\ \min & \sum_{k\in\mathcal{G}} Q \sum_{i\in\mathcal{I}} (1-p^i) z_{ik} - R h_{Nk} \\ & + \sum_{k\in\mathcal{G}} U \sum_{l\in\mathcal{G}, l>k} \Big(\sum_{i\in\mathcal{I}} z_{ik} z_{il} h_{Nk} \frac{h_{Nl}}{1-p^i}\Big) \\ \text{s.t.} & (2.20) - (2.23) \\ & (2.25) - (2.28) \\ & (2.29) - (2.31)\end{aligned} \tag{2.32}$$

Because the objective function of $\mathrm{F}^2_{\mathrm{MINLP}}$ is still nonlinear in the term $z_{ik}z_{il}h_{Nk}h_{Nl}$ of degree 4 in (2.32), we first introduce the binary variables Z and H as $Z_{ikl} = z_{ik}z_{il}$ and $H_{Nkil} = Z_{ikl}h_{Nk}$, $\forall i \in \mathcal{I}, \forall k, l \in \mathcal{G}, l > k$. We then rewrite this nonlinear term as follows.

$$\begin{aligned}\sum_{l\in\mathcal{G}, l>k} \Big(\sum_{i\in\mathcal{I}} z_{ik} z_{il}\Big) h_{Nk} &= \sum_{l\in\mathcal{G}, l>k} \sum_{i\in\mathcal{I}} Z_{ikl} h_{Nk} \\ &= \sum_{l\in\mathcal{G}, l>k} \sum_{i\in\mathcal{I}} H_{Nkil}\end{aligned} \tag{2.33}$$

We add the following linearization constraints to the model.

$$Z_{ikl} \le z_{ik} \quad \forall i \in \mathcal{I}, \forall k, l \in \mathcal{G}, l > k \tag{2.34}$$
$$Z_{ikl} \le z_{il} \quad \forall i \in \mathcal{I}, \forall k, l \in \mathcal{G}, l > k \tag{2.35}$$
$$Z_{ikl} \ge z_{ik} + z_{il} - 1 \quad \forall i \in \mathcal{I}, \forall k, l \in \mathcal{G}, l > k \tag{2.36}$$
$$H_{Nkil} \le Z_{ikl} \quad \forall i \in \mathcal{I}, \forall k, l \in \mathcal{G}, l > k \tag{2.37}$$
$$H_{Nkil} \le h_{Nk} \quad \forall i \in \mathcal{I}, \forall k, l \in \mathcal{G}, l > k \tag{2.38}$$
$$H_{Nkil} \ge h_{Nk} - (1 - Z_{ikl}) \quad \forall i \in \mathcal{I}, \forall k, l \in \mathcal{G}, l > k \tag{2.39}$$
$$Z_{ikl} \in \{0,1\} \quad \forall i \in \mathcal{I}, \forall k, l \in \mathcal{G}, l > k \tag{2.40}$$
$$H_{Nkil} \in [0,1] \quad \forall i \in \mathcal{I}, \forall k, l \in \mathcal{G}, l > k \tag{2.41}$$

The resulting MIQP (Mixed Integer Quadratic Program) formulation $\mathrm{F}^3_{\mathrm{MINLP}}$ with $\mathcal{O}(NG^2)$ variables and $\mathcal{O}(NG^2)$ constraints. Constraints (2.21) are linearized by introducing variables Z, yielding the linear constraints (2.43).

$$
\begin{aligned}
[\mathrm{F}^3_{\mathrm{MINLP}}] \min & \sum_{k\in\mathcal{G}} Q \sum_{i\in\mathcal{I}} (1-p^i) z_{ik} - R h_{Nk} \\
& + \sum_{k\in\mathcal{G}} U \sum_{l\in\mathcal{G}, l>k} \sum_{i\in\mathcal{I}} H_{Nkil} \frac{h_{Nl}}{1-p^i} && (2.42) \\
\text{s.t.} & (2.20), (2.22) - (2.23) \\
& \sum_{i\in\mathcal{I}} Z_{ikl} \leq 1 \quad \forall k, l \in \mathcal{G}, l > k && (2.43) \\
& (2.25) - (2.28) \\
& (2.29) - (2.31) \\
& (2.34) - (2.41)
\end{aligned}
$$

2.3.2 Strengthening $\mathrm{F}^3_{\mathrm{MINLP}}$ with Symmetry Breaking Constraints

The issue of symmetries is prevalent in our group testing problem, where any feasible solution to our model can be rearranged group-wise without altering the solution's efficacy. For instance, consider a feasible solution S comprising groups $G_1 = \{1, 2, 3\}$ and $G_2 = \{4, 5, 6\}$. An equivalent solution that yields the same objective value can be achieved by simply swapping the group assignments, resulting in $G_1 = \{4, 5, 6\}$ and $G_2 = \{1, 2, 3\}$. It is well-known that the resolution efficiency of mathematical models is negatively impacted from the presence of symmetries. In order to tackle this issue in our formulation, we implement lexicographic ordering constraints (Kiziltan, 2004) for the groups, ensuring a systematic and unique representation of each feasible solution. In the following, we present the lexicographic ordering constraints developed for our formulation.

First, let us introduce auxiliary variables v and associated constraints to compute the individual with the least prevalence in each group. The variable v_{ik} is defined as:

$$
v_{ik} = \begin{cases} 1, & \text{if individual } i \text{ is the individual with the least prevalence in group } G_k,\ k \in \mathcal{G} \\ 0, & \text{otherwise} \end{cases}
$$

We define the following constraints to incorporate this criterion into the model $\mathrm{F}^3_{\mathrm{MINLP}}$:

$$\sum_{i=1}^{N} v_{ik} = 1 \quad \forall k \in \mathcal{G} \tag{2.44}$$

$$v_{ik} \leq z_{ik} \quad \forall i \in \mathcal{I}, \forall k \in \mathcal{G} \tag{2.45}$$

$$z_{jk} \leq (1 - v_{ik}) \quad \forall i, j \in \mathcal{I}, p^i > p^j \text{ or } (i > j \text{ and } p^i = p^j), \forall k \in \mathcal{G} \tag{2.46}$$

$$v_{ik} + v_{j,k+1} \leq 1 \quad \forall k \in \mathcal{G}, \forall i, j \in \mathcal{I}, p^i > p^j \text{ or } (i > j \text{ and } p^i = p^j) \tag{2.47}$$

$$v_{ik} \in \{0, 1\} \quad \forall i \in \mathcal{I}, \forall k \in \mathcal{G} \tag{2.48}$$

Constraints (2.44) ensure that within every group k, there is exactly one individual identified as having the least prevalence. Constraints (2.45) link v_{ik} with z_{ik} ensuring v_{ik} can only be set to 1 if i is indeed a member of group k. Constraints (2.46) prevent any individual with a higher risk prevalence from being considered the least prevalence individual in group k if v_{ik} is set to 1. Constraints (2.47) impose lexicographical ordering between groups by ordering increasingly their least prevalence individuals. Ties are broken with the individual of the least index when individuals i and j have equal prevalences. Finally, the binary nature of v_{ik} is specified in constraints (2.48). For the rest of the paper, let $\mathrm{F}^{\mathrm{SYM}}_{\mathrm{MINLP}}$ be the strengthened formulation with the symmetry breaking constraints (2.44)-(2.48) of formulation $\mathrm{F}^{3}_{\mathrm{MINLP}}$.

2.3.3 An Extended Formulation

The formulations presented in the previous section were featuring a polynomial number of variables. However the problem under study can also be formulated by means of an exponential number of variables. The idea behind our extended reformulation is to search among all the possible groups of L individuals, the ones that satisfy the conditions ((i)-(iii)) (cf. Section 2.1) and minimize the overall expected number of false positives.

Let $\mathcal{K}$ be the set defined as $\mathcal{K} = \{1, \ldots, |\mathcal{K}| = \frac{N!}{L!(N-L)!}\}$ to be the index set of all the feasible groups i.e. all the possible groups of size L. Note that the cardinality of $\mathcal{K}$ increases exponentially. We define the set $\mathcal{K}_i$ to be the set of all feasible groups containing the individual i.

For a given group G_k, let $C_k = \mathbb{E}[FP(G_k)]$ denotes the cost of G_k, representing its contribution to the objective function due to the selection of G_k. Similarly, let $D_{kl} = \mathbb{E}[FP((G_k, G_l))]$ denotes the interaction cost between a pair of groups G_k and G_l such that $G_k \cap G_l = \{i\}$.

In our extended formulation, we use binary variables y_k, $k \in \mathcal{K}$ with $y_k = 1$ indicating that group G_k is selected in the solution, and $y_k = 0$ otherwise. Also note that, D_{kl} is only defined if groups G_k and G_l exactly have one individual in common. This leads us to define the set $\mathcal{P}(\mathcal{K}) = \{(k, l) : k, l \in \mathcal{K}, l > k : |G_k \cap G_l| = 1\}$ representing the set of pairs of groups having exactly one individual in common. For sake of simplicity, the

overall notation is summarized in Table 2.3.

Table 2.3: Notation for the extended formulation.

Sets	$\mathcal{K}$	the set of all feasible groups having L individuals
	$\mathcal{K}_i$	the set of all feasible groups having L individuals and containing the individual i
	$\mathcal{P}(\mathcal{K})$	$= \{(k,l) : k,l \in \mathcal{K}, l > k : \lvert G_k \cap G_l \rvert = 1\}$ being the set of pairs of groups having exactly one individual in common.
Variables		$y_k = \begin{cases} 1, & \text{if group } G_k \text{ is selected, } k \in \mathcal{K} \\ 0, & \text{otherwise} \end{cases}$
Parameters	C_k	the contribution of group G_k to the overall cost of S
	D_{kl}	the contribution of the pair intersecting groups (G_k, G_l) to the overall cost of S

We present the extended formulation below.

$$[\mathrm{F}^{\mathrm{EXT}}_{\mathrm{MINLP}}] \quad \min \sum_{k \in \mathcal{K}} C_k y_k + \sum_{(k,l) \in \mathcal{P}(\mathcal{K})} D_{kl} y_k y_l \tag{2.49}$$

$$\text{s.t.} \sum_{k \in \mathcal{K}_i} y_k = 2 \qquad \forall i \in \mathcal{I} \tag{2.50}$$

$$\sum_{k \in \mathcal{K}_i \cap \mathcal{K}_j} y_k \leq 1 \qquad \forall i, j \in \mathcal{I}, j > i \tag{2.51}$$

$$y_k \in \{0,1\} \qquad \forall k \in \mathcal{K} \tag{2.52}$$

The objective function (2.49) minimizes the overall misclassification error. Constraints (2.50) impose that each individual belongs to exactly two groups. Constraints (2.51) impose that each pair of individuals belongs together to at most one group. And finally, constraints (2.52) are the integrality constraints for variables y. This formulation allows us to translate the nonlinearity of the objective function (2.19) into known costs of groups.

2.4 Heuristics

In this section, we introduce first algorithms for generating feasible solutions (Section 2.4.1) and then discuss local search methods based on moves that swap individuals in different groups. There are two local search approaches - one is algorithmic explained in Section 2.4.2, and the other is based on the resolution of a mathematical model presented

in Section 2.4.3. We also present in Section 2.4.4 two heuristics from the literature known for their efficiency in the case where $L = \sqrt{N}$. Inspired by these two heuristics, we have designed three variants of our heuristics with preassigned groups as presented in Section 2.4.5. For our experiments, we do retain the five heuristics to copare their efficiencies.

2.4.1 Construction Heuristic

The construction heuristic, denoted as $\mathcal{H}_C$, is the construction algorithm described in the proof of Proposition 2.2. $\mathcal{H}_C$ proceeds according to the value of L and hence the value of $G = \frac{2N}{L}$ whether $G = 2L$, $G > 2L$ or $G < 2L$. It is worth mentioning that a feasible solution can also be obtained by solving $\mathrm{F}^1_{\mathrm{MINLP}}$ while replacing the objective function (2.19) with a constant value.

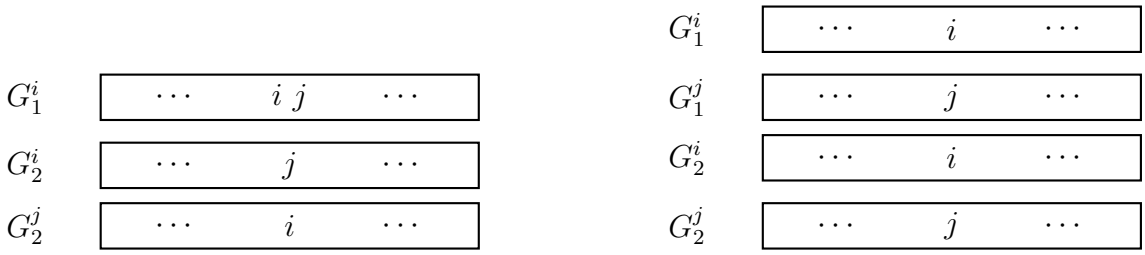
2.4.2 Swap-based Local Search

Let us first point out that for a given pair of individuals (i, j) in a feasible solution, there are two cases to consider: (i, j) belong together to one group and are not together in two other groups (cf. case 2.7a in Figure 2.7), or (i, j) do not belong together to any group (cf. case 2.7b in Figure 2.7). Let G^i_1 and G^i_2 be the two groups where i belongs, and G^j_1 and G^j_2 be the two groups where j belongs. In the first case, let us assume without loss of generality that $G^i_1 = G^j_1$. Then, we evaluate swapping i and j in the two groups where they do not belong together, G^i_2 and G^j_2. In the second case, we evaluate each of the following four possible swaps:

1. Swap i in group G^i_1 with j in group G^j_1.
2. Swap i in group G^i_1 with j in group G^j_2.
3. Swap i in group G^i_2 with j in group G^j_1.
4. Swap i in group G^i_2 with j in group G^j_2.

For any swap possibility, if the move leads to an infeasible solution or does not improve the cost, the move is not performed. Otherwise, the move is performed and the current solution is updated.

Each possible swap is evaluated, and only improving moves that preserve feasibility are considered. Among these, the best improving swap is selected and applied at each iteration. This process is repeated until no further improving swap can be found or the time limit is exceeded. The pairwise swap-based local search, denoted as $\mathcal{LS}_{PS}$, is detailed in Algorithm 1.



(a) Case with three groups.

(b) Case with four groups.

Figure 2.7: Illustration of the different configurations for individuals i and j.

Algorithm 1 Pairwise Swap-Based Local Search $\mathcal{LS}_{PS}$

Input: A feasible solution S

Output: Improvement of S if possible

while there exists a swap that improves S or time limit not exceeded **do**
  for each pair of individuals (i, j) with $i \neq j$ **do**
    Let G_1^i, G_2^i be the groups containing i and G_1^j, G_2^j be the groups containing j
    if i, j belong together in one group **then**
      Identify the two groups where i and j are not together
      Evaluate the swap of i and j in these two groups
    else
      Evaluate all four possible swaps of i and j across $G_1^i, G_2^i, G_1^j, G_2^j$
    end if
  end for
  Apply the best improving swap to S
end while
return S

2.4.3 Iterative Ejection Cycles Local Search

The iterative ejection cycles local search, denoted as $\mathcal{LS}_{IEC}$, is designed to iteratively improve an initial solution by solving a series of mixed-integer nonlinear programs that identify, at each iteration, the best moves. A move in this local search method is defined as an ejection chain (Glover, 1996), which was originally applied to the Traveling Salesman Problem (TSP) and is also well-known for Vehicle Routing Problems (VRP). In our context, an ejection chain involves removing an individual i from group G_k and replacing it by individual $j \neq i$ from group $G_l, l \neq k$, which subsequently forces individual i to be inserted elsewhere, thus creating a sequence of replacements. In our specific implementation, the ejection chains always result in cycles, as each group is of size L. This means that every individual ejected must be replaced by another individual. We impose that each group can have no more than one individual replaced in an ejection cycle. Figure 2.8 illustrates two ejection cycles for a feasible solution with $N = 9$ and

$L = 3$. The arrows indicate the sequence of individual replacements, demonstrating the cyclic nature of the ejections. The procedure, as described in Algorithm 2, starts with an initial feasible solution S, consisting of G groups, each containing L individuals. The solution is updated with these optimal moves, and the process is repeated until no further improvement is possible or a predefined termination condition is met.



(a) Two ejection cycles. (b) Result.

Figure 2.8: Two ejection cycles in a feasible solution with $N = 9$ and $L = 3$.

Algorithm 2 Iterative Ejection Cycles Local Search $\mathcal{LS}_{IEC}$.

Input: Initial feasible solution S
Output: Improvement of S if possible

1: **Repeat:**
2: Solve the $\mathrm{F}^{\mathrm{LS2}}_{\mathrm{MINLP}}$ model to find the best ejection cycles, with a maximum of one replacement per group.
3: Update the solution S with the identified best moves.
4: **Until:** No improvement is found or a termination condition (e.g., time limit, number of iterations) is met.
5: **return** S

The details of the $\mathrm{F}^{\mathrm{LS1}}_{\mathrm{MINLP}}$ model are provided below.

Let $S = \{G_1, G_2, \ldots, G_G\}$ be a feasible solution with G groups each of size L. We can perform a local search based on moves that can be decided optimally thanks to the following integer non linear programming model $\mathrm{F}^{\mathrm{LS1}}_{\mathrm{MINLP}}$.

Let a_{ik} be a binary parameter that equals 1 if individual i is in group k in the initial solution S, 0 otherwise. We define the set of eligible individuals j that can replace individual i in group k by $\mathrm{E}(i,k)$. For each group G_k where i is present, $\mathrm{E}(i,k)$ excludes any individual j that is already present in the same group G_k or has the same prevalence as individual i. Based on this definition, we only define the decision variables x^k_{ij} for $j \in \mathrm{E}(i,k)$ and for groups G_k where individual i is initially present. This ensures that the variable x^k_{ij} only considers valid and meaningful moves, thus reducing the problem size.

$$x_{ij}^k = \begin{cases} 1, & \text{if individual } j \text{ replaces individual } i \text{ in group } G_k, \forall i \in \mathcal{I}, \forall k \in \mathcal{G}, \forall j \in \mathrm{E}(i,k) \\ 0, & \text{otherwise} \end{cases}$$

We reuse decision variables z_{ik} defined for formulation $\mathrm{F}^1_{\mathrm{MINLP}}$.

Define σ_k as the sum of $(1-p^i)z_{ik}$ and π_k as the product of $(1-p^i z_{ik})$, where π_k and σ_k are positive continuous variables. They are computed as functions of a_{ik} and x_{ij}^k as follows.

$$\begin{aligned} \sigma_k &= \sum_{i\in\mathcal{I}}(1-p^i)z_{ik}, \quad \forall k \in \mathcal{G} \\ &= \sum_{i\in\mathcal{I}}(1-p^i)a_{ik} + \sum_{i\in\mathcal{I}}\sum_{j\in\mathrm{E}(i,k)}((1-p^j)-(1-p^i))x_{ij}^k, \quad \forall k \in \mathcal{G} \end{aligned}$$

$$\begin{aligned} \pi_k &= \prod_{i\in\mathcal{I}}(1-p^i z_{ik}), \quad \forall k \in \mathcal{G} \\ &= \prod_{i\in\mathcal{I}}(1-p^i a_{ik})(1+(\sum_{i\in\mathcal{I}}\sum_{j\in\mathrm{E}(i,k)}(\frac{1-p^j}{1-p^i}-1)x_{ij}^k)), \quad \forall k \in \mathcal{G} \end{aligned}$$

The objective function (2.69) minimizes the expected number of false positives. Constraints (2.54) ensure that at most one replacement occurs in each group k. Constraints (2.55) guarantee consistency in the replacements. Specifically, they ensure that if individual i is ejected from a group G_k, it is inserted into another group G_l to replace an individual $j \in G_l$. Constraints (2.56) enforce that each individual appears in exactly two groups. This is a requirement for the initial and final feasible solutions. Constraints (2.57) ensure that each pair of groups intersects in at most one individual. Constraints (2.58) specify that each group must contain exactly L individuals. Constraints (2.59) link the variables x_{ij}^k and z_{ik} with the initial solution through a_{ik}. They ensure that if an individual i is in group G_k in the initial solution and ejected (indicated by x_{ij}^k), this is accurately reflected in the variable z_{ik}, and similarly for when an individual i is inserted in a group G_k. Constraints (2.60) and (2.61) compute the values of σ_k and π_k as functions of the parameters a_{ik} representing the initial solution and the decision variables x_{ijk}. Constraints (2.62) and (2.63) define the binary nature of the decision variables x_{ij}^k and z_{ik}, respectively. Constraints (2.64) define the continuous nature of variables σ_k and π_k.

$$[\mathrm{F}^{\mathrm{LS1}}_{\mathrm{MINLP}}]\ \min \sum_{k\in\mathcal{G}} Q\sigma_k - R\pi_k + \sum_{k\in\mathcal{G}} U \sum_{l\in\mathcal{G},l>k} \sum_{i\in\mathcal{I}} z_{ik}z_{il}\pi_k \frac{\pi_l}{1-p^i} \tag{2.53}$$

$$\text{s.t.} \sum_{i\in\mathcal{I}} \sum_{j\in\mathrm{E}(i,k)} x^k_{ij} \le 1 \quad \forall k \in \mathcal{G} \tag{2.54}$$

$$\sum_{k\in\mathcal{G}} \sum_{j\in\mathrm{E}(i,k)} x^k_{ij} = \sum_{k\in\mathcal{G}} \sum_{j:a_{jk}=1, i\in\mathrm{E}(j,k)} x^k_{ji} \quad \forall i \in \mathcal{I} \tag{2.55}$$

$$\sum_{k\in\mathcal{G}} z_{ik} = 2 \quad \forall i \in \mathcal{I} \tag{2.56}$$

$$\sum_{i\in\mathcal{I}} z_{ik}z_{il} \le 1 \quad \forall k,l \in \mathcal{G}, l > k \tag{2.57}$$

$$\sum_{i\in\mathcal{I}} z_{ik} = L \quad \forall k \in \mathcal{G} \tag{2.58}$$

$$z_{ik} = a_{ik} - \sum_{j\in\mathrm{E}(i,k)} x^k_{ij} + \sum_{j:a_{jk}=1, i\in\mathrm{E}(j,k)} x^k_{ji} \quad \forall i \in \mathcal{I}, \forall k \in \mathcal{G} \tag{2.59}$$

$$\sigma_k = \sum_{i\in\mathcal{I}} (1-p^i)a_{ik} + \sum_{i\in\mathcal{I}} \sum_{j\in\mathrm{E}(i,k)} ((1-p^j)-(1-p^i))x^k_{ij} \quad \forall k \in \mathcal{G} \tag{2.60}$$

$$\pi_k = \prod_{i\in\mathcal{I}} (1-p^i a_{ik})(1 + (\sum_{i\in\mathcal{I}} \sum_{j\in\mathrm{E}(i,k)} (\frac{1-p^j}{1-p^i} - 1)x^k_{ij})) \quad \forall k \in \mathcal{G} \tag{2.61}$$

$$x^k_{ij} \in \{0,1\} \quad \forall i \in \mathcal{I}, \forall k \in \mathcal{G}, \forall j \in \mathrm{E}(i,k) \tag{2.62}$$

$$z_{ik} \in \{0,1\} \quad \forall i \in \mathcal{I}, \forall k \in \mathcal{G} \tag{2.63}$$

$$\sigma_k, \pi_k \ge 0 \quad \forall k \in \mathcal{G} \tag{2.64}$$

To linearize the term $z_{ik}z_{il}\pi_k$ in (2.69), we reuse auxiliaury variables Z_{ikl} in formulation $\mathrm{F}^3_{\mathrm{MINLP}}$ and corresponding linearization constraints ((2.34)-(2.40)) to linearize the product $z_{ik}z_{il}$. Then we linearize the product $Z_{ikl}\pi_k$ as follows. Let $\omega_{ikl} = Z_{ikl}\pi_k$ be a positive continuous variable. We add the following linearization constraints.

$$\omega_{ikl} \le Z_{ikl} \quad \forall i \in \mathcal{I}, \forall k,l \in \mathcal{G}, l > k \tag{2.65}$$

$$\omega_{ikl} \le \pi_k \quad \forall i \in \mathcal{I}, \forall k,l \in \mathcal{G}, l > k \tag{2.66}$$

$$\omega_{ikl} \ge \pi_k - (1 - Z_{ikl}) \quad \forall i \in \mathcal{I}, \forall k,l \in \mathcal{G}, l > k \tag{2.67}$$

$$\omega_{ikl} \ge 0 \quad \forall i \in \mathcal{I}, \forall k,l \in \mathcal{G}, l > k \tag{2.68}$$

Consequently, we obtain the following formulation$\mathrm{F}^{\mathrm{LS2}}_{\mathrm{MINLP}}$.

$$[\mathrm{F}^{\mathrm{LS2}}_{\mathrm{MINLP}}] \min \sum_{k\in\mathcal{G}} Q\sigma_k - R\pi_k + U \sum_{k\in\mathcal{G}} \sum_{l\in\mathcal{G},l>k} \sum_{i\in\mathcal{I}} \omega_{ikl} \frac{\pi_l}{1-p^i} \tag{2.69}$$

$$\text{s.t.} (2.54) - (2.56), (2.58) - (2.64)$$

$$\sum_{i\in\mathcal{I}} Z_{ikl} \leq 1 \quad \forall k, l \in \mathcal{G}, l > k \tag{2.70}$$

$$(2.34) - (2.40)$$

$$(2.65) - (2.68)$$

2.4.4 Gradient Design and Spiral Design from McMahan *et al.* (2012b) for Square Matrix-based Group Testing

Two heuristic approaches, namely the gradient and spiral designs, have been proposed in McMahan *et al.* (2012b) for organizing individuals in matrix-based group testing, particularly effective in settings where the population is heterogeneous.

Gradient Design

The gradient design arranges individuals within a matrix based on their risk probabilities, placing the highest-risk individual in the top-left cell and filling the matrix column by column. This design aims to localize high-risk individuals within specific columns, potentially reducing the number of positive test outcomes in low prevalence settings. Specifically, this configuration makes individuals with the lowest prevalences together in one group and the individuals with the highest prevalences together in one group.

Spiral Design

In contrast, the spiral design starts with the highest-risk individual at the top-left corner and positions subsequent individuals in a spiral pattern outward. This method seeks to isolate the individuals with the highest prevalences within a confined sub-matrix, allowing most of the matrix's rows and columns to test negative,

Evaluation and Applicability

In matrix group testing, as described in McMahan *et al.* (2012b), both designs appear to have the potential to be effective in reducing the expected number of tests. These heuristics are specific to settings that utilize the matrix format, and because of their ease of use, they might be useful in real-world applications. Still, as stated in McMahan *et al.* (2012b), the authors acknowledge that their heuristic methods, gradient and spiral designs, are not demonstrated to be optimal across all permutations and possible arrangements of individuals within the matrix. Furthermore, for a fixed value of N, these two heuristics

do not hold for all eligible values of group size L for the studied two-dimensional group testing with equal group size. Our design may utilize them exclusively when $L = \sqrt{N}$ is an integer.

2.4.5 Three Variants of The Construction Heuristic

In the context of our optimization problem, we have developed three variants of $\mathcal{H}_C$ with the goal of efficiently grouping individuals based on their prevalences. Upon analyzing the **GRADIENT** heuristic, which is known for its efficiency as discussed in McMahan *et al.* (2012b), we observed that this heuristic places the L individuals with the lowest prevalence values together, as well as the L individuals with the highest prevalence values. The three variants are designed as follows:

1. **LEAST**: This variant focuses on grouping the L individuals with the lowest prevalence values.
2. **HIGHEST**: In contrast to **LEAST**, this variant prioritizes the grouping of the L individuals with the highest prevalence values.
3. **BOTH**: The **BOTH** heuristic integrates aspects from both the **LEAST** and **HIGHEST** strategies. Initially, it groups the L individuals with the lowest prevalences, followed by the L individuals with the highest prevalences. It is important to note that the **BOTH** heuristic does not apply when the number of resulting groups G equals $L + 1$. Since the L individuals with the lowest prevalences are grouped together in one group, say G_1, each of these individuals will belong exclusively to one of the following L groups, G_g, where $g \in \{2, \cdots, L + 1\}$. Therefore, the L individuals with the highest prevalence values cannot all be grouped together.

In all three variants, we begin by grouping the corresponding individuals and then complete the solution by assigning the remaining individuals to the remaining groups thanks to an adaptation of the algorithm $\mathcal{H}_C$ or by a priori fixing the corresponding decision variables z_{ik} to the value 1 in (2.19)-(2.23) and solving the resulting feasibility model with an objective function of 0 for example.

All three resulting solutions, **BOTH** when applicable, undergo local search, $\mathcal{LS}_{PS}$ or $\mathcal{LS}_{IEC}$, for improvement without modifying the prefixed groups.

2.5 Computational Experiments

The computational experiments are designed to evaluate the performance of the five heuristics and the resolution of the three formulations in solving the problem under study. The heuristics are first applied to generate initial solutions, which are then refined using $\mathcal{LS}_{IEC}$ local search procedure. The best solution obtained from the heuristics,

after potential improvement by $\mathcal{LS}_{IEC}$ local search, is used to warm start the three mathematical formulations of the problem, which are solved using the commercial solver Gurobi. If a formulation is not solved to optimality within the given time limit, its best incumbent solution undergoes further refinement using the $\mathcal{LS}_{IEC}$ local search. The best solution across all formulations and heuristics is identified as the best-known solution for each instance, against which the performance of all heuristics is compared.

We developed our algorithms using C++ and compiled them in release mode using the 64-bit version of MS Visual Studio 2022. We solve all formulations using Gurobi 11.0.2 build v11.0.2rc0 (64-bit version). All tests were conducted on a 64-bit Windows system powered by an Intel(R) Xeon(R) Silver 4214 processor, which features 24 cores hyper-threaded to 48 virtual cores, operates at a base clock frequency of 2.2 GHz, and is equipped with 96 GB of RAM.

In this section, we first describe the instance generation. Subsequently, Section 2.5.2 compares the performance of the pairwise swap-based local search $\mathcal{LS}_{PS}$ (cf. Algorithm 1) to iterative ejection cycle based local search $\mathcal{LS}_{IEC}$ (cf. Algorithm 2). Next, we assess the effectiveness of the heuristics methods previously described in Section 2.4 in comparison to the best incumbent found by solving the three formulations. Lastly, we solve the three formulations –$\mathrm{F}^{3}_{\mathrm{MINLP}}$, $\mathrm{F}^{\mathrm{SYM}}_{\mathrm{MINLP}}$, and $\mathrm{F}^{\mathrm{EXT}}_{\mathrm{MINLP}}$– and analyze their performance.

2.5.1 Instance Generation

In order to assess the performance of our proposed method, we generate a set of random instances. Each instance consists of a number of individuals N, ranging from 6 to 12 for which the group size $L > 2$, i.e. $N \in \{6, 9, 10, 12\}$. To introduce a maximal heterogeneity in the instances, we assigned a unique prevalence value to each individual, uniformly sampled in the interval $[0.001; 0.2]$. We chose to have N distinct prevalences among the individuals in each instance so as to avoid the symmetry between individuals having the same prevalence. For each instance size N, we generated five distinct instances of risk vector values $\mathbf{p}$. Table 2.4 summarizes the properties of the instances where N denotes the number of the individuals, `# risk vector` denotes the number of risk vector values considered, `Possible group sizes (`L`)` are the eligible group sizes, Se and Sp are the values of sensitivity and specificity of the test. Finally, `Min. Prevalence` and `Max. Prevalence` are respectively the minimum value and the maximum value of the prevalences among the five risk vectors of each value of N.

Table 2.4: Characteristics of the instances including sensitivity and specificity.

N	# risk vectors	Possible group sizes (L)	Se	Sp	Min. Prevalence	Max. Prevalence
6	5	3	0.90, 0.95, 0.99	0.90, 0.95, 0.99	0.011	0.194
9	5	3	0.90, 0.95, 0.99	0.90, 0.95, 0.99	0.002	0.195
10	5	4	0.90, 0.95, 0.99	0.90, 0.95, 0.99	0.012	0.198
12	5	3, 4	0.90, 0.95, 0.99	0.90, 0.95, 0.99	0.002	0.192

2.5.2 Local Search: Comparison of $\mathcal{LS}_{IEC}$ to $\mathcal{LS}_{PS}$

In this section, we compare the performance of local search $\mathcal{LS}_{IEC}$ to local search $\mathcal{LS}_{PS}$. The evaluation is based on two key metrics: the relative gap and the improvement ratio.

The `relative gap` is defined as:

$$\text{relative gap} = \left(\frac{\text{heuristic value} - \text{best known solution}}{\text{best known solution}} \right) \times 100 \tag{2.71}$$

This metric quantifies how close the heuristic solution is to the best-known solution, with a lower relative gap indicating a higher quality solution.

The `improvement ratio` measures the improvement of the heuristic solution over the initial solution, relative to the potential improvement. It is defined as:

$$\text{improvement ratio} = \left(\frac{\text{initial value} - \text{heuristic value}}{\text{initial value} - \text{best known solution}} \right) \times 100 \tag{2.72}$$

This metric reflects the percentage of the total possible improvement achieved by the heuristic, providing insight into the effectiveness of the local search procedure.

The results in Table 2.5 demonstrate that both local searches, $\mathcal{LS}_{PS}$ and $\mathcal{LS}_{IEC}$, perform well on both relative gap and improvement ratio criteria, with $\mathcal{LS}_{IEC}$ consistently outperforming $\mathcal{LS}_{PS}$ in all cases. $\mathcal{LS}_{IEC}$ yields solutions that are closer to the best-known solution, highlighting its superior optimization capabilities. This performance advantage motivates the choice of $\mathcal{LS}_{IEC}$ for solution improvement in this study. However, we perform further investigation on the execution time so as to define an appropriate stopping criteria of $\mathcal{LS}_{IEC}$. In the following, we present, in average, the characteristics of the execution time of $\mathcal{LS}_{IEC}$ through Tables 2.7 and 2.8. For sake of simplicity, let the definition of headings in Tables 2.7 and 2.8 be summarized in Table 2.6.

Table 2.5: Average relative gaps and improvement ratios of $\mathcal{LS}_{PS}$ and $\mathcal{LS}_{IEC}$ by (Se, Sp, N) for each heuristic.

Se	Sp	N	LEAST				HIGHEST				BOTH			
			Rel. Gap (%)		Improv. Ratio (%)		Rel. Gap (%)		Improv. Ratio (%)		Rel. Gap (%)		Improv. Ratio (%)	
			$\mathcal{LS}_{PS}$	$\mathcal{LS}_{IEC}$	$\mathcal{LS}_{PS}$	$\mathcal{LS}_{IEC}$	$\mathcal{LS}_{PS}$	$\mathcal{LS}_{IEC}$	$\mathcal{LS}_{PS}$	$\mathcal{LS}_{IEC}$	$\mathcal{LS}_{PS}$	$\mathcal{LS}_{IEC}$	$\mathcal{LS}_{PS}$	$\mathcal{LS}_{IEC}$
0.9	0.9	6	0.00	0.00	59.99	59.99	0.15	0.15	50.64	50.64	-	-	-	-
		9	0.02	0.00	97.85	99.98	0.15	0.05	93.53	96.73	0.01	0.00	99.01	99.97
		10	0.00	0.00	99.85	99.95	1.15	0.00	59.60	99.99	-	-	-	-
		12	0.11	0.02	93.38	98.93	0.15	0.05	92.89	95.99	0.13	0.00	87.22	99.94
	0.95	6	0.00	0.00	60.00	60.00	0.22	0.14	50.64	53.36	-	-	-	-
		9	0.05	0.00	97.34	99.97	0.32	0.07	88.13	96.70	0.02	0.00	99.10	99.97
		10	0.00	0.00	99.85	99.95	1.56	0.00	59.54	99.99	-	-	-	-
		12	0.32	0.02	88.75	98.81	0.27	0.06	92.47	96.52	0.16	0.00	87.84	99.96
	0.99	6	0.00	0.00	59.99	59.99	0.32	0.32	50.63	50.63	-	-	-	-
		9	0.07	0.00	97.57	99.97	0.59	0.10	86.86	96.68	0.04	0.00	99.17	99.97
		10	0.00	0.00	99.86	99.96	2.07	0.00	59.49	99.99	-	-	-	-
		12	0.63	0.04	89.26	98.62	0.52	0.08	91.95	96.62	0.47	0.00	86.72	99.96
0.95	0.9	6	0.00	0.00	59.99	59.99	0.16	0.10	50.63	53.36	-	-	-	-
		9	0.02	0.00	97.86	99.96	0.15	0.05	93.52	96.72	0.02	0.00	99.01	99.96
		10	0.00	0.00	99.85	99.95	1.18	0.00	59.59	99.99	-	-	-	-
		12	0.11	0.02	93.32	98.85	0.16	0.05	92.90	96.25	0.13	0.00	87.26	99.95
	0.95	6	0.00	0.00	59.99	59.99	0.23	0.23	50.63	50.63	-	-	-	-
		9	0.05	0.00	97.36	99.97	0.32	0.07	88.12	96.70	0.02	0.00	99.11	99.97
		10	0.00	0.00	99.85	99.95	1.59	0.00	59.53	99.99	-	-	-	-
		12	0.33	0.02	88.78	98.81	0.28	0.06	92.45	96.57	0.16	0.00	87.84	99.96
	0.99	6	0.00	0.00	59.99	59.99	0.33	0.32	50.63	50.63	-	-	-	-
		9	0.07	0.00	97.58	99.98	0.59	0.10	86.86	96.68	0.03	0.00	99.18	99.98
		10	0.00	0.00	99.84	99.94	2.07	0.00	59.48	99.98	-	-	-	-
		12	0.64	0.05	89.27	98.48	0.53	0.09	91.95	96.43	0.47	0.00	86.71	99.95
0.99	0.9	6	0.00	0.00	59.99	59.99	0.16	0.16	50.64	50.64	-	-	-	-
		9	0.02	0.00	97.89	99.97	0.16	0.05	93.53	96.73	0.02	0.00	99.03	99.97
		10	0.00	0.00	99.85	99.94	1.21	0.00	59.59	99.98	-	-	-	-
		12	0.13	0.02	93.05	98.72	0.16	0.14	92.77	94.07	0.14	0.00	87.14	99.96
	0.95	6	0.00	0.00	60.00	60.00	0.23	0.15	50.64	53.36	-	-	-	-
		9	0.05	0.00	97.37	99.97	0.33	0.07	88.12	96.70	0.02	0.00	99.11	99.97
		10	0.00	0.00	99.85	99.95	1.61	0.00	59.53	99.99	-	-	-	-
		12	0.32	0.04	89.17	98.28	0.29	0.09	92.42	96.25	0.17	0.00	87.84	99.95
	0.99	6	0.00	0.00	59.99	59.99	0.33	0.32	50.63	50.63	-	-	-	-
		9	0.07	0.00	97.57	99.97	0.59	0.10	86.86	96.68	0.04	0.00	99.17	99.97
		10	0.00	0.00	99.86	99.96	2.08	0.43	59.49	91.24	-	-	-	-
		12	0.64	0.11	89.28	98.07	0.53	0.12	91.94	95.90	0.47	0.00	86.72	99.96

Table 2.6: Explanation of headings in Tables 2.7 and 2.8

Heading	Description
Avg. Time(s)	Average total time in seconds that $\mathcal{LS}_{IEC}$ took to complete for each instance.
Avg. #Iter.	Average number of iterations performed by $\mathcal{LS}_{IEC}$ before stopping.
Avg. Min. Iter. Time(s)	Average time in seconds of the fastest iteration within $\mathcal{LS}_{IEC}$.
Avg. Max. Iter. Time(s)	Average time in seconds of the slowest (maximum time) iteration within $\mathcal{LS}_{IEC}$.
Avg. FTOpt(s)	Time in seconds when the optimal solution was first found as an incumbent solution during solving $\mathrm{F}^{\mathrm{LS2}}_{\mathrm{MINLP}}$ in an iteration of $\mathcal{LS}_{IEC}$.
Avg. TCloseGap(s)	Average time in seconds required to close the gap starting from the first time where the optimal solution was found during solving $\mathrm{F}^{\mathrm{LS2}}_{\mathrm{MINLP}}$ in an iteration of $\mathcal{LS}_{IEC}$.
Avg. Iter. Time(s)	Average total time in seconds taken to solve $\mathrm{F}^{\mathrm{LS2}}_{\mathrm{MINLP}}$ to optimality in an iteration of $\mathcal{LS}_{IEC}$.

Table 2.7 highlights that the overall time generally does not exceed 16 seconds on average, except for instances with $N = 12$ and $L = 3$. Specifically, for these instances, the total time can reach nearly one hour on average. This observation suggests that the only configuration requiring significant computational time is when $N = 12$ and $L = 3$. This leads us to investigate the first time the optimal solution is found as an incumbent solution compared to the time required to close the gap. We can conclude that $\mathcal{LS}_{IEC}$ performs better in terms of runtime when there are fewer groups, even if these groups are larger in size. This is evident when comparing the algorithm's performance for $(N = 12, L = 4)$ with $(N = 12, L = 3)$, where the case with fewer, larger groups results in significantly faster execution.

Table 2.8 provides detailed insights into the timing of $\mathcal{LS}_{IEC}$, including the first time the optimal solution was found and the time required to close the gap. This analysis shows that significant improvements are often made within the first few iterations. Specifically, for $N = 12$ and $L = 3$, the optimal solution is typically found within one-third of the total time required to solve $\mathcal{LS}_{IEC}$ to optimality, averaging around 221 seconds, and generally requiring fewer than three iterations.

We also observe that the more groups present, the longer the algorithm tends to take. For instance, when comparing $N = 10$ to $N = 9$, the number of groups (G) appears to have a greater impact on time than the number of individuals (N). When $N = 9$ and $L = 3$, we have $G = 6$, whereas for $N = 10$ and $L = 4$, $G = 5$. Since at most one individual changes per group, this may explain the observed behavior. A similar pattern is noted when comparing $N = 12$ with $L = 4$ to $L = 3$. Furthermore, when the heuristic **BOTH** is applicable, the algorithm tends to converge faster because two groups are fixed, reducing combinatorial complexity and thus requiring less time compared to

Table 2.7: Aggregated characteristics of iterations in $\mathcal{LS}_{IEC}$ for each heuristic.

Se	*Sp*	*N*	*L*	**LEAST**				**HIGHEST**				**BOTH**			
				Avg. Time(s)	Avg. # Iter.	Avg. Min Iter. Time(s)	Avg. Max Iter. Time(s)	Avg. Time(s)	Avg. # Iter.	Avg. Min Iter. Time(s)	Avg. Max Iter. Time(s)	Avg. Time(s)	Avg. # Iter.	Avg. Min Iter. Time(s)	Avg. Max Iter. Time(s)
0.9	0.9	6	3	0.30	1.60	0.08	0.08	0.19	1.80	0.08	0.10	-	-	-	-
		9	3	3.83	2.60	1.27	1.53	3.73	2.60	1.30	1.53	0.65	2.40	0.24	0.28
		10	4	1.25	3.00	0.28	0.53	1.35	2.80	0.40	0.56	-	-	-	-
		12	3	2738.28	4.00	528.78	828.67	3489.13	4.00	633.49	1165.59	55.07	3.20	11.77	24.03
		12	4	14.74	4.00	2.44	5.21	11.05	4.00	2.40	3.48	3.33	4.00	0.23	1.64
	0.95	6	3	0.16	1.60	0.08	0.08	0.17	1.80	0.07	0.08	-	-	-	-
		9	3	3.78	2.60	1.35	1.54	3.86	2.60	1.34	1.57	0.67	2.40	0.26	0.27
		10	4	1.21	3.00	0.31	0.50	1.39	2.80	0.39	0.56	-	-	-	-
		12	3	1975.97	3.40	463.69	677.10	2824.59	3.40	563.19	1048.19	53.89	3.00	11.28	23.14
		12	4	14.50	3.60	2.90	5.05	11.62	4.00	2.55	3.53	3.70	3.60	0.52	1.64
	0.99	6	3	0.15	1.60	0.08	0.08	0.16	1.80	0.07	0.08	-	-	-	-
		9	3	3.64	2.60	1.24	1.52	3.73	2.60	1.34	1.46	0.68	2.40	0.25	0.29
		10	4	1.09	3.00	0.30	0.44	1.26	2.80	0.35	0.52	-	-	-	-
		12	3	1833.29	3.40	462.67	625.86	2550.44	3.40	533.31	903.21	54.58	3.00	11.76	24.19
		12	4	14.52	3.60	2.71	5.21	11.31	4.00	2.56	3.30	3.53	3.60	0.50	1.59
0.95	0.9	6	3	0.14	1.60	0.07	0.07	0.17	1.80	0.07	0.08	-	-	-	-
		9	3	3.76	2.60	1.29	1.55	3.67	2.60	1.26	1.55	0.69	2.40	0.25	0.29
		10	4	1.12	3.00	0.27	0.52	1.25	2.80	0.37	0.50	-	-	-	-
		12	3	2037.32	4.00	412.35	615.27	3024.15	4.00	458.63	1067.23	60.89	3.20	14.82	23.94
		12	4	15.31	3.80	2.89	5.35	11.76	4.00	2.56	3.61	3.65	3.80	0.53	1.65
	0.95	6	3	0.15	1.60	0.07	0.08	0.17	1.80	0.07	0.09	-	-	-	-
		9	3	3.61	2.60	1.23	1.50	3.68	2.60	1.28	1.50	0.66	2.40	0.25	0.28
		10	4	1.13	3.00	0.28	0.52	1.32	2.80	0.41	0.53	-	-	-	-
		12	3	1635.51	3.50	380.89	530.32	2420.64	3.25	544.94	909.37	55.19	3.00	13.14	22.76
		12	4	14.23	3.50	3.03	5.01	10.95	4.00	2.42	3.23	3.63	3.50	0.62	1.77
	0.99	6	3	0.14	1.60	0.07	0.08	0.16	1.80	0.07	0.08	-	-	-	-
		9	3	3.55	2.60	1.27	1.43	3.65	2.60	1.27	1.50	0.67	2.40	0.24	0.29
		10	4	1.11	3.00	0.29	0.46	1.34	2.80	0.43	0.52	-	-	-	-
		12	3	2782.10	3.75	369.63	1554.44	2100.36	3.25	372.25	784.13	50.92	3.00	10.35	23.99
		12	4	13.88	3.50	2.72	5.03	10.70	4.00	2.46	3.09	3.44	3.50	0.58	1.61
0.99	0.9	6	3	0.15	1.60	0.07	0.08	0.18	1.80	0.08	0.09	-	-	-	-
		9	3	3.73	2.60	1.31	1.55	3.79	2.60	1.35	1.57	0.67	2.40	0.25	0.29
		10	4	1.30	3.00	0.28	0.52	1.34	2.80	0.40	0.54	-	-	-	-
		12	3	1696.04	3.75	404.57	513.40	2740.44	4.00	497.22	956.71	52.63	3.25	9.87	24.69
		12	4	14.48	3.50	2.94	5.22	10.80	4.00	2.38	3.06	3.47	3.75	0.60	1.52
	0.95	6	3	0.16	1.60	0.09	0.09	0.15	1.80	0.07	0.08	-	-	-	-
		9	3	3.73	2.60	1.29	1.49	3.73	2.60	1.28	1.54	0.67	2.40	0.25	0.28
		10	4	1.14	3.00	0.27	0.49	1.33	2.80	0.41	0.50	-	-	-	-
		12	3	1471.70	3.50	344.04	483.71	2067.16	3.25	417.10	794.47	46.98	3.00	10.44	21.19
		12	4	14.05	3.50	2.69	5.31	11.37	4.00	2.40	3.35	3.63	3.50	0.65	1.70
	0.99	6	3	0.12	1.60	0.06	0.07	0.12	1.80	0.06	0.06	-	-	-	-
		9	3	3.45	2.60	1.19	1.46	3.45	2.60	1.20	1.45	0.65	2.40	0.23	0.28
		10	4	1.05	3.00	0.28	0.41	1.22	2.80	0.35	0.51	-	-	-	-
		12	3	1476.56	3.50	381.09	484.54	2015.85	3.25	362.84	792.00	49.06	3.00	11.90	23.17
		12	4	13.71	3.50	2.55	4.97	10.35	4.00	2.26	3.14	3.58	3.50	0.59	1.65

LEAST and **HIGHEST**, where only one group is fixed.

Based on these findings, we chose to set a time limit of 60 seconds per iteration, even if this leads to additional iterations, and a maximum of 600 seconds in total as a stopping criteria for $\mathcal{LS}_{IEC}$.

2.5.3 Comparison of the Five Heuristics to the best-known Solutions

The performance of each heuristic is evaluated against the best-known solution for each instance, which is determined by the optimal or best incumbent solutions found by the three mathematical formulations, potentially enhanced by $\mathcal{LS}_{IEC}$ local search. This comparative analysis allows for a comprehensive evaluation of the heuristics' effectiveness relative to the best-known solutions identified during the experiments.

For each instance, we calculate the relative gap between the heuristic solution and the best-known solution, as defined in (2.71). The aggregated results are presented in Table 2.9 categorized by population size N.

The aggregated results in Table 2.9 reveal that **LEAST** consistently outperforms other heuristics. **HIGHEST** and **BOTH** (when applicable) also perform well, providing solutions close to the best-known solutions. For $N = 9$, **GRADIENT** heuristic shows a remarkably small relative gap, underscoring its high effectiveness, while **SPIRAL** heuristic performs the least effectively. The similar relative gaps between **GRADIENT**, **HIGHEST**, and **BOTH** further highlight **GRADIENT**'s suitability for square array group testing. McMahan *et al.* (2012b) claim that these algorithms are rarely beaten in terms of efficiency and that the optimal solution would probably be only slightly better than **GRADIENT** and **SPIRAL** heuristics. Therefore, we could evaluate the effectiveness of these two designs by comparing the solutions they obtain against the optimal solution obtained by one of our formulations when the computational time is reasonable. Otherwise a performance measure is provided.

2.5.4 Empirical comparison of $\mathbf{F}^{3}_{\mathbf{MINLP}}$, $\mathbf{F}^{\mathbf{SYM}}_{\mathbf{MINLP}}$ and $\mathbf{F}^{\mathbf{EXT}}_{\mathbf{MINLP}}$

We compare the three formulations presented in Section 2.3 based on different criteria, such as running time and the gap at the root node. Table 2.10 provides the column headings used in the subsequent tables. We use the default parameters of Gurobi and modify only the following ones: `GRB_IntParam_NumericFocus` = 1 (improves numerical stability), `GRB_DoubleParam_MIPGap` = 0 (requires proven optimality; no early stop on gap), and `GRB_IntParam_NonConvex` = 2 (enables solving non-convex quadratic models). For each experiment, we set a time limit of 3600 seconds. We recall that the three models are warm-started with the same solution, which is the best solution found by the heuristics.

Table 2.8: Aggregated First Time Optimal Solution Found per Iteration in $\mathcal{LS}_{IEC}$

Se	*Sp*	*N*	*L*	**LEAST**			**HIGHEST**			**BOTH**		
				Avg. FTOpt(s)	Avg. TCloseGap(s)	Avg. Iter. Time(s)	Avg. FTOpt(s)	Avg. TCloseGap(s)	Avg. Iter. Time(s)	Avg. FTOpt(s)	Avg. TCloseGap(s)	Avg. Iter. Time(s)
0.9	0.9	6	3	0.00	0.07	0.07	0.00	0.08	0.08	-	-	-
		9	3	0.08	1.32	1.40	0.15	1.27	1.42	0.00	0.26	0.26
		10	4	0.08	0.32	0.40	0.09	0.38	0.47	-	-	-
		12	3	200.15	484.39	684.54	214.45	657.80	872.25	3.88	13.31	17.19
		12	4	1.41	2.26	3.67	0.64	2.11	2.75	0.08	0.74	0.82
	0.95	6	3	0.00	0.07	0.07	0.00	0.07	0.07	-	-	-
		9	3	0.00	1.44	1.44	0.08	1.39	1.47	0.00	0.27	0.27
		10	4	0.00	0.39	0.39	0.00	0.49	0.49	-	-	-
		12	3	130.88	450.26	581.14	348.12	482.61	830.73	3.93	14.01	17.94
		12	4	1.44	2.57	4.01	0.70	2.19	2.89	0.17	0.85	1.01
	0.99	6	3	0.00	0.07	0.07	0.00	0.07	0.07	-	-	-
		9	3	0.08	1.30	1.38	0.08	1.35	1.42	0.00	0.27	0.27
		10	4	0.00	0.35	0.35	0.00	0.44	0.44	-	-	-
		12	3	139.35	399.83	539.18	244.65	505.45	750.10	1.80	16.37	18.17
		12	4	0.94	3.08	4.02	0.65	2.16	2.81	0.11	0.86	0.97
0.95	0.9	6	3	0.00	0.06	0.06	0.00	0.07	0.07	-	-	-
		9	3	0.15	1.28	1.43	0.08	1.32	1.40	0.00	0.27	0.27
		10	4	0.08	0.29	0.36	0.08	0.36	0.44	-	-	-
		12	3	130.45	378.86	509.31	269.15	486.86	756.01	4.00	15.01	19.01
		12	4	1.39	2.63	4.02	0.73	2.20	2.93	0.25	0.70	0.95
	0.95	6	3	0.00	0.07	0.07	0.00	0.07	0.07	-	-	-
		9	3	0.08	1.30	1.38	0.15	1.25	1.40	0.00	0.26	0.26
		10	4	0.00	0.36	0.36	0.00	0.46	0.46	-	-	-
		12	3	160.82	308.36	469.18	358.82	383.44	742.27	3.40	16.82	20.22
		12	4	1.17	2.81	3.98	0.55	2.22	2.77	0.22	0.77	0.99
	0.99	6	3	0.00	0.06	0.06	0.00	0.07	0.07	-	-	-
		9	3	0.00	1.35	1.35	0.00	1.39	1.39	0.00	0.26	0.26
		10	4	0.00	0.36	0.36	0.00	0.47	0.47	-	-	-
		12	3	165.88	292.74	458.62	285.06	372.98	658.04	3.40	14.45	17.85
		12	4	0.94	2.92	3.86	0.50	2.22	2.72	0.22	0.73	0.95
0.99	0.9	6	3	0.00	0.06	0.06	0.00	0.08	0.08	-	-	-
		9	3	0.00	1.42	1.42	0.08	1.37	1.44	0.00	0.27	0.27
		10	4	0.07	0.35	0.42	0.11	0.36	0.47	-	-	-
		12	3	119.37	336.52	455.89	262.10	417.82	679.92	2.94	13.86	16.79
		12	4	1.61	2.30	3.91	0.91	1.80	2.72	0.29	0.63	0.92
	0.95	6	3	0.00	0.07	0.07	0.00	0.06	0.06	-	-	-
		9	3	0.08	1.34	1.42	0.08	1.35	1.42	0.00	0.26	0.26
		10	4	0.00	0.37	0.37	0.00	0.46	0.46	-	-	-
		12	3	190.35	230.42	420.77	240.18	398.03	638.21	2.47	13.73	16.20
		12	4	1.00	2.85	3.85	0.75	2.13	2.88	0.39	0.61	1.00
	0.99	6	3	0.00	0.06	0.06	0.00	0.05	0.05	-	-	-
		9	3	0.00	1.31	1.31	0.08	1.24	1.31	0.00	0.26	0.26
		10	4	0.00	0.34	0.34	0.00	0.42	0.42	-	-	-
		12	3	252.82	168.40	421.23	281.06	332.91	613.97	3.53	14.24	17.78
		12	4	0.94	2.87	3.81	0.40	2.26	2.66	0.33	0.65	0.98

Table 2.9: Comparison of heuristics with Relative Gap (%).

N	Relative Gap (%)				
	GRADIENT	SPIRAL	LEAST	HIGHEST	BOTH
6	-	-	0.000	0.237	-
9	0.073	4.555	0.001	0.073	0.073
10	-	-	0.000	1.613	-
12	-	-	0.036	0.081	0.070

Table 2.10: Column headings.

Column heading	**Description**
ID	ID of the risk vector instance
Obj	value of the best solution obtained
Runtime (s)	total computation time in seconds (equals to 3600 seconds if optimality is not achieved, denoted by TL (Time Limit)
Nodes	number of nodes in the search tree
Gap_r (%)	gap at the root node $Gap_r = \frac{UB-LB}{UB} \times 100$, UB is the upper bound given as a warm start defined as the best solution value of the five heuristics
Gap (%)	gap at the termination/at the time limit: $Gap = \frac{Obj-LB}{Obj} \times 100$
Avg. Time (s)	the average runtime in seconds
Avg. #Nodes	the average number of nodes
Avg. Gap_r (%)	the average gap at the root node
#Opt./#Inst.	the number of instances solved to optimality over the number of instances

We present in Table 2.11 the aggregated results per population size N. Detailed results for each instance can be found in Tables 4.10 to 4.13 in the appendix.

It is observed in Table 2.11 that $\text{F}^3_{\text{MINLP}}$ model struggles to solve the instances to optimality starting from $N = 9$, as indicated by the non-zero optimality gaps and high run times. Despite not solving the instances to optimality within the given time limit, $\text{F}^3_{\text{MINLP}}$ often finds the optimal solution as the best incumbent solution. This is evidenced by the fact that the best incumbent found by $\text{F}^3_{\text{MINLP}}$ matches the optimal solution identified by the $\text{F}^{\text{SYM}}_{\text{MINLP}}$ and $\text{F}^{\text{EXT}}_{\text{MINLP}}$ models. However, the weakness of $\text{F}^3_{\text{MINLP}}$ lies in its ability to

Table 2.11: Aggregated performance comparison of formulations by N

N	$\text{F}^3_{\text{MINLP}}$				$\text{F}^{\text{SYM}}_{\text{MINLP}}$				$\text{F}^{\text{EXT}}_{\text{MINLP}}$			
	Avg. Time (s)	Avg. #Nodes	Avg. Gap_r (%)	#Opt. /#Inst.	Avg. Time (s)	Avg. #Nodes	Avg. Gap_r (%)	#Opt. /#Inst.	Avg. Time (s)	Avg. #Nodes	Avg. Gap_r (%)	#Opt. /#Inst.
6	0.62	1484.16	543.69	45/45	0.34	143.07	207.46	45/45	0.09	2.18	25.11	45/45
9	TL	1388022.29	1657.0	0/45	780.27	205664.27	1236.33	45/45	44.79	14107.02	747.68	45/45
10	3459.34	2437954.8	489.87	11/45	208.67	132953.33	384.93	45/45	39.73	61320.89	432.44	45/45
12	TL	480580.26	1656.78	0/90	TL	568779.24	1368.79	0/90	TL	11176738.63	1402.76	0/90

close the optimality gap, which is primarily due to its lower bound not being as tight as those of the other models as shown in Tables 2.11 for instances with $N = 9$ and $N = 10$ respectively.

The $\mathrm{F}^{\mathrm{SYM}}_{\mathrm{MINLP}}$ model shows improved performance compared with $\mathrm{F}^{3}_{\mathrm{MINLP}}$, often solving instances to optimality faster and with fewer nodes explored. This improvement is due to the symmetry-breaking constraints (2.44)-(2.48) incorporated in the $\mathrm{F}^{\mathrm{SYM}}_{\mathrm{MINLP}}$ model, which reduce the search space and enhance the efficiency of the solver.

The $\mathrm{F}^{\mathrm{EXT}}_{\mathrm{MINLP}}$ model consistently outperforms both $\mathrm{F}^{3}_{\mathrm{MINLP}}$ and $\mathrm{F}^{\mathrm{SYM}}_{\mathrm{MINLP}}$ in terms of runtime, solving instances with $N \in \{6, 9, 10\}$ to optimality within a few seconds. This highlights that $\mathrm{F}^{\mathrm{EXT}}_{\mathrm{MINLP}}$ model is worth studying as the nonlinear cost of each group C_k and of each intersections of groups D_{kl} are already computed and known. Although $\mathrm{F}^{\mathrm{EXT}}_{\mathrm{MINLP}}$ has superior performance, the lower bound obtained is weak for $N \geq 9$. It is worth of strengthening it which define potential future research avenues to improve performance of $\mathrm{F}^{\mathrm{EXT}}_{\mathrm{MINLP}}$ over all instances. Here, we could enumerate all the groups in $\mathrm{F}^{\mathrm{EXT}}_{\mathrm{MINLP}}$ only because of the small size of the populations. Additionally, we can remark that all the three warm-started models, initialized with the same best heuristic solution, either confirm its optimality of often improve it.

From the computational results, formulations $\mathrm{F}^{\mathrm{SYM}}_{\mathrm{MINLP}}$ and $\mathrm{F}^{\mathrm{EXT}}_{\mathrm{MINLP}}$ are not comparable computationally. In fact, it does not seem that one formulation outperforms that other. Indeed, both formulations $\mathrm{F}^{\mathrm{EXT}}_{\mathrm{MINLP}}$ and $\mathrm{F}^{\mathrm{SYM}}_{\mathrm{MINLP}}$ solve to optimality the instances when $N \in \{6, 9, 10\}$ with $\mathrm{F}^{\mathrm{EXT}}_{\mathrm{MINLP}}$ performing better in runtime compared to $\mathrm{F}^{\mathrm{SYM}}_{\mathrm{MINLP}}$. However, for $N \geq 10$, the gap at the root node is explicitly worse for $\mathrm{F}^{\mathrm{EXT}}_{\mathrm{MINLP}}$ compared with the gap at the root node of $\mathrm{F}^{\mathrm{SYM}}_{\mathrm{MINLP}}$.

2.5.4.1 Some Properties of best-known Solutions

In the bar plot analysis (Figure 2.9), we present the characteristics of the best-known solutions for various combination values of (Se, Sp, N).

For $N = 6$, $N = 9$, and $N = 10$, the L least risk individuals are consistently grouped in the optimal solutions, indicating that minimizing false positives is achieved through grouping lower-risk individuals. On the other hand, the L highest-risk individuals are grouped together less frequently, suggesting variability in the optimal solutions based on specific values of Se, Sp, and $\mathbf{p}$. This analysis provides deeper insights into solution properties and highlights the performance of heuristic approaches, such as the **GRADIENT** heuristic, particularly in matrix group testing for $N = 9$. For $N = 12$, new insights emerge, revealing more diverse group characteristics.

2.6 Conclusion and Future Work

In this chapter, we focus on the non-adaptive risk-based 2D-GTEG problem in a heterogeneous population and with imperfect tests. We highlight the novelty and ease of

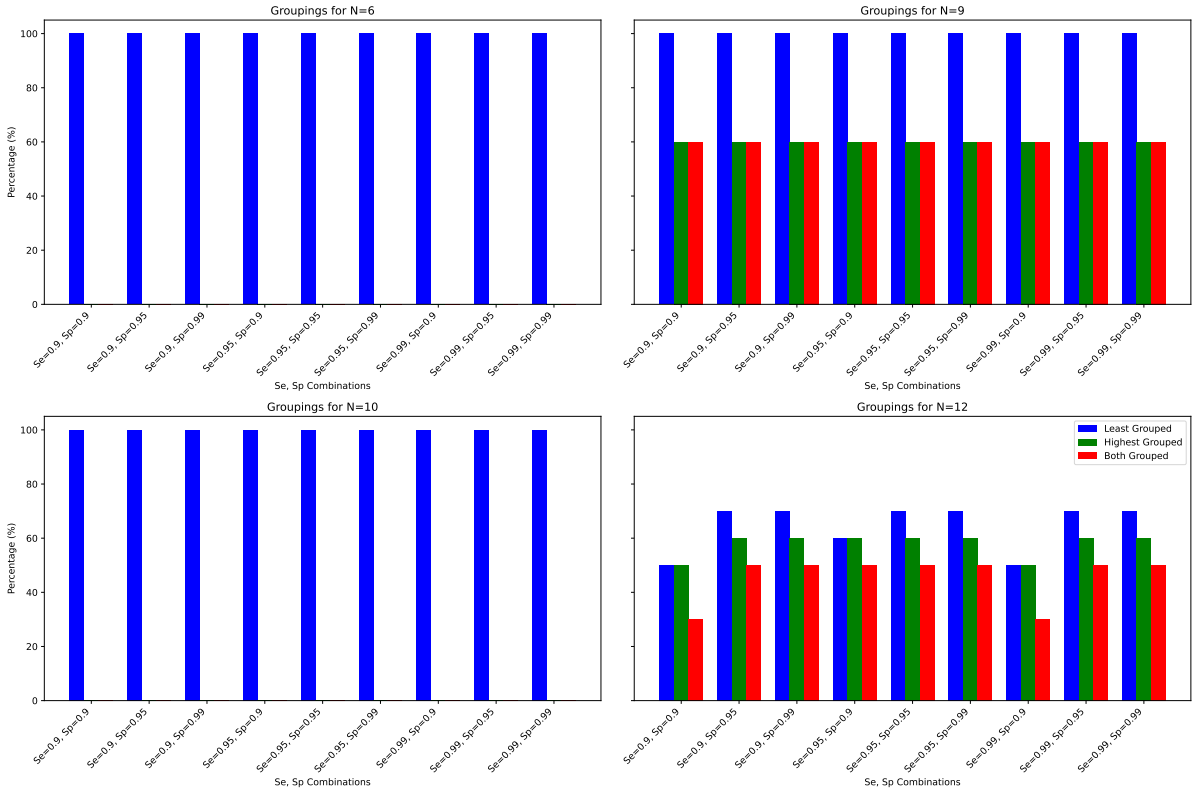


Figure 2.9: Solution properties in optimal solution or best incumbent by varying (Se, Sp)

applicability of this design compared to known square array designs. First, we focus on the statistical calculations regarding misclassification errors and the expected number of tests in our setting. We formulate the problem with three mathematical models - $\mathrm{F}^{3}_{\mathrm{MINLP}}$, $\mathrm{F}^{\mathrm{SYM}}_{\mathrm{MINLP}}$, and $\mathrm{F}^{\mathrm{EXT}}_{\mathrm{MINLP}}$. Additionally, we provide several heuristics to construct feasible solutions and two local search methods to improve the solutions. In our experiments on small instances, we compare the computational performance of the three models and our methods to two heuristics from the literature when applicable.

Computational results on the three formulations show that, on average, $\mathrm{F}^{\mathrm{EXT}}_{\mathrm{MINLP}}$ is the best, followed by formulation $\mathrm{F}^{\mathrm{SYM}}_{\mathrm{MINLP}}$. Formulation $\mathrm{F}^{\mathrm{EXT}}_{\mathrm{MINLP}}$ performs the best on instances with N values of 6, 9, and 10 according to the running time and the gap criteria. However, the gap at the root node tends to be significant, indicating the need of improvements.

Interestingly, our experiments consistently reveal that grouping the least risk individuals leads to minimize false positives. It is worth noting that grouping the highest-risk individuals is not always a feature of optimal solutions and depends on the instance. Our analysis offers a promising direction for future strategies. Furthermore, our experiments provided an evaluation of the **GRADIENT** and **SPIRAL** heuristics of McMahan *et al.* (2012b) with respect to the optimal solutions.

We were only able to run and compare the three models on small instances because experiments revealed the significant limitations of all three models, especially the $\mathrm{F}^{\mathrm{EXT}}_{\mathrm{MINLP}}$ model when $N = 12$. Chapter 3 explores how to solve this exponentially sized formulation

by using column generation-based methods, and how to improve the lower bound with valid inequalities.

Chapter 3

A Branch-and-Price Algorithm for Risk-based Non-adaptive Two-Dimensional Group Testing with Equal Group Size

In the previous chapter, we introduced an extended formulation $\mathrm{F}^{\mathrm{EXT}}_{\mathrm{MINLP}}$ that enumerates all feasible groups to select those that ensure a feasible solution while minimizing the objective function. Although solving this formulation to optimality was possible for instances with a size of $N \leq 10$ in less than 45 seconds of runtime, it has limitations due to the impracticality of enumerating all possible groups and its weak lower bound at the root node. To address these challenges, this chapter proposes an enhanced extended formulation. We solve its linear relaxation using simultaneous column-and-row generation. To restore integrality, we embed this approach within a Branch-and-Price framework. This algorithm aims to overcome the limitations identified in the previous chapter, providing a more scalable solution methodology.

The chapter is organized as follows. Section 3.1 introduces the enhanced extended formulation and provides a mathematical comparison of both formulations. Section 3.2 describes the simultaneous column-and-row generation approach used to solve the linear relaxation of the enhanced formulation, including the definitions of the Restricted Master Problem and the Pricing Problem, solution methods for the latter, and the computation of a Lagrangian lower bound. Section 3.3 presents the Branch-and-Price algorithm that integrates the simultaneous column-and-row generation method to restore solution integrality, along with branching rules and a primal heuristic. Section 3.4 provides computational experiments that discuss the effectiveness and the limits of the proposed approach. Finally, Section 3.5 concludes the chapter with a summary of key findings and outlines future research directions.

3.1 Enhanced Extended Formulation

In this section, we present an enhanced version of the extended formulation $\mathrm{F}^{\mathrm{EXT}}_{\mathrm{MINLP}}$. To obtain it, we first linearize the original quadratic formulation $\mathrm{F}^{\mathrm{EXT}}_{\mathrm{MINLP}}$, and then we derive a family of valid inequalities which are used to obtain the new formulation. Finally, we provide a comparison of the two formulations, supported by mathematical proofs, to highlight the improvements achieved with the enhanced formulation.

3.1.1 Linearization of $\mathbf{F}^{\mathbf{EXT}}_{\mathbf{MINLP}}$

The product $y_k y_l$ of binary variables which appears in the objective function of $\mathrm{F}^{\mathrm{EXT}}_{\mathrm{MINLP}}$ can be linearized by introducing auxiliary binary variables $x_{kl} = y_k y_l, \forall (k,l) \in \mathcal{P}(\mathcal{K})$ and the corresponding linearization constraints as follows:

$$\min \sum_{k \in \mathcal{K}} C_k y_k + \sum_{(k,l) \in \mathcal{P}(\mathcal{K})} D_{kl} x_{kl} \tag{3.1}$$

$$\text{s.t.} \sum_{k \in \mathcal{K}_i} y_k = 2 \qquad \forall i \in \mathcal{I} \tag{3.2}$$

$$\sum_{k \in \mathcal{K}_i \cap \mathcal{K}_j} y_k \leq 1 \qquad \forall i, j \in \mathcal{I}, j > i \tag{3.3}$$

$$y_k + y_l - x_{kl} \leq 1 \qquad \forall (k,l) \in \mathcal{P}(\mathcal{K}) \tag{3.4}$$

$$y_k - x_{kl} \geq 0 \qquad \forall (k,l) \in \mathcal{P}(\mathcal{K}) \tag{3.5}$$

$$y_l - x_{kl} \geq 0 \qquad \forall (k,l) \in \mathcal{P}(\mathcal{K}) \tag{3.6}$$

$$y_k \in \{0,1\} \qquad \forall k \in \mathcal{K} \tag{3.7}$$

$$x_{kl} \in \{0,1\} \qquad \forall (k,l) \in \mathcal{P}(\mathcal{K}) \tag{3.8}$$

Constraints (3.4), (3.5) and (3.6) express the linearization of the product $y_k y_l$. Constraints (3.8) are the binary requirements for variables x_{kl}. Notice that as $D_{kl} \geq 0$, the linearization constraints (3.5) and (3.6) may be omitted from the model. Consequently, only the constraints (3.4) are sufficient to linearize the product $y_k y_l$ with the variable x_{kl}. We therefore obtain the following model denoted by $\mathrm{F}^{\mathrm{EXT}}_{\mathrm{LIN}}$:

$$[\mathrm{F}^{\mathrm{EXT}}_{\mathrm{LIN}}] \quad \min \sum_{k\in\mathcal{K}} C_k y_k + \sum_{(k,l)\in\mathcal{P}(\mathcal{K})} D_{kl} x_{kl} \tag{3.9}$$

$$\text{s.t.} \sum_{k\in\mathcal{K}_i} y_k = 2 \qquad \forall i \in \mathcal{I} \tag{3.10}$$

$$\sum_{k\in\mathcal{K}_i\cap\mathcal{K}_j} y_k \leq 1 \qquad \forall i,j \in \mathcal{I}, j > i \tag{3.11}$$

$$y_k + y_l - x_{kl} \leq 1 \qquad \forall (k,l) \in \mathcal{P}(\mathcal{K}) \tag{3.12}$$

$$y_k \in \{0,1\} \qquad \forall k \in \mathcal{K} \tag{3.13}$$

$$x_{kl} \in \{0,1\} \qquad \forall (k,l) \in \mathcal{P}(\mathcal{K}) \tag{3.14}$$

3.1.2 An Alternative Extended Formulation

For a wide variety of discrete combinatorial and continuous non-convex programming problems, the Reformulation-Linearization Technique (RLT) of Adams & Sherali (1986, 1990) and Sherali & Adams (1990, 1994, 1998, 2013) is well renowned for generating tight linear programming relaxations, as well as for proposing effective heuristic solutions. It essentially involves two phases: reformulation and linearization. In the reformulation phase, existing constraints and variable bounds are multiplied to generate additional valid constraints. These products often capture hidden relationships in the original problem, helping to tighten the relaxation. The linearization phase introduces new variables to replace nonlinear terms, thereby obtaining a linear model.

In our context, let i be an individual. Let us multiply the constraints (3.10) by y_l where $l \in \mathcal{K}_i$. This leads to $\sum_{k\in\mathcal{K}_i} y_k y_l = 2y_l$ that can be decomposed in

$$\sum_{k\in\mathcal{K}_i, G_k\cap G_l=\{i\}} y_k y_l + \sum_{k\in\mathcal{K}_i, |G_k\cap G_l|\geq 2} y_k y_l + y_l y_l = 2y_l \tag{3.15}$$

Since the product $y_k y_l$ for $|G_k \cap G_l| \geq 2$ represents pairs of groups (G_k, G_l) that share two or more individuals, the conflict constraints in (3.11) prevent both y_k and y_l from being equal to 1 simultaneously. As a result, $y_k y_l$ for $|G_k \cap G_l| \geq 2$ will always be equal to zero, and the corresponding terms can be removed from the equation (3.15). Then, for the products of variables representing groups that have exactly i in common, we can replace, by definition, the product $y_k y_l, G_k \cap G_l = \{i\}$ by x_{kl}. Then, since y_l is binary, it holds that $y_l y_l = y_l$. Let $\mathcal{P}(\mathcal{K}_i) = \{(k,l); k,l \in \mathcal{K}_i, G_k \cap G_l = \{i\}\}$ be the set of pairs of groups intersecting exactly in individual i. This simplifies the expression to:

$$\sum_{k:(k,l)\in\mathcal{P}(\mathcal{K}_i)} x_{kl} = y_l \quad \forall i \in G_l \tag{3.16}$$

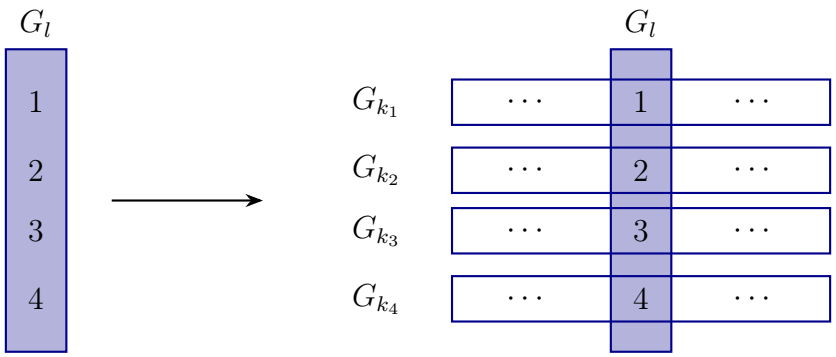


Figure 3.1: Illustration of the constraint (3.16). If G_l is selected in the solution, one group G_{k_i} intersecting with G_l in i must also be selected in the solution $\forall i \in G_l$.

Let us now analyze constraints (3.16) for a group G_l and an individual $i \in G_l$. The constraint enforces that group G_l, which contains individual i, must intersect with exactly one other group G_k in individual i when $y_l = 1$. In other words, if G_l is selected, it must intersect with another group in individual i, and this is true for all $i \in G_l$. Figure 3.1 illustrates this case. Let the following model $\mathrm{F}^{\mathrm{EXT}}_{\mathrm{RLT}}$ be an alternative extended formulation for 2D-GTEG including inequalities (3.16). It reads as follows:

$$[\mathrm{F}^{\mathrm{EXT}}_{\mathrm{RLT}}] \quad \min \sum_{k\in\mathcal{K}} C_k y_k + \sum_{(k,l)\in\mathcal{P}(\mathcal{K})} D_{kl} x_{kl} \tag{3.17}$$

$$\text{s.t.} \sum_{k\in\mathcal{K}_i} y_k = 2 \qquad \forall i \in \mathcal{I} \tag{3.18}$$

$$y_k - \sum_{l:(k,l)\in\mathcal{P}(\mathcal{K}_i)} x_{kl} = 0 \qquad \forall k \in \mathcal{K}, \forall i \in G_k \tag{3.19}$$

$$y_k \in \{0,1\} \qquad \forall k \in \mathcal{K} \tag{3.20}$$

$$x_{kl} \in \{0,1\} \qquad \forall (k,l) \in \mathcal{P}(\mathcal{K}) \tag{3.21}$$

Constraints (3.19) ensure that if a group G_k is selected ($y_k = 1$), then the specific individual $i \in G_k$ must be the intersection with exactly one other group that shares exactly i with G_k. If G_k is not selected, all variables x_{kl} and x_{lk} related to individual i in that group are set to 0. It can be observed that constraints (3.18) with (3.19) and the variable definitons are sufficient to provide a valid formulation for 2D-GTEG. Indeed, as showed by Proposition 3.2 the two formulations provide the same optimal solutions.

3.1.3 Comparison of the Formulations

In this section, we compare the two formulations, $\mathrm{F}_{\mathrm{LIN}}^{\mathrm{EXT}}$ and $\mathrm{F}_{\mathrm{RLT}}^{\mathrm{EXT}}$, to establish the superiority of the latter. While both formulations yield the same optimal integer solutions, as stated in Proposition 3.1, the strength of their linear relaxations differs significantly. In particular, Proposition 3.2 demonstrates that the linear relaxation of $\mathrm{F}_{\mathrm{RLT}}^{\mathrm{EXT}}$ provides a tighter bound, making it a stronger formulation overall.

Proposition 3.1. *Both formulations F_{LIN}^{EXT} and F_{RLT}^{EXT} have the same set of optimal integer solutions.*

Proof. Let $(\hat{y}, \hat{x})$ be an optimal integer solution for $\mathrm{F}_{\mathrm{LIN}}^{\mathrm{EXT}}$. We show that $(\hat{y}, \hat{x})$ is feasible for $\mathrm{F}_{\mathrm{RLT}}^{\mathrm{EXT}}$. First, constraints (3.10) and (3.18) are the same family of constraints. Therefore, $(\hat{y}, \hat{x})$ satisfies (3.18). Now, we show that $(\hat{y}, \hat{x})$ satisfy constraints (3.19). We consider first that $\hat{y_k} = 0$ for $k \in \mathcal{K}$. Since $(\hat{y}, \hat{x})$ is optimal for $\mathrm{F}_{\mathrm{LIN}}^{\mathrm{EXT}}$, we have $\hat{x_{kl}} = 0$ for all $(k, l) \in \mathcal{P}(\mathcal{K})$ and (3.19) are satisfied. We assume now that $\hat{y_k} = 1$ for $k \in \mathcal{K}$. Since constraints (3.10) impose that each individual is in two groups and constraints (3.11) ensure that any two groups share no more than one individual, there exists a unique $l \in \mathcal{K}_i$ such that $\hat{y_l} = 1$ and $(k, l) \in \mathcal{P}(\mathcal{K}_i)$. Due to constraints (3.12), we have $\hat{x_{kl}} = 1$ and constraint (3.19) is satisfied.

We now prove that any feasible solution (y, x) of formulation $\mathrm{F}_{\mathrm{RLT}}^{\mathrm{EXT}}$ is a feasible solution of $\mathrm{F}_{\mathrm{LIN}}^{\mathrm{EXT}}$. Again, constraints constraints (3.10) and (3.18) are the same family of constraints. Therefore, (y, x) satisfies (3.10).

We now show that constraints (3.18)-(3.19) imply constraints (3.11).

Let us fix two distinct individuals $i, j \in \mathcal{I}$ with $i < j$.

$$
\begin{aligned}
2 - \sum_{k \in \mathcal{K}_i \cap \mathcal{K}_j} y_k &= \sum_{k \in \mathcal{K}_i \setminus \mathcal{K}_j} y_k \quad \text{from (3.18)} \\
&= \sum_{k \in \mathcal{K}_i \setminus \mathcal{K}_j} \sum_{l:(k,l) \in \mathcal{P}(\mathcal{K}_i)} x_{kl} \quad \text{using (3.19)} \\
&= \sum_{(k,l) \in \mathcal{P}(\mathcal{K}_i): k \in \mathcal{K}_i \setminus \mathcal{K}_j} x_{kl} \\
&\geq \sum_{(k,l) \in \mathcal{P}(\mathcal{K}_i): k \in \mathcal{K}_i \setminus \mathcal{K}_j, l \in \mathcal{K}_i \cap \mathcal{K}_j} x_{kl} \\
&= \sum_{l \in \mathcal{K}_i \cap \mathcal{K}_j} \sum_{k:(k,l) \in \mathcal{P}(\mathcal{K}_i)} x_{kl} \quad \text{by definition of } \mathcal{P}(\mathcal{K}_i) \\
&= \sum_{l \in \mathcal{K}_i \cap \mathcal{K}_j} y_l \quad \text{from (3.19)}
\end{aligned}
\tag{3.22}
$$

This implies that constraints (3.11) are satisfied.

Last, we show that constraints (3.18)-(3.19) imply constraints (3.12). Let us fix (k, l) such that $(k, l) \in \mathcal{P}(\mathcal{K}_i)$.

$$
\begin{aligned}
2 - y_k - y_l &= \sum_{m \in \mathcal{K}_i \setminus \{k,l\}} y_m \quad \text{from (3.18)} \\
&= \sum_{(m,n) \in \mathcal{P}(\mathcal{K}_i): m \in \mathcal{K}_i \setminus \{k,l\}} x_{mn} \quad \text{using (3.19)} \\
&= \sum_{(m,n) \in \mathcal{P}(\mathcal{K}_i): m,n \in \mathcal{K}_i \setminus \{k,l\}} x_{mn} \\
&+ \sum_{m:(m,k) \in \mathcal{P}(\mathcal{K}_i): m \in \mathcal{K}_i \setminus \{k,l\}} x_{mk} \\
&+ \sum_{m:(m,l) \in \mathcal{P}(\mathcal{K}_i): m \in \mathcal{K}_i \setminus \{k,l\}} x_{ml} \\
&\geq \sum_{m:(m,k) \in \mathcal{P}(\mathcal{K}_i)} x_{mk} + \sum_{m:(m,l) \in \mathcal{P}(\mathcal{K}_i)} x_{ml} - 2x_{kl} \\
&= y_k - x_{kl} + y_l - x_{kl} \quad \text{from (3.19)}
\end{aligned}
\tag{3.23}
$$

This implies that constraints (3.12) are satisfied.

Therefore, all feasible solution of $\mathrm{F}_{\mathrm{RLT}}^{\mathrm{EXT}}$ are feasible solutions of $\mathrm{F}_{\mathrm{LIN}}^{\mathrm{EXT}}$. □

Proposition 3.2. *Let LP_{LIN} and LP_{RLT} denote the linear relaxations of F_{LIN}^{EXT} and F_{RLT}^{EXT}, with corresponding optimal values $v(LP_{LIN})$ and $v(LP_{RLT})$, then $v(LP_{RLT}) \geq v(LP_{LIN})$.*

Proof. First, we can observe that any feasible solution of LP_{RLT} is also feasible for LP_{LIN}. Indeed, the second part of the proof of Proposition 3.1 remains valid for the linear relaxations. However, the reverse does not hold, as demonstrated by the following counterexample. Consider an instance with 6 individuals, where $Se = Sp = 0.95$, $\mathbf{p} = (0.01, 0.02, 0.03, 0.04, 0.05, 0.06)$, and all possible groups of size 3 are listed, with values of C_k and D_{kl} multiplied by a factor of 100000 are provided in Table 4.19 in the appendix. The respective optimal solutions of LP_{LIN} and LP_{RLT} are compared.

For LP_{RLT}: $\bar{y}_1 = \bar{y}_8 = \bar{y}_{15} = \bar{y}_{19} = 1$ with the corresponding x variables $\bar{x}_{1,8} = \bar{x}_{1,15} = \bar{x}_{1,19} = \bar{x}_{8,15} = \bar{x}_{8,19} = \bar{x}_{15,19} = 1$ and with the optimal value $v(LP_{\mathrm{RLT}}) = 94.58$. For LP_{LIN}: $\hat{y}_1 = \hat{y}_2 = \hat{y}_6 = \hat{y}_8 = \hat{y}_{13} = \hat{y}_{15} = \hat{y}_{19} = \hat{y}_{20} = 0.5$ with the optimal value $v(LP_{\mathrm{LIN}}) = -23782.99$. In $(\hat{y}, \hat{x})$, we have $\forall (k,l) \in \mathcal{P}(\mathcal{K}_i) : \hat{y}_k + \hat{y}_l \leq 1$ and $\hat{x}_{kl} = 0$. In particular, we have the following:

$$
\underbrace{\hat{y}_k}_{>0} - \underbrace{\sum_{(k,l) \in \mathcal{P}(\mathcal{K}_i)} \hat{x}_{kl} - \sum_{(l,k) \in \mathcal{P}(\mathcal{K}_i)} \hat{x}_{lk}}_{=0} \neq 0 \tag{3.24}
$$

And thus (3.19) are not satisfied. Consequently, $(\hat{y}, \hat{x})$ is not feasible in LP_{RLT}.

□

3.2 Simultaneous Column-and-Row Generation

Column generation (Lübbecke & Desrosiers, 2005) is a well-known method for resolving large-scale linear programming (LP) problems. Initially pioneered by Dantzig & Wolfe (1960) and Gilmore & Gomory (1961), this approach is often used to solve mixed-integer programming problems with an exponential number of variables by leveraging LP relaxations. The core concept is to solve the linear relaxation of the original problem, called the Master Problem (MP) by considering initially a limited set of variables (or columns), that is the Restricted Master Problem (RMP), and by generating new columns as required. This is achieved by solving a pricing problem, which identifies columns with negative reduced costs to be added to the RMP until optimality is reached.

However, the conventional column generation approach assumes that the constraints in the RMP are explicitly known. In our case, new linking constraints must be introduced with newly generated columns, making our problem a Column-Dependent-Row problem (CDR). CDR-problems, require simultaneous column-and-row generation to guarantee the correctness of the solution. In his PhD thesis (Muter, 2011), Muter first introduced a general algorithm for simultaneous column-and-row generation. This approach involves solving several pricing problems to generate both necessary columns and corresponding rows. The design of these pricing problems is critical, requiring problem-specific customization for each column-dependent-row formulation.

In the following sections, we detail our approach for solving the linear relaxation of $\mathrm{F}_{\mathrm{RLT}}^{\mathrm{EXT}}$ by the simultaneous column-and-row generation. Section 3.2.1 introduces the Restricted Master Problem, while Section 3.2.2 provides a detailed formulation of the Pricing Problem. Section 3.2.3 discusses the solution methods for the Pricing Problem, including heuristic and exact approaches. Section 3.2.4 presents the initialization strategies for the RMP to provide a strong starting point for the column generation procedure. In Section 3.2.5, we discuss the Lagrangian lower bound, used as an early termination criterion for the column generation. Finally, Section 3.2.6 presents the complete simultaneous column-and-row generation algorithm, integrating the different components.

3.2.1 Restricted Master Problem

In the remaining of the chapter, we refer to the master problem MP as the linear relaxation of $\mathrm{F}_{\mathrm{RLT}}^{\mathrm{EXT}}$ where we replace the equality constraints (3.19) by the inequality constraints (3.27) to master the sign of the corresponding dual variables λ to be negative instead of free. We can do that due to the fact that we solve a minimization problem where $D_{kl} \geq 0$. The following mathematical model presents MP with the corresponding dual variables in brackets.

$$[\text{MP}]\ \min \sum_{k\in\mathcal{K}} C_k y_k + \sum_{(k,l)\in\mathcal{P}(\mathcal{K})} D_{kl} x_{kl} \tag{3.25}$$

$$\text{s.t.} \sum_{k\in\mathcal{K}_i} y_k = 2 \qquad (\alpha_i) \quad \forall i \in \mathcal{I} \tag{3.26}$$

$$y_k - \sum_{l:(k,l)\in\mathcal{P}(\mathcal{K}_i)} x_{kl} \leq 0 \qquad (\lambda_{ki}) \quad \forall k \in \mathcal{K}, \forall i \in G_k \tag{3.27}$$

$$y_k \geq 0 \qquad \forall k \in \mathcal{K} \tag{3.28}$$

$$x_{kl} \geq 0 \qquad \forall (k,l) \in \mathcal{P}(\mathcal{K}) \tag{3.29}$$

We refer to the problem below as the Restricted Master Problem $RMP(\bar{\mathcal{K}})$ defined over a subset of columns $\bar{\mathcal{K}} \subset \mathcal{K}$.

$$[RMP(\bar{\mathcal{K}})]\ \min \sum_{k\in\bar{\mathcal{K}}} C_k y_k + \sum_{(k,l)\in\mathcal{P}(\bar{\mathcal{K}})} D_{kl} x_{kl} \tag{3.30}$$

$$\text{s.t.} \sum_{k\in\bar{\mathcal{K}}_i} y_k = 2 \qquad (\alpha_i) \quad \forall i \in \mathcal{I} \tag{3.31}$$

$$y_k - \sum_{l:(k,l)\in\mathcal{P}(\bar{\mathcal{K}}_i)} x_{kl} \leq 0 \qquad (\lambda_{ki}) \quad \forall k \in \bar{\mathcal{K}}, \forall i \in G_k \tag{3.32}$$

$$y_k \geq 0 \qquad \forall k \in \bar{\mathcal{K}} \tag{3.33}$$

$$x_{kl} \geq 0 \qquad \forall (k,l) \in \mathcal{P}(\bar{\mathcal{K}}) \tag{3.34}$$

3.2.2 Pricing Problem

Let α and λ respectively be the dual variables associated to constraints (3.26) and (3.27). The dual model of the MP is then written as follows.

$$[\text{DMP}]\ \max \sum_{i\in\mathcal{I}} 2\alpha_i \tag{3.35}$$

$$\text{s.t.} \sum_{i\in G_k} \alpha_i + \sum_{i\in G_k} \lambda_{ki} \leq C_k \qquad \forall k \in \mathcal{K} \tag{3.36}$$

$$-\lambda_{ki} - \lambda_{li} \leq D_{kl} \qquad \forall (k,l) \in \mathcal{P}(\mathcal{K}), G_k \cap G_l = \{i\} \tag{3.37}$$

$$\alpha_i \in \mathbb{R} \qquad \forall i \in \mathcal{I} \tag{3.38}$$

$$\lambda_{ki} \leq 0 \qquad \forall k \in \mathcal{K}, \forall i \in G_k \tag{3.39}$$

Given the optimal dual variables obtained from the solution of the current $RMP(\bar{\mathcal{K}})$, we define the associated pricing subproblem in the form of a row-generating subproblem. This formulation allows us to evaluate whether a new group y_k, not yet included in the restricted set $\bar{\mathcal{K}}$, has a negative reduced cost and should be introduced into $RMP(\bar{\mathcal{K}})$.

Formally, the pricing subproblem is defined as:

$$\bar{C}^* = \min_{k \in \mathcal{K} \setminus \bar{\mathcal{K}}} \left\{ C_k - \sum_{i \in G_k} \alpha_i - \sum_{i \in G_k} \lambda_{ki} \right\} \tag{3.40}$$

Upon the addition of a new variable y_k to $RMP(\bar{\mathcal{K}})$, new coupling constraints must be introduced. Specifically, for each individual $i \in G_k$, we include the constraint (3.32) $y_k - \sum_{l \in \bar{\mathcal{K}}_i, G_l \cap G_k = \{i\}} x_{lk} \leq 0$ along with the corresponding auxiliary variables x_{lk}. If no group $l \in \bar{\mathcal{K}}_i$ exists such that $G_l \cap G_k = \{i\}$, the constraint reduces to $y_k \leq 0$, ensuring that y_k cannot take a positive value in the solution unless new compatible groups are introduced in subsequent iterations. In that case, the corresponding dual variable λ_{ki} is not active and is set to zero. This dependency structure characterizes our model as a *column-dependent row problem with restricted pairs*, where each new variable y_k introduces not only a column but also a specific subset of induced constraints and variables determined by its individual overlaps with existing groups in $\bar{\mathcal{K}}$.

The main challenge lies in evaluating the reduced cost $\bar{C}_k^*$ when the dual variables λ_{ki} do not exist in the current $RMP(\bar{\mathcal{K}})$. Neglecting these terms would result in an underestimation of the true reduced cost, potentially leading to the inclusion of non-beneficial columns y_k with falsely negative reduced costs. Hence, to ensure the optimality of the column-and-row generation process, a principled estimation of the missing dual variables λ_{ki} is necessary.

In the framework of Muter et al. Muter *et al.* (2013), three types of pricing problems are defined: *y-pricing*, which evaluates reduced cost using only existing dual variables; *x-pricing*, which evaluates auxiliary variables independently; and *row-generating pricing*, which accounts for new variables along with their induced constraints. In our setting, *y-pricing* is inappropriate because omitting λ_{ki} may systematically produce negative reduced costs. *x-pricing* is also inapplicable, as the x_{kl} variables are purely auxiliary–they can only be active when both y_k and y_l are in the model and selected. Thus, the appropriate pricing approach is the *row-generating pricing* problem.

The row-generating pricing problem, tailored to our formulation, is written as:

$$\bar{C}^* = \min_{k \in \mathcal{K} \setminus \bar{\mathcal{K}}} \quad C_k - \sum_{i \in G_k} \alpha_i - \sum_{i \in G_k} \lambda_{ki} \tag{3.41}$$

$$\text{s.t.} \quad -\lambda_{ki} \leq D_{lk} + \lambda_{li} \qquad \forall i \in G_k,\ \forall l \in \bar{\mathcal{K}}_i : G_l \cap G_k = \{i\} \tag{3.42}$$

$$\lambda_{ki} \leq 0 \qquad \forall i \in G_k \tag{3.43}$$

$$\text{at least one constraint in (3.42)-(3.43) is tight} \forall i \in G_k. \tag{3.44}$$

where constraints (3.44) impose the feasibility of the basis.

The value of λ_{ki} is trivial to compute: for each individual $i \in G_k$, we take the minimum of all values $D_{lk}+\lambda_{li}$ such that $l \in \bar{\mathcal{K}}_i$ and $G_l \cap G_k = \{i\}$, and we only consider those values that are *positive*. If no such group l exists, or if all resulting expressions are non-positive, then we set $\lambda_{ki} = 0$. Formally, we define:

$$\lambda_{ki} = \min\left\{\{0\} \cup \left\{-(D_{lk} + \lambda_{li}) \,\middle|\, l \in \bar{\mathcal{K}}_i,\ G_l \cap G_k = \{i\},\ D_{lk} + \lambda_{li} > 0\right\}\right\} \tag{3.45}$$

This guarantees that $\lambda_{ki} \leq 0$, satisfies the dual constraints, and enforces tightness whenever a positive bound exists.

Define for each pair (k, i) the index set:

$$\mathcal{M}_{ki} = \left\{l \in \bar{\mathcal{K}}_i \,\middle|\, G_l \cap G_k = \{i\},\ D_{lk} + \lambda_{li} > 0\right\} \tag{3.46}$$

Then the simplified pricing objective becomes:

$$\bar{C}^* = \min_{k \in \mathcal{K} \setminus \bar{\mathcal{K}}} \left\{ C_k - \sum_{i \in G_k} \alpha_i + \sum_{i \in G_k} \min\left\{\{0\} \cup \{-(D_{lk} + \lambda_{li}) \,|\, l \in \mathcal{M}_{ki}\}\right\} \right\} \tag{3.47}$$

This formulation ensures that the pricing problem evaluates each potential column y_k consistently enabling an optimal column-and-row generation algorithm.

In what follows, we denote by $G'_k \subset \mathcal{I}, k' \in \mathcal{K} \setminus \bar{\mathcal{K}}$ the candidate group of L individuals. Once constructed, if its reduced cost is negative, G'_k will be added to the $RMP(\bar{\mathcal{K}})$ as a new column.

Let us introduce the binary variable ω_i which equals 1 if individual i is selected, 0 otherwise. An integer nonlinear formulation of the PP is as follows (please refer to the definition of constants Q, R, U in 2.18 in (2.18) in Section 2.2.3).

$$\begin{aligned}
[\mathrm{F}^2_{\mathrm{PP}}] \ \min \quad & Q \sum_{i \in \mathcal{I}} (1 - p^i)\omega_i \\
& - R \prod_{i \in \mathcal{I}} (1 - p^i \omega_i) \\
& - \sum_{i \in \mathcal{I}} \alpha_i \omega_i + \sum_{i \in \mathcal{I}} \omega_i \min\left\{\{0\} \cup \{-(D_{lk} + \lambda_{li}) \,|\, l \in \mathcal{M}_{k'i}\}\right\} && (3.48) \\
\text{s.t.} \quad & \sum_{i \in \mathcal{I}} \omega_i = L && (3.49) \\
& \omega_i \in \{0, 1\} \qquad \forall i \in \mathcal{I} && (3.50)
\end{aligned}$$

The term $D_{lk'}$ is computed for the group G'_k, for the individual $i \in G'_k$, for an existing group $l \in \bar{\mathcal{K}}_i, G_l \cap G'_k = \{i\}$ as:

$$D_{lk'} = U(1 - p^i) \prod_{j \in \mathcal{J}, j \neq i} (1 - p^j \omega_j) \prod_{h \in \mathcal{J}, h \neq i} (1 - p^h c_{hl}) \tag{3.51}$$

with c_{hl} a binary parameter indicating if individual h is present in group $G_l, l \in \bar{\mathcal{K}}$.

3.2.3 Solution Methods for the Pricing Problem

Solving the formulation $\mathrm{F}^2_{\mathrm{PP}}$ is challenging. In particular, estimating the missing dual variables λ involves an inner minimization that can only be performed once the group under construction is fully defined.

In this section, we present a nonlinear formulation for the PP, adapted from formulation $\mathrm{F}^2_{\mathrm{PP}}$, that incorporates this inner minimization directly, and can be solved using a commercial solver capable of handling nonlinear expressions. We also introduce an exact labeling algorithm and a heuristic adaptation.

3.2.3.1 A Nonlinear Formulation for the PP

Unlike the formulation in Section 2.3, where the equivalent product $\prod_{i \in \mathcal{J}}(1 - p^i \omega_i)$ was linearized, we now propose a nonlinear formulation that retains this product in its original form. More importantly, we embed the *inner minimization* used to estimate the missing dual variables $\lambda_{k'i}$ directly within the pricing problem.

When a candidate group $G_{k'}$ is considered (i.e. $\sum_{i \in \mathcal{J}} \omega_i = L$), the corresponding dual variable $\lambda_{k'i}$ for individual i must be computed by minimizing over groups $G_l \in \bar{\mathcal{K}}_i$ that intersect $G_{k'}$ only at i, and whose cost $D_{lk'} + \lambda_{li}$ is non-negative. If such groups exist, the minimum of these costs is used to estimate $\lambda_{k'i}$. Otherwise, $\lambda_{k'i}$ is set to zero.

To model this, we introduce binary variables $\gamma_{il} \in \{0, 1\}$, which equal 1 when group $G_l \in \bar{\mathcal{K}}_i$ is selected for individual i in the dual estimation. Their contribution to the objective function is:

$$\sum_{i \in \mathcal{J}} \sum_{l \in \bar{\mathcal{K}}_i} \gamma_{il} \left[U \cdot \frac{\prod_{h \in \mathcal{J}}(1 - p^h c_{hl})}{1 - p^i} \cdot \prod_{j \in \mathcal{J}} (1 - p^j \omega_j) + \lambda_{li} \right].$$

To control the validity of each group selection, we define indicator binary variables $\varphi_{il}, \psi_{il} \in \{0, 1\}$ and $\xi_i \in \{0, 1\}$. Here, $\varphi_{il} = 1$ if G_l intersects $G_{k'}$ exactly at i; $\psi_{il} = 1$ if the cost associated with selecting G_l is non-negative; and $\xi_i = 1$ if there exists at least one such valid group.

We enforce these structural constraints:

$$\varphi_{il} \leq \omega_i, \qquad \forall i \in \mathcal{I},\ l \in \bar{\mathcal{K}}_i, \tag{3.52}$$

$$\varphi_{il} + \omega_j \leq 1, \qquad \forall i \in \mathcal{I},\ j \in G_l \setminus \{i\}, \tag{3.53}$$

$$\varphi_{il} \geq \omega_i - \sum_{j \in G_l \setminus \{i\}} \omega_j, \qquad \forall i \in \mathcal{I},\ l \in \bar{\mathcal{K}}_i, \tag{3.54}$$

$$\varphi_{il} \in \{0,1\}, \qquad \forall i \in \mathcal{I},\ l \in \bar{\mathcal{K}}_i. \tag{3.55}$$

Define the cost expression for group G_l as:

$$\mu_{il} = (1-Sp)(Se+Sp-1)^2 \cdot \frac{\prod_{h \in \mathcal{J}}(1-p^h c_{hl})}{1-p^i} \cdot \prod_{j \in \mathcal{J}}(1-p^j\omega_j) + \lambda_{li}.$$

We model the activation of ψ_{il} based on whether $\mu_{il} \geq 0$ using a two-sided big-M formulation:

$$\mu_{il} \leq M_{il}^{\text{up}} \cdot \psi_{il}, \qquad \forall i \in \mathcal{I},\ l \in \bar{\mathcal{K}}_i, \tag{3.56}$$

$$\mu_{il} \geq M_{il}^{\text{low}} \cdot (\psi_{il} - 1), \qquad \forall i \in \mathcal{I},\ l \in \bar{\mathcal{K}}_i, \tag{3.57}$$

$$\psi_{il} \leq \varphi_{il}, \qquad \forall i \in \mathcal{I},\ l \in \bar{\mathcal{K}}_i, \tag{3.58}$$

$$\psi_{il} \in \{0,1\}, \qquad \forall i \in \mathcal{I},\ l \in \bar{\mathcal{K}}_i. \tag{3.59}$$

The constants M_{il}^{up} and M_{il}^{low} are customized for each pair (i,l) to tightly bound the expression μ_{il}, defined as:

$$M_{il}^{\text{up}} = U \cdot \frac{\prod_{h \in \mathcal{J}}(1-p^h c_{hl})}{1-p^i} \cdot \prod_{j \in \mathcal{S}^{\min}}(1-p^j) + \lambda_{li},$$

where $\mathcal{S}^{\min}$ denotes the set of L individuals with the smallest values of $(1-p^j)$, to obtain an upper bound on the product term.

Similarly, we set:

$$M_{il}^{\text{low}} = U \cdot \frac{\prod_{h \in \mathcal{J}}(1-p^h c_{hl})}{1-p^i} \cdot \prod_{j \in \mathcal{S}^{\max}}(1-p^j) + \lambda_{li},$$

where $\mathcal{S}^{\max}$ is the set of L individuals with the largest values of $(1-p^j)$, ensuring that the lower bound accommodates the worst-case (smallest) value of μ_{il} over all feasible ω configurations.

To evaluate the existence of at least one valid group for i, we impose:

$$\xi_i \geq \varphi_{il} \cdot \psi_{il}, \qquad \forall i \in \mathcal{I},\ l \in \bar{\mathcal{K}}_i, \tag{3.60}$$

$$\xi_i \leq \sum_{l \in \bar{\mathcal{K}}_i} \varphi_{il} \cdot \psi_{il}, \qquad \forall i \in \mathcal{I}, \tag{3.61}$$

$$\xi_i \in \{0, 1\}, \qquad \forall i \in \mathcal{I}. \tag{3.62}$$

In addition, to ensure that group G_l is selected for i only when it both intersects exactly at i and has a non-negative cost, we impose:

$$\gamma_{il} \leq \varphi_{il}, \qquad \forall i \in \mathcal{I},\ l \in \bar{\mathcal{K}}_i, \tag{3.63}$$

$$\gamma_{il} \leq \psi_{il}, \qquad \forall i \in \mathcal{I},\ l \in \bar{\mathcal{K}}_i. \tag{3.64}$$

Finally, to enforce that the selection of individual i in G'_k depends on the existence of an exact intersection in i and with corresponding $D_{lk'} + \lambda_{li} \geq 0$, we couple these auxiliary variables with the following constraints:

$$\sum_{l \in \bar{\mathcal{K}}_i} \gamma_{il} = \omega_i \cdot \xi_i \quad \forall i \in \mathcal{I}. \tag{3.65}$$

The full PP ($\mathrm{F}^3_{\mathrm{PP}}$) is then:

$$\begin{aligned}
[\mathrm{F}^3_{\mathrm{PP}}]\ \min\quad & Q \sum_{i \in \mathcal{I}} (1 - p^i)\omega_i - R \prod_{i \in \mathcal{I}} (1 - p^i \omega_i) - \sum_{i \in \mathcal{I}} \alpha_i \omega_i \\
& + \sum_{i \in \mathcal{I}} \sum_{l \in \bar{\mathcal{K}}_i} \gamma_{il} \left[U \frac{\prod_{h \in \mathcal{I}} (1 - p^h c_{hl})}{1 - p^i} \prod_{i \in \mathcal{I}} (1 - p^i \omega_i) + \lambda_{li} \right] \\
\text{s.t.}\quad & (3.49) - (3.50), (3.52) - (3.65).
\end{aligned} \tag{3.66}$$

3.2.3.2 Exact Labeling Algorithm for the PP

The PP can be modeled as a constrained shortest path problem on an acyclic graph, where each path must have exactly $L+1$ arcs. Below, we describe how the graph is built and outline our solution approach.

Let $G = (V, A)$ be the acyclic graph with node set $V = \{0\} \cup \mathcal{I} \cup \{N+1\}$, where $\mathcal{I}$ represents the individuals and 0 and $N+1$ are two artificial individuals with risks $p^0 = p^{N+1} = 0$. The arc set is defined as $A = \{(i, j) : i, j \in V,\ i < j\}$. Selecting an arc (i, j) implies that individuals i and j are in the group. By construction, the graph is acyclic since an ordered group of size L represents all permutations of its members. The objective is to find the shortest path from node 0 to node $N+1$ that uses exactly $L+1$ arcs, which corresponds to selecting a group of L individuals with minimum reduced cost.

The algorithm is based on a labeling approach, extending labels from node to node

while maintaining column feasibility. However, the reduced cost in the objective function of $\mathrm{F}^2_{\mathrm{PP}}$ does not have a cumulative property. Let $Q = \frac{(1-Sp)Se^2}{2}$ and $R = L(1-Sp)Se(Se+Sp-1)$ be two constant coefficients in the objective function in $\mathrm{F}^2_{\mathrm{PP}}$. Given a candidate group G'_k, the reduced cost of the corresponding column can be expressed as:

$$\bar{C} = \underbrace{\sum_{i \in G'_k} \left(Q(1-p^i) - \alpha_i\right)}_{\text{Additive Part}} + \underbrace{R \prod_{i \in G'_k} (1-p^i)}_{\text{Multiplicative Part}} + \underbrace{\sum_{i \in G'_k} \min\left\{\{0\} \cup \{-(D_{lk} + \lambda_{li}) \,|\, l \in \mathcal{M}_{k'i}\}\right\}}_{\text{Minimization Part (when group } G'_k \text{ is complete)}} \tag{3.67}$$

The last term can only be computed once a full group G'_k of size L is formed. It accounts for the estimation of missing dual variables λ_{li} using existing columns in the current master problem that overlap with G'_k on exactly one individual.

Unfortunately, this structure prevents the use of standard dynamic programming techniques, making it harder to develop effective dominance rules or lower bounds that help reduce the search space. Consequently, the labeling algorithm must explore all possible groups of size L and applies dominance rules only to complete groups.

The exact pricing labeling algorithm can be viewed as a smart enumeration technique. While it currently lacks dominance rules for partial labels (i.e., incomplete groups of size L) and does not incorporate bounding strategies for early pruning, it becomes notably more effective once a group is fully constructed, enabling the application of dominance rules. Its key strength lies in its ability to generate not only the optimal reduced-cost column but also multiple columns with negative reduced costs. This significantly reduces the need for repeated calls to the pricing algorithm, thereby lowering the overall computational effort. As a result, it proves particularly powerful for small-sized instances, where guided enumeration remains both feasible and efficient.

Technically, each path $P_{0,j} = \{0, i_1, i_2, \cdots, j\}$ of length less than or equal to $L+1$ (representing a subgroup of size less than or equal to L) is represented by a label $\mathcal{L} = (\{i : i \in P_{0,j}\}, \theta_1, \theta_2, \bar{C})$, where θ_1 is the first objective term involving the linear term $\sum_{i \in \mathcal{J}}(Q(1-p^i) - \alpha_i)\omega_i$, θ_2 is the second objective term dealing with the nonlinear part $R\prod_{i \in \mathcal{J}}(1-p^i\omega_i)$ of the objective function, and $\bar{C}$ being the computation of the complete reduced cost when the path $P_{0,j}$ is of length $L+1$ representing a group of exactly L individuals. $\bar{C}$ is computed only when the corresponding G'_k is completed and only when this is satisfied, we compute $\bar{C}$ as $\bar{C} = \theta_1 - \theta_2 + \sum_{i \in G'_k} \min\{\{0\} \cup \{-(D_{lk} + \lambda_{li}) \,|\, l \in \mathcal{M}_{k'i}\}\}$. When a path $P_{0,j}$ is of length $L+1$, the path is extended to node $N+1$.

For each individual j in the sequence, the algorithm extends existing labels by evaluating all preceding individuals i, updating the labels. When a label represents a complete group, dominance rules are applied. Consider two labels, $\mathcal{L}^i_1$ and $\mathcal{L}^i_2$, each corresponding to a group of size L at node i. We say that $\mathcal{L}^i_1$ dominates $\mathcal{L}^i_2$ if $\theta_1^{\mathcal{L}^i_1} \leq \theta_1^{\mathcal{L}^i_2}$, $\theta_2^{\mathcal{L}^i_1} \geq \theta_2^{\mathcal{L}^i_2}$, and $\bar{C}_1 \leq \bar{C}_2$. Only non-dominated labels, which offer the best trade-off between the ob-

jectives, are retained. These labels form the Pareto front representing the best possible groups.

The algorithm continues extending and evaluating labels until all paths in the graph have been explored. For efficiency, since adding a column (y_k) to the $RMP(\bar{\mathcal{K}})$ also entails introducing all associated x_{lk} variables and linking constraints (3.32), we do not incorporate every column from the Pareto front. Instead, for each individual, we select the best column to add to the $RMP(\bar{\mathcal{K}})$. The entire procedure is summarized in Algorithm 3.

3.2.3.3 Heuristics Based on the Exact Labeling Algorithm

Before applying the exact labeling algorithm, we invoke heuristic labeling approaches to accelerate the solution of the PP and reduce the computational burden for large populations. In particular, we use two heuristics: the *Sub-population Decomposition Heuristic* and the *Label Limit Heuristic*.

Sub-population Decomposition Heuristic. This heuristic partitions the initial population $\mathcal{I}$ (with N individuals) into s sub-populations, where s is chosen such that $2 \leq s \leq N/L$ and each sub-population contains at least L individuals to ensure feasibility. Let $q = \lfloor N/s \rfloor$ and $r = N - s \cdot q$. In practice, if $r = 1$, then the first $s - 1$ sub-populations contain q individuals each, while the last sub-population contains $q + 1$ individuals. In each run, $\mathcal{I}$ is randomly shuffled and partitioned accordingly, and the exact labeling algorithm is applied independently to each sub-population. The resulting columns are then added to the $RMP(\bar{\mathcal{K}})$.

Label Limit Heuristic. To further reduce complexity, this heuristic restricts the number of labels maintained at each node. Based on preliminary experiments, we limit the number of labels for each incomplete group size (from 3 to $L - 1$) to at most 10. Specifically, after extending labels from node i to node j (for all $i < j$), we prune in node j the set of labels for each intermediate group size $L' \in [3, L - 1]$ to a maximum of 10 labels based on the smallest objectives values θ_1 and $-\theta_2$.

Overall, to solve the PP $\mathrm{F}^2_{\mathrm{PP}}$, we employ a heuristic chain that begins with these heuristics and finishes with an exact pricing algorithm either the one described in Section 3.2.3.1 or in Section 3.2.3.2. If the heuristics do not yield columns with negative reduced costs, the exact pricing algorithm is applied. This structured approach efficiently explores negatively priced columns, starting with computationally less demanding methods and moving to exact pricing algorithm as needed.

Algorithm 3 Exact Labeling Algorithm for $\mathrm{F}^2_{\mathrm{PP}}$

Input: Population $\mathcal{I}$, Group size L, (α, λ), $\bar{\mathcal{K}}$
Output: Set of best labels (Pareto front) representing complete groups of size L
Initialize: Graph $G = (V, A)$, Node set $V = \{0, \mathcal{I}, N+1\}$, Arc set $A = \{(i,j) : i, j \in V, i < j\}$
Initialize: Set of labels $\mathcal{L} = \emptyset$, Start at node 0
for all nodes $j \in V \setminus \{0\}$ **do**
    for all nodes $i < j$ **do**
        for all labels $\mathcal{L}$ ending at node i **do**
            if adding j does not violate constraints **then**
                Extend label $\mathcal{L}$ to j
                Update label $\mathcal{L}$ with new objectives terms θ_1 and θ_2
                if label $\mathcal{L}$ forms a complete group (size L) **then**
                    Compute full reduced cost $\bar{C}_{\mathcal{L}}$
                    for all existing labels $\mathcal{L}'$ at node $N+1$ **do**
                        if $\theta_1^{\mathcal{L}'} \leq \theta_1^{\mathcal{L}}$ and $\theta_2^{\mathcal{L}'} \leq \theta_2^{\mathcal{L}}$ and $\bar{C}_{\mathcal{L}'} \leq \bar{C}_{\mathcal{L}}$ **then**
                            Do not extend label $\mathcal{L}$ to node $N+1$ (label $\mathcal{L}'$ dominates $\mathcal{L}$)
                            continue to next label
                        else if $\theta_1^{\mathcal{L}} \leq \theta_1^{\mathcal{L}'}$ and $\theta_2^{\mathcal{L}} \leq \theta_2^{\mathcal{L}'}$ and $\bar{C}_{\mathcal{L}} \leq \bar{C}_{\mathcal{L}'}$ **then**
                            Mark label $\mathcal{L}'$ as dominated
                        end if
                    end for
                    Remove all dominated labels at node $N+1$
                    Add label $\mathcal{L}$ to node $N+1$ if not dominated
                end if
            end if
        end for
    end for
end for
Return the best column for each individual at node $N+1$

3.2.4 Initialization of $RMP(\bar{\mathcal{K}})$

To accelerate the simultaneous column-and-row generation, we populate the set $\bar{\mathcal{K}}$ with columns generated by heuristics from the literature–**GRADIENT** and **SPIRAL** (when applicable)–as well as our heuristics: **LEAST**, **HIGHEST**, and **BOTH** (when applicable), all previously described in Section 2.4. Additionally, we include columns refined through the Iterative Ejection Cycles local search, $\mathcal{LS}_{IEC}$ (see Algorithm 2). Duplicate columns are removed.

Once these columns are added to the $RMP(\bar{\mathcal{K}})$, we solve it with y_k as binary to com-

pute an upper bound that may be better than the best individual heuristic solution. This step guarantees an efficient starting point for the subsequent column-and-row generation.

3.2.5 Lagrangian Lower Bound

In the following, we compute the Lagrangian lower bound on the optimal value of the MP. Let us reconsider the MP to which we add the two redundant constraints (3.71) and (3.72). Constraint (3.71) ensures that the number of groups is equal to $\frac{2N}{L}$. Constraints (3.72) impose that each individual is exactly in one intersection. The dual variables corresponding to the constraints are given in brackets.

$$\min \sum_{k\in\mathcal{K}} C_k y_k + \sum_{(k,l)\in\mathcal{P}(\mathcal{K})} D_{kl} x_{kl} \tag{3.68}$$

$$\text{s.t.} \sum_{k\in\mathcal{K}_i} y_k = 2 \qquad (\alpha_i) \quad \forall i \in \mathcal{I} \tag{3.69}$$

$$y_k - \sum_{l:(k,l)\in\mathcal{P}(\mathcal{K}_i)} x_{kl} \leq 0 \qquad (\lambda_{ki}) \quad \forall k \in \mathcal{K}, \forall i \in G_k \tag{3.70}$$

$$\sum_{k\in\mathcal{K}} y_k = \frac{2N}{L} \qquad (\pi) \tag{3.71}$$

$$\sum_{(k,l)\in\mathcal{P}(\mathcal{K}_i)} x_{kl} = 1 \qquad (\beta_i) \quad \forall i \in \mathcal{I} \tag{3.72}$$

$$y_k \geq 0 \qquad \forall k \in \mathcal{K} \tag{3.73}$$

$$x_{kl} \geq 0 \qquad \forall (k,l) \in \mathcal{P}(\mathcal{K}) \tag{3.74}$$

We relax constraints (3.69) and (3.70) by dualizing them in the objective function with respective multipliers α and λ. We factorize by y_k and x_{kl} in the objective function. Let $L(\alpha,\lambda) : \mathbb{R}^{|\mathcal{I}|} \times \mathbb{R}_{\leq 0}^{|\mathcal{K}|\times L} \to \mathbb{R}$ be the *dual function* defined as in (3.75).

$$\begin{aligned} L(\alpha,\lambda) = \min \Bigg\{ & \sum_{i\in\mathcal{I}} 2\alpha_i + \min \sum_{k\in\mathcal{K}} \left(C_k - \sum_{i\in G_k} \alpha_i - \sum_{i\in G_k} \lambda_{ki} \right) y_k \\ & + \sum_{i\in\mathcal{I}} \sum_{(k,l)\in\mathcal{P}(\mathcal{K}_i)} (D_{kl} + \lambda_{ki} + \lambda_{li})\, x_{kl} : (3.71), (3.74) \Bigg\}. \end{aligned} \tag{3.75}$$

The problem defined by $L(\alpha,\lambda)$, where $\alpha \in \mathbb{R}^{|\mathcal{I}|}$ and $\lambda \in \mathbb{R}_{\leq 0}^{|\mathcal{K}|}$, is a relaxation of the master problem MP. Therefore, for each $\alpha \in \mathbb{R}^{|\mathcal{I}|}$ and $\lambda \in \mathbb{R}_{\leq 0}^{|\mathcal{K}|\times L}$, the value $L(\alpha,\lambda)$ serves as a lower bound for the optimal value $\tilde{z}$ of the MP. The corresponding *Lagrangian dual problem* is defined as:

$$\text{[LGD]} \quad \max\{L(\alpha,\lambda) : \alpha \in \mathbb{R}^{|\mathcal{I}|}, \lambda \in \mathbb{R}_{\leq 0}^{|\mathcal{K}|\times L}\} \tag{3.76}$$

and it provides the best possible lower bound among these values.

By duality, problem LGD can be reformulated as a linear program which corresponds to the MP. The dual of the inner minimization problem $L(\alpha, \lambda)$ is the following.

$$\max \frac{2N}{L}\pi + \sum_{i\in\mathcal{I}} \beta_i \tag{3.77}$$

$$\text{s.t.} \sum_{i\in G_k} \alpha_i + \sum_{i\in G_k} \lambda_{ki} + \pi \leq C_k \qquad \forall k \in \mathcal{K} \tag{3.78}$$

$$\beta_i - \lambda_{ki} - \lambda_{li} \leq D_{kl} \qquad \forall i \in \mathcal{I}, \forall (k,l) \in \mathcal{P}(\mathcal{K}_i) \tag{3.79}$$

$$\beta_i \in \mathbb{R} \qquad \forall i \in \mathcal{I} \tag{3.80}$$

$$\pi \in \mathbb{R} \tag{3.81}$$

The Lagrangian dual problem becomes then:

$$\text{[LGDD]} \quad \max \sum_{i\in\mathcal{I}} 2\alpha_i + \sum_{i\in\mathcal{I}} \beta_i + \frac{2N}{L}\pi \tag{3.82}$$

$$\text{s.t.} \sum_{i\in G_k} \alpha_i + \sum_{i\in G_k} \lambda_{ki} + \pi \leq C_k \qquad \forall k \in \mathcal{K} \tag{3.83}$$

$$\beta_i - \lambda_{ki} - \lambda_{li} \leq D_{kl} \qquad \forall i \in \mathcal{I}, \forall (k,l) \in \mathcal{P}(\mathcal{K}_i) \tag{3.84}$$

$$\beta_i \in \mathbb{R} \qquad \forall i \in \mathcal{I} \tag{3.85}$$

$$\pi \in \mathbb{R} \tag{3.86}$$

$$\alpha_i \in \mathbb{R} \qquad \forall i \in \mathcal{I} \tag{3.87}$$

$$\lambda_{ki} \leq 0 \qquad \forall k \in \mathcal{K}, \forall i \in G_k \tag{3.88}$$

If we note y and x the dual variables associated with constraints (3.83) and (3.84) respectively, then the dual of the Lagrangian dual problem LGDD is the MP.

Now, let $(\bar{\alpha}, \bar{\lambda}, \bar{\beta}, \bar{\pi})$ be an optimal solution of the dual of the $RMP(\bar{\mathcal{K}})$. We first write the Lagrangian $L(\bar{\alpha}, \bar{\lambda})$ in terms of the optimal values of the $RMP(\bar{\mathcal{K}})$ and of the PP F^1_{PP}.

$$
\begin{aligned}
L(\bar{\alpha},\bar{\lambda}) = & \sum_{i\in\mathcal{I}} 2\bar{\alpha}_i \\
& + \min\left\{\sum_{k\in\bar{\mathcal{K}}}\left(C_k - \sum_{i\in G_k}\bar{\alpha}_i - \sum_{i\in G_k}\bar{\lambda}_{ki}\right) y_k \right. \\
& \left. + \sum_{i\in\mathcal{I}}\sum_{(k,l)\in\mathcal{P}(\mathcal{K}_i)}\left(D_{kl} + \bar{\lambda}_{ki} + \bar{\lambda}_{li}\right) x_{kl}\right\} \\
\text{s.t.} & \sum_{k\in\bar{\mathcal{K}}} y_k = \frac{2N}{L}, && && (3.89)\\
& \sum_{(k,l)\in\mathcal{P}(\bar{\mathcal{K}}_i)} x_{kl} = 1, && \forall i\in\mathcal{I}, && (3.90)\\
& y_k \geq 0, && \forall k\in\bar{\mathcal{K}}, && (3.91)\\
& x_{kl} \geq 0, && \forall (k,l)\in\mathcal{P}(\bar{\mathcal{K}}). && (3.92)
\end{aligned}
$$

Remark that given $(\bar{\alpha},\bar{\lambda},\bar{\beta},\bar{\pi})$ an optimal solution of the dual of the $RMP(\bar{\mathcal{K}})$, the reduced cost of a variable y_k is $\bar{C}_k = C_k - \sum_{i\in G_k}\bar{\alpha}_i - \sum_{i\in G_k}\bar{\lambda_{ki}} - \bar{\pi}$. Hence we have $\bar{C}_k + \bar{\pi} = C_k - \sum_{i\in G_k}\bar{\alpha}_i - \sum_{i\in G_k}\bar{\lambda_{ki}}$.

We know that $\sum_{i\in\mathcal{I}} 2\bar{\alpha}_i + \sum_{i\in\mathcal{I}}\bar{\beta}_i + \frac{2N}{L}\bar{\pi}$ is the optimal value of the dual of the $RMP(\bar{\mathcal{K}})$ by strong duality. We have $\sum_{i\in\mathcal{I}} 2\bar{\alpha}_i + \sum_{i\in\mathcal{I}}\bar{\beta}_i + \frac{2N}{L}\bar{\pi} = z^*$.

We can then write:

$$
\begin{aligned}
L(\bar{\alpha},\bar{\lambda}) = & z^* - \sum_{i\in\mathcal{I}}\bar{\beta}_i - \frac{2N}{L}\bar{\pi} \\
& + \min\left\{\sum_{k\in\bar{\mathcal{K}}}\left(\bar{C}_k + \bar{\pi}\right) y_k \right. \\
& \left. + \sum_{i\in\mathcal{I}}\sum_{(k,l)\in\mathcal{P}(\mathcal{K}_i)}\left(D_{kl} + \bar{\lambda}_{ki} + \bar{\lambda}_{li}\right) x_{kl}\right\} \\
\text{s.t.} & \sum_{k\in\bar{\mathcal{K}}} y_k = \frac{2N}{L}, && && (3.93)\\
& \sum_{(k,l)\in\mathcal{P}(\bar{\mathcal{K}}_i)} x_{kl} = 1, && \forall i\in\mathcal{I}, && (3.94)\\
& y_k \geq 0, && \forall k\in\bar{\mathcal{K}}, && (3.95)\\
& x_{kl} \geq 0, && \forall (k,l)\in\mathcal{P}(\bar{\mathcal{K}}). && (3.96)
\end{aligned}
$$

Minimizing the term $\sum_{i\in\mathcal{I}}\sum_{(k,l)\in\mathcal{P}(\mathcal{K}_i)}\left(D_{kl} + \bar{\lambda}_{ki} + \bar{\lambda}_{li}\right) x_{kl}$ in the objective function, along with the constraints (3.94) and (3.96), has a straightforward solution. Specifically,

this part simplifies to $\sum_{i\in\mathcal{I}} \min_{(k,l)\in\mathcal{P}(\mathcal{K}_i)}\{D_{kl}+\bar{\lambda}_{ki}+\bar{\lambda}_{li}\}$. Substituting this term into the expression for $L(\bar{\alpha},\bar{\lambda})$ gives:

$$\begin{aligned} L(\bar{\alpha},\bar{\lambda}) = z^* &- \sum_{i\in\mathcal{I}} \bar{\beta}_i - \frac{2N}{L}\bar{\pi} \\ &+ \sum_{i\in\mathcal{I}} \min_{(k,l)\in\mathcal{P}(\mathcal{K}_i)} \{D_{kl}+\bar{\lambda}_{ki}+\bar{\lambda}_{li}\} \\ &+ \min \sum_{k\in\bar{\mathcal{K}}} (\bar{C}_k+\bar{\pi})y_k \\ \text{s.t.} \sum_{k\in\bar{\mathcal{K}}} y_k &= \frac{2N}{L}, \qquad (3.97) \\ y_k &\geq 0, \quad \forall k\in\bar{\mathcal{K}}. \qquad (3.98) \end{aligned}$$

However, as previously noted, the term $\sum_{i\in\mathcal{I}} \bar{\beta}_i$ is equivalent to $\sum_{i\in\mathcal{I}} \min_{(k,l)\in\mathcal{P}(\mathcal{K}_i)}\{D_{kl}+\bar{\lambda}_{ki}+\bar{\lambda}_{li}\}$. Substituting this term into the equation, $L(\bar{\alpha},\bar{\lambda})$ simplifies further to:

$$\begin{aligned} L(\bar{\alpha},\bar{\lambda}) = z^* &- \frac{2N}{L}\bar{\pi} + \min \sum_{k\in\bar{\mathcal{K}}} (\bar{C}_k+\bar{\pi})y_k \\ \text{s.t.} \sum_{k\in\bar{\mathcal{K}}} y_k &= \frac{2N}{L}, \qquad (3.99) \\ y_k &\geq 0, \quad \forall k\in\bar{\mathcal{K}}. \qquad (3.100) \end{aligned}$$

The inner minimization problem related to the sum over k, given by the term $\sum_{k\in\bar{\mathcal{K}}}(\bar{C}_k+\bar{\pi})y_k$ together with constraints (3.99)-(3.100), has a trivial solution:

$$\hat{y_k} = \begin{cases} \frac{2N}{L} & \text{if } k = k^* \\ 0 & \text{otherwise} \end{cases}$$

where k^* is the optimal solution of the PP defined in $\mathrm{F}^1_{\mathrm{PP}}$. Substituting this into the expression for $L(\bar{\alpha},\bar{\lambda})$ gives:

$$L(\bar{\alpha},\bar{\lambda}) = z^* - \frac{2N}{L}\bar{\pi} + \frac{2N}{L}(\bar{C}_{k^*}+\bar{\pi}) = z^* + \frac{2N}{L}\bar{C}_{k^*}. \qquad (3.101)$$

Thus, at every iteration of the column and row generation process, a lower bound on the optimal value of the MP is determined by the expression (3.101).

3.2.6 Simultaneous Column-and-Row Generation Overview

Algorithm 4 begins with the initialization of $RMP(\bar{\mathcal{K}})$ using a set of feasible solutions as described in Section 3.2.4. Then, the column-and-row generation process is iteratively

applied as follows:

1. Solve the current $RMP(\bar{\mathcal{K}})$.
2. Solve the pricing problem $\mathrm{F}^1_{\mathrm{PP}}$ to generate new columns.
3. Calculate the Lagrangian lower bound $L(\bar{\alpha}, \bar{\lambda})$ at each iteration. If the pricing problem is solved heuristically, the lower bound is a heuristic bound, which tends to overestimate the value. If the pricing problem is solved exactly, the Lagrangian lower bound is exact.
4. If the heuristic lower bound is below a specified threshold (e.g., a 1% gap with the value of the $RMP(\bar{\mathcal{K}})$), the heuristic is deactivated in subsequent iterations. This allows the algorithm to pass control to another heuristic or the exact pricing algorithm, ensuring better columns are found and mitigating the tailing-off effect.
5. If the pricing problem is solved exactly and the gap between the Lagrangian lower bound and the $RMP(\bar{\mathcal{K}})$ value is below 1%, the algorithm proceeds to check the solution type:
   - If the solution is fractional, the column-and-row generation process is finished with a gap below 1%.
   - If the solution is integer, the algorithm continues to check whether or not the solution is optimal by repeating the process until either the solution becomes fractional or no further improving columns are found. This step is crucial in the Branch-and-Price context, as an integer solution at a 1% gap may otherwise lead to prematurely terminating the node exploration, leaving no fractional variables to branch on.
6. If no improving columns are found by any method, the column-and-row generation process terminates.

The approach ensures that, when new columns are found, they are added to the $RMP(\bar{\mathcal{K}})$ along with the corresponding induced variables x_{lk} and linking constraints (3.32). Additionally, for existing variables y_l, the constraints (3.32) may be adjusted to consider potential intersections with the new columns through x_{lk}. This iterative process continues until either the gap between the Lagrangian lower bound and the $RMP(\bar{\mathcal{K}})$ value falls below 1%, or no more improving columns are found. If the time limit for the column-and-row generation process is reached before invoking the exact pricing algorithm, the algorithm switches to the exact pricing algorithm to obtain a valid Lagrangian lower bound to compute an optimality gap.

Algorithm 4 Simultaneous column-and-row Generation

Output: a solution within 1% gap for MP.

1: Initialize $RMP(\bar{\mathcal{K}})$ with a set of feasible solutions.
2: **repeat**
3: Solve $RMP(\bar{\mathcal{K}})$ and obtain dual variables α and λ.
4: Solve $\mathrm{F}^1_{\mathrm{PP}}$ starting from heuristics and moving to the exact pricing algorithm if necessary.
5: Add new negatively priced columns y_k to $RMP(\bar{\mathcal{K}})$.
6: Add new induced variables x_{lk} to $RMP(\bar{\mathcal{K}})$.
7: Add new induced constraints (3.32) to $RMP(\bar{\mathcal{K}})$.
8: Add the corresponding new induced variables x_{lk} in constraints (3.32) for the already existing groups G_l, $\forall i \in G_k$ if $G_l \cap G_k = \{i\}$.
9: **until** no column is found with a negative reduced cost or a gap of 1% or less is reached and the solution is fractional.

If during an iteration of Algorithm 4 the solution of $RMP(\bar{\mathcal{K}})$ is integer, we compare its value to the best known upper bound. If it is better than the latter, we update the best upper bound.

3.3 Branch-and-Price Algorithm

To solve $\mathrm{F}^{\mathrm{EXT}}_{\mathrm{RLT}}$, we have developed a Branch-and-Price algorithm (Desrosiers & Lübbecke, 2011) that embeds the column-and-row generation previously presented. This approach is a variant on the Branch-and-Bound technique, where a column generation procedure solves the linear relaxation of the restricted master problem at each node. In our context, the Branch-and-Bound search tree is explored using the depth-first strategy to quickly find integer solutions and potentially improve the upper bound. In the following, we present the branching rules used and the primal heuristic designed.

3.3.1 Branching Rules

In the following, let $(\bar{y}, \bar{x})$ be a fractional solution of MP at a given node of the Branch-and-Bound tree. In this section, we introduce two types of branching rules, which will be compared empirically to assess their individual effectiveness.

3.3.1.1 Highest Fractional Variable Branching Rules

At each node, we branch on the variable with the highest fractional value (the closest to 1). We chose to branch on the highest fractional variable instead of the most fractional variable (the closest to 0.5) because preliminary empirical experiments show its superiority. Specifically, we consider two rules.

Highest fractional y_k If $\bar{y_k}$ is the highest fractional value, we impose $y_k = 1$ (including G_k) or $y_k = 0$ (excluding G_k).

Highest fractional x_{kl} If $\bar{x_{kl}}$ is the highest fractional value, we impose $x_{kl} = 1$ (forcing $y_k + y_l = 2$) or $x_{kl} = 0$ (forcing $y_k + y_l \leq 1$).

3.3.1.2 Ryan and Foster Branching Rule

When observing the structure of a feasible integer solution, two individuals i, j with $j > i$ are either together in only one group or are not together in any group which is imposed by constraints (3.11). Thus, we can use Ryan and Foster (Ryan & Foster, 1981) branching rule. The fundamental principle is to select two individuals that either have to be grouped together or cannot be grouped together. Specifically, if the optimal solution of the $RMP(\bar{\mathcal{K}})$ is fractional, then there must exist at least one pair of individuals (i, j) such that the sum of columns including i and j is fractional. That is $0 < \sum_{k \in \bar{\mathcal{K}}_i \cap \bar{\mathcal{K}}_j} \bar{y_k} < 1$. We therefore select the pair of individuals (i, j) having the highest fractional $\sum_{k \in \bar{\mathcal{K}}_i \cap \bar{\mathcal{K}}_j} \bar{y_k}$ (the closest to 1). The branching constraints are then

$$\sum_{k \in \bar{\mathcal{K}}_i \cap \bar{\mathcal{K}}_j} y_k \leq 0 \tag{3.102}$$

$$\sum_{k \in \bar{\mathcal{K}}_i \cap \bar{\mathcal{K}}_j} y_k \geq 1 \tag{3.103}$$

In the "separate" branch where i and j can not be together, we add in the pricing problem $\mathrm{F}^1_{\mathrm{PP}}$ a constraint that prevents $\mathrm{F}^1_{\mathrm{PP}}$ from generating negatively priced columns that include both i and j. However, in the "together" branch, $\mathrm{F}^1_{\mathrm{PP}}$ does not need to be modified.

Remark 3.3. *To prevent potential conflicts caused by branching constraints during the solution process, we introduce a set of dummy variables $\{\delta_i\}_{i \in \mathcal{I}}$–one for each individual (Feillet, 2010). These are added to the constraints (3.31):*

$$\sum_{k \in \bar{\mathcal{K}}_i} y_k + \delta_i = 2 \quad \forall i \in \mathcal{I},$$

and penalized in the objective function (3.30) with a large constant M:

$$\min \sum_{k \in \bar{\mathcal{K}}} C_k y_k + \sum_{(k,l) \in \mathcal{P}(\bar{\mathcal{K}})} D_{kl} x_{kl} + M \sum_{i \in \mathcal{I}} \delta_i.$$

This ensures $RMP(\bar{\mathcal{K}})$ remains feasible at all times, even if future branching decisions introduce conflicting constraints.

3.3.2 Primal Heuristic

Our approach exploits the structure of the original (compact) formulation $\mathrm{F}^{\mathrm{SYM}}_{\mathrm{MINLP}}$ to fix those individuals whose group membership is already determined by the branching rules. To do so, we construct a residual feasibility compact formulation, one with an objective function of minimizing 0, by adding the equivalent fixing constraints imposed by the branching decisions. In particular, depending on the branching decision, we add the following sets of constraints to the residual model.

Rule $y_k = 1$ or $x_{kl} = 1$ Let $\mathcal{C}$ be the indices of the groups involved in these branching constraints in the current node ($\mathcal{C} = \{k\}$ or $\mathcal{C} = \{k, l\}$) We know that the assignment of the individuals to the solution of $\mathrm{F}^{\mathrm{SYM}}_{\mathrm{MINLP}}$ must be associated with the corresponding fixed groups. To model this, we introduce the following binary variables.

$$\varphi_{kg} = \begin{cases} 1, & \text{if group } G_k \text{ is assigned to group } G_g, c \in \mathcal{C}, g \in \mathcal{G} \\ 0, & \text{otherwise.} \end{cases}$$

Then, for every fixed group G_k we impose the fixing constraints

$$\sum_{g \in \mathcal{G}} \varphi_{kg} = 1, \quad \forall\, k \in \mathcal{C}, \tag{3.104}$$

$$\sum_{i \in G_k} z_{ig} \geq L\, \varphi_{kg}, \quad \forall\, g \in \mathcal{G}, \forall\, k \in \mathcal{C} \tag{3.105}$$

Constraints (3.104) and (3.105) ensure that the individuals in each fixed group should be together in exactly one group.

Rule $y_k = 0$ Adding no-good cut constraints (3.106) where we forbid having groups that contain the individuals of the forbidden group.

$$\sum_{i \in G_c} z_{im} \leq L - 1, \quad \forall\, m \in \mathcal{G}, \forall\, c \in \mathcal{C} \tag{3.106}$$

Rule $x_{kl} = 0$ Adding no-good cut constraints (3.107) where we forbid the simultaneous full selection of two groups that are not allowed to appear together. In particular, for each pair (G_k, G_l) for which $x_{kl} = 0$ is fixed, we impose

$$\sum_{i \in G_k} z_{im} + \sum_{i \in G_l} z_{in} \leq 2L - 1 \quad \forall\, m, n \in \mathcal{G}, m < n, \tag{3.107}$$

Rule Ryan and Foster "Together": When the branching decision requires that individuals i and j must appear together in exactly one group, we add constraint (3.108)

to enforce that there exists precisely one group in which both individuals are assigned.

$$\sum_{m \in \mathcal{G}} z_{im} z_{jm} = 1 \tag{3.108}$$

Rule Ryan and Foster "Separate" Conversely, when the branching decision requires that individuals i and j must *not* be together in any group, we add the constraint (3.109) to the original formulation that forbids any group from containing both i and j.

$$\sum_{m \in \mathcal{G}} z_{im} z_{jm} = 0 \tag{3.109}$$

This residual $\mathrm{F}^{\mathrm{SYM}}_{\mathrm{MINLP}}$ is then solved for one purpose. At children nodes at depth d in the Branch-and-Bound tree where $d \mod L = 0$ and the solution is fractional, we solve the residual model. If this yields a feasible solution, we then apply the swap-based local search $\mathcal{LS}_{PS}$ to improve it. If the improved solution yields a better objective value than the current best upper bound, the upper bound is updated and any newly generated groups (not already present) are added to $RMP(\bar{\mathcal{K}})$.

3.3.3 Branch-and-Price Algorithm Overview

This section provides an overview of the Branch-and-Price algorithm developed for solving $\mathrm{F}^{\mathrm{EXT}}_{\mathrm{RLT}}$. The algorithm integrates the simultaneous column-and-row generation approach described in Algorithm 4 within a Branch-and-Bound framework, incorporating the primal heuristic and one of the previously described branching rules.

Algorithm 5 Branch-and-Price Algorithm

```
initialize RMP(K̄) with a feasible set of columns.
create the root node and add it to the set of active node.
while list of active nodes is not empty or time limit not reached do
    select the next active node from the list of nodes using a depth-first search.
    check feasibility of the current node and prune it if infeasible
    apply Algorithm 4 to solve RMP(K̄).
    if the RMP(K̄) solution is fractional then
        apply the primal heuristic.
        perform branching and add the children nodes to active nodes.
    else
        update the incumbent solution if the new solution has a better objective value.
    end if
end while
if time limit is reached and list of active nodes is not empty then
    perform LS_IEC on the best incumbent solution.
end if
```

The Algorithm 5 begins by initializing the set of active nodes with the root node and

$RMP(\bar{\mathcal{K}})$ with a set of feasible columns as described in Section 3.2.4. The algorithm solves the root node with simultaneous column-and-row generation (Algorithm 4). If the $RMP(\bar{\mathcal{K}})$ solution remains fractional, a branching step is performed. After branching, the algorithm adds the children nodes to the set of active nodes. The primal heuristic is called at nodes at depth d in the Branch-and-Bound tree such that $d \mod L = 0$. Note that, at each iteration of Algorithm 4, if an integer solution is found and its value is better than the current upper bound, the upper bound is updated with this solution. The algorithm selects the next active node to explore, using a depth-first search strategy and gives priority to nodes where the last branching applied branching rule involves $x_{kl} = 1$ or $y_k = 1$ or $\sum_{k \in \bar{\mathcal{K}}_i \cap \bar{\mathcal{K}}_j} y_k \geq 1$. This helps to explore first nodes with groups or individual membership fixed at 1 which increases the potential for quickly finding integer solutions or pruning infeasible nodes. The process continues until either the list of active nodes is empty or a time limit is reached. Finally, if the time limit is reached and the list of active nodes is not empty, the algorithm performs $\mathcal{LS}_{IEC}$ (see Algorithm 2) on the best incumbent solution to further improve the solution value.

3.4 Computational Experiments

This section evaluates the performance of the developed Branch-and-Price algorithm. We first describe the instances in Section 2.5.1. Then, in Section 3.4.2 we provide the performance of $\mathrm{F}^{\mathrm{EXT}}_{\mathrm{RLT}}$ compared to $\mathrm{F}^{\mathrm{EXT}}_{\mathrm{MINLP}}$ to solve instances $N \in \{6, 9, 10, 12\}$ to show the superiority of the former formulation. Then, we assess the efficiency of the simultaneous column-and-row generation features, particularly the choice of the exact pricing methods (see Section 3.4.3). Once the best empirical setting for the exact pricing algorithm is established, we evaluate the efficiency of the branching rules (see Section 3.4.4). All experiments were conducted using the same software and hardware configurations as in the previous chapter (see Section 2.5) except for the commercial solver where we use Gurobi `12.0` instead of Gurobi `11.0.2` to solve $RMP(\bar{\mathcal{K}})$ and to solve $\mathrm{F}^{3}_{\mathrm{PP}}$. The latest release of Gurobi can handle multiple nonlinear expressions and functions and thus we do not linearize the highly nonlinear product in the objective function. We rely on Gurobi's `Expression Tree` representation (a directed tree of operator/function nodes whose leaves are constants and decision variables, used to store and evaluate nonlinear formulas) and on the C++ API routine `addGenConstrNL` (which registers a general nonlinear constraint by linking a nonlinear expression tree to a variable/constraint, so Gurobi can treat the relation natively with its nonlinear machinery) to model the nonlinearity in our formulation $\mathrm{F}^{3}_{\mathrm{PP}}$.

3.4.1 Instance Description

The instances considered here are as in the previous chapter (see Section 2.5.1), with the addition of larger instances generated in the same manner. Table 3.1 presents all instance parameters including those with $N \in \{16, 25, 36, 49, 64, 81, 100\}$.

Table 3.1: Characteristics of the instances including sensitivity and specificity.

N	# instances	Possible group sizes (L)	Se	Sp	Min. Prevalence	Max. Prevalence
6	5	3	0.90, 0.95, 0.99	0.90, 0.95, 0.99	0.011	0.194
9	5	3	0.90, 0.95, 0.99	0.90, 0.95, 0.99	0.002	0.195
10	5	4	0.90, 0.95, 0.99	0.90, 0.95, 0.99	0.012	0.198
12	5	3, 4	0.90, 0.95, 0.99	0.90, 0.95, 0.99	0.002	0.192
16	5	4	0.90, 0.95, 0.99	0.90, 0.95, 0.99	0.002	0.198
25	5	5	0.90, 0.95, 0.99	0.90, 0.95, 0.99	0.003	0.194
36	5	3, 4, 6, 8	0.90, 0.95, 0.99	0.90, 0.95, 0.99	0.002	0.199
49	5	7	0.90, 0.95, 0.99	0.90, 0.95, 0.99	0.001	0.199
64	5	4, 8	0.90, 0.95, 0.99	0.90, 0.95, 0.99	0.001	0.199
81	5	3, 6, 9	0.90, 0.95, 0.99	0.90, 0.95, 0.99	0.001	0.199
100	5	4, 5, 8, 10	0.90, 0.95, 0.99	0.90, 0.95, 0.99	0.001	0.199

3.4.2 Empirical Comparison of $\mathrm{F}^{\mathrm{EXT}}_{\mathrm{RLT}}$ and $\mathrm{F}^{\mathrm{EXT}}_{\mathrm{MINLP}}$

We compare solving $\mathrm{F}^{\mathrm{EXT}}_{\mathrm{RLT}}$ with all enumerated columns to solving $\mathrm{F}^{\mathrm{EXT}}_{\mathrm{MINLP}}$ as we did in the previous chapter. Table 3.2 shows the aggregated results per value of N. Whereas both formulations solve to optimality the instances where $N \in \{6, 9, 10\}$, $\mathrm{F}^{\mathrm{EXT}}_{\mathrm{RLT}}$ solves these instances within less than 0.6 seconds in average and mostly in the root node. Then, when it comes for $N = 12$, $\mathrm{F}^{\mathrm{EXT}}_{\mathrm{RLT}}$ solves all the 90 instances within 44 seconds in average and with an average gap at the root node $\mathrm{Gap}_r \leq 0.01\%$. While $\mathrm{F}^{\mathrm{EXT}}_{\mathrm{MINLP}}$ solves none of the 90 instances to optimality within the time limit and with an average Gap_r of $\approx 1402\%$. These results show the strong quality of $\mathrm{F}^{\mathrm{EXT}}_{\mathrm{RLT}}$ compared to $\mathrm{F}^{\mathrm{EXT}}_{\mathrm{MINLP}}$.

3.4.3 Evaluation of the Exact Pricing Algorithms

Let the considered configurations be labeled as follows. `CRG` denotes the simultaneous column-and-row generation process. The two exact pricing methods are denoted as

Table 3.2: Aggregated performance comparison of extended formulations by N

N	$\mathrm{F}^{\mathrm{EXT}}_{\mathrm{MINLP}}$				$\mathrm{F}^{\mathrm{EXT}}_{\mathrm{RLT}}$			
	Avg. Time (s)	Avg. #Nodes	Avg. Gap_r (%)	#Opt./#Inst.	Avg. Time (s)	Avg. #Nodes	Avg. Gap_r (%)	#Opt./#Inst.
6	0.09	2.18	25.11	45/45	0.02	1.0	0.0	45/45
9	44.79	14107.02	747.68	45/45	0.06	1.0	0.0	45/45
10	39.73	61320.89	432.44	45/45	0.58	1.53	0.0	45/45
12	TL	11176738.63	1402.76	0/90	43.13	817.86	0.01	90/90

$\texttt{EXT}_{\texttt{GUR}}$, which solves the PP via formulation F^3_{PP} using Gurobi, and $\texttt{EXT}_{\texttt{LAB}}$, which solves F^1_{PP} using the labeling-based Algorithm 3. In what follows, we compare $\texttt{CRG-EXT}_{\texttt{GUR}}$ to $\texttt{CRG-EXT}_{\texttt{LAB}}$ at the root node.

Note that, since solving F^3_{PP} with Gurobi yields only the optimal column when it is found within the time limit, we developed a callback that captures all negatively priced columns whenever an integer solution is found during the Branch-and-Bound process and stores them in a pool. This pool is then added to $RMP(\bar{\mathcal{K}})$ instead of including only the optimal column.

First, we initialize $RMP(\bar{\mathcal{K}})$ as described in Section 3.2.4. The experiments are then conducted according to the chosen configuration. Note that we do not report all results on the instances listed in Table 3.1. In these experiments, we set $Se = Sp = 0.95$ and consider only the first realization of the risk vector $\mathbf{p}$ for each instance size (Instance $ID = 1$). Table 3.3 summarizes the results, reporting the objective value of $RMP(\bar{\mathcal{K}})$ (`OBJ`), the Lagrangian lower bound (`LB`), and the best upper bound found by the heuristic (`UB`). In addition, we report the minimum and maximum iteration times (`minIterTime` and `maxIterTime`), as well as the total execution time ($\texttt{Time}_r$ `(s)`) of the simultaneous column-and-row generation process at the root node. Note that `LB` is computed as $\texttt{LB} = max(0, (L(\bar{\alpha}, \bar{\lambda}))$ since we are minimizing the misclassification error which is a positive measure. We report the gap at root node as $\texttt{Gap}_r$ which is computed as $\frac{OBJ-LB}{LB} \times 100$ when $LB > 0$, otherwise the gaps are infinite and report them as '-' in the table.

Table 3.3: Comparison of $\texttt{CRG-EXT}_{\texttt{LAB}}$ and $\texttt{CRG-EXT}_{\texttt{GUR}}$ when $Se = Sp = 0.95$ with Instance $ID = 1$.

N	L	Configuration	OBJ	LB	UB	minIterTime	maxIterTime	# iterations	Total Time (s)	Gap (%)
6	3	$\texttt{CRG-EXT}_{\texttt{LAB}}$	1548.31	1548.31	1548.31	0.00	0.00	5	0.01	0.00
6	3	$\texttt{CRG-EXT}_{\texttt{GUR}}$	1548.31	1548.31	1548.31	0.22	0.35	5	1.39	0.00
9	3	$\texttt{CRG-EXT}_{\texttt{LAB}}$	3015.46	3015.46	3015.46	0.00	0.01	7	0.04	0.00
9	3	$\texttt{CRG-EXT}_{\texttt{GUR}}$	3015.46	3015.46	3015.46	4.16	37.64	9	297.87	0.00
10	4	$\texttt{CRG-EXT}_{\texttt{LAB}}$	4710.81	4710.81	4710.81	0.00	0.02	25	0.25	0.00
10	4	$\texttt{CRG-EXT}_{\texttt{GUR}}$	4711.03	0.00	4711.03	0.66	1804.50	17	TL	-
12	3	$\texttt{CRG-EXT}_{\texttt{LAB}}$	2589.43	2589.43	2600.28	0.01	0.02	8	0.11	0.42
12	3	$\texttt{CRG-EXT}_{\texttt{GUR}}$	2590.63	2567.48	2600.28	21.27	336.43	7	969.07	1.28
12	4	$\texttt{CRG-EXT}_{\texttt{LAB}}$	4619.70	4619.70	4624.98	0.01	0.05	21	0.60	0.11
12	4	$\texttt{CRG-EXT}_{\texttt{GUR}}$	4624.98	0.00	4624.98	1.22	1290.63	11	TL	-
16	4	$\texttt{CRG-EXT}_{\texttt{LAB}}$	6689.44	6689.44	6720.07	0.03	0.13	20	1.56	0.46
16	4	$\texttt{CRG-EXT}_{\texttt{GUR}}$	6716.20	0.00	6720.07	96.65	2388.38	6	TL	-
25	5	$\texttt{CRG-EXT}_{\texttt{LAB}}$	16652.88	16652.88	16658.76	0.71	4.42	44	102.18	0.04
25	5	$\texttt{CRG-EXT}_{\texttt{GUR}}$	16658.76	0.00	16658.76	212.47	2820.37	4	TL	-

Table 3.3 summarizes the results for both $\texttt{EXT}_{\texttt{LAB}}$ and $\texttt{EXT}_{\texttt{GUR}}$ up to $N = 25$. Across all these cases, $\texttt{EXT}_{\texttt{LAB}}$ consistently outperforms $\texttt{EXT}_{\texttt{GUR}}$ in terms of runtime. The slower runtime performance of $\texttt{EXT}_{\texttt{GUR}}$ is mainly due to the weak linear relaxation of F^3_{PP}. Furthermore, the higher quality of the columns generated with $\texttt{EXT}_{\texttt{LAB}}$ leads to a faster con-

vergence. In contrast, $\texttt{EXT}_{\texttt{GUR}}$ relies on a set of negative columns obtained via callbacks during the resolution, which are of comparatively lower quality. Although a critical observation is that the performance of both $\texttt{EXT}_{\texttt{LAB}}$ and $\texttt{EXT}_{\texttt{GUR}}$ degrades as iterations progress due to the increasing size of the $RMP(\bar{\mathcal{K}})$ for computing the missing dual variables λ. However, note that for larger values of N, in most cases, when $\texttt{EXT}_{\texttt{GUR}}$ is used, the weak lower bound of $\mathrm{F}^3_{\mathrm{PP}}$ makes the Lagrangian lower bound negative, and thus we could not compute a nonzero valid lower bound on MP. Given the poor scalability of $\texttt{EXT}_{\texttt{GUR}}$ beyond $N = 25$, there is no practical benefit to testing it on larger instances.

Table 3.4: Performance of $\texttt{CRG-EXT}_{\texttt{LAB}}$ when $Se = Sp = 0.95$ with Instance $ID = 1$.

N	L	OBJ	LB	UB	minIterTime	maxIterTime	# iterations	Total Time (s)	Gap (%)
6	3	1548.31	1548.31	1548.31	0.00	0.00	5	0.01	0.00
9	3	3015.46	3015.46	3015.46	0.00	0.01	7	0.04	0.00
10	4	4710.81	4710.81	4710.81	0.00	0.02	25	0.25	0.00
12	3	2589.43	2589.43	2600.28	0.01	0.02	8	0.11	0.42
	4	4619.70	4619.70	4624.98	0.01	0.05	21	0.60	0.11
16	4	6689.44	6689.44	6720.07	0.03	0.13	20	1.56	0.46
25	5	16652.88	16652.88	16658.76	0.71	4.42	44	102.18	0.04
36	3	8643.31	8643.31	8649.79	0.06	0.20	18	2.56	0.08
	4	15441.33	15441.33	15455.88	0.65	2.23	36	53.24	0.09
	6	30931.22	30250.06	30931.22	99.18	586.13	23	TL	2.25
	8	46823.33	0.00	46823.33	TL	TL	1	TL	-
49	7	51369.70	0.00	51369.70	TL	TL	1	TL	-
64	4	23525.45	23525.45	23535.43	9.89	172.99	56	3394.83	0.04
	8	71889.01	0.00	72437.73	TL	TL	1	TL	-
81	3	14498.25	14498.25	14504.19	1.99	5.66	34	135.53	0.04
	6	53016.76	8416.88	53016.76	TL	TL	1	TL	-
	9	92508.87	0.00	95006.26	TL	TL	1	TL	-
100	4	36435.20	36435.20	36435.20	1.15	154.09	34	TL	0.00
	5	54603.40	39718.26	54603.40	388.18	3211.82	2	TL	37.48
	8	122281.36	0.00	122281.36	TL	TL	1	TL	-
	10	148263.28	0.00	148263.28	TL	TL	1	TL	-

Table 3.4 reports the performance of $\texttt{EXT}_{\texttt{LAB}}$ alone for larger instances, to assess its scalability limits. As N increases, the performance of $\texttt{EXT}_{\texttt{LAB}}$ deteriorates significantly. Moreover, for a fixed N, increasing L further worsens runtime and often prevents the method from solving the pricing problem to optimality. This degradation is mainly due to the explosion in the number of labels combined with memory limitations, originating from the lack of effective dominance rules during group construction and the absence of strong lower bounding techniques. As a result, $\texttt{EXT}_{\texttt{LAB}}$ remains effective only for small population sizes ($N \leq 25$) or for very small group sizes on larger populations, namely $(N, L) \in \{(36, 3), (36, 4), (36, 6), (64, 4), (81, 3), (100, 4)\}$. These cases define the feasi-

ble range of instances for which $\texttt{EXT}_{\texttt{LAB}}$ can be used in the subsequent Branch-and-Price experiments.

Based on these observations, we only consider the set of instances for which $\texttt{EXT}_{\texttt{LAB}}$ can be used. We introduce the set $\mathcal{N}$ of instance pairs (N, L) considered in our experiments, defined as $\mathcal{N} = \{(N, L) \mid N \leq 25\} \cup \{(36, 3), (36, 4), (36, 6), (64, 4), (81, 3), (100, 4)\}$. Consequently, the final configuration selected is $\texttt{CRG-H+EXT}_{\texttt{LAB}}\texttt{+LG}$. We use the heuristics for the pricing, then the exact pricing algorithm $\texttt{EXT}_{\texttt{LAB}}$ is called either for obtaining the optimal negative reduced column or to compute the Lagrangian lower bound on the value of MP. `LG` stands for the use of the Lagrangian lower bound. It is used for an early termination criteria and in the management of the heuristics.

3.4.4 Evaluation of the Branching Rules

To compare the performance of the three branching rules described in Section 3.3.1.1 and Section 3.3.1.2, we conduct computational experiments on the entire test bed presented in Table 3.1. In our evaluation, we solve $\text{F}_{\text{RLT}}^{\text{EXT}}$ using the Branch-and-Price algorithm (Algorithm 5) with each branching rule applied separately. The tested configurations, summarized in Table 3.5, include `BP-RF` (Ryan and Foster rule), `BP-HFY` (branching on the highest fractional y_k variable), and `BP-HFX` (branching on the highest fractional x_{kl} variable).

Configuration name	Branching rule involved
`BP-RF`	Ryan and Foster
`BP-HFY`	Highest Fractional y_k
`BP-HFX`	Highest Fractional x_{kl}

Table 3.5: Tested configurations of Algorithm 5.

Table 3.6 presents the aggregated results across the entire test bed. Detailed results per instance are provided in Appendix 4.4. For each value of N and each eligible value of L, we compare the three branching rules. To improve readability, the values of N, L, and the metrics at the root node—namely the average execution time (`Avg. Time`$_r$ `(s)`) and the average optimality gap at the root (`Avg. Gap`$_r$ `(%)`)—are grouped together, as they remain constant across the three branching strategies. The remaining metrics are reported individually for each branching rule. We include the total execution time over the solved instances to proven optimality only (`Total Time (s) - Opt.`) with its average, minimum, and maximum values. For the instances not solved to proven optimality, we report the final optimality gap at the time limit (`Final Gap (%) - notOpt`) with its average, minimum, and maximum values. We also report the average number of branching nodes explored (`# Nodes`) and the average improvement in the upper bound (Δ`UB (%)`), computed as $\Delta\text{UB} = \frac{\text{Initial UB} - \text{Final UB}}{\text{Initial UB}} \times 100$. Finally, the number of instances solved to optimality out of the 45 instances is reported (`# Opt. / # Inst.`).

Table 3.6: Aggregated comparison of the three branching rules.

N	L	Config	Root Node		Total Time (s) – Opt.			Final Gap (%) – notOpt.			# Nodes	Δ UB (%)	# Opt./# Inst.
			Avg. Time_r (s)	Avg. Gap_r (%)	Avg.	Min.	Max.	Avg.	Min.	Max.			
6	3	BP-HFX	0.01	0.00	0.02	0.01	0.03	opt	0.00	0.00	1.00	0.0001	45/45
		BP-HFY			0.02	0.01	0.03	opt	0.00	0.00	1.00	0.0001	45/45
		BP-RF			0.02	0.01	0.03	opt	0.00	0.00	1.00	0.0001	45/45
9	3	BP-HFX	0.04	0.01	0.07	0.01	0.32	opt	0.00	0.00	1.98	0.0013	45/45
		BP-HFY			0.06	0.01	0.14	opt	0.00	0.00	1.31	0.0013	45/45
		BP-RF			0.11	0.01	0.53	opt	0.00	0.00	2.24	0.0013	45/45
10	4	BP-HFX	0.28	0.18	6.36	0.11	54.89	opt	0.00	0.00	21.93	0.0013	45/45
		BP-HFY			0.50	0.11	1.20	opt	0.00	0.00	1.58	0.0013	45/45
		BP-RF			2.71	0.12	29.47	opt	0.00	0.00	10.02	0.0013	45/45
12	3	BP-HFX	0.09	1.04	667.57	57.69	3568.82	1.25	0.38	3.12	990.82	0.184	34/45
		BP-HFY			621.91	3.42	3436.45	2.50	0.67	4.42	767.31	0.1227	41/45
		BP-RF			1342.83	64.84	3403.58	1.26	0.16	3.60	1389.78	0.1675	26/45
	4	BP-HFX	0.57	0.93	593.99	1.90	1590.38	0.57	0.07	1.27	440.47	0.1161	27/45
		BP-HFY			178.88	1.64	1409.33	opt	0.00	0.00	129.44	0.1134	45/45
		BP-RF			521.91	7.04	3195.66	1.59	0.84	2.73	304.00	0.0917	40/45
16	4	BP-HFX	0.61	0.76	385.55	0.85	1358.05	0.40	0.01	0.76	136.16	0.0168	6/45
		BP-HFY			474.63	0.87	2409.64	0.53	0.09	1.15	198.71	0.0209	21/45
		BP-RF			1025.28	22.70	3354.35	0.72	0.11	1.43	191.13	0.0214	7/45
25	5	BP-HFX	5.98	0.74	TL	TL	TL	0.71	0.04	1.22	60.44	0.0057	0/45
		BP-HFY			TL	TL	TL	0.68	0.44	1.06	93.84	0.0109	0/45
		BP-RF			TL	TL	TL	0.66	0.44	1.13	46.80	0.0047	0/45
36	3	BP-HFX	0.91	0.45	18.53	0.76	53.79	0.47	0.02	1.10	629.71	0.0053	3/45
		BP-HFY			571.16	0.69	1004.82	0.46	0.02	0.98	697.98	0.0108	3/45
		BP-RF			2.03	2.03	2.03	0.46	0.02	0.96	587.60	0.0095	1/45
	4	BP-HFX	5.60	0.55	1419.60	4.91	2178.26	0.58	0.05	1.23	105.36	0.0046	3/45
		BP-HFY			8.44	4.91	11.98	0.54	0.04	1.01	129.58	0.0115	2/45
		BP-RF			8.51	8.51	8.51	0.56	0.01	1.13	101.00	0.0001	1/45
	6	BP-HFX	1129.12	2.04	TL	TL	TL	2.09	0.47	12.48	2.67	0.0	0/45
		BP-HFY			TL	TL	TL	1.98	0.54	13.43	2.78	0.0	0/45
		BP-RF			TL	TL	TL	1.53	0.48	12.41	3.78	0.0	0/45
64	4	BP-HFX	61.27	0.36	104.36	56.90	151.82	0.38	0.02	1.08	16.00	0.0	2/45
		BP-HFY			67.22	57.89	76.56	0.38	0.01	1.16	16.96	0.0	2/45
		BP-RF			66.26	66.26	66.26	0.35	0.01	1.07	22.44	0.0	1/45
81	3	BP-HFX	16.94	0.46	807.52	603.55	947.83	0.39	0.02	1.25	86.00	0.0926	3/45
		BP-HFY			1063.72	1063.72	1063.72	0.36	0.02	1.07	94.51	0.0983	1/45
		BP-RF			TL	TL	TL	0.40	0.02	0.89	109.22	0.0462	0/45
100	4	BP-HFX	552.46	1.48	TL	TL	TL	1.47	0.40	2.48	5.80	0.0	0/45
		BP-HFY			TL	TL	TL	1.45	0.40	2.47	5.76	0.0	0/45
		BP-RF			TL	TL	TL	1.45	0.40	2.50	6.00	0.0	0/45

BP-HFY emerges as the most effective branching rule in terms of gap closure, solving to optimality 242 out of 270 instances for $N \leq 16$. When compared to BP-HFX and BP-RF over the subset of instances that all three configurations solve to optimality, BP-HFY consistently outperforms both in terms of runtime and number of explored nodes. BP-RF ranks second with 208 solved instances, followed by BP-HFX with 202. For $N \in \{25, 100\}$ and for $(N, L) = (36, 6)$, none of the three configurations solve the instances to optimality. However, for the remaining instances, i.e., $(N, L) \in \{(36, 3), (36, 4), (64, 4), (81, 3)\}$, BP-HFX solves 11 instances to optimality, compared to 8 for BP-HFY and 4 for BP-RF. This may be attributed to BP-HFX fixing two groups simultaneously at each branch for $x_{kl} = 1$, whereas BP-HFY fixes only a single group at a time for $y_k = 1$. Both methods, however, struggle when branching on $x_{kl} = 0$ or $y_k = 0$, particularly for $x_{kl} = 0$, which translates into the constraint $y_k + y_l \leq 1$, a known limitation of conventional fractional-based branching rules. Nevertheless, both BP-HFX and BP-HFY outperform BP-RF, which only restricts group membership for two individuals. Since BP-HFX and BP-HFY directly affect one or two complete groups in the integer solution among $G = \frac{2N}{L}$ groups, they apply a stronger branching effect than BP-RF, which imposes comparatively weaker constraints on the feasible space.

Table 3.7: Aggregated final results with BP-HFY.

N	L	**Root Node**		**Total Time (s) – Opt.**			**Final Gap (%) – notOpt.**			**#** **Nodes**	**Δ** **UB (%)**	**# Opt./# Inst.**
		Avg. Time_r (s)	Avg. Gap_r (%)	Avg.	Min.	Max.	Avg.	Min.	Max.			
6	3	0.01	0.00	0.02	0.01	0.03	opt	0.00	0.00	1.00	0.0001	45/45
9	3	0.04	0.01	0.06	0.01	0.14	opt	0.00	0.00	1.31	0.0013	45/45
10	4	0.28	0.18	0.50	0.11	1.20	opt	0.00	0.00	1.58	0.0013	45/45
12	3	0.09	1.04	621.91	3.42	3436.45	2.50	0.67	4.42	767.31	0.1227	41/45
	4	0.57	0.93	178.88	1.64	1409.33	opt	0.00	0.00	129.44	0.1134	45/45
16	4	0.61	0.76	474.63	0.87	2409.64	0.53	0.09	1.15	198.71	0.0209	21/45
25	5	5.98	0.74	TL	TL	TL	0.68	0.44	1.06	93.84	0.0109	0/45
36	3	0.91	0.45	571.16	0.69	1004.82	0.46	0.02	0.98	697.98	0.0108	3/45
	4	5.60	0.55	8.44	4.91	11.98	0.54	0.04	1.01	129.58	0.0115	2/45
	6	1129.12	2.04	TL	TL	TL	1.98	0.54	13.43	2.78	0.0	0/45
64	4	61.27	0.36	67.22	57.89	76.56	0.38	0.01	1.16	16.96	0.0	2/45
81	3	16.94	0.46	1063.72	1063.72	1063.72	0.36	0.02	1.07	94.51	0.0983	1/45
100	4	552.46	1.48	TL	TL	TL	1.45	0.40	2.47	5.76	0.0	0/45

Furthermore, we observe from Table 3.6 that the Branch-and-Price algorithm leads to small improvements of upper bound in most cases (at most 0.184%). This suggests that the initial upper bounds provided by the heuristics obtained with the local search method are of strong quality and often close to optimality. Among the tested branching rules, BP-HFY and BP-HFX are the most effective in improving the upper bound when

such improvements occur. Therefore, `BP-HFY` is the retained configuration. We report in Table 3.7 the performance of the retained configuration.

Overall, the developed Branch-and-Price algorithm rarely manages to fully close the optimality gap for $N \geq 25$. Within the one-hour time limit, the gap reduction for instances not solved to optimality is negligible or even nonexistent. Nevertheless, the final gap averages at most 2.5%. This confirms, first, that most of the computational effort is concentrated at the root node, and second, that both the quality of the linear relaxation of the RLT-based formulation and the effectiveness of the heuristics are noteworthy. However, the developed branching rules quickly struggle to reach optimality as the combinatorial complexity of the instances increases.

These results highlight that even if a Branch-and-Price algorithm can be a possible method to solve the studied problem, its strength highly depends on the scalability of the exact pricing algorithm and the quality of the branching rules.

On the one hand, it would have been desirable to further advance the scientific frontier by solving all benchmark instances to optimality, particularly those with $N \leq 36$, a goal that remains highly challenging. On the other hand, exploring larger values of N and L is also of theoretical interest; however, in practical applications, group testing is generally performed on small groups to mitigate dilution effects, and the process is typically conducted in batches. These practical considerations, together with the results reported in this section, highlight the effectiveness of the developed *ad hoc* heuristics in addressing real-world scenarios encountered in medical laboratories.

3.4.5 Some Properties of Best Known Solutions

Similarly to Section 2.5.4.1 in the previous chapter, we are curious to observe the characteristics of the best known solutions for various combination values of (Se, Sp, N) for $N \in \{12, 16, 25, 36, 49, 64, 81, 100\}$.

Figures 3.2 and 3.3 show that in general and depending on the instances and values of Se and Sp, the L least risk individuals are mostly grouped in the best known solutions, indicating that minimizing false positives is likely achieved through grouping lower-risk individuals. Thus, one can use the heuristic **LEAST** complemented by $\mathcal{LS}_{IEC}$ local search and obtain a good quality solution.

3.5 Conclusion and Perspectives

This chapter proposed a Branch-and-Price algorithm for non-adaptive 2D-GTEG. The approach combines a strengthened extended formulation developed thanks to RLT cuts. The linear relaxation of the formulation is solved with simultaneous column-and-row generation, which addresses the challenge of estimating missing dual variables. The algorithm developed efficiently solves small instances and provides a performance guarantee,

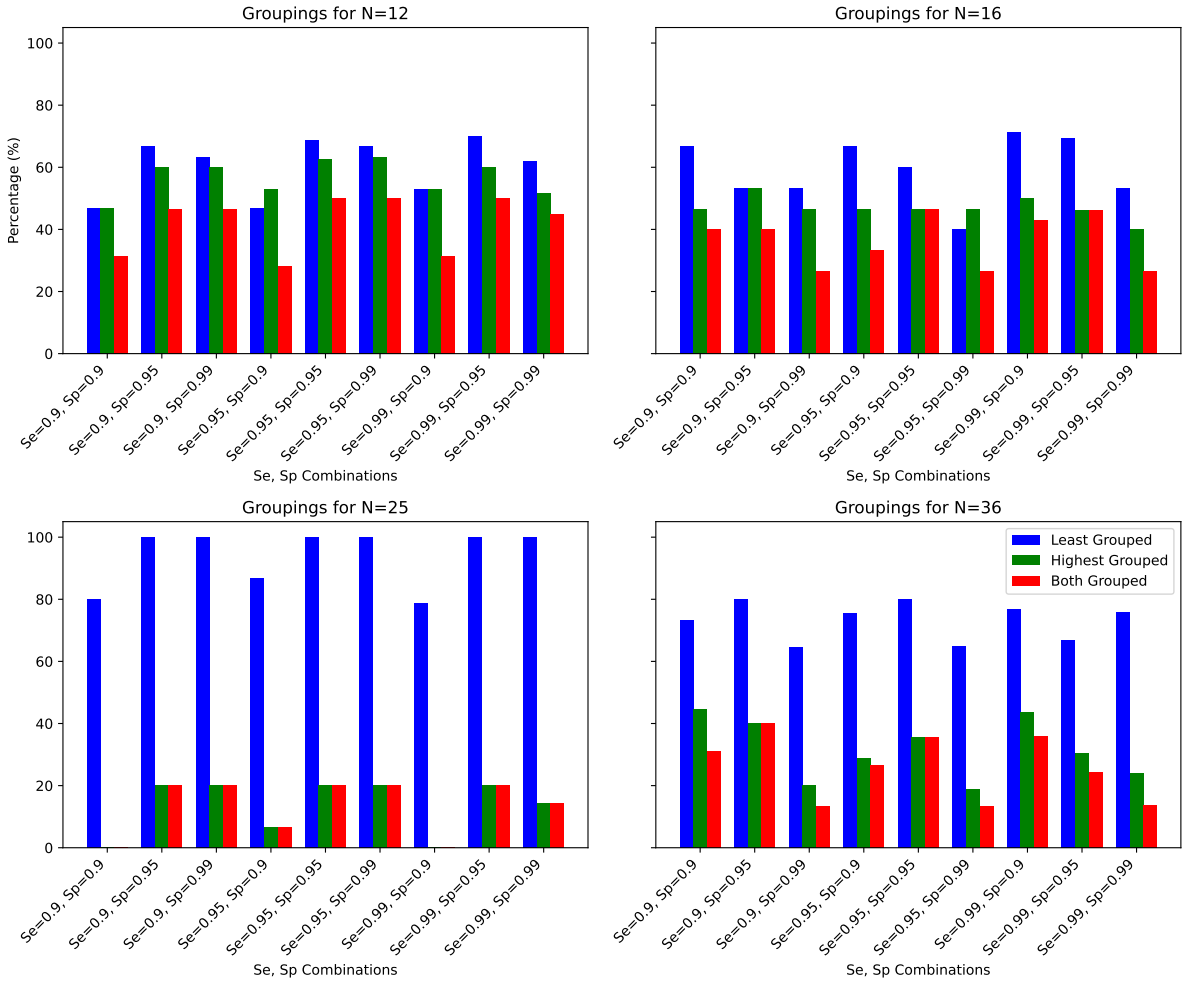


Figure 3.2: Solution properties in optimal or best incumbent solutions by varying (Se, Sp) for $N \in \{12, 16, 25, 36\}$.

which has never been done in the literature prior to this work, but scalability remains limited for larger populations due to the complexity of the Pricing Problem. Future work could focus on enhancing the linear relaxation of $\mathrm{F}^3_{\mathrm{PP}}$ with valid inequalities to improve its resolution. Our perspectives involve mainly enhancing the scalability of our methods to better address large-scale instances and potentially exploring alternative formulations.

A natural extension involves relaxing the equal group size constraint to allow for two distinct group sizes, analogous to rectangular array testing. This generalization introduces row groups of size L_1 and column groups of size L_2, enhancing flexibility while preserving the core analytical structure.

Adapting the Branch-and-Price framework to this rectangular-like setting requires solving two separate Pricing Problems, one for each group size. Thus, the missing dual variables need to be correctly estimated accordingly. The adaptation of the Lagrangian lower bound is required. Once all of these adaptations are done, the overall algorithmic framework remains applicable.

The next chapter adapts the developed methods to a real-world application for early

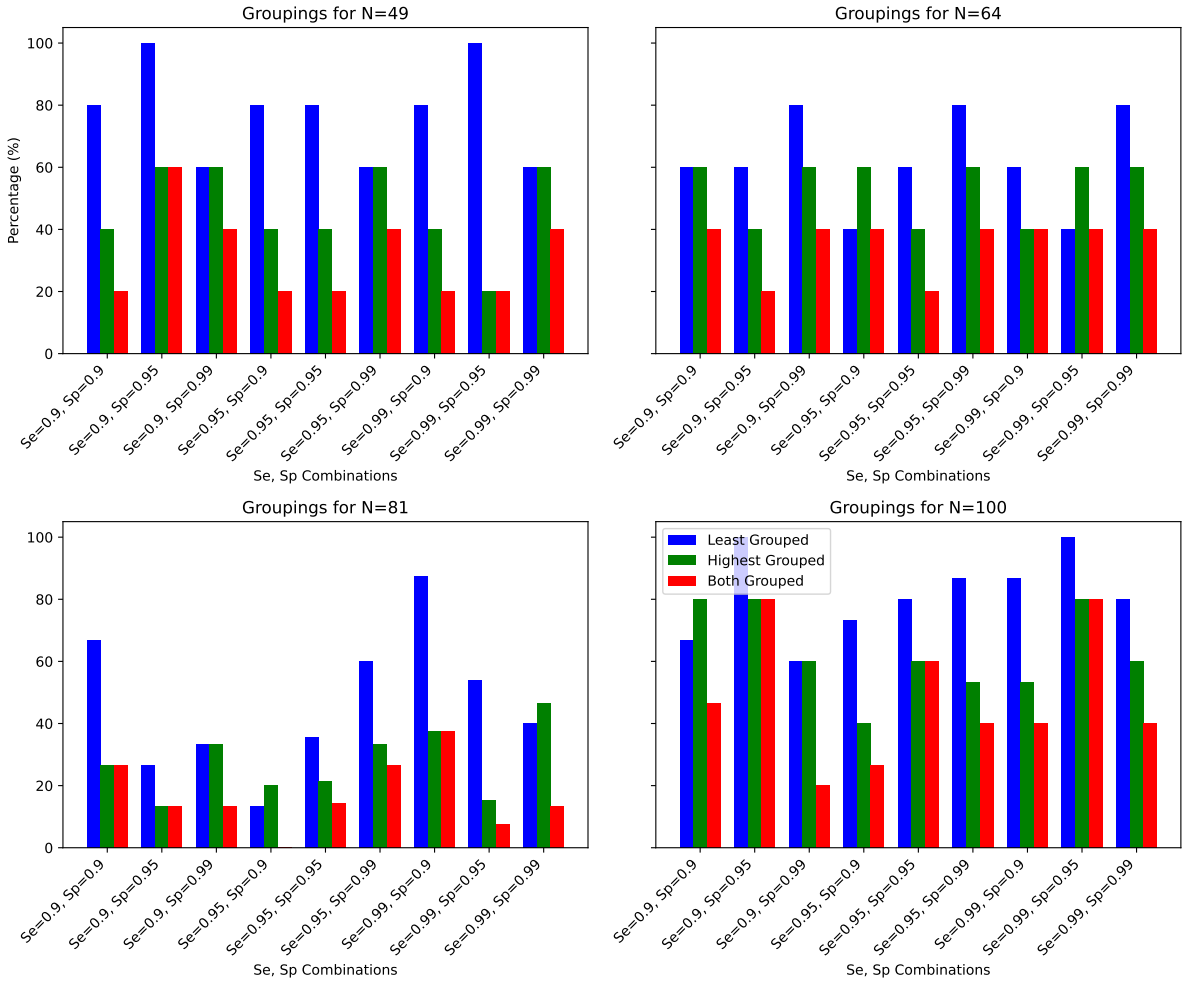


Figure 3.3: Solution properties in optimal or best incumbent solutions by varying (Se, Sp) for $N \in \{49, 64, 81, 100\}$.

detection of rare autoimmune diseases. In collaboration with *Lille University Hospital*, we extend the performance measures, the compact formulation, and the local search algorithms to handle multiplex assays that detect simultaneously multiple antinuclear antibodies (ANAs), key biomarkers for autoimmune disorders, enabling large-scale, cost-efficient screening.

Chapter 4

Risk-based Non-adaptive Two-Dimensional Group Testing with multiplex Antinuclear Antibody assays: Application for Rare Autoimmune Disease Prevention

This chapter is the result of a collaboration with researchers from Lille University Hospital, including Clément CHAUVET, Aurélien CHEPY, Aurore COLLET, Sylvain DUBUCQUOI, Adan JOSÉ GARCIA, and Vincent SOBANSKI.

In this chapter, we apply two-dimensional group testing to a rare disease prevention project in collaboration with Lille University Hospital. This chapter is a real-world application chapter that extends the models and methods developed in previous chapters to a multi-disease screening context. This chapter demonstrates that our formulations and methods, originally developed for single-disease screening, can be readily extended to multi-disease screening, underscoring their versatility and practical potential. Notably, the focus is on the extendability of our approach rather than on new methodology, as the underlying techniques remain unchanged.

This chapter is organized as follows. We first introduce in Section 4.1 the background and motivation of the project. Section 4.2 introduces new definitions specific to the multi-ANA screening context and describes how the already developed compact and extended formulations, along with the associated algorithms in the previous chapters, remain applicable for this new setting. In Section 4.3, we conduct an experimental study based on two real-world datasets from the literature and discuss our findings. Finally, Section 4.4 concludes the chapter and outlines directions for future research.

4.1 Background and Motivation

Autoimmune diseases occur when the body's immune system mistakenly identifies its own healthy cells as threats and attacks them. Normally, the immune system protects the body by producing antibodies that specifically target harmful pathogens such as viruses and bacteria. However, in autoimmune disorders, this mechanism fails: the immune system generates autoantibodies–antibodies that wrongly recognize the body's own cells as foreign. A notable class of autoantibodies is antinuclear antibodies (ANA), which target proteins located in the nucleus of the body's own cells. These misguided immune responses can lead to chronic inflammation and damage to various organs and tissues.

Systemic sclerosis (SSc), also called scleroderma, is a rare autoimmune disease that causes skin and organ fibrosis along with vascular damage. It has high morbidity, high impact on patient life, and high mortality that is greater than any other rheumatic disease (Denton & Khanna, 2017). Statistics in France show that SSc affects mainly women (about 80% of cases) with an average diagnosis age of around 42 years. The prevalence in France is estimated at 132–228 cases per million adults, with an annual incidence of roughly 2–3 per 100,000 inhabitants (Agard & Mekinian, 2023).

In their articles Chépy *et al.* (2022, 2024), the authors explore the potential role of ANAs in SSc. Although ANAs are commonly considered biomarkers, the study suggests that they could play a more direct role in the pathogenesis of the disease. They highlight that ANAs often precede disease onset by several years, correlated with disease severity, and may be linked to disease progression. This indicates the potential importance of ANA in the persistence of SSc and supports the need for earlier diagnosis and interventions, as early detection could improve patient outcomes by facilitating timely treatments. As such, many autoimmune diseases, if diagnosed early, can be treated to prevent life-threatening serious complications. Unfortunately, late diagnosis often results in irreversible damage. Having a timely diagnosis through mass screening programs can significantly improve patient outcomes (Chépy *et al.*, 2024).

In practice, the standard protocol for ANA testing in cohorts generally follows a two-step process. First, an indirect immunofluorescence test (IIF) is used as a screening tool because of its high sensitivity and its ability to reveal characteristic fluorescence patterns. Individuals with a positive IIF result then undergo a confirmatory multiplex assay to identify specific ANA types. Multiplex assays allow simultaneous screening for multiple autoantibodies; in our context, the *Bioplex 2000* assay is used to test for up to 14 ANAs (Laboratories, 2023). Determining the precise ANA profile is critical because different autoimmune diseases, such as lupus or systemic sclerosis, are associated with distinct autoantibody patterns (e.g., anti-SSA, anti-Scl-70). Figure 4.1 illustrates the traditional two-step ANA screening process.

In the literature of group testing, Bilder *et al.* (2019, 2021); Hou *et al.* (2020) study one-dimensional and matrix-based group testing while considering multiplex assays. These

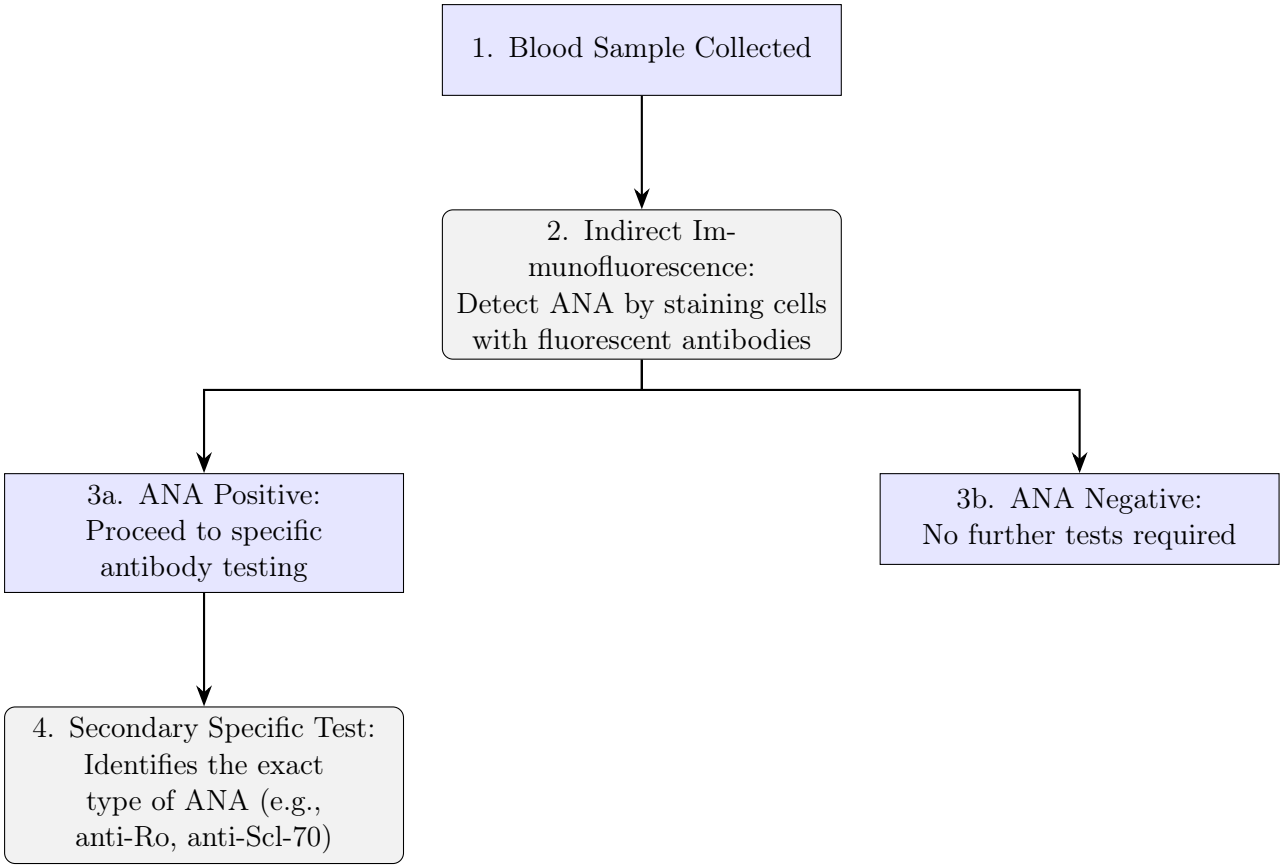


Figure 4.1: ANA Testing Process: Immunofluorescence followed by Specific Testing for Positive Samples

works consider group testing and multiplex assays for even more efficiency. They applied an adaptation of the already described heuristics Gradient Design and Spiral Design from McMahan *et al.* (2012b) for square matrix-based group testing in this new context for the simultaneous detection of chlamydia and gonorrhea, two sexually transmitted diseases.

In collaboration with Lille University Hospital, we are exploring the possibility of preventing autoimmune diseases through massive screening in the Haut-de-France region in France. This project will use ANA testing as a screening tool to identify individuals at risk of developing autoimmune diseases, allowing for early diagnosis and treatment. Our research focuses on applying the non-adaptive 2D-GTEG to this screening initiative. Through this collaboration, we hope to motivate healthcare investors to fund the necessary equipment and infrastructure to implement this large-scale prevention initiative. The combination of multiplex biomarker-based diagnostics and optimized group testing offers a powerful strategy for improving public health in the region, and may be scaled to the national or international level.

All this being said, in what follows we present the specific adaptations made to extend our approach to multi-ANA screening.

4.2 Problem Description

The objective of this section is to provide a structured and self-contained description of the problem studied in this chapter. We recall the key elements previously introduced in earlier chapters and introduce the new notation and definitions that are specific to the multi-ANA screening context.

We build on the `AND` testing scheme introduced in Section 2.1, Chapter 2, and extend it to account for the multiplex nature of ANA assays, where multiple antibodies are tested simultaneously. Unlike the single-disease setting–where a group testing positive indicates the presence of a single target disease–a multiplex assay returns results for all ANAs in a single test, whether applied to an individual sample or to a group of samples. In this context, we define a group or an individual as *positive* if the test detects at least one ANA. Under this setting, the `AND` scheme is adapted as follows: an individual $i \in G_k \cap G_l$ is retested only if both groups G_k and G_l test positive for at least one ANA.

Let $\mathcal{I} = \{1, 2, \ldots, N\}$ be the population of individuals to be tested, and let $\mathcal{R} = \{1, 2, \ldots, R\}$ be the index set of ANAs considered. Each individual $i \in \mathcal{I}$ is associated with a risk vector $(p_r^i)_{r \in \mathcal{R}}$, where p_r^i is the probability that individual i is positive for ANA r.

We make the following assumptions throughout this chapter:

Assumption 4.1. *Individuals are independent. The positivity of an individual i is independent of the positivity of any other individual j.*

Assumption 4.2. *For each individual, the presence of different ANAs is independent. That is, for any individual i, the event of being positive for ANA r does not influence the probability of being positive for any other ANA $r' \neq r$.*

Assumption 4.3. *Test outcomes are independent across groups. Even though groups may overlap by design, we assume no dependency is introduced by the testing process itself.*

Assumption 4.4. *For each ANA r, the sensitivity Se_r and specificity Sp_r remain the same whether the test is applied to an individual or to a group.*

We assume that a multiplex ANA assay is used to simultaneously test all ANAs. For each ANA $r \in \mathcal{R}$, the assay is characterized by a known sensitivity Se_r and specificity Sp_r. Whether applied to an individual or to a group, the assay provides a response for all ANAs. We denote the result of testing an individual or a group by $\tau(\cdot) \in \{0, 1\}$. A value $\tau(\cdot) = 1$ indicates a positive test result, while $\tau(\cdot) = 0$ indicates a negative result. The true status of an individual or a group is denoted by $(\cdot)^+$ if it is truly positive, and by $(\cdot)^-$ if it is truly negative. Based on this, we define the overall sensitivity Se and specificity Sp of the multiplex assay. Se is the probability that the test returns a positive result given that the tested entity (either an individual or a group) is truly positive for at least one ANA. Sp is the probability that the test returns a negative result given that

the tested entity (individual or group) is truly negative for all ANAs. These expressions apply whether the test is performed on an individual or on a group of individuals:

$$Se = P(\tau(\cdot) = 1 \mid (\cdot)^+) = 1 - \prod_{r \in \mathcal{R}} (1 - Se_r), \tag{4.1}$$

$$Sp = P(\tau(\cdot) = 0 \mid (\cdot)^-) = \prod_{r \in \mathcal{R}} Sp_r. \tag{4.2}$$

A feasible solution is defined by a collection of groups $S = \{G_1, G_2, \ldots, G_G\}$, where conditions ((i))–((iii)) (cf. Section 2.1) are satisfied. Specifically, given S, each individual belongs to exactly two groups, each pair of groups intersect at most in one individual and each group contains exactly L individuals. Additionally, as previously done in Chapters 2 and 3, we consider $\mathbb{E}[FN(S)]$, $\mathbb{E}[FP(S)]$ and $\mathbb{E}[T(S)]$ to evaluate S. We recall that these performance measures respectively quantify: the expected number of truly positive individuals who are incorrectly classified as negative ($\mathbb{E}[FN(S)]$); the expected number of truly negative individuals who are incorrectly classified as positive ($\mathbb{E}[FP(S)]$); and the expected total number of tests performed, including both the initial group tests and the confirmatory individual tests ($\mathbb{E}[T(S)]$).

The optimization problem studied in this chapter is the same as the one introduced in Chapter 2. It consists in computing a solution that satisfies conditions ((i))–((iii)) and minimizes a convex combination of the expected number of false negatives, false positives, and tests. For completeness, we recall the formal definition of the problem below.

Let $\mathcal{S}$ be the set of all solutions satisfying conditions ((i))–((iii)). For each feasible solution $S \in \mathcal{S}$, let $\mathbb{E}[FN(S)]$, $\mathbb{E}[FP(S)]$, and $\mathbb{E}[T(S)]$ respectively denote the expected number of false negatives, false positives, and tests of S.

The optimization problem- already defined in Chapter 2.1 as Problem (2.1)- is recalled as follows:

$$\min_{S \in \mathcal{S}} \quad \lambda_1 \mathbb{E}[FN(S)] + \lambda_2 \mathbb{E}[FP(S)] + (1 - \lambda_1 - \lambda_2)\mathbb{E}[T(S)]$$

where $\lambda_1, \lambda_2 \in [0, 1]$ with $\lambda_1 + \lambda_2 \leq 1$. The weights λ_1, λ_2, and $1 - \lambda_1 - \lambda_2$ reflect the importance assigned to each of the three performance measures by the decision-maker.

By defining $q^i = \prod_{r \in \mathcal{R}} (1 - p_r^i)$ as the probability that individual i is negative for all ANAs and setting $p^i = 1 - q^i$, we recover the probability that individual i is positive for at least one ANA. With this transformation, and using the expressions of Se and Sp respectively in (4.1) and (4.2), all performance measures $\mathbb{E}[FN(S)]$, $\mathbb{E}[FP(S)]$, and $\mathbb{E}[T(S)]$ reduce exactly to the single-disease case presented in Chapter 2, Section 2.2.

Consequently, all mathematical formulations and algorithms developed in Chapters 2 and 3 remain valid and require no structural changes. The only necessary adaptation is to compute the aggregated probability $p^i = 1 - \prod_{r \in \mathcal{R}} (1 - p_r^i)$, Se and Sp prior to applying

the models and solution methods.

4.3 Computational Experiments

In this section, we describe our computational experiments designed to evaluate the proposed methods to solve the problem studied. First, Section 4.3.1 details the instance generation process. In this section, we generate instances based on estimated prevalences derived from two real-world aggregated datasets of the literature (Guo *et al.*, 2014; Hayashi *et al.*, 2008). These datasets provide the risk distribution of specific ANA positivity by age and sex in the general population, which we use to simulate realistic instances. We assess the performance of our simultaneous column-and-row generation procedure at the root node of the Branch-and-Price algorithm. This provides a performance guarantee on the solutions obtained using our heuristics, which are improved by $\mathcal{LS}_{PS}$ local search method for its rapidity rather than $\mathcal{LS}_{IEC}$. We focus on the root node because, as noted in Section 3.4.4, the majority of the computational effort is concentrated, and the gap at the time limit is rarely improved after branching. Section 4.3.3 explains the design of the experiments and provides preliminary results.

All experiments were conducted using the same software and hardware configurations as in the previous chapter (see Section 2.5).

4.3.1 Instance Generation

To generate realistic population instances for multi-ANA screening, we use aggregated datasets from two large population-based studies. These studies report ANA prevalence estimates by age and sex, which are necessary for simulating real-world risk distributions. In contrast, the Lille University Hospital cohort does not provide such prevalence data on the general population because most of the patients screened for ANAs are mostly positive: patients are referred to Lille University Hospital only when a city physician suspects an autoimmune disease. For this reason, we base our probability estimates on the general population data from Guo *et al.* (2014) and Hayashi *et al.* (2008). However, we use clinical insights from the Lille cohort to guide the selection of ANA types. Our collaborators there focus on six ANAs strongly associated with autoimmune diseases such as systemic lupus erythematosus, systemic sclerosis, and Gougerot–Sjögren syndrome. Table 4.1 lists the sensitivities and specificities of the multiplex assay used, along with the diseases associated with each ANA.

The first dataset is from the study by (Guo *et al.*, 2014), which includes 20,970 individuals from China who underwent routine health check-ups. Among them, 10,420 are female and 10,550 are male. ANA testing was conducted using indirect immunofluorescence, and 1,243 individuals tested positive to ANA. Table 4.2 shows the number of ANA-positive individuals by sex and age group. These ANA positive individuals under-

ANA	Associated pathology(ies)	Test sensitivity	Test specificity
Anti-dsDNA	Systemic lupus	0.86	1.00
Anti-Sm	Systemic lupus	0.71	1.00
Anti-CB	Systemic sclerosis	1.00	0.97
Anti-Scl-70	Systemic sclerosis	0.76	0.96
Anti-SSA	Systemic sclerosis + Systemic lupus + Goujerot-Sjögren	0.915	1.00
Anti-SSB	Goujerot-Sjögren	1.00	0.99

Table 4.1: Sensitivities and specificities of Bioplex Assay for various ANA antibodies and their associated pathologies.

went a further LIA test (Line Immunoassay Damoiseaux *et al.* (2005)) for specific ANA positivity. Table 4.3 provides the number of individuals who tested positive for each specific ANA, again organized by sex and three age groups: ≤ 20 years, 21–49 years, and ≥ 50 years.

Age group (y)	Male	Female
2–<10	21/1300	33/1200
10–<20	55/2200	176/2150
20–<30	39/1700	143/1680
30–<40	48/1800	109/1840
40–<50	49/1500	105/1480
50–<60	43/1000	138/970
60–<70	43/600	95/550
70–<80	30/350	79/400
80+	12/100	25/150
Total	340/10,550	903/10,420

Table 4.2: Distribution of antinuclear antibody positive frequency in male and female participants at different ages adapted from (Guo *et al.*, 2014).

The second dataset comes from the study by (Hayashi *et al.*, 2008), which followed 2,181 residents of a town in Japan over a 5-year period. Participants were aged between 20 and 93 years and were tested during annual physical examinations. Among them, 1,409 are female and 772 are male. A total of 566 individuals tested positive for ANA. Specific ANA positivity was assessed for eight specific ANA types using individual disease-specific ANA assays ELISA (Enzyme-linked immunosorbent assay (Shah & Maghsoudlou, 2016)). Table 4.4 reports the number of ANA-positive individuals for each ANA type, by sex and

Antibody	By Sex			By Age Group			
	Male	Female	Total	≤ 20 y	21–49 y	≥ 50 y	Total
Anti-nRNP	16	37	53	13	14	25	52
Anti-Sm	10	24	34	6	8	17	31
Anti-SSA	30	93	123	21	40	67	128
Anti-Ro52	40	123	163	25	43	98	166
Anti-SSB	11	24	35	6	10	19	35
Anti-Jo-1	6	13	19	0	3	14	17
Anti-Scl-70	0	6	6	0	3	3	6
Anti-CB	5	60	65	5	22	38	65
Anti-dsDNA	8	33	41	8	11	22	41
Anti-his	16	41	57	6	16	35	57
Anti-PCNA	5	19	24	16	0	8	24
Anti-Nuk	8	10	18	0	6	11	17
Anti-Rib	5	24	29	2	8	19	29
Anti-M2	32	121	153	25	17	112	154
Anti-PM	13	27	40	6	8	24	38
Total	205	655	860	139	209	512	860

Table 4.3: Numbers of ANA-specific antibodies in positive sera: breakdown by sex and by age group adapted from (Guo *et al.*, 2014).

age group. The population is divided into seven age groups: 20–30, 30–40, 40–50, 50–60, 60–70, 70–80, and over 80 years.

In what follows, let Φ_G and Φ_H denote, respectively, the datasets from Guo *et al.* (2014) and Hayashi *et al.* (2008). For dataset Φ_H, the specific ANA positivity risk for an antibody a in an age group γ and sex s is computed directly from the data as

$$P(\tau(a) = 1 \mid \gamma, s) = \frac{n_{a,\gamma,s}}{N_{\gamma,s}},$$

where $N_{\gamma,s}$ is the number of individuals tested and $n_{a,\gamma,s}$ is the number of individuals positive for ANA a in subgroup (γ, s).

In contrast, dataset Φ_G provides aggregated data that do not directly yield $n_{a,\gamma,s}$. Instead, we only have the overall conditional probabilities aggregated by sex, $P(\tau(a) = 1 \mid ANA^+, s)$, and by age group, $P(\tau(a) = 1 \mid ANA^+, \gamma)$ for the individuals who are ANA positive overall (ANA^+). We therefore estimate the specific ANA positivity risk

Antibody	20–30 y		31–40 y		41–50 y		51–60 y		61–70 y		71–80 y		81–93 y		Total
	F	M	F	M	F	M	F	M	F	M	F	M	F	M	
Anti-U1RNP	1	0	2	0	2	0	2	0	3	0	0	1	0	0	11 (7 F)
Anti-dsDNA	0	0	1	0	1	1	1	0	2	1	1	2	0	0	10 (3 F)
Anti-Sm	0	0	0	0	0	0	0	0	0	0	0	0	0	0	0 (0 F)
Anti-CB	1	0	1	0	3	0	4	1	8	2	6	1	0	0	30 (23 F)
Anti-Scl-70	0	0	0	0	0	0	0	0	0	0	0	0	0	0	0 (0 F)
Anti-SSA	2	0	4	0	6	0	13	1	14	3	11	3	0	1	58 (50 F)
Anti-SSB	0	0	1	0	0	0	1	0	1	1	1	0	0	0	5 (1 F)
Anti-Jo-1	0	0	0	0	0	0	0	0	0	0	0	0	0	0	0 (0 F)
Females	4/178		9/245		12/232		18/202		26/308		15/209		1/35		85/1409
Males	0/80		0/90		1/137		2/99		5/208		6/134		1/24		15/772

Table 4.4: Number of positive individuals for each ANA by age group, distinguishing females (F) and males (M), adapted from (Hayashi *et al.*, 2008).

by averaging these two conditional probabilities:

$$P(\tau(a) = 1 \mid \gamma, s) \approx \frac{P(\tau(a) = 1 \mid ANA^+, s) + P(\tau(a) = 1 \mid ANA^+, \gamma)}{2}.$$

For example, for the age group $[0, 20]$, for females, and for Anti-SSB, we have:

1. The overall ANA positivity in this subgroup is given by

$$P(ANA^+ \mid F, [0, 20]) = \frac{33 + 176}{1200 + 2150}.$$

2. Based on sex,

$$P(\tau(\text{Anti-SSB}) = 1 \mid ANA^+, F) = \frac{24}{903},$$

where 903 is the total number of ANA-positive females.

3. Based on age,

$$P(\tau(\text{Anti-SSB}) = 1 \mid ANA^+, [0, 20]) = \frac{6}{21 + 55 + 33 + 176}.$$

The estimated specific ANA positivity risks are reported in Tables 4.5 and 4.6 for Φ_G and Φ_H datasets, respectively.

Using these computed ANA specific prevalences, we simulate 4 realistic populations per dataset Φ_G^N and Φ_H^N of sizes $N \in \{50, 100, 150, 200\}$. In practice, laboratories process specimens in batches typically between 40 and 200 samples (Aprahamian, 2018), so our chosen population sizes reflect real-world testing conditions. In our simulation, each

individual is assigned an age group γ and sex s according to the discrete distribution following Table 4.7 for Φ_G^N or Table 4.8 for Φ_H^N, and is then assigned the corresponding ANA specific positivity risk with respect to the 6 ANAs reported in Table 4.1.

Concerning the dilution effect, preliminary experiments conducted by our collaborators at Lille University Hospital have shown that the multiplex assay maintains its specific ANA sensitivities and specificities only for group sizes up to $L_{\max} = 5$. Therefore, for each population of size N, we consider only eligible group sizes $L \leq L_{\max}$.

Sex	M			F		
Age	≤ 20 y	21-49 y	≥ 50 y	≤ 20 y	21-49 y	≥ 50 y
ANA						
Anti-CB	0.0005	0.0018	0.0031	0.0040	0.0070	0.0135
Anti-Jo-1	0.0003	0.0006	0.0018	0.0006	0.0012	0.0038
Anti-M2	0.0029	0.0032	0.0117	0.0114	0.0095	0.0328
Anti-Nuk	0.0003	0.0009	0.0019	0.0005	0.0016	0.0030
Anti-PCNA	0.0012	0.0003	0.0012	0.0045	0.0010	0.0036
Anti-PM	0.0009	0.0014	0.0034	0.0026	0.0028	0.0072
Anti-Rib	0.0003	0.0009	0.0019	0.0016	0.0027	0.0060
Anti-Ro52	0.0032	0.0055	0.0121	0.0115	0.0140	0.0309
Anti-SSA	0.0025	0.0046	0.0087	0.0091	0.0119	0.0222
Anti-SSB	0.0008	0.0014	0.0028	0.0025	0.0030	0.0060
Anti-Scl-70	0.0000	0.0002	0.0002	0.0003	0.0008	0.0012
Anti-Sm	0.0008	0.0012	0.0026	0.0025	0.0027	0.0057
Anti-dsDNA	0.0008	0.0012	0.0026	0.0034	0.0037	0.0076
Anti-his	0.0010	0.0021	0.0046	0.0033	0.0050	0.0107
Anti-nRNP	0.0015	0.0020	0.0040	0.0047	0.0044	0.0086

Table 4.5: Prevalences of ANA specificities by sex and age group (in $[0, 1]$) computed from Guo *et al.* (2014).

These simulated instances form our experimental benchmark for evaluating our methods for multi-ANA screening.

4.3.2 Experiment Design

For each instance, our experimental design focuses on evaluating the performance of the simultaneous column-and-row generation procedure at the root node of the Branch-and-Price algorithm. First, we initialize $RMP(\bar{\mathcal{K}})$ as described in Section 3.2.4 with the adapted objective and cost functions of the heuristics and local search method as described at the end of Section 4.2. The adopted process for pricing algorithms and the lower

Antibody	20-30 y		31-40 y		41-50 y		51-60 y		61-70 y		71-80 y		81-93 y	
	F	M	F	M	F	M	F	M	F	M	F	M	F	M
Anti-U1RNP	0.0056	0.0000	0.0082	0.0000	0.0086	0.0000	0.0099	0.0000	0.0097	0.0000	0.0000	0.0075	0.0000	0.0000
Anti-Sm	0.0000	0.0000	0.0000	0.0000	0.0000	0.0000	0.0000	0.0000	0.0000	0.0000	0.0000	0.0000	0.0000	0.0000
Anti-SSA/Ro	0.0112	0.0000	0.0163	0.0000	0.0259	0.0000	0.0644	0.0101	0.0455	0.0144	0.0526	0.0224	0.0000	0.0417
Anti-SSB/La	0.0000	0.0000	0.0041	0.0000	0.0000	0.0000	0.0050	0.0000	0.0032	0.0048	0.0048	0.0000	0.0000	0.0000
Anti-Scl-70	0.0000	0.0000	0.0000	0.0000	0.0000	0.0000	0.0000	0.0000	0.0000	0.0000	0.0000	0.0000	0.0000	0.0000
Anti-Jo-1	0.0000	0.0000	0.0000	0.0000	0.0000	0.0000	0.0000	0.0000	0.0000	0.0000	0.0000	0.0000	0.0000	0.0000
Anti-centromere	0.0056	0.0000	0.0041	0.0000	0.0129	0.0000	0.0198	0.0101	0.0260	0.0096	0.0287	0.0075	0.0000	0.0000
Anti-dsDNA	0.0000	0.0000	0.0041	0.0000	0.0043	0.0073	0.0050	0.0000	0.0065	0.0048	0.0048	0.0149	0.0000	0.0000

Table 4.6: Probability of being positive for each ANA by age group and sex (in $[0, 1]$) computed from Hayashi *et al.* (2008).

Age Group	F	M
2-10	5.72	6.20
10-20	10.25	10.49
20-30	8.01	8.11
30-40	8.77	8.58
40-50	7.06	7.15
50-60	4.63	4.77
60-70	2.62	2.86
70-80	1.91	1.67
80+	0.72	0.48

Table 4.7: Proportion (in %) by age group and sex from Table 4.2.

Age Group	F	M
20-30	8.16	3.67
31-40	11.23	4.13
41-50	10.64	6.28
51-60	9.26	4.54
61-70	14.12	9.54
71-80	9.58	6.14
81-93	1.60	1.10

Table 4.8: Proportion (in %) by age group and sex from Table 4.4.

bound is the configuration retained in the previous chapter (see Section 3.4.3). Namely, we use the chain of pricing heuristics and the suitable exact pricing algorithm depending on the values of N and L and the computation of the lower bound as $\texttt{LB} = max(0, (L(\bar{\alpha}, \bar{\lambda}))$. Preliminary experiments show that the labeling pricing algorithm configuration $\texttt{EXT}_{\texttt{LAB}}$ can be called to solve the pricing problem to optimality only for the instances with $(N, L) \in \{(50, 4), (50, 5), (100, 4), (150, 3)\}$.

4.3.3 Results

Table 4.9 summarizes the results. We report the Lagrangian lower bound (LB), and the best upper bound found by the heuristics ($\mathbb{E}[FP(S)]$). Additionally, we report the expected number of false negatives ($\mathbb{E}[FN(S)]$) and the expected number of tests ($\mathbb{E}[T(S)]$). Note that $\mathbb{E}[T(S)]$ can be compared to the number of groups in each solution G. These

measures provide a clear view of the potential gains in terms of misclassification errors and testing costs if the proposed screening strategy was implemented in practice. We recall that $\mathbb{E}[FN(S)]$ is not affected by how the individuals are arranged in the groups. In addition, we report the total execution time ($\texttt{Time}_r$ $\texttt{(s)}$) of the simultaneous column-and-row generation process in the root node. We also report the number of y and x variables. Note that $\texttt{LB}$ is computed as $\texttt{LB} = max(0, (L(\bar{\alpha}, \bar{\lambda}))$ since we are minimizing the misclassification error, which is a positive measure. We report the gap at root node as $\texttt{Gap}_r$, which is computed as $\frac{OBJ-LB}{LB} \times 100$ when $LB > 0$; otherwise, the gaps are infinite and are reported as '-' in the table.

Table 4.9 shows that for $N = 50$, we could solve the root node in less than 26 seconds for all the datasets Φ_G^{50} and Φ_H^{50} and providing a gap at the root node $\leq 0.45\%$ with the minimum gap of 0.04%. Datasets Φ_G^{100} and Φ_H^{100} with group sizes of $L = 4$ are solved in less than 6 minutes and with a gap at the root node of 0.84%. Datasets Φ_G^{150} and Φ_H^{150} with $L = 3$ are solved in less than 96 seconds with a gap at the root node of $\leq 3.53\%$ with Φ_H^{150} with $L = 3$ solved in 40 seconds and with a gap of 1.96%. These are the instances for which we can provide a performance guarantee within less than 6 minutes of runtime. For the remaining instances, we could not compute a performance guarantee due to the lower bound being equal to 0.

In conclusion, similarly to the last chapter, all in all, only instances for which $\texttt{EXT}_{\texttt{LAB}}$ can be called are the instances for which we can provide the performance guarantee.

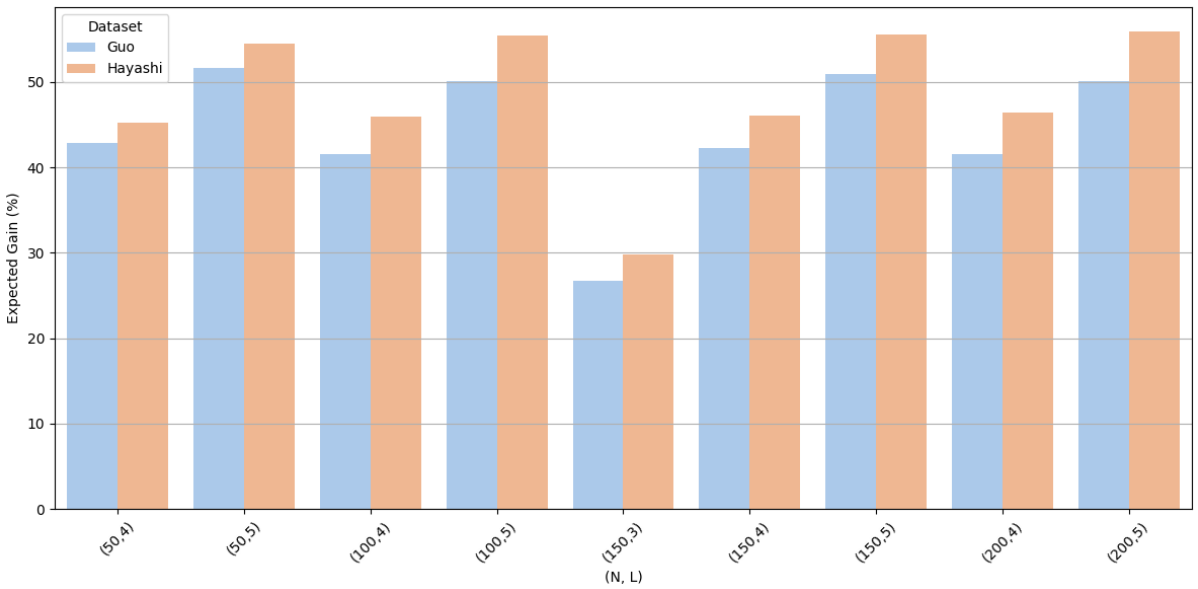


Figure 4.2: Expected gain in the number of tests compared to individual testing, for each dataset and configuration (N, L). The gain is computed as $\left(1 - \frac{\mathbb{E}[T(S)]}{N}\right) \times 100$.

Figure 4.2 highlights the expected gain in the number of tests achieved by our two-dimensional group testing strategy with equal group sizes, compared to individual testing. The expected gain (%) is computed as $\left(1 - \frac{\mathbb{E}[T(S)]}{N}\right) \times 100$ and is shown for each dataset

and configuration (N, L).

The results demonstrate that our approach can reduce the number of tests by approximately 42% to 56%, depending on the population size and group size. The gain tends to increase with larger group sizes L and is generally higher for the Φ_H due to its prevalence distribution. For instance, with $N = 100$ and $L = 5$, the expected gain reaches over 55%. Our approach saves more than half of the tests required by individual testing. In other words, with the same 100 tests, we can test up to 155 individuals by using the 55 saved tests for individual testing (i.e., 100 + 55). Alternatively, we can apply two-dimensional group testing to a new batch of 100 individuals, potentially testing up to 200 people in total, assuming no confirmatory retesting is necessary.

These gains highlight the practical value of our method, especially in large-scale screening scenarios. While exact methods can provide performance guarantees for small to medium-sized instances–based on the best heuristic solutions–the use of heuristics becomes essential to handle larger instances within acceptable computation times efficiently.

From an economic perspective, group testing offers substantial economic savings compared to individual testing, particularly in the context of high-throughput laboratories such as the one at Lille University Hospital. In the current system, patients are not charged directly for ANA tests. Instead, the laboratory bills the French social security system. Billing is based on test outcomes: a negative result costs 20.80 €, while a positive result costs 35.36 €, due to the additional confirmatory analyses required to identify specific ANA patterns. This pricing structure reflects actual resource usage because more steps and reagents are involved in positive cases, as shown in the hospital's pricing policy (Biology and Genetic Pathology Center - Lille University Hospital , 2025).

With individual testing, each patient incurs a cost of at least 20.8 €, even when the entire population is negative. However, when employing group testing, the laboratory uses fewer tests to screen the same population, leading to a direct reduction in testing costs and, consequently, in the amount billed to social security. For instance, in our experiments with a population of $N = 100$ and group size $L = 5$, our optimization algorithms reduce the expected number of tests by approximately 55%. In the hypothetical case where all individuals test negative, this translates to a cost of $20.8 \times 100 \times 0.45 = 936$ € compared with 2080 € in the individual testing setting, resulting in an expected savings of 1144 € for the social security.

Nevertheless, it is essential to recognize that group testing introduces extra operational complexity for the laboratory. Preparing and managing group mixtures requires more work from laboratory personnel and may necessitate an investment in dedicated platforms or equipment to automate and track sample pooling. Furthermore, confirmatory testing is needed for individuals suspected to be positive based on group results, which adds to the workflow.

This raises important policy questions regarding the distribution of cost savings and labor burden. While social security benefits from reduced expenses, laboratories must

bear the operational overhead introduced by group testing. Addressing this imbalance is crucial for practical adoption and may require revisiting reimbursement policies and regulations. A fair redistribution model or incentivizing laboratories through adjusted billing schemes could unlock the full potential of group testing in public health screening programs.

These results provide valuable information for planning the next steps of the project. They can help determine whether to focus on small batches of individuals, where we can compute performance guarantees using our exact methods, or larger batches, where such guarantees are unavailable but our heuristics still provide high-quality solutions. The trade-off between performance assurance and scalability will guide the practical implementation of the proposed screening strategy.

N	L	G	Dataset	LB	$\mathbb{E}[FP(S)]$	$\mathbb{E}[FN(S)]$	$\mathbb{E}[T(S)]$	$\#y$	$\#x$	# Iter.	Time$_r$ (s)	Gap$_r$ (%)
50	4	25	Φ_H^{50}	0.11885	0.11938	2.03065	28.55900	428	22402	33	23.18	0.45
50	4	25	Φ_G^{50}	0.08200	0.08236	1.33574	27.39017	336	13540	26	22.74	0.44
50	5	20	Φ_H^{50}	0.16480	0.16504	2.03065	24.14351	423	30479	40	25.58	0.15
50	5	20	Φ_G^{50}	0.10872	0.10876	1.33574	22.72807	322	17428	28	19.32	0.04
100	4	50	Φ_H^{100}	0.28503	0.28632	4.73939	58.40492	733	36957	49	354.49	0.76
100	4	50	Φ_G^{100}	0.14178	0.14251	2.23162	54.05599	568	22068	45	356.32	0.84
100	5	40	Φ_H^{100}	0.00000	0.40125	4.73939	49.87629	724	53803	53	1042.71	-
100	5	40	Φ_G^{100}	0.00000	0.18412	2.23162	44.58879	592	36278	42	1164.19	-
150	3	100	Φ_H^{150}	0.25632	0.26302	6.47373	109.84091	991	28093	103	95.39	3.53
150	3	100	Φ_G^{150}	0.15434	0.15666	3.24440	105.24993	643	11529	78	39.68	1.96
150	4	75	Φ_H^{150}	0.00000	0.39925	6.47373	86.58499	1234	75172	99	1186.73	-
150	4	75	Φ_G^{150}	0.00000	0.21081	3.24440	80.94326	965	46018	79	863.31	-
150	5	60	Φ_H^{150}	0.00000	0.55391	6.47373	73.56501	1223	107686	101	TL	-
150	5	60	Φ_G^{150}	0.00000	0.27042	3.24440	66.70637	1098	87571	90	TL	-
200	4	100	Φ_H^{200}	0.00000	0.58749	9.25632	116.77748	1487	83192	119	2696.66	-
200	4	100	Φ_G^{200}	0.00000	0.25835	3.83936	107.14672	1128	48239	103	2030.03	-
200	5	80	Φ_H^{200}	0.00000	0.82014	9.25632	99.75584	1471	120647	122	TL	-
200	5	80	Φ_G^{200}	0.00000	0.32751	3.83936	88.03219	1199	80391	95	TL	-

Table 4.9: Results of the simultaneous column-and-row generation on the root node

4.4 Conclusion and Perspectives

In this chapter, we extended our previously developed methods for single-disease group testing to the context of multi-disease (multi-ANA) screening, in collaboration with the Lille University Hospital. The goal is to support a large-scale screening initiative for the

early detection of rare autoimmune diseases. To achieve this, we adapted the statistical performance measures, expected number of false positives, false negatives, and tests, to account for multiple ANA targets per individual. Once these adaptations were made, we demonstrated the genericity and flexibility of our approach: the existing mathematical formulations required only minimal changes, primarily in the objective and cost functions, while the general framework remained unchanged.

We then conducted computational experiments on simulated data based on two real case studies in the literature. These experiments aimed to evaluate the performance of our simultaneous column-and-row generation method, complemented by construction heuristics and local search procedures. The goal was to provide mathematical and practical insights into the potential of our methods for this collaboration.

The results show that our heuristics and local search can already yield solutions of interest. However, what we consider more valuable is the ability to compute a lower bound and obtain a performance guarantee on the quality of these solutions. Our experiments indicate that this is currently achievable only for small population sizes and small group sizes, due to the computational limits of our exact pricing algorithms. Nevertheless, even with this limitation, the method can still be used to generate batches for around 50 individuals at a time, which remains practical for the intended application.

Looking forward, our main research perspective lies in assessing the real-world validity of our approach. In particular, we aim to evaluate how closely the expected values used in our methods–such as the number of tests and misclassification errors–align with real-world empirical results. This will be the focus of the next steps in our ongoing collaboration with the Lille University Hospital.

Conclusions and Perspectives

Conclusions

This research is the first to study exact methods for the problem of risk-based non-adaptive two-dimensional group testing under realistic conditions. The objective is to minimize a convex combination of the expected number of tests and the misclassification error, accounting for population heterogeneity and imperfect tests.

Chapter 1 presents a literature review focused on the application of Combinatorial Optimization techniques to group testing problems. The majority of existing research, namely Aprahamian *et al.* (2019), addresses one-dimensional risk-based group testing variants where each individual belongs to a single group. Notably, no exact methods have been proposed for the two-dimensional group testing problem under realistic assumptions of heterogeneity and imperfect testing. The closest works include McMahan *et al.* (2012b), who proposed heuristics for risk-based matrix group testing, and Xiong *et al.* (2019), who introduced the concept of maximal overlapping group designs, albeit assuming population homogeneity. This identified gap motivated the development of a more general and exact approach for non-adaptive risk-based two-dimensional group testing.

Chapter 2 presents a generalized risk-based non-adaptive two-dimensional group testing design with equal group sizes, where each individual is assigned to exactly two groups and each group contains L individuals. The design minimizes a convex combination of expected tests and misclassification errors, with L constrained to clinical limits to reduce dilution effects. A key contribution is the characterization of eligible group sizes for which such designs are feasible. Unlike matrix-based designs, constructing solutions for generalized design was non-trivial. We introduced several variants of constructive algorithms and local search heuristics. Another significant contribution was the development of several mathematical formulations to model the problem. Starting with a nonlinear compact formulation, we transformed it to a quadratic formulation and strengthened it with symmetry-breaking constraints to create a tighter mixed-integer quadratic program. We also proposed an extended quadratic formulation by enumerating all possible groups of size L, shifting nonlinear terms into precomputed costs. Computational experiments on randomly generated instances show that our Least-prevalence heuristic outperforms prior work, with average relative gaps of 0.036% for $N \leq 12$ and 0.001% for $N = 9$. In comparison, the Gradient heuristic had an average gap of 0.073%, and the Spiral design

performed worst, with a gap of 4.555% for $N = 9$. These results demonstrate the effectiveness of our heuristics. For exact methods, we solved instances to optimality for $N \leq 10$ using the extended formulation, with an average runtime of under 45 seconds. However, scalability remains a limitation. For $N \geq 12$, none of the three formulations could achieve optimality within a one-hour time limit due to weak lower bounds and the combinatorial complexity.

Chapter 3 addresses the scalability challenge by developing a Branch-and-Price algorithm for large-scale instances. We first propose a tighter formulation obtained by applying the Reformulation and Linearization Technique (RLT) (Adams & Sherali, 1986) to the linearized extended formulation. This formulation enables optimal solutions for $N \leq 10$ in under 0.6 seconds and for $N = 12$ in around 44 seconds–far surpassing previous formulations. To solve its linear relaxation, we developed a simultaneous column-and-row generation algorithm (Muter, 2011). This algorithm incorporates auxiliary variables representing intersections of groups, transforming the nonlinear objective terms into the pricing problem. A major challenge was to estimate correctly the missing dual variables for assessing the optimality of the simultaneous column-and-row generation. Two exact pricing algorithms are developed: one solves a formulated pricing problem with a commercial solver, and the other uses a problem-specific labeling algorithm. The labeling approach, while efficient, currently lacks dominance and completion bounding techniques due to the pricing problem's complexity. We also implement heuristics derived from the labeling algorithm to further improve scalability. We compute a Lagrangian lower bound to obtain a valid global lower bound on the optimal value of the master problem, improving the solution quality assessment during optimization. The experiments on the proposed Branch-and-Price algorithm revealed that most computational effort and improvement occur at the root node, where the optimality gap is already quite low (e.g., less than 1.85%). Branching and tree exploration reduce the gap marginally, suggesting that additional computational time beyond the root node yields limited benefit in closing the gap further neither to improve the upper bound. This highlights the efficiency of the developed heuristics making them well-suited for massive screening applications.

Chapter 4 extends the methods developed in previous chapters to a multi-risk screening context, in collaboration with Lille University Hospital, focusing on antinuclear antibody (ANA) screening for autoimmune diseases. The framework originally designed for single-disease screening was successfully adapted for this multi-risk setting. Each individual has a risk vector for each ANA, and we defined positivity as being positive for at least one ANA, reflecting the multiplex nature of the assay. We adapted the cost function of the heuristics and objective functions of the mathematical formulations to account for the misclassification error and the expected number of tests required in this multi-ANA setup. Despite these changes, the overall framework from earlier chapters remained intact. Experiments with populations of 50 to 200 individuals from real-world studies demonstrated significant savings in the expected number of tests, ranging from

27% to 56%. The multiplex assay achieved high performance with minimal misclassification error, and optimality gaps range from 0.04% to 3.53%. These results validate the efficiency of the proposed methods for large-scale applications. Future work will apply these findings in real-world studies to assess the practical impact and further compare the observed results with the expected outcomes.

In conclusion, a key strength of this research lies in the reusability and adaptability of the proposed methods. The models and algorithms can be applied to various large-scale screening problems across diverse fields, including public health, medical diagnostics, and industrial quality control. The methodology requires only the population's risk levels, the test characteristics, and the group size constraints, making it highly flexible for different applications.

Perspectives and Future Directions of Research

While this research presented several contributions to the field of non-adaptive two-dimensional group testing with heterogeneous populations, several key future research directions remain.

A significant obstacle we encountered throughout our methods, particularly when solving the mathematical formulations, was the weak lower bound. This issue also affected the mathematical programming based local search heuristic and the pricing problem formulation. Despite being able to find the optimal solution as the best incumbent, closing the gap efficiently remained a bottleneck. Future research should focus on improving the lower bound or investigating hidden problem structures that could help strengthen it. Exploring valid inequalities, tighter reformulations, or other mathematical techniques is essential for improving the computational performance of the methods proposed.

The scalability of exact pricing algorithms also posed a challenge, particularly due to the lack of dominance rules and completion bounds, which is a consequence of the complex objective function in the pricing problem. These issues hindered the scalability of our methods. Overcoming these challenges by finding new ways to tighten the pricing formulation could significantly improve the scalability and applicability of the methods to large-scale problems.

While constructive algorithms and local search heuristics were developed and proved effective for small instances, there is room to explore alternative solution approaches. Investigating the suitability of metaheuristics could provide further improvements in solution quality when dealing with large-scale instances where exact methods become computationally prohibitive. For example, Genetic Algorithms (GAs) could be explored; however, a major challenge lies first in designing a solution encoding that respects the problem's structural constraints–namely, two-group membership, intersection conditions, and equal group sizes. Efficient crossover and mutation operators tailored to this encoding would be essential to maintain feasibility and performance. Alternatively, matheuristics–

hybrid approaches combining heuristic strategies with mathematical programming components– have shown strong potential. In particular, our work on the ejection cycle operator, which integrates a mathematical programming model into local search, opens the door to deeper exploration of this paradigm. Given its promising results, further extensions in this direction could yield scalable and effective solution methods for even larger problem instances.

From a modeling perspective, one promising direction would be to consider relaxing the equality constraint on group sizes could enable more flexible and practically viable designs. This would allow the algorithm to automatically decide the optimal group sizes that allow for the minimal misclassification error.

The complexity of the proposed problem remains an open question. A formal study of its computational complexity, including hardness results and identification of tractable subclasses if any, could provide valuable insights and guide algorithmic development.

In addition to the algorithmic improvements, we also need to address the practical implementation of the proposed methods, particularly in real-world scenarios. One such avenue of future research involves the physical execution of sample mixtures in large-scale screening. The proposed solutions require groups of individuals to be formed, a task that can be difficult to execute manually, especially in high-throughput screening facilities. A pipetting robot could automate this process, but the question arises: how can we optimize the pipetting robot's actions based on the solutions we have developed? This problem presents a new layer of complexity and could be approached by optimizing the pipetting sequence, focusing on minimizing either the number of pipetting changes or the distance traveled by the robot, while considering its handling capacity and physical constraints.

The importance of practice in evaluating the efficiency of the proposed methods cannot be overstated. While the theoretical and algorithmic contributions are critical, their true value lies in their practical applicability. Ensuring that the solutions we propose can be implemented efficiently in real-world settings is key to bridging the gap between theory and practice.

Last but not least, an extension to higher-dimensional designs, where each individual is tested in more than two groups, may further enhance detection accuracy and reduce false classifications. While this increases the modeling and computational complexity, it opens up new structural possibilities in the design of multi-dimensional group testing.

Finally, we hope that the work presented in this thesis inspires further research in both the field of group testing and optimization problems in general. While the methods developed here are specifically tailored to non-adaptive two-dimensional group testing with heterogeneous populations, we believe that the framework can be adapted to tackle similar optimization problems in various domains.

Bibliography

Adams, W.P. & Sherali, H.D. (1986). A tight linearization and an algorithm for zero-one quadratic programming problems. *Management Science*, **32**, 1274–1290. 59, 110

Adams, W.P. & Sherali, H.D. (1990). Linearization strategies for a class of zero-one mixed integer programming problems. *Operations Research*, **38**, 217–226. 59

Agard, C. & Mekinian, A. (2023). Épidémiologie de la sclérodermie systémique. https://sclerodermie.net/epidemiologie-de-la-sclerodermie-systemique/. Accessed: March 24, 2025. 94

Almeftah, T., Brotcorne, L., Cattaruzza, D., Fortz, B., Keita, K., Labbé, M., Ogier, M. & Semet, F. (2020). Group design in group testing for COVID-19: A french case-study. *arXiv preprint arXiv:2011.06927*. 9, 10

Anthony, M., Boros, E., Crama, Y. & Gruber, A. (2017). Quadratic reformulations of nonlinear binary optimization problems. *Mathematical Programming*, **162**, 115–144. 33

Aprahamian, H. & El-Amine, H. (2022). Optimal screening of populations with heterogeneous risk profiles under the availability of multiple tests. *INFORMS Journal on Computing*, **34**, 150–164. 10, 12

Aprahamian, H., Bish, E.K. & Bish, D.R. (2018). Adaptive risk-based pooling in public health screening. *IISE Transactions*, **50**, 753–766. 9, 10

Aprahamian, H., Bish, D.R. & Bish, E.K. (2019). Optimal risk-based group testing. *Management Science*, **65**, 4365–4384. 2, 9, 10, 11, 109

Aprahamian, H., Bish, D.R. & Bish, E.K. (2020a). Optimal group testing: Structural properties and robust solutions, with application to public health screening. *INFORMS Journal on Computing*, **32**, 895–911. 10, 11

Aprahamian, H., Bish, E.K. & Bish, D.R. (2020b). Static risk-based group testing schemes under imperfectly observable risk. *Stochastic Systems*, **10**, 361–390. 10, 11

Aprahamian, H.Y.B. (2018). *Optimal Risk-based Pooled Testing in Public Health Screening, with Equity and Robustness Considerations*. Ph.D. thesis. 101

Ben-Ami, R., Klochendler, A., Seidel, M., Sido, T., Gurel-Gurevich, O., Yassour, M., Meshorer, E., Benedek, G., Fogel, I., Oiknine-Djian, E., Gertler, A., Rotstein, Z., Lavi, B., Dor, Y., Wolf, D., Salton, M. & Drier, Y. (2020). Large-scale implementation of pooled RNA extraction and RT-PCR for SARS-CoV-2 detection. *Clinical Microbiology and Infection*, **26**, 1248–1253. 2

Bilder, C.R., Tebbs, J.M. & McMahan, C.S. (2019). Informative group testing for multiplex assays. *Biometrics*, **75**, 278–288. 94

Bilder, C.R., Tebbs, J.M. & McMahan, C.S. (2021). Informative array testing with multiplex assays. *Statistics in Medicine*, **40**, 3021–3034. 94

Biology and Genetic Pathology Center - Lille University Hospital (2025). ANA Test Pricing. https://biologiepathologie.chu-lille.fr/catalogue-analyses/Detail.php?codeCatalogueAnalyses=4302. Accessed: June 23, 2025. 105

Bish, D.R., Bish, E.K., El-Hajj, H. & Aprahamian, H. (2021). A robust pooled testing approach to expand COVID-19 screening capacity. *Plos One*, **16**, e0246285. 10, 12

Blass, A. & Gurevich, Y. (2002). Y. gurevich: The logic in computer science column pairwise testing. *Bulletin-European Association for Theoretical Computer Science*, **78**, 100–132. 2

Bui, T.V., Huynh, C.N. & Nguyen, T.D. (2013). Early detection for networking anomalies using non-adaptive group testing. In *2013 International Conference on ICT Convergence (ICTC)*, 984–987, IEEE. 2

Burer, S. & Letchford, A.N. (2012). Non-convex mixed-integer nonlinear programming: A survey. *Surveys in Operations Research and Management Science*, **17**, 97–106. 33

Chépy, A., Bourel, L., Koether, V., Launay, D., Dubucquoi, S. & Sobanski, V. (2022). Can antinuclear antibodies have a pathogenic role in systemic sclerosis? *Frontiers in Immunology*, **13**, 930970. 94

Chépy, A., Collet, A., Sobanski, V. & Dubucquoi, S. (2024). Les anticorps antinucléaires: spectateurs ou acteurs? exemple de la sclérodermie systémique. *Revue Francophone des Laboratoires*, **2024**, 31–38. 94

Colosi, L.M., Barry, K.E., Kotay, S.M., Porter, M.D., Poulter, M.D., Ratliff, C., Simmons, W., Steinberg, L.I., Wilson, D.D., Morse, R. *et al.* (2021). Development of wastewater pooled surveillance of severe acute respiratory syndrome coronavirus 2 (SARS-CoV-2) from congregate living settings. *Applied and Environmental Microbiology*, **87**, e00433–21. 2

Damoiseaux, J., Boesten, K., Giesen, J., Austen, J. & Cohen Tervaert, J. (2005). Evaluation of a novel line-blot immunoassay for the detection of antibodies to extractable nuclear antigens. *Annals of the New York Academy of Sciences*, **1050**, 340–347. 99

Daniel, E.A., Anbalagan, S., Muthuramalingam, K., Karunaianantham, R., Karunakaran, L.P., Nesakumar, M., Selvachithiram, M., Pattabiraman, S., Natarajan, S., Tripathy, S.P. *et al.* (2021). Pooled testing strategies for SARS-CoV-2 diagnosis: A comprehensive review. *Diagnostic Microbiology and Infectious Disease*, **101**, 115432. 3

Dantzig, G.B. & Wolfe, P. (1960). Decomposition principle for linear programs. *Operations Research*, **8**, 101–111. 63

Denton, C.P. & Khanna, D. (2017). Systemic sclerosis. *The Lancet*, **390**, 1685–1699. 94

Desrosiers, J. & Lübbecke, M.E. (2011). Branch-price-and-cut algorithms. *Encyclopedia of Operations Research and Management Science. John Wiley & Sons, Chichester*, 109–131. 78

Dorfman, R. (1943). The detection of defective members of large populations. *The Annals of Mathematical Statistics*, **14**, 436–440. 1

El Hajj, H., Bish, D.R., Bish, E.K. & Aprahamian, H. (2022a). Screening multidimensional heterogeneous populations for infectious diseases under scarce testing resources, with application to COVID-19. *Naval Research Logistics (NRL)*, **69**, 3–20. 10, 12

El Hajj, H., Bish, D.R., Bish, E.K. & Kay, D.M. (2022b). Novel pooling strategies for genetic testing, with application to newborn screening. *Management Science*. 10

Elloumi, S. & Verchère, Z. (2023). Efficient linear reformulations for binary polynomial optimization problems. *Computers & Operations Research*, **155**, 106240. 33

Feillet, D. (2010). A tutorial on column generation and branch-and-price for vehicle routing problems. *4OR*, **8**, 407–424. 79

Gilmore, P.C. & Gomory, R.E. (1961). A linear programming approach to the cutting-stock problem. *Operations Research*, **9**, 849–859. 63

Glover, F. (1996). Ejection chains, reference structures and alternating path methods for traveling salesman problems. *Discrete Applied Mathematics*, **65**, 223–253. 39

Guo, Y.P., Wang, C.G., Liu, X., Huang, Y.Q., Guo, D.L., Jing, X.Z., Yuan, C.G., Yang, S., Liu, J.M., Han, M.S. *et al.* (2014). The prevalence of antinuclear antibodies in the general population of china: a cross-sectional study. *Current Therapeutic Research*, **76**, 116–119. xi, xii, 98, 99, 100, 102

Gurobi Optimization, LLC (2024). Gurobi Optimizer Reference Manual. 33

Habtesllassie, Y., Haines, L.M., Mwambi, H. & Odhiambo, J. (2015). Array-based schemes for group screening with test errors which incorporate a concentration effect. *Journal of Statistical Planning and Inference*, **167**, 41–57. 18, 26

Hayashi, N., Koshiba, M., Nishimura, K., Sugiyama, D., Nakamura, T., Morinobu, S., Kawano, S. & Kumagai, S. (2008). Prevalence of disease-specific antinuclear antibodies in general population: estimates from annual physical examinations of residents of a small town over a 5-year period. *Modern Rheumatology*, **18**, 153–160. xii, 98, 99, 100, 101, 103

Hou, P., Tebbs, J.M., Wang, D., McMahan, C.S. & Bilder, C.R. (2020). Array testing for multiplex assays. *Biostatistics*, **21**, 417–431. 94

Hourfar, M.K., Themann, A., Eickmann, M., Puthavathana, P., Laue, T., Seifried, E. & Schmidt, M. (2007). Blood screening for influenza. *Emerging Infectious Diseases*, **13**, 1081. 2

Hudgens, M.G. & Kim, H.Y. (2011). Optimal configuration of a square array group testing algorithm. *Communications in Statistics–Theory and Methods*, **40**, 436–448. 14

Kainkaryam, R.M. & Woolf, P.J. (2009). Pooling in high-throughput drug screening. *Current Opinion in Drug Discovery & Development*, **12**, 339. 2

Kim, H.Y. & Hudgens, M.G. (2009). Three-dimensional array-based group testing algorithms. *Biometrics*, **65**, 903–910. 14

Kiziltan, Z. (2004). *Symmetry breaking ordering constraints*. Ph.D. thesis, Data-och Systemvetenskap. 35

Laboratories, B.R. (2023). Bioplex 2200 ANA Screen With MDSS. https://www.bio-rad.com/en-fr/product/bioplex-2200-ana-screen-with-mdss?ID=fa9a5d96-922d-4b5e-8d76-4e7417b3dd37. Accessed: March 24, 2025. 94

Lin, J., Aprahamian, H. & Golovko, G. (2024a). Optimal targeted mass screening in non-uniform populations with multiple tests and schemes. *Naval Research Logistics (NRL)*, **71**, 87–108. 10, 12

Lin, J., Aprahamian, H. & Golovko, G. (2024b). An optimization framework for large-scale screening under limited testing capacity with application to COVID-19. *Health Care Management Science*, 1–16. 10, 12

Lin, J., Aprahamian, H. & Golovko, G. (2024c). A proactive/reactive mass screening approach with uncertain symptomatic cases. *PLOS Computational Biology*, **20**, e1012308. 10, 12

Lübbecke, M.E. & Desrosiers, J. (2005). Selected topics in column generation. *Operations Research*, **53**, 1007–1023. 63

McMahan, C.S., Tebbs, J.M. & Bilder, C.R. (2012a). Informative dorfman screening. *Biometrics*, **68**, 287–296. 9, 10

McMahan, C.S., Tebbs, J.M. & Bilder, C.R. (2012b). Two-dimensional informative array testing. *Biometrics*, **68**, 793–804. vi, 14, 43, 44, 50, 54, 95, 109

Mullis, K.B. (1994). *The polymerase chain reaction*, vol. 41. Springer science & business media. 17

Muter, İ. (2011). *Simultaneous column-and-row generation for solving large-scale linear programs with column-dependent-rows*. Ph.D. thesis. 63, 110

Muter, I., Birbil, Ş.İ. & Bülbül, K. (2013). Simultaneous column-and-row generation for large-scale linear programs with column-dependent-rows. *Mathematical Programming*, **142**, 47–82. 65

Mutesa, L., Ndishimye, P., Butera, Y., Souopgui, J., Uwineza, A., Rutayisire, R., Ndoricimpaye, E.L., Musoni, E., Rujeni, N., Nyatanyi, T. *et al.* (2021). A pooled testing strategy for identifying SARS-CoV-2 at low prevalence. *Nature*, **589**, 276–280. 14

Pasquali, F., De Cesare, A., Valero, A., Olsen, J.E. & Manfreda, G. (2014). Improvement of sampling plans for salmonella detection in pooled table eggs by use of real-time PCR. *International Journal of Food Microbiology*, **184**, 31–34. 2

Pevzner, P.A. & Lipshutz, R.J. (1994). Towards dna sequencing chips. In *International Symposium on Mathematical Foundations of Computer Science*, 143–158, Springer. 2

Phatarfod, R. & Sudbury, A. (1994). The use of a square array scheme in blood testing. *Statistics in Medicine*, **13**, 2337–2343. 4, 14

Ryan, D.M. & Foster, B.A. (1981). An integer programming approach to scheduling. *Computer Scheduling of Public Transport Urban Passenger Vehicle and Crew Scheduling*, 269–280. 79

Shah, K. & Maghsoudlou, P. (2016). Enzyme-linked immunosorbent assay (elisa): the basics. *British journal of hospital medicine*, **77**, C98–C101. 99

Sherali, H.D. & Adams, W.P. (1990). A hierarchy of relaxations between the continuous and convex hull representations for zero-one programming problems. *SIAM Journal on Discrete Mathematics*, **3**, 411–430. 59

Sherali, H.D. & Adams, W.P. (1994). A hierarchy of relaxations and convex hull characterizations for mixed-integer zero–one programming problems. *Discrete Applied Mathematics*, **52**, 83–106. 59

Sherali, H.D. & Adams, W.P. (1998). Reformulation-linearization techniques for discrete optimization problems. In *Handbook of Combinatorial Optimization*, 479–532, Springer. 59

Sherali, H.D. & Adams, W.P. (2013). *A reformulation-linearization technique for solving discrete and continuous nonconvex problems*, vol. 31. Springer Science & Business Media. 59

Sobel, M. & Groll, P.A. (1959). Group testing to eliminate efficiently all defectives in a binomial sample. *Bell System Technical Journal*, **38**, 1179–1252. 2

Weusten, J., Vermeulen, M., van Drimmelen, H. & Lelie, N. (2011). Refinement of a viral transmission risk model for blood donations in seroconversion window phase screened by nucleic acid testing in different pool sizes and repeat test algorithms. *Transfusion*, **51**, 203–215. 2

Xiong, W., Ding, J., He, Y. & Li, Q. (2019). Improved matrix pooling. *Statistical Methods in Medical Research*, **28**, 211–222. 19, 109

Yelin, I., Aharony, N., Tamar, E.S., Argoetti, A., Messer, E., Berenbaum, D., Shafran, E., Kuzli, A., Gandali, N., Shkedi, O. *et al.* (2020). Evaluation of COVID-19 RT-qPCR test in multi sample pools. *Clinical Infectious Diseases*, **71**, 2073–2078. 2

Appendix

Appendix for Chapter 2

Square Matrix Layout Check Problem $\mathbf{F_{SQUARE}}$ when $L = \sqrt{N}$

Any solution to the model (2.1) can be verified to see if it can be expressed as a matrix where L groups represent the rows and L other groups represent the columns, with each individual being the intersection of a row and a column. By definition, the model (2.1) may not guarantee this property as it does not incorporate such constraints. Thus, we modeled a problem that takes as a parameter the optimal solution of (2.1) and tries to constitute the corresponding matrix if possible. Let $\mathcal{L} = \{1, \ldots, L\}$, where L is the size of each group and $\mathcal{G}$ indexes the groups from 1 to G, with $G = \frac{2N}{L}$. Note, when $L = \sqrt{N}$, G equals $2L$. The binary variables are defined as follows. Let $w^i_{mn} = 1$ if individual i is in cell $(m, n), \forall i \in \mathcal{I}$, $m, n \in \mathcal{L}$, 0 otherwise; $r_{mk} = 1$ if group $G_k, k \in \mathcal{G}$ represents the row $m \in \mathcal{L}$, 0 otherwise; and $c_{nk} = 1$ if group $G_k, k \in \mathcal{G}$ represents the column $n \in \mathcal{L}$, 0 otherwise. The optimization problem is formulated in $\mathrm{F}_{\mathrm{SQUARE}}$.

Constraints (4.4) impose exactly one cell (m, n) for each individual i. Constraints (4.5) impose exactly one individual i per cell (m, n). Constraints (4.6) impose exactly L groups to be chosen as columns. Constraints (4.7) impose exactly L groups to be chosen as rows. Constraints (4.8) express that if a group k is chosen to be the column m, then all the individuals i belonging to group G_k have to be assigned to this row m. Similarly, constraints (4.9) express that if a group k is chosen to be the row n, then all the individuals i belonging to group G_k have to be assigned to this column n. Finally, constraints (4.10), (4.11), and (4.12) are integrality constraints for the variables w^i_{mn}, c_{mg}, and r_{ng}. The model does not have an objective function as stated in (4.3) as the formulation above models a feasibility problem.

$$[\text{F}_{\text{SQUARE}}] \quad \min \quad 0 \tag{4.3}$$

$$\text{s.t.} \sum_{m\in\mathcal{L}}\sum_{n\in\mathcal{L}} w^i_{mn} = 1 \qquad \forall i \in \mathcal{I} \tag{4.4}$$

$$\sum_{i\in\mathcal{I}} w^i_{mn} = 1 \qquad \forall m,n \in \mathcal{L} \tag{4.5}$$

$$\sum_{m\in\mathcal{L}}\sum_{k\in\mathcal{G}} c_{mk} = L \tag{4.6}$$

$$\sum_{n\in\mathcal{L}}\sum_{k\in\mathcal{G}} r_{nk} = L \tag{4.7}$$

$$\sum_{i\in G_k}\sum_{m\in\mathcal{L}} w^i_{mn} - Lc_{mk} \geq 0 \qquad \forall m \in \mathcal{L}, k \in \mathcal{G} \tag{4.8}$$

$$\sum_{i\in G_k}\sum_{n\in\mathcal{L}} w^i_{mn} - Lr_{nk} \geq 0 \qquad \forall n \in \mathcal{L}, k \in \mathcal{G} \tag{4.9}$$

$$w^i_{mn} \in \{0,1\} \qquad \forall m,n \in \mathcal{L}, i \in \mathcal{I} \tag{4.10}$$

$$c_{mg} \in \{0,1\} \qquad \forall m \in \mathcal{L}, k \in \mathcal{G} \tag{4.11}$$

$$r_{ng} \in \{0,1\} \qquad \forall n \in \mathcal{L}, k \in \mathcal{G} \tag{4.12}$$

Detailed Experimental Results

Remark 4.5. *The values of* $\mathbb{E}[FP(S)]$ *in our experiments are very small. Therefore, for ease of interpretation, all* $\mathbb{E}[FP(S)]$ *values reported in our tables are multiplied by a factor of* $100,000$.

Appendix for Chapter 3

Table 4.50: Comparison of Branching Rules for N=36, L=3, Instance ID = 1

L	Se	Sp	Configuration	LB	UB	Δ UB (%)	$\#y$	$\#x$	# nodes	Time_r (s)	Total Time (s)	Gap_r (%)	Gap (%)
3	0.9	0.9	BP-HFX	22167.03	22261.17	0.0002	1082	160080	650	0.69	TL	0.42	0.42
3	0.9	0.9	BP-HFY	22167.03	22261.17	0.0002	979	122843	748	0.72	TL	0.42	0.42
3	0.9	0.9	BP-RF	22167.03	22261.17	0.0002	1246	194812	473	0.71	TL	0.42	0.42
3	0.9	0.95	BP-HFX	7863.42	7921.22	0.0	879	106045	692	1.14	TL	0.74	0.74
3	0.9	0.95	BP-HFY	7868.67	7921.22	0.0	850	100547	756	0.80	TL	0.67	0.67
3	0.9	0.95	BP-RF	7874.49	7921.22	0.0	942	120708	645	1.25	TL	0.59	0.59
3	0.9	0.99	BP-HFX	1139.62	1140.12	0.0	615	52508	847	0.66	TL	0.04	0.04
3	0.9	0.99	BP-HFY	1139.64	1140.12	0.0	576	45327	903	0.59	TL	0.04	0.04
3	0.9	0.99	BP-RF	1139.67	1140.12	0.0	686	58393	744	0.59	TL	0.04	0.04
3	0.95	0.9	BP-HFX	23866.04	24006.69	0.0001	943	122265	597	0.90	TL	0.59	0.59
3	0.95	0.9	BP-HFY	23897.81	24006.69	0.0001	995	132274	669	1.10	TL	0.46	0.46
3	0.95	0.9	BP-RF	23884.44	24006.69	0.0001	1181	175302	480	0.92	TL	0.51	0.51
3	0.95	0.95	BP-HFX	8587.89	8649.79	0.0	941	119308	607	1.19	TL	0.72	0.72
3	0.95	0.95	BP-HFY	8598.83	8649.79	0.0	870	103665	701	1.58	TL	0.59	0.59
3	0.95	0.95	BP-RF	8605.70	8649.79	0.0	1003	130908	528	1.42	TL	0.51	0.51
3	0.95	0.99	BP-HFX	1263.60	1264.28	0.0001	737	75161	799	0.76	TL	0.05	0.05
3	0.95	0.99	BP-HFY	1263.57	1264.28	0.0001	648	57247	982	0.66	TL	0.06	0.06
3	0.95	0.99	BP-RF	1263.52	1264.28	0.0001	725	66210	673	1.04	TL	0.06	0.06
3	0.99	0.9	BP-HFX	25273.96	25439.43	0.0	1039	145576	713	0.60	TL	0.65	0.65
3	0.99	0.9	BP-HFY	25273.96	25439.40	0.0	926	115646	713	0.58	TL	0.65	0.65
3	0.99	0.9	BP-RF	25273.96	25439.40	0.0	1183	180733	447	0.60	TL	0.65	0.65
3	0.99	0.95	BP-HFX	9200.87	9257.62	0.0	957	124254	661	0.77	TL	0.62	0.62
3	0.99	0.95	BP-HFY	9200.87	9257.62	0.0	857	102455	811	0.77	TL	0.62	0.62
3	0.99	0.95	BP-RF	9184.52	9257.62	0.0	914	106760	460	1.78	TL	0.80	0.80
3	0.99	0.99	BP-HFX	1367.11	1368.22	0.0001	722	70191	868	0.67	TL	0.08	0.08
3	0.99	0.99	BP-HFY	1367.11	1368.22	0.0001	690	61770	983	0.70	TL	0.08	0.08
3	0.99	0.99	BP-RF	1367.11	1368.22	0.0001	747	73025	896	0.67	TL	0.08	0.08

Table 4.51: Comparison of Branching Rules for N=36, L=4, Instance ID = 1

L	Se	Sp	Configuration	LB	UB	Δ UB (%)	$\#y$	$\#x$	# nodes	Time$_r$ (s)	Total Time (s)	Gap$_r$ (%)	Gap (%)
4	0.9	0.9	BP-HFX	35218.19	35472.07	0.0001	1490	430290	86	3.21	TL	0.72	0.72
4	0.9	0.9	BP-HFY	35285.13	35472.07	0.0001	1520	455519	160	3.77	TL	0.53	0.53
4	0.9	0.9	BP-RF	35220.12	35472.07	0.0001	1561	429484	101	3.81	TL	0.72	0.72
4	0.9	0.95	BP-HFX	13959.19	14054.60	0.0	1402	372953	96	5.68	TL	0.68	0.68
4	0.9	0.95	BP-HFY	13943.63	14054.60	0.0	1444	402783	84	4.22	TL	0.80	0.80
4	0.9	0.95	BP-RF	13940.16	14054.60	0.0	1489	388497	66	6.53	TL	0.82	0.82
4	0.9	0.99	BP-HFX	2250.71	2278.31	0.0	1024	199283	217	5.31	TL	1.23	1.23
4	0.9	0.99	BP-HFY	2275.38	2277.84	0.0205	1252	306591	231	6.11	TL	0.13	0.11
4	0.9	0.99	BP-RF	2252.80	2278.31	0.0	1132	233770	216	4.56	TL	1.13	1.13
4	0.95	0.9	BP-HFX	38338.62	38613.50	0.0	1476	425460	76	4.20	TL	0.72	0.72
4	0.95	0.9	BP-HFY	38380.00	38613.50	0.0	1477	423059	148	4.08	TL	0.61	0.61
4	0.95	0.9	BP-RF	38382.45	38613.50	0.0	1588	447206	63	5.36	TL	0.60	0.60
4	0.95	0.95	BP-HFX	15344.94	15455.88	0.0001	1352	352430	157	5.65	TL	0.72	0.72
4	0.95	0.95	BP-HFY	15346.84	15455.88	0.0001	1528	442864	66	5.90	TL	0.71	0.71
4	0.95	0.95	BP-RF	15346.74	15455.88	0.0001	1519	414213	80	5.93	TL	0.71	0.71
4	0.95	0.99	BP-HFX	2527.67	2531.03	0.0	1283	318592	159	4.54	TL	0.13	0.13
4	0.95	0.99	BP-HFY	2527.61	2531.03	0.0	1063	219512	211	4.26	TL	0.14	0.14
4	0.95	0.99	BP-RF	2504.68	2531.03	0.0	1340	327681	152	6.77	TL	1.05	1.05
4	0.99	0.9	BP-HFX	40944.35	41226.40	0.0	1598	506445	139	4.44	TL	0.69	0.69
4	0.99	0.9	BP-HFY	40944.35	41226.40	0.0	1612	517220	98	4.55	TL	0.69	0.69
4	0.99	0.9	BP-RF	40944.35	41226.40	0.0	1583	448146	94	4.66	TL	0.69	0.69
4	0.99	0.95	BP-HFX	16481.16	16624.40	0.0	1567	480260	106	7.40	TL	0.87	0.87
4	0.99	0.95	BP-HFY	16481.16	16624.16	0.0015	1424	375100	166	7.32	TL	0.87	0.87
4	0.99	0.95	BP-RF	16491.34	16624.22	0.0011	1566	423160	105	7.58	TL	0.81	0.81
4	0.99	0.99	BP-HFX	2715.33	2742.78	0.0	1190	269133	164	4.10	TL	1.01	1.01
4	0.99	0.99	BP-HFY	2715.33	2742.78	0.0	1161	258664	222	4.17	TL	1.01	1.01
4	0.99	0.99	BP-RF	2738.80	2742.78	0.0	1250	299236	148	5.52	TL	0.15	0.15

Table 4.52: Comparison of Branching Rules for N=36, L=6, Instance ID = 1

L	Se	Sp	Configuration	LB	UB	Δ UB (%)	$\#y$	$\#x$	# nodes	Time_r (s)	Total Time (s)	Gap_r (%)	Gap (%)
6	0.9	0.9	BP-HFX	63439.87	63896.30	0.0	697	96011	3	281.88	TL	0.72	0.72
6	0.9	0.9	BP-HFY	63247.43	63896.30	0.0	700	95220	3	1570.95	TL	1.03	1.03
6	0.9	0.9	BP-RF	63441.15	63896.30	0.0	580	66158	5	301.99	TL	0.72	0.72
6	0.9	0.95	BP-HFX	27630.76	27964.40	0.0	731	104727	3	1434.88	TL	1.21	1.21
6	0.9	0.95	BP-HFY	27777.00	27964.40	0.0	721	101407	3	653.87	TL	0.67	0.67
6	0.9	0.95	BP-RF	27584.47	27964.40	0.0	471	43052	2	2927.86	TL	1.38	1.38
6	0.9	0.99	BP-HFX	4903.10	4989.99	0.0	698	96901	3	1530.30	TL	1.77	1.77
6	0.9	0.99	BP-HFY	4952.26	4989.99	0.0	827	132085	3	491.36	TL	0.76	0.76
6	0.9	0.99	BP-RF	4950.66	4989.99	0.0	622	76505	4	468.27	TL	0.79	0.79
6	0.95	0.9	BP-HFX	69719.84	70236.40	0.0	661	78802	3	1164.33	TL	0.74	0.74
6	0.95	0.9	BP-HFY	69125.88	70236.40	0.0	900	160388	4	286.89	TL	1.61	1.61
6	0.95	0.9	BP-RF	69779.21	70236.40	0.0	571	64310	5	692.49	TL	0.66	0.66
6	0.95	0.95	BP-HFX	30670.14	30931.20	0.0	819	132924	3	280.70	TL	0.85	0.85
6	0.95	0.95	BP-HFY	30660.48	30931.20	0.0	740	106186	3	546.03	TL	0.88	0.88
6	0.95	0.95	BP-RF	30599.28	30931.20	0.0	620	74778	4	794.29	TL	1.08	1.08
6	0.95	0.99	BP-HFX	5495.35	5551.20	0.0	837	137492	3	581.12	TL	1.02	1.02
6	0.95	0.99	BP-HFY	5496.44	5551.20	0.0	767	115371	3	549.42	TL	1.00	1.00
6	0.95	0.99	BP-RF	5506.85	5551.20	0.0	608	71701	4	580.67	TL	0.81	0.81
6	0.99	0.9	BP-HFX	74963.25	75504.26	0.0001	761	114865	3	683.42	TL	0.72	0.72
6	0.99	0.9	BP-HFY	74963.25	75504.26	0.0001	611	72677	3	675.54	TL	0.72	0.72
6	0.99	0.9	BP-RF	74963.25	75504.26	0.0001	611	72999	5	687.20	TL	0.72	0.72
6	0.99	0.95	BP-HFX	33136.44	33439.38	0.0	720	102975	3	507.09	TL	0.91	0.91
6	0.99	0.95	BP-HFY	33136.44	33439.40	0.0	827	134101	4	506.78	TL	0.91	0.91
6	0.99	0.95	BP-RF	33136.44	33439.40	0.0	600	70272	4	496.17	TL	0.91	0.91
6	0.99	0.99	BP-HFX	5965.43	6020.40	0.0	860	145205	3	541.55	TL	0.92	0.92
6	0.99	0.99	BP-HFY	5965.43	6020.40	0.0	885	153825	3	536.85	TL	0.92	0.92
6	0.99	0.99	BP-RF	5967.53	6020.40	0.0	671	86488	4	494.63	TL	0.89	0.89

Table 4.53: Comparison of Branching Rules for N=36, L=3, Instance ID = 2

L	Se	Sp	Configuration	LB	UB	Δ UB (%)	$\#y$	$\#x$	# nodes	Time$_r$ (s)	Total Time (s)	Gap$_r$ (%)	Gap (%)
3	0.9	0.9	BP-HFX	19954.24	20021.09	0.0011	966	127200	648	0.86	TL	0.34	0.34
3	0.9	0.9	BP-HFY	19954.24	20020.36	0.0047	971	125188	685	0.86	TL	0.34	0.33
3	0.9	0.9	BP-RF	19954.24	20021.30	0.0	1221	185189	413	0.84	TL	0.34	0.34
3	0.9	0.95	BP-HFX	6860.12	6907.33	0.0083	837	92167	763	0.84	TL	0.70	0.69
3	0.9	0.95	BP-HFY	6866.32	6907.90	0.0	885	109012	608	0.75	TL	0.61	0.61
3	0.9	0.95	BP-RF	6866.39	6906.97	0.0135	1009	128619	568	0.81	TL	0.60	0.59
3	0.9	0.99	BP-HFX	960.55	960.96	0.0022	789	85907	739	0.54	TL	0.05	0.04
3	0.9	0.99	BP-HFY	960.59	960.93	0.0053	738	73895	843	0.59	TL	0.04	0.04
3	0.9	0.99	BP-RF	960.58	960.98	0.0	764	70715	789	0.65	TL	0.04	0.04
3	0.95	0.9	BP-HFX	21415.53	21523.49	0.0075	881	105217	585	0.60	TL	0.51	0.50
3	0.95	0.9	BP-HFY	21416.59	21524.61	0.0023	885	103726	684	0.58	TL	0.51	0.50
3	0.95	0.9	BP-RF	21411.85	21525.08	0.0001	1110	163526	415	0.63	TL	0.53	0.53
3	0.95	0.95	BP-HFX	7491.51	7530.76	0.0001	870	99869	644	1.25	TL	0.52	0.52
3	0.95	0.95	BP-HFY	7488.94	7530.76	0.0001	969	124841	604	1.26	TL	0.56	0.56
3	0.95	0.95	BP-RF	7480.17	7530.76	0.0001	1029	135566	422	1.01	TL	0.68	0.68
3	0.95	0.99	BP-HFX	1064.10	1064.10	0.0883	397	18423	25	0.68	53.79	0.04	0.00
3	0.95	0.99	BP-HFY	1064.60	1064.86	0.017	771	78363	852	0.80	TL	0.04	0.02
3	0.95	0.99	BP-RF	1064.59	1065.04	0.0	744	68210	742	0.79	TL	0.04	0.04
3	0.99	0.9	BP-HFX	22658.84	22766.57	0.0001	911	113885	554	0.98	TL	0.48	0.48
3	0.99	0.9	BP-HFY	22598.32	22766.34	0.0011	935	117879	590	0.99	TL	0.74	0.74
3	0.99	0.9	BP-RF	22632.32	22762.16	0.0195	1041	138884	481	0.65	TL	0.59	0.57
3	0.99	0.95	BP-HFX	7991.19	8048.73	0.0	956	125472	550	0.87	TL	0.72	0.72
3	0.99	0.95	BP-HFY	8015.84	8047.96	0.0096	973	131045	540	1.20	TL	0.41	0.40
3	0.99	0.95	BP-RF	8004.74	8048.73	0.0	1140	165309	494	1.15	TL	0.55	0.55
3	0.99	0.99	BP-HFX	1150.99	1150.99	0.0	188	3670	1	0.64	0.76	0.00	0.00
3	0.99	0.99	BP-HFY	1150.99	1150.99	0.0	188	3670	1	0.58	0.69	0.00	0.00
3	0.99	0.99	BP-RF	1150.99	1150.99	0.0	198	4088	3	0.59	2.03	0.00	0.00

Table 4.54: Comparison of Branching Rules for N=36, L=4, Instance ID = 2

L	Se	Sp	Configuration	LB	UB	Δ UB (%)	$\#y$	$\#x$	# nodes	Time_r (s)	Total Time (s)	Gap_r (%)	Gap (%)
4	0.9	0.9	BP-HFX	31490.60	31647.10	0.0	1554	473066	77	3.17	TL	0.50	0.50
4	0.9	0.9	BP-HFY	31483.76	31640.47	0.0209	1357	346862	196	4.51	TL	0.52	0.50
4	0.9	0.9	BP-RF	31429.08	31647.10	0.0	1603	458762	102	3.58	TL	0.69	0.69
4	0.9	0.95	BP-HFX	12134.92	12235.70	0.0	1474	421030	87	3.92	TL	0.83	0.83
4	0.9	0.95	BP-HFY	12154.84	12227.03	0.0709	1299	315996	104	3.68	TL	0.67	0.59
4	0.9	0.95	BP-RF	12150.69	12235.70	0.0	1467	376360	75	3.70	TL	0.70	0.70
4	0.9	0.99	BP-HFX	1932.06	1932.11	0.0	1094	214070	187	5.47	TL	0.00	0.00
4	0.9	0.99	BP-HFY	1932.11	1932.11	0.0	256	10624	3	4.43	11.98	0.01	0.00
4	0.9	0.99	BP-RF	1931.96	1932.11	0.0	993	171926	196	5.75	TL	0.01	0.01
4	0.95	0.9	BP-HFX	34182.78	34373.90	0.0	1496	425538	54	8.86	TL	0.56	0.56
4	0.95	0.9	BP-HFY	34211.89	34373.90	0.0	1479	429943	58	4.02	TL	0.47	0.47
4	0.95	0.9	BP-RF	34159.87	34373.90	0.0	1524	430457	91	5.29	TL	0.63	0.63
4	0.95	0.95	BP-HFX	13333.63	13435.37	0.0003	1244	289017	113	5.37	TL	0.76	0.76
4	0.95	0.95	BP-HFY	13341.73	13435.37	0.0003	1499	434925	122	6.02	TL	0.70	0.70
4	0.95	0.95	BP-RF	13314.05	13435.37	0.0003	1540	432534	79	3.95	TL	0.91	0.91
4	0.95	0.99	BP-HFX	2122.92	2145.62	0.0	1113	231133	185	4.31	TL	1.07	1.07
4	0.95	0.99	BP-HFY	2124.04	2145.52	0.0045	1091	222603	225	4.81	TL	1.02	1.01
4	0.95	0.99	BP-RF	2145.31	2145.62	0.0	1153	238899	205	4.78	TL	0.01	0.01
4	0.99	0.9	BP-HFX	36431.89	36638.07	0.0001	1434	389087	91	6.08	TL	0.57	0.57
4	0.99	0.9	BP-HFY	36410.35	36638.07	0.0001	1417	378609	115	3.68	TL	0.63	0.63
4	0.99	0.9	BP-RF	36430.37	36638.07	0.0001	1591	451863	119	3.94	TL	0.57	0.57
4	0.99	0.95	BP-HFX	14319.82	14432.83	0.0095	1404	377515	131	5.11	TL	0.80	0.79
4	0.99	0.95	BP-HFY	14319.82	14432.38	0.0126	1264	300168	160	5.19	TL	0.80	0.79
4	0.99	0.95	BP-RF	14324.41	14434.16	0.0003	1578	449777	126	5.62	TL	0.77	0.77
4	0.99	0.99	BP-HFX	2323.43	2323.43	0.0	248	9810	1	3.74	4.91	0.00	0.00
4	0.99	0.99	BP-HFY	2323.43	2323.43	0.0	248	9810	1	3.75	4.91	0.00	0.00
4	0.99	0.99	BP-RF	2323.43	2323.43	0.0	271	11752	1	8.35	8.51	0.00	0.00

Table 4.55: Comparison of Branching Rules for N=36, L=6, Instance ID = 2

L	Se	Sp	Configuration	LB	UB	Δ UB (%)	$\#y$	$\#x$	# nodes	Time_r (s)	Total Time (s)	Gap_r (%)	Gap (%)
6	0.9	0.9	BP-HFX	56832.19	57234.30	0.0	436	36499	2	732.37	TL	0.71	0.71
6	0.9	0.9	BP-HFY	56751.35	57234.30	0.0	426	34645	2	960.50	TL	0.85	0.85
6	0.9	0.9	BP-RF	56817.76	57234.30	0.0	476	44417	4	1403.08	TL	0.73	0.73
6	0.9	0.95	BP-HFX	24484.14	24615.39	0.0	457	41056	2	1351.06	TL	0.54	0.54
6	0.9	0.95	BP-HFY	24462.69	24615.39	0.0	467	42751	2	1299.04	TL	0.62	0.62
6	0.9	0.95	BP-RF	24469.47	24615.39	0.0	527	54341	4	1466.04	TL	0.60	0.60
6	0.9	0.99	BP-HFX	4290.83	4324.59	0.0	506	50457	2	426.59	TL	0.79	0.79
6	0.9	0.99	BP-HFY	4287.41	4324.59	0.0	785	123403	4	228.61	TL	0.87	0.87
6	0.9	0.99	BP-RF	4283.72	4324.59	0.0	628	77432	4	469.85	TL	0.95	0.95
6	0.95	0.9	BP-HFX	62505.72	62800.70	0.0	436	36818	2	1363.98	TL	0.47	0.47
6	0.95	0.9	BP-HFY	62463.80	62800.70	0.0	416	33840	2	1774.31	TL	0.54	0.54
6	0.95	0.9	BP-RF	62409.41	62800.70	0.0	536	56826	5	780.88	TL	0.63	0.63
6	0.95	0.95	BP-HFX	27005.85	27202.29	0.0	427	36204	2	1017.46	TL	0.73	0.73
6	0.95	0.95	BP-HFY	27027.75	27202.29	0.0	437	36730	2	1098.61	TL	0.65	0.65
6	0.95	0.95	BP-RF	27020.80	27202.29	0.0	487	46097	4	984.77	TL	0.67	0.67
6	0.95	0.99	BP-HFX	4771.13	4809.90	0.0001	875	153073	4	480.88	TL	0.81	0.81
6	0.95	0.99	BP-HFY	4767.43	4809.90	0.0001	795	124768	4	692.58	TL	0.89	0.89
6	0.95	0.99	BP-RF	4770.03	4809.90	0.0001	594	70109	4	465.59	TL	0.84	0.84
6	0.99	0.9	BP-HFX	67041.51	67444.30	0.0	427	35582	2	476.24	TL	0.60	0.60
6	0.99	0.9	BP-HFY	66932.49	67444.30	0.0	507	49530	3	509.61	TL	0.76	0.76
6	0.99	0.9	BP-RF	67036.71	67444.30	0.0	477	43186	4	1224.24	TL	0.61	0.61
6	0.99	0.95	BP-HFX	29165.53	29365.18	0.0001	467	42658	2	275.91	TL	0.68	0.68
6	0.99	0.95	BP-HFY	29165.53	29365.18	0.0001	497	47945	2	266.00	TL	0.68	0.68
6	0.99	0.95	BP-RF	29056.24	29365.18	0.0001	577	64953	5	940.46	TL	1.06	1.06
6	0.99	0.99	BP-HFX	5177.71	5211.79	0.0	487	46876	2	1204.69	TL	0.66	0.66
6	0.99	0.99	BP-HFY	5177.97	5211.79	0.0	457	40655	2	1394.04	TL	0.65	0.65
6	0.99	0.99	BP-RF	5179.00	5211.79	0.0	464	41735	2	1730.30	TL	0.63	0.63

Table 4.56: Comparison of Branching Rules for N=36, L=3, Instance ID = 3

L	Se	Sp	Configuration	LB	UB	Δ UB (%)	$\#y$	$\#x$	# nodes	Time_r (s)	Total Time (s)	Gap_r (%)	Gap (%)
3	0.9	0.9	BP-HFX	15882.90	15958.40	0.0	1187	191184	391	0.97	TL	0.48	0.48
3	0.9	0.9	BP-HFY	15882.90	15958.40	0.0	1127	169513	366	0.93	TL	0.48	0.48
3	0.9	0.9	BP-RF	15882.90	15958.40	0.0	1137	167265	414	0.91	TL	0.48	0.48
3	0.9	0.95	BP-HFX	4988.92	5028.97	0.045	944	119617	581	1.41	TL	0.85	0.80
3	0.9	0.95	BP-HFY	4993.15	5031.24	0.0	886	102815	781	1.38	TL	0.76	0.76
3	0.9	0.95	BP-RF	4985.67	5030.02	0.0242	1074	150248	577	1.41	TL	0.91	0.89
3	0.9	0.99	BP-HFX	615.72	616.22	0.0	764	74914	761	0.63	TL	0.08	0.08
3	0.9	0.99	BP-HFY	615.59	616.22	0.0	691	65246	842	0.62	TL	0.10	0.10
3	0.9	0.99	BP-RF	615.52	616.22	0.0	812	79857	649	0.95	TL	0.11	0.11
3	0.95	0.9	BP-HFX	16910.25	17031.79	0.0042	981	128754	614	1.17	TL	0.72	0.72
3	0.95	0.9	BP-HFY	16916.56	17032.49	0.0001	1085	155861	537	1.32	TL	0.69	0.69
3	0.95	0.9	BP-RF	16935.11	17031.76	0.0043	1025	136683	546	1.44	TL	0.58	0.57
3	0.95	0.95	BP-HFX	5390.91	5450.47	0.0	1036	144783	623	1.39	TL	1.10	1.10
3	0.95	0.95	BP-HFY	5408.76	5450.47	0.0	979	126308	589	1.95	TL	0.77	0.77
3	0.95	0.95	BP-RF	5394.33	5446.10	0.0802	1081	153200	505	1.69	TL	1.04	0.96
3	0.95	0.99	BP-HFX	680.40	681.39	0.0	756	78663	1461	1.24	TL	0.15	0.15
3	0.95	0.99	BP-HFY	680.67	681.34	0.0078	811	89336	1662	0.93	TL	0.11	0.10
3	0.95	0.99	BP-RF	680.65	681.00	0.0578	760	75008	832	0.63	TL	0.11	0.05
3	0.99	0.9	BP-HFX	17780.91	17912.96	0.0002	1094	162702	457	1.20	TL	0.74	0.74
3	0.99	0.9	BP-HFY	17806.90	17903.25	0.0544	1150	179539	413	1.54	TL	0.60	0.54
3	0.99	0.9	BP-RF	17813.44	17911.57	0.008	1092	159441	473	0.95	TL	0.56	0.55
3	0.99	0.95	BP-HFX	5748.29	5796.92	0.0126	1016	138951	488	2.26	TL	0.86	0.85
3	0.99	0.95	BP-HFY	5740.48	5793.02	0.0799	926	115682	603	1.46	TL	1.00	0.92
3	0.99	0.95	BP-RF	5740.73	5790.23	0.128	1166	168396	359	0.99	TL	0.99	0.86
3	0.99	0.99	BP-HFX	734.81	735.89	0.0	712	68136	861	0.74	TL	0.15	0.15
3	0.99	0.99	BP-HFY	734.81	735.49	0.0543	755	77384	891	0.74	TL	0.15	0.09
3	0.99	0.99	BP-RF	734.81	735.89	0.0	845	89260	801	0.74	TL	0.15	0.15

Table 4.57: Comparison of Branching Rules for N=36, L=4, Instance ID = 3

L	Se	Sp	Configuration	LB	UB	Δ UB (%)	$\#y$	$\#x$	# nodes	Time_r (s)	Total Time (s)	Gap_r (%)	Gap (%)
4	0.9	0.9	BP-HFX	24570.18	24766.07	0.0001	1745	603482	42	6.02	TL	0.80	0.80
4	0.9	0.9	BP-HFY	24538.48	24766.07	0.0001	1548	449332	107	3.76	TL	0.93	0.93
4	0.9	0.9	BP-RF	24573.46	24766.07	0.0001	1562	437405	64	3.80	TL	0.78	0.78
4	0.9	0.95	BP-HFX	8841.01	8917.12	0.0	1526	445544	49	4.80	TL	0.86	0.86
4	0.9	0.95	BP-HFY	8845.54	8912.22	0.055	1442	370081	148	5.46	TL	0.81	0.75
4	0.9	0.95	BP-RF	8830.10	8917.12	0.0	1555	442483	91	4.63	TL	0.99	0.99
4	0.9	0.99	BP-HFX	1296.06	1297.40	0.0	1143	250912	129	6.42	TL	0.10	0.10
4	0.9	0.99	BP-HFY	1296.05	1297.40	0.0	1092	224753	147	6.76	TL	0.10	0.10
4	0.9	0.99	BP-RF	1295.99	1297.40	0.0	1095	212847	85	8.97	TL	0.11	0.11
4	0.95	0.9	BP-HFX	26518.34	26732.60	0.0	1677	537493	85	4.63	TL	0.81	0.81
4	0.95	0.9	BP-HFY	26556.90	26732.60	0.0	1541	447564	77	4.85	TL	0.66	0.66
4	0.95	0.9	BP-RF	26516.53	26732.60	0.0	1718	528907	62	6.31	TL	0.81	0.81
4	0.95	0.95	BP-HFX	9662.70	9735.95	0.1155	1502	422935	57	7.55	TL	0.87	0.76
4	0.95	0.95	BP-HFY	9673.64	9747.21	0.0	1449	387451	92	7.33	TL	0.76	0.76
4	0.95	0.95	BP-RF	9666.20	9747.21	0.0	1584	440622	94	5.81	TL	0.84	0.84
4	0.95	0.99	BP-HFX	1437.22	1438.91	0.0001	1171	263538	106	8.45	TL	0.12	0.12
4	0.95	0.99	BP-HFY	1437.22	1438.91	0.0001	1229	286775	139	8.44	TL	0.12	0.12
4	0.95	0.99	BP-RF	1437.16	1438.91	0.0001	1154	238259	137	6.58	TL	0.12	0.12
4	0.99	0.9	BP-HFX	28087.43	28349.97	0.0001	1722	559993	57	4.65	TL	0.93	0.93
4	0.99	0.9	BP-HFY	28164.33	28348.42	0.0056	1415	388074	95	4.58	TL	0.66	0.65
4	0.99	0.9	BP-RF	28133.86	28349.97	0.0001	1602	450822	44	5.34	TL	0.77	0.77
4	0.99	0.95	BP-HFX	10437.67	10437.67	0.0003	1466	394357	37	7.58	2075.64	0.94	0.00
4	0.99	0.95	BP-HFY	10360.71	10430.28	0.0711	1552	445165	128	5.59	TL	0.74	0.67
4	0.99	0.95	BP-RF	10343.56	10437.67	0.0003	1592	461495	95	4.78	TL	0.91	0.91
4	0.99	0.99	BP-HFX	1555.46	1558.73	0.0002	1217	276366	184	6.40	TL	0.21	0.21
4	0.99	0.99	BP-HFY	1555.64	1557.66	0.0685	1145	244408	215	7.27	TL	0.20	0.13
4	0.99	0.99	BP-RF	1555.33	1558.73	0.0002	1204	261643	160	8.34	TL	0.22	0.22

Table 4.58: Comparison of Branching Rules for N=36, L=6, Instance ID = 3

L	Se	Sp	Configuration	LB	UB	Δ UB (%)	$\#y$	$\#x$	# nodes	Time$_r$ (s)	Total Time (s)	Gap$_r$ (%)	Gap (%)
6	0.9	0.9	BP-HFX	43099.59	44384.60	0.0	628	78387	1	3598.50	TL	2.98	2.98
6	0.9	0.9	BP-HFY	43758.90	44384.60	0.0	818	133276	3	1797.84	TL	1.43	1.43
6	0.9	0.9	BP-RF	43788.92	44384.60	0.0	638	80918	4	613.17	TL	1.36	1.36
6	0.9	0.95	BP-HFX	17445.86	18187.50	0.0	1037	218804	3	1346.26	TL	4.25	4.25
6	0.9	0.95	BP-HFY	16797.34	18187.50	0.0	918	165210	2	1836.06	TL	8.28	8.28
6	0.9	0.95	BP-RF	17678.68	18187.50	0.0	838	136819	3	1383.39	TL	2.88	2.88
6	0.9	0.99	BP-HFX	2704.92	3042.53	0.0	1134	254400	1	3450.94	TL	12.48	12.48
6	0.9	0.99	BP-HFY	2755.15	3042.53	0.0	1007	199524	3	2336.35	TL	10.43	10.43
6	0.9	0.99	BP-RF	2956.76	3042.53	0.0	1167	278437	3	1374.01	TL	2.90	2.90
6	0.95	0.9	BP-HFX	46455.44	48481.79	0.0	871	147195	3	1792.45	TL	4.36	4.36
6	0.95	0.9	BP-HFY	45922.02	48481.79	0.0	915	162341	3	1942.67	TL	5.57	5.57
6	0.95	0.9	BP-RF	47616.99	48481.79	0.0	648	83933	3	1949.02	TL	1.82	1.82
6	0.95	0.95	BP-HFX	19201.57	20040.09	0.0	919	169315	3	1454.87	TL	4.37	4.37
6	0.95	0.95	BP-HFY	19306.22	20040.09	0.0	1030	215971	3	1616.57	TL	3.80	3.80
6	0.95	0.95	BP-RF	19119.96	20040.09	0.0	778	119264	2	3134.32	TL	4.81	4.81
6	0.95	0.99	BP-HFX	3160.96	3383.44	0.0001	843	139255	1	3596.06	TL	7.04	7.04
6	0.95	0.99	BP-HFY	2982.82	3383.44	0.0001	1152	263052	1	3589.89	TL	13.43	13.43
6	0.95	0.99	BP-RF	3009.85	3383.44	0.0001	1115	242321	2	2184.99	TL	12.41	12.41
6	0.99	0.9	BP-HFX	48305.58	51889.00	0.0	994	190958	3	814.92	TL	7.42	7.42
6	0.99	0.9	BP-HFY	51374.33	51889.00	0.0	1081	245421	4	729.45	TL	1.00	1.00
6	0.99	0.9	BP-RF	50881.18	51889.00	0.0	688	94214	4	1422.97	TL	1.98	1.98
6	0.99	0.95	BP-HFX	20674.36	21586.70	0.0	955	180666	3	1911.73	TL	4.41	4.41
6	0.99	0.95	BP-HFY	20674.36	21586.70	0.0	798	125220	2	1958.69	TL	4.41	4.41
6	0.99	0.95	BP-RF	21148.12	21586.70	0.0	738	109067	3	684.85	TL	2.07	2.07
6	0.99	0.99	BP-HFX	3293.25	3671.57	0.0	1045	209570	3	2033.52	TL	11.49	11.49
6	0.99	0.99	BP-HFY	3447.49	3671.57	0.0	1030	214053	2	2392.48	TL	6.50	6.50
6	0.99	0.99	BP-RF	3506.44	3671.57	0.0	842	142021	2	3089.45	TL	4.71	4.71

Table 4.59: Comparison of Branching Rules for N=36, L=3, Instance ID = 4

L	Se	Sp	Configuration	LB	UB	Δ UB (%)	$\#y$	$\#x$	# nodes	Time$_r$ (s)	Total Time (s)	Gap$_r$ (%)	Gap (%)
3	0.9	0.9	BP-HFX	17486.12	17628.90	0.0	1003	136156	605	0.66	TL	0.82	0.82
3	0.9	0.9	BP-HFY	17486.12	17628.90	0.0	1021	146538	632	0.64	TL	0.82	0.82
3	0.9	0.9	BP-RF	17486.12	17627.51	0.0079	1120	167220	491	0.66	TL	0.82	0.81
3	0.9	0.95	BP-HFX	5769.55	5811.71	0.0	935	118589	611	0.90	TL	0.73	0.73
3	0.9	0.95	BP-HFY	5771.83	5810.81	0.0155	893	109481	828	0.92	TL	0.69	0.68
3	0.9	0.95	BP-RF	5768.10	5811.71	0.0	1086	145515	523	0.86	TL	0.76	0.76
3	0.9	0.99	BP-HFX	761.35	761.91	0.0	693	67959	847	0.54	TL	0.07	0.07
3	0.9	0.99	BP-HFY	761.26	761.91	0.0	663	58898	953	0.52	TL	0.09	0.09
3	0.9	0.99	BP-RF	761.22	761.91	0.0	718	63151	932	0.59	TL	0.09	0.09
3	0.95	0.9	BP-HFX	18802.90	18879.70	0.0	895	109609	546	1.04	TL	0.41	0.41
3	0.95	0.9	BP-HFY	18775.72	18879.70	0.0	964	124366	681	0.96	TL	0.55	0.55
3	0.95	0.9	BP-RF	18779.55	18877.66	0.0108	1156	175761	496	0.63	TL	0.53	0.52
3	0.95	0.95	BP-HFX	6283.06	6316.19	0.0	889	113368	630	1.08	TL	0.53	0.53
3	0.95	0.95	BP-HFY	6277.88	6316.19	0.0	840	97190	694	1.15	TL	0.61	0.61
3	0.95	0.95	BP-RF	6259.77	6314.65	0.0243	1016	133937	697	0.85	TL	0.90	0.88
3	0.95	0.99	BP-HFX	842.68	843.34	0.0	916	114380	856	0.55	TL	0.08	0.08
3	0.95	0.99	BP-HFY	842.68	843.03	0.0365	657	54885	1017	0.54	TL	0.08	0.04
3	0.95	0.99	BP-RF	842.68	843.12	0.0261	769	77201	901	0.55	TL	0.08	0.05
3	0.99	0.9	BP-HFX	19785.18	19910.26	0.0002	1013	134617	580	1.02	TL	0.63	0.63
3	0.99	0.9	BP-HFY	19769.22	19910.26	0.0002	1046	151383	486	0.92	TL	0.71	0.71
3	0.99	0.9	BP-RF	19812.94	19910.26	0.0002	1140	172085	620	0.96	TL	0.49	0.49
3	0.99	0.95	BP-HFX	6686.72	6734.36	0.0051	1007	137676	551	1.22	TL	0.72	0.71
3	0.99	0.95	BP-HFY	6693.64	6734.70	0.0	892	103519	769	1.02	TL	0.61	0.61
3	0.99	0.95	BP-RF	6680.34	6734.70	0.0	1188	175637	440	0.74	TL	0.81	0.81
3	0.99	0.99	BP-HFX	911.02	911.70	0.0201	695	67245	983	0.56	TL	0.10	0.08
3	0.99	0.99	BP-HFY	911.02	911.64	0.0269	714	69638	915	0.56	TL	0.10	0.07
3	0.99	0.99	BP-RF	911.02	911.89	0.0	766	80300	889	0.53	TL	0.10	0.10

Table 4.60: Comparison of Branching Rules for N=36, L=4, Instance ID = 4

L	Se	Sp	Configuration	LB	UB	Δ UB (%)	$\#y$	$\#x$	# nodes	Time$_r$ (s)	Total Time (s)	Gap$_r$ (%)	Gap (%)
4	0.9	0.9	BP-HFX	27447.85	27561.40	0.0	1511	425988	81	7.24	TL	0.41	0.41
4	0.9	0.9	BP-HFY	27402.54	27561.40	0.0	1563	479448	103	6.54	TL	0.58	0.58
4	0.9	0.9	BP-RF	27294.98	27561.40	0.0	1626	478210	90	4.87	TL	0.98	0.98
4	0.9	0.95	BP-HFX	10210.58	10275.33	0.0094	1474	425154	78	4.03	TL	0.64	0.63
4	0.9	0.95	BP-HFY	10215.60	10276.30	0.0	1440	403570	95	3.40	TL	0.59	0.59
4	0.9	0.95	BP-RF	10202.98	10276.30	0.0	1388	354338	72	3.02	TL	0.72	0.72
4	0.9	0.99	BP-HFX	1559.32	1560.73	0.0002	1092	235109	186	4.04	TL	0.09	0.09
4	0.9	0.99	BP-HFY	1558.97	1560.73	0.0002	1073	227719	161	6.06	TL	0.11	0.11
4	0.9	0.99	BP-RF	1559.36	1560.73	0.0002	1036	188261	151	3.34	TL	0.09	0.09
4	0.95	0.9	BP-HFX	29667.89	29839.19	0.0	1440	412171	86	8.90	TL	0.58	0.58
4	0.95	0.9	BP-HFY	29634.42	29839.19	0.0	1431	388049	134	6.26	TL	0.69	0.69
4	0.95	0.9	BP-RF	29699.29	29839.19	0.0	1546	424155	74	7.67	TL	0.47	0.47
4	0.95	0.95	BP-HFX	11187.03	11258.40	0.0	1566	482843	38	6.61	TL	0.64	0.64
4	0.95	0.95	BP-HFY	11192.49	11254.98	0.0304	1474	434240	82	3.82	TL	0.59	0.56
4	0.95	0.95	BP-RF	11187.68	11258.40	0.0	1469	400239	80	3.56	TL	0.63	0.63
4	0.95	0.99	BP-HFX	1730.44	1732.13	0.0	1169	263806	135	4.98	TL	0.10	0.10
4	0.95	0.99	BP-HFY	1730.44	1732.13	0.0	1090	226034	158	5.13	TL	0.10	0.10
4	0.95	0.99	BP-RF	1730.25	1732.13	0.0	1112	221990	139	6.00	TL	0.11	0.11
4	0.99	0.9	BP-HFX	31561.72	31725.77	0.0001	1574	482546	86	4.91	TL	0.52	0.52
4	0.99	0.9	BP-HFY	31502.57	31718.50	0.023	1547	465169	54	4.93	TL	0.71	0.69
4	0.99	0.9	BP-RF	31560.46	31725.77	0.0001	1618	484963	62	4.06	TL	0.52	0.52
4	0.99	0.95	BP-HFX	11990.34	12076.30	0.0	1478	426957	65	5.02	TL	0.72	0.72
4	0.99	0.95	BP-HFY	11977.44	12072.30	0.0332	1430	395779	79	4.24	TL	0.83	0.79
4	0.99	0.95	BP-RF	12012.54	12076.30	0.0	1462	376205	58	3.45	TL	0.53	0.53
4	0.99	0.99	BP-HFX	1873.58	1875.69	0.0002	1315	342421	163	6.81	TL	0.11	0.11
4	0.99	0.99	BP-HFY	1873.58	1875.04	0.0345	1118	239902	214	7.08	TL	0.11	0.08
4	0.99	0.99	BP-RF	1873.51	1875.69	0.0002	1139	226852	160	6.74	TL	0.12	0.12

Table 4.61: Comparison of Branching Rules for N=36, L=6, Instance ID = 4

L	Se	Sp	Configuration	LB	UB	Δ UB (%)	$\#y$	$\#x$	# nodes	Time_r (s)	Total Time (s)	Gap_r (%)	Gap (%)
6	0.9	0.9	BP-HFX	49354.21	49732.90	0.0	787	120866	3	595.36	TL	0.77	0.77
6	0.9	0.9	BP-HFY	49396.70	49732.90	0.0	398	32389	2	693.81	TL	0.68	0.68
6	0.9	0.9	BP-RF	49380.12	49732.90	0.0	518	53783	5	958.10	TL	0.71	0.71
6	0.9	0.95	BP-HFX	20847.89	20847.89	0.0001	368	27332	1	1770.54	TL	0.00	0.00
6	0.9	0.95	BP-HFY	20727.36	20847.89	0.0001	408	33877	1	1763.35	TL	0.58	0.58
6	0.9	0.95	BP-RF	20748.78	20847.89	0.0001	408	33281	1	1872.13	TL	0.48	0.48
6	0.9	0.99	BP-HFX	3545.52	3574.34	0.0	518	54046	2	1177.53	TL	0.81	0.81
6	0.9	0.99	BP-HFY	3542.69	3574.34	0.0	850	144011	3	458.14	TL	0.89	0.89
6	0.9	0.99	BP-RF	3537.16	3574.34	0.0	565	63546	4	445.73	TL	1.05	1.05
6	0.95	0.9	BP-HFX	53996.40	54439.58	0.0	886	156992	4	288.40	TL	0.82	0.82
6	0.95	0.9	BP-HFY	54113.67	54439.58	0.0	418	35041	2	791.51	TL	0.60	0.60
6	0.95	0.9	BP-RF	53884.24	54439.58	0.0	548	61011	4	260.06	TL	1.03	1.03
6	0.95	0.95	BP-HFX	22870.48	23003.50	0.0	408	34287	2	1804.78	TL	0.58	0.58
6	0.95	0.95	BP-HFY	23002.96	23003.50	0.0	388	31176	1	1709.04	TL	0.00	0.00
6	0.95	0.95	BP-RF	22867.34	23003.50	0.0	438	39516	2	1947.79	TL	0.60	0.60
6	0.95	0.99	BP-HFX	3938.94	3974.11	0.0001	711	101595	3	886.32	TL	0.89	0.89
6	0.95	0.99	BP-HFY	3938.94	3974.11	0.0001	787	122939	3	871.64	TL	0.89	0.89
6	0.95	0.99	BP-RF	3933.82	3974.11	0.0001	627	79478	4	470.98	TL	1.02	1.02
6	0.99	0.9	BP-HFX	57954.51	58359.20	0.0	399	32149	2	470.92	TL	0.70	0.70
6	0.99	0.9	BP-HFY	57925.31	58359.20	0.0	409	32922	2	740.98	TL	0.75	0.75
6	0.99	0.9	BP-RF	57954.90	58359.20	0.0	569	65973	6	258.91	TL	0.70	0.70
6	0.99	0.95	BP-HFX	24661.40	24804.30	0.0	448	40513	2	1580.39	TL	0.58	0.58
6	0.99	0.95	BP-HFY	24627.66	24804.30	0.0	438	38710	2	1372.93	TL	0.72	0.72
6	0.99	0.95	BP-RF	24656.81	24804.30	0.0	398	32151	2	1547.24	TL	0.60	0.60
6	0.99	0.99	BP-HFX	4260.68	4309.50	0.0	912	166610	4	240.89	TL	1.15	1.15
6	0.99	0.99	BP-HFY	4260.68	4309.50	0.0	771	119096	3	234.96	TL	1.15	1.15
6	0.99	0.99	BP-RF	4270.60	4309.50	0.0	651	85751	4	262.66	TL	0.91	0.91

Table 4.62: Comparison of Branching Rules for N=36, L=3, Instance ID = 5

L	Se	Sp	Configuration	LB	UB	Δ UB (%)	$\#y$	$\#x$	# nodes	Time$_r$ (s)	Total Time (s)	Gap$_r$ (%)	Gap (%)
3	0.9	0.9	BP-HFX	17518.40	17625.90	0.0	1077	157959	528	0.81	TL	0.61	0.61
3	0.9	0.9	BP-HFY	17518.40	17624.60	0.0074	1039	145504	584	0.80	TL	0.61	0.61
3	0.9	0.9	BP-RF	17518.40	17625.90	0.0	1129	163553	437	0.90	TL	0.61	0.61
3	0.9	0.95	BP-HFX	5764.81	5804.81	0.0	1053	154156	578	1.00	TL	0.69	0.69
3	0.9	0.95	BP-HFY	5758.91	5799.70	0.0881	1070	154902	543	1.01	TL	0.80	0.71
3	0.9	0.95	BP-RF	5756.96	5804.81	0.0	1036	137544	582	1.09	TL	0.83	0.83
3	0.9	0.99	BP-HFX	758.64	758.78	0.0001	727	70411	857	0.61	TL	0.02	0.02
3	0.9	0.99	BP-HFY	758.50	758.50	0.0376	674	59184	381	0.62	1004.82	0.03	0.00
3	0.9	0.99	BP-RF	758.65	758.78	0.0001	726	63931	808	0.55	TL	0.02	0.02
3	0.95	0.9	BP-HFX	18778.93	18875.98	0.0001	1028	144830	552	1.07	TL	0.52	0.52
3	0.95	0.9	BP-HFY	18763.11	18872.29	0.0196	1103	162454	627	0.98	TL	0.60	0.58
3	0.95	0.9	BP-RF	18753.60	18872.05	0.0209	1066	144071	502	0.81	TL	0.65	0.63
3	0.95	0.95	BP-HFX	6273.10	6304.71	0.0	981	131864	528	1.40	TL	0.50	0.50
3	0.95	0.95	BP-HFY	6243.29	6304.71	0.0	965	124416	569	1.12	TL	0.98	0.98
3	0.95	0.95	BP-RF	6274.92	6304.71	0.0	1025	132906	401	1.59	TL	0.47	0.47
3	0.95	0.99	BP-HFX	839.89	839.89	0.0	170	3001	3	0.41	1.04	0.00	0.00
3	0.95	0.99	BP-HFY	839.73	839.73	0.0185	603	48196	347	0.39	707.96	0.00	0.00
3	0.95	0.99	BP-RF	839.86	839.89	0.0	698	59419	836	0.42	TL	0.00	0.00
3	0.99	0.9	BP-HFX	19783.79	19897.20	0.0387	1202	196869	351	1.03	TL	0.61	0.57
3	0.99	0.9	BP-HFY	19792.68	19904.90	0.0	951	117605	570	0.98	TL	0.57	0.57
3	0.99	0.9	BP-RF	19814.93	19904.90	0.0	1106	160910	534	0.75	TL	0.45	0.45
3	0.99	0.95	BP-HFX	6681.90	6721.57	0.0061	1071	153859	589	0.92	TL	0.60	0.59
3	0.99	0.95	BP-HFY	6681.90	6721.98	0.0	1053	149529	560	0.96	TL	0.60	0.60
3	0.99	0.95	BP-RF	6681.90	6721.98	0.0	1003	133125	640	0.93	TL	0.60	0.60
3	0.99	0.99	BP-HFX	907.84	908.04	0.0	680	63363	962	0.56	TL	0.04	0.02
3	0.99	0.99	BP-HFY	907.63	908.04	0.0	696	64253	896	0.55	TL	0.04	0.04
3	0.99	0.99	BP-RF	907.63	908.04	0.0	676	58809	884	0.54	TL	0.04	0.04

Table 4.63: Comparison of Branching Rules for N=36, L=4, Instance ID = 5

L	Se	Sp	Configuration	LB	UB	Δ UB (%)	$\#y$	$\#x$	# nodes	Time_r (s)	Total Time (s)	Gap_r (%)	Gap (%)
4	0.9	0.9	BP-HFX	27452.60	27568.56	0.0002	1509	429178	68	4.81	TL	0.42	0.42
4	0.9	0.9	BP-HFY	27453.72	27568.56	0.0002	1411	370540	97	9.84	TL	0.42	0.42
4	0.9	0.9	BP-RF	27442.74	27568.56	0.0002	1548	426224	60	8.88	TL	0.46	0.46
4	0.9	0.95	BP-HFX	10199.44	10276.49	0.0001	1516	422510	98	7.15	TL	0.76	0.76
4	0.9	0.95	BP-HFY	10211.85	10273.01	0.034	1314	315949	136	4.06	TL	0.63	0.60
4	0.9	0.95	BP-RF	10198.23	10276.49	0.0001	1470	391837	63	4.25	TL	0.77	0.77
4	0.9	0.99	BP-HFX	1557.82	1558.57	0.0	1055	201171	221	4.49	TL	0.05	0.05
4	0.9	0.99	BP-HFY	1557.78	1558.57	0.0	1116	231018	192	5.23	TL	0.05	0.05
4	0.9	0.99	BP-RF	1557.87	1558.57	0.0	1007	173039	137	3.75	TL	0.05	0.05
4	0.95	0.9	BP-HFX	29713.19	29845.29	0.0	1535	444140	71	7.50	TL	0.44	0.44
4	0.95	0.9	BP-HFY	29732.84	29845.29	0.0	1620	502303	64	8.94	TL	0.38	0.38
4	0.95	0.9	BP-RF	29703.18	29845.29	0.0	1660	508433	44	7.25	TL	0.48	0.48
4	0.95	0.95	BP-HFX	11181.26	11258.08	0.0002	1490	415296	67	4.96	TL	0.69	0.69
4	0.95	0.95	BP-HFY	11157.77	11258.08	0.0002	1507	425241	151	3.62	TL	0.90	0.90
4	0.95	0.95	BP-RF	11180.31	11258.08	0.0002	1600	455009	75	5.86	TL	0.70	0.70
4	0.95	0.99	BP-HFX	1728.48	1729.71	0.0	1243	293907	195	4.34	TL	0.07	0.07
4	0.95	0.99	BP-HFY	1728.48	1729.71	0.0	1276	318759	238	4.29	TL	0.07	0.07
4	0.95	0.99	BP-RF	1728.33	1729.71	0.0	1128	222774	143	5.73	TL	0.08	0.08
4	0.99	0.9	BP-HFX	31597.15	31730.88	0.0001	1750	562235	60	8.62	TL	0.42	0.42
4	0.99	0.9	BP-HFY	31425.75	31730.88	0.0001	1589	478504	43	7.82	TL	0.97	0.97
4	0.99	0.9	BP-RF	31608.01	31730.88	0.0001	1586	443301	42	9.18	TL	0.39	0.39
4	0.99	0.95	BP-HFX	11997.50	12072.39	0.0001	1566	452780	78	4.25	TL	0.62	0.62
4	0.99	0.95	BP-HFY	11997.50	12072.39	0.0001	1469	397917	94	4.24	TL	0.62	0.62
4	0.99	0.95	BP-RF	11966.19	12072.39	0.0001	1530	411731	46	5.62	TL	0.89	0.89
4	0.99	0.99	BP-HFX	1871.65	1871.65	0.07	1267	294056	93	6.16	2178.26	0.07	0.00
4	0.99	0.99	BP-HFY	1871.68	1872.43	0.0285	1068	213963	218	6.06	TL	0.07	0.04
4	0.99	0.99	BP-RF	1871.65	1872.96	0.0	985	171661	198	3.76	TL	0.07	0.07

Table 4.64: Comparison of Branching Rules for N=36, L=6, Instance ID = 5

L	Se	Sp	Configuration	LB	UB	Δ UB (%)	$\#y$	$\#x$	# nodes	Time$_r$ (s)	Total Time (s)	Gap$_r$ (%)	Gap (%)
6	0.9	0.9	BP-HFX	49057.18	49782.10	0.0	699	94102	3	1579.64	TL	1.48	1.48
6	0.9	0.9	BP-HFY	49242.29	49782.10	0.0	786	123663	4	489.18	TL	1.10	1.10
6	0.9	0.9	BP-RF	49242.29	49782.10	0.0	619	74237	4	522.43	TL	1.10	1.10
6	0.9	0.95	BP-HFX	20714.59	20866.90	0.0	529	56204	2	287.94	TL	0.74	0.74
6	0.9	0.95	BP-HFY	20540.39	20866.90	0.0	1078	228194	4	1240.33	TL	1.59	1.59
6	0.9	0.95	BP-RF	20619.39	20866.90	0.0	639	79194	4	290.75	TL	1.20	1.20
6	0.9	0.99	BP-HFX	3502.36	3577.16	0.0001	1021	209383	4	662.06	TL	2.14	2.14
6	0.9	0.99	BP-HFY	3524.32	3577.16	0.0001	804	128400	3	2190.48	TL	1.50	1.50
6	0.9	0.99	BP-RF	3432.62	3577.16	0.0001	637	79771	5	261.52	TL	4.21	4.21
6	0.95	0.9	BP-HFX	53707.32	54456.89	0.0	709	98732	3	1826.65	TL	1.40	1.40
6	0.95	0.9	BP-HFY	54076.76	54456.89	0.0	700	96581	3	530.94	TL	0.70	0.70
6	0.95	0.9	BP-RF	54043.13	54456.89	0.0	629	78782	4	496.64	TL	0.77	0.77
6	0.95	0.95	BP-HFX	22788.28	23018.70	0.0	1014	205234	3	292.76	TL	1.01	1.01
6	0.95	0.95	BP-HFY	22818.51	23018.70	0.0	734	108358	3	276.98	TL	0.88	0.88
6	0.95	0.95	BP-RF	22813.88	23018.70	0.0	509	52262	3	522.06	TL	0.90	0.90
6	0.95	0.99	BP-HFX	3912.49	3977.22	0.0	966	182011	3	505.87	TL	1.65	1.65
6	0.95	0.99	BP-HFY	3912.49	3977.22	0.0	892	154372	3	510.98	TL	1.65	1.65
6	0.95	0.99	BP-RF	3930.97	3977.22	0.0	682	92561	4	224.39	TL	1.18	1.18
6	0.99	0.9	BP-HFX	57838.35	58375.50	0.0	658	84284	4	502.81	TL	0.93	0.93
6	0.99	0.9	BP-HFY	57864.12	58375.50	0.0	867	147415	4	283.30	TL	0.88	0.88
6	0.99	0.9	BP-RF	57893.31	58375.50	0.0	538	57014	5	248.35	TL	0.83	0.83
6	0.99	0.95	BP-HFX	24555.15	24822.70	0.0	856	144845	3	1078.76	TL	1.09	1.09
6	0.99	0.95	BP-HFY	24555.15	24822.73	0.0	982	195913	4	1058.49	TL	1.09	1.09
6	0.99	0.95	BP-RF	24625.24	24822.70	0.0	637	84373	5	297.27	TL	0.80	0.80
6	0.99	0.99	BP-HFX	4240.28	4305.35	0.0	935	175266	4	925.26	TL	1.53	1.53
6	0.99	0.99	BP-HFY	4240.28	4305.35	0.0	848	143896	3	907.11	TL	1.53	1.53
6	0.99	0.99	BP-RF	4250.80	4305.35	0.0	654	84469	5	466.00	TL	1.28	1.28

Table 4.70: Comparison of Branching Rules for N=81, L=3, Instance ID = 1

L	Se	Sp	Configuration	LB	UB	Δ UB (%)	$\#y$	$\#x$	# nodes	Time$_r$ (s)	Total Time (s)	Gap$_r$ (%)	Gap (%)
3	0.9	0.9	BP-HFX	40245.65	40480.90	0.0	2159	300995	47	23.76	TL	0.58	0.58
3	0.9	0.9	BP-HFY	40245.65	40426.28	0.1349	2237	318099	54	22.42	TL	0.58	0.45
3	0.9	0.9	BP-RF	40245.65	40480.90	0.0	1813	187022	53	23.46	TL	0.58	0.58
3	0.9	0.95	BP-HFX	13281.14	13347.89	0.2288	1864	226159	78	21.35	TL	0.73	0.50
3	0.9	0.95	BP-HFY	13210.84	13351.88	0.199	1862	228424	76	17.88	TL	1.27	1.07
3	0.9	0.95	BP-RF	13266.40	13378.50	0.0	1691	176595	84	20.47	TL	0.84	0.84
3	0.9	0.99	BP-HFX	1748.00	1750.92	0.0074	1129	85412	166	9.67	TL	0.17	0.17
3	0.9	0.99	BP-HFY	1747.97	1751.05	0.0	1143	94766	151	9.00	TL	0.18	0.18
3	0.9	0.99	BP-RF	1748.78	1749.67	0.0789	1244	111648	188	5.70	TL	0.13	0.05
3	0.95	0.9	BP-HFX	43148.63	43345.50	0.0	2200	311284	45	20.41	TL	0.46	0.46
3	0.95	0.9	BP-HFY	43178.17	43291.01	0.1257	2236	321105	47	17.17	TL	0.39	0.26
3	0.95	0.9	BP-RF	43177.81	43345.50	0.0	1846	196248	55	19.28	TL	0.39	0.39
3	0.95	0.95	BP-HFX	14423.11	14504.19	0.0001	1864	233234	74	15.93	TL	0.56	0.56
3	0.95	0.95	BP-HFY	14431.12	14504.19	0.0001	1906	244301	86	14.16	TL	0.51	0.51
3	0.95	0.95	BP-RF	14422.63	14504.19	0.0001	1732	188302	89	15.65	TL	0.57	0.57
3	0.95	0.99	BP-HFX	1935.49	1938.21	0.0	1124	89345	153	5.91	TL	0.14	0.14
3	0.95	0.99	BP-HFY	1935.33	1936.56	0.0852	1165	98190	160	7.51	TL	0.15	0.06
3	0.95	0.99	BP-RF	1935.10	1936.54	0.0863	1277	106453	208	7.58	TL	0.16	0.07
3	0.99	0.9	BP-HFX	45527.02	45719.70	0.0	2095	265866	39	22.07	TL	0.42	0.42
3	0.99	0.9	BP-HFY	45523.69	45719.70	0.0	2262	311784	42	21.06	TL	0.43	0.43
3	0.99	0.9	BP-RF	45496.96	45719.70	0.0	1767	174690	49	20.07	TL	0.49	0.49
3	0.99	0.95	BP-HFX	15391.39	15473.11	0.169	2024	268435	65	24.66	TL	0.70	0.53
3	0.99	0.95	BP-HFY	15388.06	15481.21	0.1167	1943	243582	86	21.58	TL	0.72	0.61
3	0.99	0.95	BP-RF	15396.11	15499.30	0.0	1826	205808	84	24.88	TL	0.67	0.67
3	0.99	0.99	BP-HFX	2091.74	2095.59	0.0001	1222	102066	147	9.06	TL	0.18	0.18
3	0.99	0.99	BP-HFY	2092.02	2095.59	0.0	1231	118691	156	6.57	TL	0.17	0.17
3	0.99	0.99	BP-RF	2091.63	2094.60	0.0474	1318	117994	160	12.60	TL	0.19	0.14

Table 4.71: Comparison of Branching Rules for N=81, L=3, Instance ID = 2

L	Se	Sp	Configuration	LB	UB	Δ UB (%)	$\#y$	$\#x$	# nodes	Time$_r$ (s)	Total Time (s)	Gap$_r$ (%)	Gap (%)
3	0.9	0.9	BP-HFX	47108.41	47262.00	0.0	2119	290991	47	18.72	TL	0.33	0.33
3	0.9	0.9	BP-HFY	47108.41	47211.45	0.107	2124	286771	68	17.49	TL	0.33	0.22
3	0.9	0.9	BP-RF	47108.41	47262.00	0.0	1843	204599	67	18.65	TL	0.33	0.33
3	0.9	0.95	BP-HFX	16378.72	16491.25	0.1003	1831	224595	86	16.33	TL	0.79	0.69
3	0.9	0.95	BP-HFY	16411.50	16485.32	0.1362	1864	222935	108	15.71	TL	0.59	0.45
3	0.9	0.95	BP-RF	16399.93	16486.47	0.1292	1658	170087	104	16.23	TL	0.66	0.53
3	0.9	0.99	BP-HFX	2320.78	2320.78	0.1283	932	55406	44	7.35	871.17	0.13	0.00
3	0.9	0.99	BP-HFY	2320.79	2321.63	0.0918	1051	79081	170	7.81	TL	0.13	0.04
3	0.9	0.99	BP-RF	2320.85	2321.95	0.0781	1230	100675	197	7.23	TL	0.13	0.05
3	0.95	0.9	BP-HFX	50693.86	50808.52	0.1118	2167	289280	48	17.79	TL	0.34	0.23
3	0.95	0.9	BP-HFY	50694.70	50817.78	0.0936	2215	312163	57	16.98	TL	0.34	0.24
3	0.95	0.9	BP-RF	50672.49	50865.40	0.0	1866	208709	65	16.53	TL	0.38	0.38
3	0.95	0.95	BP-HFX	17901.71	17982.64	0.1508	1765	209784	92	18.01	TL	0.60	0.45
3	0.95	0.95	BP-HFY	17913.17	17993.56	0.0902	1814	215819	87	16.65	TL	0.54	0.45
3	0.95	0.95	BP-RF	17904.54	17982.76	0.1501	1668	172038	98	18.96	TL	0.59	0.44
3	0.95	0.99	BP-HFX	2572.82	2574.96	0.0358	1147	94757	158	8.90	TL	0.12	0.08
3	0.95	0.99	BP-HFY	2571.99	2575.59	0.0111	1086	84218	172	8.35	TL	0.15	0.14
3	0.95	0.99	BP-RF	2572.50	2573.03	0.1108	1097	77710	206	7.81	TL	0.13	0.02
3	0.99	0.9	BP-HFX	53674.37	53843.20	0.0	2172	287812	44	21.07	TL	0.31	0.31
3	0.99	0.9	BP-HFY	53616.66	53843.20	0.0	2231	313877	46	15.25	TL	0.42	0.42
3	0.99	0.9	BP-RF	53659.90	53775.60	0.1256	1453	113877	59	19.24	TL	0.34	0.22
3	0.99	0.95	BP-HFX	19151.42	19221.19	0.1916	1841	207774	72	21.42	TL	0.56	0.36
3	0.99	0.95	BP-HFY	19159.22	19251.35	0.0351	1859	226003	90	16.65	TL	0.52	0.48
3	0.99	0.95	BP-RF	19221.28	19258.10	0.0	1720	180671	89	17.89	TL	0.19	0.19
3	0.99	0.99	BP-HFX	2782.18	2782.18	0.1701	1025	68785	44	11.19	947.83	0.16	0.00
3	0.99	0.99	BP-HFY	2782.56	2786.92	0.0002	1287	122057	149	10.12	TL	0.16	0.16
3	0.99	0.99	BP-RF	2782.39	2784.93	0.0713	1296	112756	178	10.65	TL	0.16	0.09

Table 4.72: Comparison of Branching Rules for N=81, L=3, Instance ID = 3

L	Se	Sp	Configuration	LB	UB	Δ UB (%)	$\#y$	$\#x$	# nodes	Time_r (s)	Total Time (s)	Gap_r (%)	Gap (%)
3	0.9	0.9	BP-HFX	44144.36	44307.35	0.0008	2281	338564	55	15.34	TL	0.37	0.37
3	0.9	0.9	BP-HFY	44144.36	44269.52	0.0862	2196	307505	52	15.59	TL	0.37	0.28
3	0.9	0.9	BP-RF	44144.36	44307.70	0.0	1831	197163	66	16.95	TL	0.37	0.37
3	0.9	0.95	BP-HFX	15026.41	15107.02	0.169	1883	233380	90	16.36	TL	0.71	0.54
3	0.9	0.95	BP-HFY	15030.22	15113.95	0.1232	1780	200628	98	15.63	TL	0.68	0.56
3	0.9	0.95	BP-RF	15034.91	15128.85	0.0248	1725	191246	103	16.13	TL	0.65	0.62
3	0.9	0.99	BP-HFX	2067.81	2069.64	0.1064	1149	91587	164	10.91	TL	0.20	0.09
3	0.9	0.99	BP-HFY	2068.58	2069.23	0.1265	1083	85112	171	6.04	TL	0.16	0.03
3	0.9	0.99	BP-RF	2067.83	2070.94	0.0439	1222	106143	194	9.77	TL	0.19	0.15
3	0.95	0.9	BP-HFX	47003.52	47590.30	0.0	2261	317812	45	16.64	TL	1.25	1.25
3	0.95	0.9	BP-HFY	47417.56	47590.30	0.0	2270	324571	52	16.69	TL	0.36	0.36
3	0.95	0.9	BP-RF	47405.22	47590.30	0.0	1806	183031	53	20.16	TL	0.39	0.39
3	0.95	0.95	BP-HFX	16379.84	16464.94	0.1035	1958	255523	79	18.86	TL	0.62	0.52
3	0.95	0.95	BP-HFY	16386.34	16453.21	0.1747	1882	217388	97	17.55	TL	0.58	0.41
3	0.95	0.95	BP-RF	16382.86	16481.98	0.0001	1696	181416	84	16.89	TL	0.61	0.61
3	0.95	0.99	BP-HFX	2291.61	2292.58	0.0391	1208	105008	162	6.19	TL	0.08	0.04
3	0.95	0.99	BP-HFY	2290.83	2292.45	0.0451	1143	90601	150	9.46	TL	0.12	0.07
3	0.95	0.99	BP-RF	2291.13	2293.48	0.0	1178	91960	169	9.70	TL	0.10	0.10
3	0.99	0.9	BP-HFX	50237.73	50239.80	0.1435	1911	204237	64	17.16	TL	0.41	0.00
3	0.99	0.9	BP-HFY	50106.41	50312.00	0.0	2226	306799	45	18.52	TL	0.41	0.41
3	0.99	0.9	BP-RF	50121.76	50238.96	0.1452	1625	143772	48	19.19	TL	0.38	0.23
3	0.99	0.95	BP-HFX	17508.84	17582.12	0.1254	1946	243711	88	21.93	TL	0.54	0.42
3	0.99	0.95	BP-HFY	17508.84	17604.20	0.0	2007	266688	58	25.01	TL	0.54	0.54
3	0.99	0.95	BP-RF	17508.84	17604.20	0.0	1759	188330	78	21.97	TL	0.54	0.54
3	0.99	0.99	BP-HFX	2477.89	2481.44	0.0	1148	94856	148	7.67	TL	0.14	0.14
3	0.99	0.99	BP-HFY	2477.89	2481.44	0.0	1247	115023	145	7.40	TL	0.14	0.14
3	0.99	0.99	BP-RF	2477.89	2479.75	0.0682	1307	119673	189	7.56	TL	0.14	0.07

Table 4.73: Comparison of Branching Rules for N=81, L=3, Instance ID = 4

L	Se	Sp	Configuration	LB	UB	Δ UB (%)	$\#y$	$\#x$	# nodes	Time$_r$ (s)	Total Time (s)	Gap$_r$ (%)	Gap (%)
3	0.9	0.9	BP-HFX	39975.08	40171.70	0.0	2205	302576	42	18.40	TL	0.49	0.49
3	0.9	0.9	BP-HFY	39975.08	40171.70	0.0	2156	285338	43	18.26	TL	0.49	0.49
3	0.9	0.9	BP-RF	39975.08	40171.70	0.0	1844	197558	54	18.46	TL	0.49	0.49
3	0.9	0.95	BP-HFX	13106.80	13214.72	0.0384	2015	266201	79	22.08	TL	0.86	0.82
3	0.9	0.95	BP-HFY	13107.66	13182.83	0.2796	1945	246936	75	23.65	TL	0.86	0.57
3	0.9	0.95	BP-RF	13090.62	13198.81	0.1588	1789	200295	91	20.93	TL	0.99	0.83
3	0.9	0.99	BP-HFX	1713.54	1715.98	0.1512	1210	106696	146	14.30	TL	0.29	0.14
3	0.9	0.99	BP-HFY	1713.39	1714.91	0.2138	1279	117462	157	12.37	TL	0.30	0.09
3	0.9	0.99	BP-RF	1714.25	1718.58	0.0	1237	107522	187	6.20	TL	0.25	0.25
3	0.95	0.9	BP-HFX	42784.04	43019.60	0.0	2143	272659	39	22.56	TL	0.55	0.55
3	0.95	0.9	BP-HFY	42790.34	43019.60	0.0	2193	289233	40	21.71	TL	0.54	0.54
3	0.95	0.9	BP-RF	42806.88	43019.60	0.0	1920	205284	50	20.11	TL	0.50	0.50
3	0.95	0.95	BP-HFX	14245.60	14321.59	0.3493	1950	245316	77	26.36	TL	0.89	0.53
3	0.95	0.95	BP-HFY	14238.36	14327.65	0.3072	1940	241753	78	25.04	TL	0.94	0.63
3	0.95	0.95	BP-RF	14244.73	14371.80	0.0	1826	203232	78	23.83	TL	0.89	0.89
3	0.95	0.99	BP-HFX	1896.60	1903.24	0.0002	1330	130490	141	8.27	TL	0.35	0.35
3	0.95	0.99	BP-HFY	1896.88	1899.18	0.2132	1134	89870	150	11.98	TL	0.34	0.12
3	0.95	0.99	BP-RF	1896.54	1902.28	0.0503	1384	144100	178	11.31	TL	0.35	0.30
3	0.99	0.9	BP-HFX	45125.08	45368.50	0.0	2193	282834	34	22.81	TL	0.54	0.54
3	0.99	0.9	BP-HFY	45075.52	45368.50	0.0	2143	270656	36	19.45	TL	0.65	0.65
3	0.99	0.9	BP-RF	45087.21	45368.50	0.0	1880	195624	47	21.40	TL	0.62	0.62
3	0.99	0.95	BP-HFX	15187.29	15265.08	0.3376	1991	249203	65	27.55	TL	0.85	0.51
3	0.99	0.95	BP-HFY	15196.91	15297.94	0.1232	2088	274025	60	27.36	TL	0.79	0.66
3	0.99	0.95	BP-RF	15183.16	15316.80	0.0	1812	194882	76	24.37	TL	0.88	0.88
3	0.99	0.99	BP-HFX	2049.64	2052.32	0.1892	1257	106747	129	14.94	TL	0.32	0.13
3	0.99	0.99	BP-HFY	2049.21	2050.24	0.2902	1188	95502	139	12.81	TL	0.34	0.05
3	0.99	0.99	BP-RF	2050.03	2051.93	0.2083	1320	116492	172	8.09	TL	0.30	0.09

Table 4.74: Comparison of Branching Rules for N=81, L=3, Instance ID = 5

L	Se	Sp	Configuration	LB	UB	Δ UB (%)	$\#y$	$\#x$	# nodes	Time$_r$ (s)	Total Time (s)	Gap$_r$ (%)	Gap (%)
3	0.9	0.9	BP-HFX	40666.78	40799.17	0.0412	2198	304197	52	23.77	TL	0.37	0.33
3	0.9	0.9	BP-HFY	40666.78	40765.23	0.1244	2223	305089	53	24.07	TL	0.37	0.24
3	0.9	0.9	BP-RF	40666.78	40816.00	0.0	1880	207472	66	22.61	TL	0.37	0.37
3	0.9	0.95	BP-HFX	13521.84	13536.77	0.1389	1820	216051	83	18.59	TL	0.25	0.11
3	0.9	0.95	BP-HFY	13455.95	13538.04	0.1295	1916	249097	79	17.39	TL	0.74	0.61
3	0.9	0.95	BP-RF	13444.13	13555.60	0.0	1829	211113	96	19.06	TL	0.83	0.83
3	0.9	0.99	BP-HFX	1785.58	1790.96	0.0	1379	149438	127	6.93	TL	0.30	0.30
3	0.9	0.99	BP-HFY	1785.26	1785.59	0.3001	1285	107068	146	12.92	TL	0.32	0.02
3	0.9	0.99	BP-RF	1785.47	1789.89	0.0599	1256	107767	186	8.43	TL	0.31	0.25
3	0.95	0.9	BP-HFX	43578.18	43735.90	0.0	2258	313492	42	23.28	TL	0.36	0.36
3	0.95	0.9	BP-HFY	43570.60	43735.90	0.0	2168	282729	38	24.20	TL	0.38	0.38
3	0.95	0.9	BP-RF	43547.23	43735.90	0.0	1876	198838	49	21.93	TL	0.43	0.43
3	0.95	0.95	BP-HFX	14630.45	14733.39	0.0394	1942	248031	77	21.44	TL	0.74	0.70
3	0.95	0.95	BP-HFY	14637.21	14717.48	0.1474	1952	252309	76	24.88	TL	0.70	0.55
3	0.95	0.95	BP-RF	14638.46	14739.20	0.0	1745	186848	86	21.08	TL	0.69	0.69
3	0.95	0.99	BP-HFX	1976.26	1980.29	0.1438	1129	93579	143	12.83	TL	0.35	0.20
3	0.95	0.99	BP-HFY	1976.72	1983.14	0.0	1392	135999	133	9.88	TL	0.32	0.32
3	0.95	0.99	BP-RF	1976.76	1983.14	0.0	1289	114906	171	7.94	TL	0.32	0.32
3	0.99	0.9	BP-HFX	46074.44	46074.44	0.17	1252	82854	23	21.72	603.55	0.42	0.00
3	0.99	0.9	BP-HFY	46073.77	46073.77	0.1715	1485	118607	41	21.42	1063.72	0.39	0.00
3	0.99	0.9	BP-RF	46070.76	46071.77	0.1758	1532	126755	56	24.11	TL	0.41	0.00
3	0.99	0.95	BP-HFX	15613.82	15694.54	0.2185	2028	268072	65	24.13	TL	0.74	0.52
3	0.99	0.95	BP-HFY	15618.64	15679.90	0.3115	1903	231938	81	24.36	TL	0.71	0.39
3	0.99	0.95	BP-RF	15613.82	15728.90	0.0	1848	200963	75	24.03	TL	0.74	0.74
3	0.99	0.99	BP-HFX	2136.40	2136.90	0.3677	1171	95348	162	7.90	TL	0.39	0.02
3	0.99	0.99	BP-HFY	2136.40	2144.16	0.0293	1224	112173	155	7.85	TL	0.39	0.36
3	0.99	0.99	BP-RF	2136.40	2139.06	0.2674	1259	105332	180	7.98	TL	0.39	0.12

Table 4.75: Comparison of Branching Rules for N=100, L=4, Instance ID = 1

L	Se	Sp	Configuration	LB	UB	Δ UB (%)	$\#y$	$\#x$	# nodes	Time_r (s)	Total Time (s)	Gap_r (%)	Gap (%)
4	0.9	0.9	BP-HFX	86175.31	86523.86	0.0001	1509	164226	4	641.00	TL	0.40	0.40
4	0.9	0.9	BP-HFY	86175.31	86523.86	0.0001	1498	161850	4	686.48	TL	0.40	0.40
4	0.9	0.9	BP-RF	86175.31	86523.86	0.0001	1499	161105	4	693.69	TL	0.40	0.40
4	0.9	0.95	BP-HFX	32948.56	33509.76	0.0	1532	169807	6	367.01	TL	1.70	1.70
4	0.9	0.95	BP-HFY	33066.04	33545.65	0.0	1522	167106	5	397.36	TL	1.45	1.45
4	0.9	0.95	BP-RF	33066.04	33545.65	0.0	1371	135619	6	396.67	TL	1.45	1.45
4	0.9	0.99	BP-HFX	5198.35	5271.45	0.0	846	51232	8	363.65	TL	1.41	1.41
4	0.9	0.99	BP-HFY	5198.45	5271.45	0.0	751	40311	9	292.86	TL	1.40	1.40
4	0.9	0.99	BP-RF	5198.02	5271.45	0.0	710	35820	9	781.78	TL	1.41	1.41
4	0.95	0.9	BP-HFX	93460.71	94565.89	0.0	1501	162896	4	664.50	TL	1.18	1.18
4	0.95	0.9	BP-HFY	93564.37	94565.89	0.0	1547	172229	4	689.93	TL	1.07	1.07
4	0.95	0.9	BP-RF	93598.89	94565.89	0.0	1558	175192	4	660.81	TL	1.03	1.03
4	0.95	0.95	BP-HFX	36277.17	36435.30	0.0	1516	167050	6	314.63	TL	0.44	0.44
4	0.95	0.95	BP-HFY	36290.58	36435.30	0.0	1462	153598	6	331.97	TL	0.40	0.40
4	0.95	0.95	BP-RF	36275.90	36435.30	0.0	1382	137385	6	332.01	TL	0.44	0.44
4	0.95	0.99	BP-HFX	5771.35	5845.68	0.0	816	48147	9	355.48	TL	1.29	1.29
4	0.95	0.99	BP-HFY	5771.41	5845.68	0.0	833	49740	7	319.00	TL	1.29	1.29
4	0.95	0.99	BP-RF	5710.42	5853.30	0.0	756	40955	8	424.12	TL	2.50	2.50
4	0.99	0.9	BP-HFX	99646.72	100761.43	0.0	1581	180192	4	667.39	TL	1.12	1.12
4	0.99	0.9	BP-HFY	99646.29	100834.53	0.0	1398	140384	4	741.38	TL	1.19	1.19
4	0.99	0.9	BP-RF	99671.14	100834.53	0.0	1514	164213	4	720.63	TL	1.17	1.17
4	0.99	0.95	BP-HFX	38940.05	39577.30	0.0	1577	179458	5	427.55	TL	1.64	1.64
4	0.99	0.95	BP-HFY	38970.11	39577.30	0.0	1509	163780	5	486.58	TL	1.56	1.56
4	0.99	0.95	BP-RF	38976.71	39577.30	0.0	1452	151839	5	434.43	TL	1.54	1.54
4	0.99	0.99	BP-HFX	6194.22	6332.50	0.0	909	59348	8	257.37	TL	2.23	2.23
4	0.99	0.99	BP-HFY	6195.11	6340.89	0.0	839	50414	8	432.22	TL	2.35	2.35
4	0.99	0.99	BP-RF	6251.07	6340.89	0.0	833	49745	7	893.63	TL	1.44	1.44

Table 4.76: Comparison of Branching Rules for N=100, L=4, Instance ID = 2

L	Se	Sp	Configuration	LB	UB	Δ UB (%)	$\#y$	$\#x$	# nodes	Time$_r$ (s)	Total Time (s)	Gap$_r$ (%)	Gap (%)
4	0.9	0.9	BP-HFX	73328.78	74381.11	0.0	1607	185701	4	700.68	TL	1.44	1.44
4	0.9	0.9	BP-HFY	73293.90	74391.74	0.0	1591	182501	4	704.03	TL	1.50	1.50
4	0.9	0.9	BP-RF	73328.78	74381.11	0.0	1514	164238	4	698.28	TL	1.44	1.44
4	0.9	0.95	BP-HFX	26935.52	27387.33	0.0	1504	162718	5	410.06	TL	1.68	1.68
4	0.9	0.95	BP-HFY	26929.00	27387.33	0.0	1518	165367	5	390.19	TL	1.70	1.70
4	0.9	0.95	BP-RF	26863.32	27387.33	0.0	1381	136711	6	379.10	TL	1.95	1.95
4	0.9	0.99	BP-HFX	4035.09	4135.01	0.0	872	54848	8	302.29	TL	2.48	2.48
4	0.9	0.99	BP-HFY	4035.16	4135.01	0.0	786	44156	8	438.19	TL	2.47	2.47
4	0.9	0.99	BP-RF	4035.38	4135.01	0.0	744	39638	8	499.69	TL	2.47	2.47
4	0.95	0.9	BP-HFX	79255.91	80379.39	0.0	1530	168839	4	806.47	TL	1.42	1.42
4	0.95	0.9	BP-HFY	79270.04	80379.39	0.0	1520	165580	4	800.66	TL	1.40	1.40
4	0.95	0.9	BP-RF	79285.10	80379.39	0.0	1558	173115	4	818.03	TL	1.38	1.38
4	0.95	0.95	BP-HFX	29518.26	30038.25	0.0	1571	177879	5	479.78	TL	1.87	1.76
4	0.95	0.95	BP-HFY	29480.86	30038.25	0.0	1499	162273	5	430.91	TL	1.89	1.89
4	0.95	0.95	BP-RF	29459.74	30038.25	0.0	1491	159348	5	438.14	TL	1.96	1.96
4	0.95	0.99	BP-HFX	4476.55	4574.02	0.0	861	53275	8	298.71	TL	2.18	2.18
4	0.95	0.99	BP-HFY	4476.70	4574.02	0.0	815	47700	7	467.33	TL	2.17	2.17
4	0.95	0.99	BP-RF	4476.31	4574.02	0.0	765	41627	7	849.89	TL	2.18	2.18
4	0.99	0.9	BP-HFX	84139.36	85406.23	0.0	1364	133269	3	841.38	TL	1.51	1.51
4	0.99	0.9	BP-HFY	84207.00	85406.23	0.0	1422	145579	4	788.90	TL	1.42	1.42
4	0.99	0.9	BP-RF	84195.07	85406.23	0.0	1391	138250	3	874.29	TL	1.44	1.44
4	0.99	0.95	BP-HFX	31656.12	32199.49	0.0	1619	187996	5	453.05	TL	1.84	1.72
4	0.99	0.95	BP-HFY	31608.56	32199.49	0.0	1593	181772	5	689.70	TL	1.87	1.87
4	0.99	0.95	BP-RF	31605.52	32199.49	0.0	1485	158137	5	451.60	TL	1.88	1.88
4	0.99	0.99	BP-HFX	4846.16	4952.45	0.0	901	58355	7	555.88	TL	2.19	2.19
4	0.99	0.99	BP-HFY	4846.19	4952.45	0.0	849	51447	8	400.08	TL	2.19	2.19
4	0.99	0.99	BP-RF	4846.28	4952.45	0.0	782	43849	8	558.27	TL	2.19	2.19

Table 4.77: Comparison of Branching Rules for N=100, L=4, Instance ID = 3

L	Se	Sp	Configuration	LB	UB	Δ UB (%)	$\#y$	$\#x$	# nodes	Time$_r$ (s)	Total Time (s)	Gap$_r$ (%)	Gap (%)
4	0.9	0.9	BP-HFX	77896.93	78859.70	0.0	1589	182857	4	732.99	TL	1.24	1.24
4	0.9	0.9	BP-HFY	77898.02	78775.34	0.0	1582	180619	4	691.33	TL	1.13	1.13
4	0.9	0.9	BP-RF	77896.93	78859.70	0.0	1537	170227	4	752.00	TL	1.24	1.24
4	0.9	0.95	BP-HFX	29114.96	29597.13	0.0	1509	165864	5	342.51	TL	1.66	1.66
4	0.9	0.95	BP-HFY	29115.71	29597.13	0.0	1543	172657	6	369.25	TL	1.65	1.65
4	0.9	0.95	BP-RF	29111.39	29597.13	0.0	1393	139860	6	370.16	TL	1.67	1.67
4	0.9	0.99	BP-HFX	4450.74	4532.83	0.0	798	45624	10	475.85	TL	1.84	1.84
4	0.9	0.99	BP-HFY	4450.49	4532.83	0.0	759	41109	7	489.52	TL	1.85	1.85
4	0.9	0.99	BP-RF	4450.81	4532.83	0.0	766	41936	10	479.93	TL	1.84	1.84
4	0.95	0.9	BP-HFX	84277.82	85405.70	0.0	1556	175730	4	729.20	TL	1.34	1.34
4	0.95	0.9	BP-HFY	84366.31	85405.68	0.0	1583	180083	4	727.02	TL	1.23	1.23
4	0.95	0.9	BP-RF	84374.13	85430.41	0.0	1578	178646	4	735.75	TL	1.25	1.25
4	0.95	0.95	BP-HFX	31889.21	32438.94	0.0	1604	185709	5	429.80	TL	1.72	1.72
4	0.95	0.95	BP-HFY	31901.73	32438.94	0.0	1527	167946	6	399.49	TL	1.68	1.68
4	0.95	0.95	BP-RF	31907.20	32438.94	0.0	1485	159437	5	408.88	TL	1.67	1.67
4	0.95	0.99	BP-HFX	4939.19	5031.17	0.0	825	48495	8	469.46	TL	1.86	1.86
4	0.95	0.99	BP-HFY	4939.43	5031.17	0.0	771	42436	8	748.72	TL	1.86	1.86
4	0.95	0.99	BP-RF	4939.77	5023.24	0.0	794	45276	8	435.90	TL	1.69	1.69
4	0.99	0.9	BP-HFX	89706.20	90874.00	0.0	1408	143020	4	776.46	TL	1.30	1.30
4	0.99	0.9	BP-HFY	89701.95	90874.00	0.0	1391	139189	3	927.05	TL	1.31	1.31
4	0.99	0.9	BP-RF	89684.06	90769.73	0.0	1539	169904	4	813.71	TL	1.21	1.21
4	0.99	0.95	BP-HFX	34241.15	34849.72	0.0	1637	193593	5	466.17	TL	1.78	1.78
4	0.99	0.95	BP-HFY	34251.08	34849.72	0.0	1621	189871	5	497.02	TL	1.75	1.75
4	0.99	0.95	BP-RF	34190.81	34805.78	0.0	1551	173472	5	442.16	TL	1.80	1.80
4	0.99	0.99	BP-HFX	5348.87	5448.56	0.0	781	43580	7	779.35	TL	1.86	1.86
4	0.99	0.99	BP-HFY	5348.43	5448.56	0.0	819	48217	7	847.84	TL	1.87	1.87
4	0.99	0.99	BP-RF	5349.02	5448.56	0.0	763	41427	9	344.33	TL	1.86	1.86

Table 4.78: Comparison of Branching Rules for N=100, L=4, Instance ID = 4

L	Se	Sp	Configuration	LB	UB	Δ UB (%)	$\#y$	$\#x$	# nodes	Time$_r$ (s)	Total Time (s)	Gap$_r$ (%)	Gap (%)
4	0.9	0.9	BP-HFX	80509.60	81441.82	0.0	1474	155985	4	634.95	TL	1.16	1.16
4	0.9	0.9	BP-HFY	80509.60	81441.82	0.0	1481	158476	4	639.98	TL	1.16	1.16
4	0.9	0.9	BP-RF	80509.60	81441.82	0.0	1395	140042	5	634.35	TL	1.16	1.16
4	0.9	0.95	BP-HFX	30421.47	30849.10	0.0	1419	145127	6	346.96	TL	1.41	1.41
4	0.9	0.95	BP-HFY	30403.75	30890.10	0.0	1458	153573	6	367.05	TL	1.60	1.60
4	0.9	0.95	BP-RF	30419.33	30849.10	0.0	1360	134139	6	381.97	TL	1.41	1.41
4	0.9	0.99	BP-HFX	4704.32	4775.94	0.0	743	39605	9	450.08	TL	1.52	1.52
4	0.9	0.99	BP-HFY	4704.59	4767.34	0.0	701	35062	9	305.19	TL	1.33	1.33
4	0.9	0.99	BP-RF	4704.65	4775.94	0.0	695	34623	9	243.66	TL	1.52	1.52
4	0.95	0.9	BP-HFX	87322.75	88415.66	0.0	1514	165665	4	702.68	TL	1.25	1.25
4	0.95	0.9	BP-HFY	87300.82	88365.03	0.0	1630	191527	4	723.98	TL	1.22	1.22
4	0.95	0.9	BP-RF	87324.50	88365.03	0.0	1490	159072	4	705.22	TL	1.19	1.19
4	0.95	0.95	BP-HFX	33288.46	33814.03	0.0	1493	161332	5	397.13	TL	1.58	1.58
4	0.95	0.95	BP-HFY	33359.36	33861.28	0.0	1449	150688	5	407.87	TL	1.50	1.50
4	0.95	0.95	BP-RF	33337.07	33814.03	0.0	1387	138812	6	359.78	TL	1.43	1.43
4	0.95	0.99	BP-HFX	5221.30	5292.39	0.0	723	37367	8	473.43	TL	1.36	1.36
4	0.95	0.99	BP-HFY	5221.58	5292.39	0.0	762	41529	7	496.46	TL	1.36	1.36
4	0.95	0.99	BP-RF	5221.52	5292.39	0.0	744	39651	8	355.35	TL	1.36	1.36
4	0.99	0.9	BP-HFX	92912.04	94079.54	0.0	1486	160414	4	740.14	TL	1.26	1.26
4	0.99	0.9	BP-HFY	92900.12	94141.54	0.0	1334	127954	3	1261.31	TL	1.34	1.34
4	0.99	0.9	BP-RF	92888.50	94079.54	0.0	1483	157819	4	768.20	TL	1.28	1.28
4	0.99	0.95	BP-HFX	35799.24	36301.65	0.0	1569	179650	5	451.62	TL	1.40	1.40
4	0.99	0.95	BP-HFY	35739.84	36301.65	0.0	1431	148018	5	431.82	TL	1.57	1.57
4	0.99	0.95	BP-RF	35748.93	36301.65	0.0	1458	153813	5	465.09	TL	1.55	1.55
4	0.99	0.99	BP-HFX	5599.80	5732.18	0.0	815	47970	7	695.23	TL	2.36	2.36
4	0.99	0.99	BP-HFY	5654.90	5732.18	0.0	816	47767	9	436.86	TL	1.37	1.37
4	0.99	0.99	BP-RF	5655.28	5732.18	0.0	749	40248	8	307.09	TL	1.36	1.36

Table 4.79: Comparison of Branching Rules for N=100, L=4, Instance ID = 5

L	Se	Sp	Configuration	LB	UB	Δ UB (%)	$\#y$	$\#x$	# nodes	Time$_r$ (s)	Total Time (s)	Gap$_r$ (%)	Gap (%)
4	0.9	0.9	BP-HFX	78873.37	79598.86	0.0	1614	187886	5	590.73	TL	1.04	0.92
4	0.9	0.9	BP-HFY	78759.55	79598.86	0.0	1626	190571	5	578.05	TL	1.07	1.07
4	0.9	0.9	BP-RF	78781.13	79598.86	0.0	1558	175164	5	583.61	TL	1.04	1.04
4	0.9	0.95	BP-HFX	29550.98	29917.05	0.0	1451	152638	6	356.02	TL	1.24	1.24
4	0.9	0.95	BP-HFY	29550.98	29917.05	0.0	1461	154393	6	356.79	TL	1.24	1.24
4	0.9	0.95	BP-RF	29564.82	29917.05	0.0	1383	138613	6	348.20	TL	1.19	1.19
4	0.9	0.99	BP-HFX	4539.74	4600.53	0.0	761	41363	9	527.94	TL	1.34	1.34
4	0.9	0.99	BP-HFY	4539.88	4600.53	0.0	745	39408	9	472.08	TL	1.34	1.34
4	0.9	0.99	BP-RF	4539.85	4600.53	0.0	687	33571	9	622.98	TL	1.34	1.34
4	0.95	0.9	BP-HFX	85359.93	86195.58	0.0	1562	177399	4	727.10	TL	0.98	0.98
4	0.95	0.9	BP-HFY	85369.01	86195.58	0.0	1557	175114	4	692.04	TL	0.97	0.97
4	0.95	0.9	BP-RF	85367.76	86195.58	0.0	1522	167833	4	662.19	TL	0.97	0.97
4	0.95	0.95	BP-HFX	32397.60	32792.55	0.0	1505	164727	6	503.68	TL	1.22	1.22
4	0.95	0.95	BP-HFY	32401.72	32792.55	0.0	1567	177941	5	364.58	TL	1.21	1.21
4	0.95	0.95	BP-RF	32400.25	32792.55	0.0	1430	147485	6	376.31	TL	1.21	1.21
4	0.95	0.99	BP-HFX	5038.31	5106.65	0.0	761	41375	7	827.82	TL	1.36	1.36
4	0.95	0.99	BP-HFY	5038.00	5106.65	0.0	771	42935	9	562.81	TL	1.36	1.36
4	0.95	0.99	BP-RF	5038.47	5106.65	0.0	730	38653	8	628.66	TL	1.35	1.35
4	0.99	0.9	BP-HFX	90792.73	91707.33	0.0	1564	176235	4	718.58	TL	1.01	1.01
4	0.99	0.9	BP-HFY	90748.76	91707.33	0.0	1595	184347	4	735.50	TL	1.06	1.06
4	0.99	0.9	BP-RF	90797.62	91707.33	0.0	1486	158196	4	726.12	TL	1.00	1.00
4	0.99	0.95	BP-HFX	34755.51	35189.74	0.0	1583	181103	5	428.91	TL	1.25	1.25
4	0.99	0.95	BP-HFY	34766.12	35189.74	0.0	1492	161607	5	396.85	TL	1.22	1.22
4	0.99	0.95	BP-RF	34759.58	35189.74	0.0	1451	152803	6	390.52	TL	1.24	1.24
4	0.99	0.99	BP-HFX	5456.31	5530.55	0.0	798	45482	8	331.10	TL	1.36	1.36
4	0.99	0.99	BP-HFY	5456.60	5530.55	0.0	780	43836	8	446.60	TL	1.36	1.36
4	0.99	0.99	BP-RF	5456.07	5530.55	0.0	763	41583	9	590.41	TL	1.37	1.37

Table 4.10: Performance Comparison of the Formulations for $N = 6$

Instance					F^{3}_{MINLP}					F^{SYM}_{MINLP}					F^{EXT}_{MINLP}				
ID	N	L	Se	Sp	Obj	Runtime (s)	Nodes	Gap_r (%)	Gap (%)	Obj	Runtime (s)	Nodes	Gap_r (%)	Gap (%)	Obj	Runtime (s)	Nodes	Gap_r (%)	Gap (%)
1	6	3	0.9	0.9	3893.84	0.95	1457	309	0	3893.84	0.63	143	159	0	3893.84	0.33	1	0	0
1	6	3	0.9	0.95	1415.34	0.85	1547	474	0	1415.34	0.52	143	240	0	1415.34	0.3	1	0	0
1	6	3	0.9	0.99	209.73	0.62	1495	691	0	209.73	0.54	143	342	0	209.73	0.34	1	0	0
1	6	3	0.95	0.9	4205.28	0.61	1546	323	0	4205.28	0.28	143	167	0	4205.28	0.08	1	0	0
1	6	3	0.95	0.95	1548.31	0.58	1495	485	0	1548.31	0.28	143	243	0	1548.31	0.07	1	0	0
1	6	3	0.95	0.99	232.68	0.6	1460	697	0	232.68	0.27	143	377	0	232.68	0.07	1	0	0
1	6	3	0.99	0.9	4463.01	0.57	1461	333	0	4463.01	0.28	143	157	0	4463.01	0.08	1	0	0
1	6	3	0.99	0.95	1658.97	0.62	1566	492	0	1658.97	0.26	145	279	0	1658.97	0.07	1	0	0
1	6	3	0.99	0.99	251.9	0.55	1465	700	0	251.9	0.27	143	398	0	251.9	0.07	1	0	0
2	6	3	0.9	0.9	3433.36	0.72	1451	348	0	3433.36	0.39	143	82	0	3433.36	0.08	1	0	0
2	6	3	0.9	0.95	1197.61	0.6	1440	556	0	1197.61	0.31	141	264	0	1197.61	0.08	1	0	0
2	6	3	0.9	0.99	168.93	0.59	1560	856	0	168.93	0.32	143	194	0	168.93	0.08	1	0	0
2	6	3	0.95	0.9	3694.6	0.63	1540	364	0	3694.6	0.32	143	162	0	3694.6	0.08	1	0	0
2	6	3	0.95	0.95	1306.6	0.53	1448	570	0	1306.6	0.31	142	261	0	1306.6	0.08	1	0	0
2	6	3	0.95	0.99	187.27	0.61	1460	865	0	187.27	0.34	141	198	0	187.27	0.08	1	0	0
2	6	3	0.99	0.9	3910.4	0.55	1451	377	0	3910.4	0.29	143	143	0	3910.4	0.08	1	0	0
2	6	3	0.99	0.95	1397.2	0.55	1453	583	0	1397.2	0.28	143	236	0	1397.2	0.07	1	0	0
2	6	3	0.99	0.99	202.62	0.59	1452	865	0	202.62	0.3	142	411	0	202.62	0.08	1	0	0
3	6	3	0.9	0.9	2788.27	0.67	1453	344	0	2788.27	0.34	145	123	0	2788.27	0.08	1	0	0
3	6	3	0.9	0.95	911.43	0.59	1444	589	0	911.43	0.27	144	252	0	911.43	0.09	1	0	0
3	6	3	0.9	0.99	118.98	0.59	1505	984	0	118.98	0.28	143	359	0	118.98	0.07	1	0	0
3	6	3	0.95	0.9	2983.31	0.55	1450	363	0	2983.31	0.28	143	128	0	2983.31	0.07	1	0	0
3	6	3	0.95	0.95	990.19	0.52	1469	612	0	990.19	0.29	146	304	0	990.19	0.07	1	0	0
3	6	3	0.95	0.99	131.73	0.6	1534	991	0	131.73	0.27	143	431	0	131.73	0.08	1	0	0
3	6	3	0.99	0.9	3144.01	0.63	1439	378	0	3144.01	0.28	143	135	0	3144.01	0.08	1	0	0
3	6	3	0.99	0.95	1055.53	0.62	1451	622	0	1055.53	0.28	143	198	0	1055.53	0.07	1	0	0
3	6	3	0.99	0.99	142.4	0.58	1479	1025	0	142.4	0.26	143	565	0	142.4	0.07	1	0	0
4	6	3	0.9	0.9	4252.19	0.74	1464	276	0	4252.2	0.35	143	159	0	4252.2	0.12	16	170	0
4	6	3	0.9	0.95	1574.77	0.62	1494	414	0	1574.77	0.3	143	228	0	1574.78	0.11	11	276	0
4	6	3	0.9	0.99	237.62	0.65	1530	594	0	237.62	0.37	143	155	0	237.62	0.08	1	0	0
4	6	3	0.95	0.9	4600.53	0.6	1457	286	0	4600.54	0.31	143	144	0	4600.54	0.08	1	0	0
4	6	3	0.95	0.95	1724.61	0.6	1498	423	0	1724.61	0.3	143	114	0	1724.61	0.07	1	0	0
4	6	3	0.95	0.99	263.7	0.56	1464	597	0	263.7	0.28	143	179	0	263.7	0.08	1	0	0
4	6	3	0.99	0.9	4888.97	0.6	1450	298	0	4888.98	0.27	141	180	0	4888.98	0.09	1	0	0
4	6	3	0.99	0.95	1849.37	0.57	1450	430	0	1849.37	0.29	143	257	0	1849.37	0.11	16	287	0
4	6	3	0.99	0.99	285.53	0.61	1530	599	0	285.53	0.31	143	151	0	285.53	0.11	14	397	0
5	6	3	0.9	0.9	3501.57	0.63	1476	307	0	3501.57	0.34	143	74	0	3501.57	0.08	1	0	0
5	6	3	0.9	0.95	1219.68	0.62	1446	490	0	1219.68	0.49	141	147	0	1219.68	0.07	1	0	0
5	6	3	0.9	0.99	171.08	0.69	1550	763	0	171.08	0.51	143	53	0	171.08	0.07	1	0	0
5	6	3	0.95	0.9	3768.03	0.58	1514	323	0	3768.03	0.43	142	71	0	3768.03	0.07	1	0	0
5	6	3	0.95	0.95	1330.42	0.64	1516	501	0	1330.42	0.29	143	179	0	1330.42	0.07	1	0	0
5	6	3	0.95	0.99	189.63	0.62	1497	763	0	189.63	0.45	143	65	0	189.63	0.07	1	0	0
5	6	3	0.99	0.9	3988.06	0.6	1532	331	0	3988.06	0.29	149	84	0	3988.06	0.07	1	0	0
5	6	3	0.99	0.95	1422.44	0.65	1470	511	0	1422.44	0.58	143	27	0	1422.44	0.05	1	0	0
5	6	3	0.99	0.99	205.15	0.62	1478	764	0	205.15	0.28	143	265	0	205.15	0.06	1	0	0

Table 4.11: Performance Comparison of the Formulations for $N = 9$

Instance					F^{3}_{MINLP}					F^{SYM}_{MINLP}					F^{EXT}_{MINLP}				
ID	N	L	Se	Sp	Obj	Runtime (s)	Nodes	Gap_r (%)	Gap (%)	Obj	Runtime (s)	Nodes	Gap_r (%)	Gap (%)	Obj	Runtime (s)	Nodes	Gap_r (%)	Gap (%)
1	9	3	0.9	0.9	7179.75	TL	602593	536	241	7179.76	119.64	187267	420	0	7179.76	2.76	2651	98	0
1	9	3	0.9	0.95	2747.8	TL	1054551	782	235	2747.81	1099.39	258536	597	0	2747.82	5.4	986	113	0
1	9	3	0.9	0.99	429.89	TL	2479097	1076	365	429.89	550.5	200341	812	0	429.89	3.47	1384	212	0
1	9	3	0.95	0.9	7791.14	TL	2314385	558	213	7791.18	318.46	191214	437	0	7791.18	0.75	1	0	0
1	9	3	0.95	0.95	3015.44	TL	1821922	796	285	3015.45	750.06	193572	611	0	3015.46	0.84	1	0	0
1	9	3	0.95	0.99	477.33	TL	1128702	1068	383	477.33	944.6	197508	840	0	477.33	1.78	22	78	0
1	9	3	0.99	0.9	8298.16	TL	1292961	569	178	8298.16	1063.17	188237	459	0	8298.18	1.02	1	0	0
1	9	3	0.99	0.95	3238.49	TL	1254852	808	288	3238.5	1361.6	195513	621	0	3238.51	7.21	1092	119	0
1	9	3	0.99	0.99	517.06	TL	679542	1086	329	517.07	1407.29	193925	861	0	517.07	2.38	20	78	0
2	9	3	0.9	0.9	4540.93	TL	749930	910	288	4540.93	151.18	260769	666	0	4540.94	18.54	34601	691	0
2	9	3	0.9	0.95	1519.01	TL	1635194	1502	354	1519.01	777.58	200655	1121	0	1519.02	3.68	1124	319	0
2	9	3	0.9	0.99	203.44	TL	2297243	2484	1154	203.44	716.25	193280	1814	0	203.45	2.38	325	306	0
2	9	3	0.95	0.9	4868.71	TL	1836364	961	456	4868.74	187.6	205732	707	0	4868.76	1.8	272	135	0
2	9	3	0.95	0.95	1652.66	TL	1458174	1572	744	1652.67	242.32	184255	1155	0	1652.68	2.58	941	316	0
2	9	3	0.95	0.99	225.33	TL	1224828	2502	1282	225.34	806.41	185658	1827	0	225.34	2.96	466	311	0
2	9	3	0.99	0.9	5139.03	TL	1506241	981	272	5139.04	886.92	189611	700	0	5139.06	2.75	329	143	0
2	9	3	0.99	0.95	1763.61	TL	1314769	1606	441	1763.62	1181.44	262850	1156	0	1763.63	3.89	866	336	0
2	9	3	0.99	0.99	243.65	TL	1089091	2423	656	243.66	1263.1	194968	1837	0	243.66	4.4	584	308	0
3	9	3	0.9	0.9	4022.33	TL	714905	1016	287	4022.34	136.01	188279	744	0	4022.35	14.68	31413	801	0
3	9	3	0.9	0.95	1269.75	TL	1233892	1846	554	1269.75	1126.61	201985	1400	0	1269.76	118.96	32947	1434	0
3	9	3	0.9	0.99	155.89	TL	2265381	3281	805	155.89	951.07	200674	2358	0	155.89	86.4	34223	2565	0
3	9	3	0.95	0.9	4292.77	TL	1343987	1084	269	4292.78	945.71	182116	841	0	4292.79	106.45	33450	847	0
3	9	3	0.95	0.95	1375.68	TL	670819	1766	993	1375.69	1301.86	193640	1401	0	1375.69	156.35	32423	1484	0
3	9	3	0.95	0.99	172.39	TL	655921	3227	940	172.39	1389.92	197342	2405	0	172.39	194.91	33323	2587	0
3	9	3	0.99	0.9	4515.09	TL	578796	1132	351	4515.1	1515.5	184226	858	0	4515.11	212.56	31754	883	0
3	9	3	0.99	0.95	1463.41	TL	564493	1921	611	1463.42	1626.6	185773	1452	0	1463.42	220.83	32361	1522	0
3	9	3	0.99	0.99	186.19	TL	507487	3265	1022	186.19	1681.32	194178	2397	0	186.19	221.13	32945	2602	0
4	9	3	0.9	0.9	4298.11	TL	1035182	954	247	4298.13	155.09	259972	699	0	4298.14	17.79	28383	737	0
4	9	3	0.9	0.95	1400.97	TL	7204830	1631	764	1400.98	526.42	265297	1252	0	1400.99	19.81	30512	1278	0
4	9	3	0.9	0.99	180.67	TL	1412741	2692	723	180.67	190.97	200812	2099	0	180.67	37.26	29695	2175	0
4	9	3	0.95	0.9	4598.77	TL	1153687	987	608	4598.79	451.84	185249	754	0	4598.8	70.59	28725	778	0
4	9	3	0.95	0.95	1521.41	TL	1186677	1674	846	1521.42	510.5	197471	1277	0	1521.43	61.04	30511	1320	0
4	9	3	0.95	0.99	199.98	TL	999598	2783	1541	199.98	669.64	264508	2121	0	199.98	61.99	30052	2192	0
4	9	3	0.99	0.9	4846.34	TL	1124500	1030	516	4846.36	678.31	195453	794	0	4846.38	61.11	28904	809	0
4	9	3	0.99	0.95	1621.29	TL	1010694	1704	450	1621.3	885.51	265501	1198	0	1621.31	85.71	30740	1351	0
4	9	3	0.99	0.99	216.12	TL	1431329	2765	786	216.13	858.56	201132	2084	0	216.13	154.71	42611	2205	0
5	9	3	0.9	0.9	4125.75	TL	789619	970	284	4125.76	131.58	193492	755	0	4125.78	1.88	562	132	0
5	9	3	0.9	0.95	1316.93	TL	3674327	1738	777	1316.94	719.24	188384	1325	0	1316.94	1.51	90	236	0
5	9	3	0.9	0.99	164.4	TL	960701	3021	836	164.4	300.5	193592	2180	0	164.4	2.1	347	128	0
5	9	3	0.95	0.9	4407.09	TL	1012725	1059	545	4407.11	484.63	188567	782	0	4407.11	1.92	192	147	0
5	9	3	0.95	0.95	1427.94	TL	862703	1803	926	1427.94	876.95	205225	1340	0	1427.95	16.98	6427	507	0
5	9	3	0.95	0.99	181.86	TL	1213608	3028	837	181.86	670.52	196968	2154	0	181.86	3.57	751	582	0
5	9	3	0.99	0.9	4638.48	TL	821257	1093	598	4638.51	794.27	183918	809	0	4638.51	1.47	46	133	0
5	9	3	0.99	0.95	1519.9	TL	927056	1851	988	1519.92	888.3	191993	1383	0	1519.93	12.96	5475	519	0
5	9	3	0.99	0.99	196.46	TL	1363649	3024	890	196.46	817.04	265254	2132	0	196.46	2.39	288	130	0

Table 4.12: Performance Comparison of the Formulations for $N = 10$

Instance					F^{3}_{MINLP}					F^{SYM}_{MINLP}					F^{EXT}_{MINLP}				
ID	N	L	Se	Sp	Obj	Runtime (s)	Nodes	Gap_r (%)	Gap (%)	Obj	Runtime (s)	Nodes	Gap_r (%)	Gap (%)	Obj	Runtime (s)	Nodes	Gap_r (%)	Gap (%)
1	10	4	0.9	0.9	10642.81	TL	863159	327	86	10642.82	50.82	120088	249	0	10642.84	6.07	59585	242	0
1	10	4	0.9	0.95	4280.02	2941.56	4328422	448	0	4280.03	286.93	117093	334	0	4280.03	59.73	61424	339	0
1	10	4	0.9	0.99	703.76	TL	640769	583	174	703.76	681.91	169935	447	0	703.76	98.15	59994	451	0
1	10	4	0.95	0.9	11603.44	TL	2918945	339	61	11603.46	173.17	169247	252	0	11603.48	41.6	62182	249	0
1	10	4	0.95	0.95	4710.78	3083.32	4424725	459	0	4710.81	44.81	167673	340	0	4710.81	7.76	62632	346	0
1	10	4	0.95	0.99	781.98	3201.52	4691969	582	0	781.99	71.25	168597	439	0	781.99	30.21	57460	454	0
1	10	4	0.99	0.9	12401.63	2795.1	4308554	347	0	12401.64	69.49	166453	256	0	12401.66	25.55	60116	257	0
1	10	4	0.99	0.95	5070.25	2528.82	4414697	463	0	5070.27	57.83	163017	343	0	5070.27	20.97	62857	349	0
1	10	4	0.99	0.99	847.54	2557.8	4467343	594	0	847.54	58.63	169570	446	0	847.54	21.62	62711	455	0
2	10	4	0.9	0.9	13964.95	TL	1208928	248	67	13964.97	66.33	112259	193	0	13964.98	5.83	63609	147	0
2	10	4	0.9	0.95	5947.46	3345.17	7374858	323	0	5947.47	483.31	106189	254	0	5947.48	70.95	63681	195	0
2	10	4	0.9	0.99	1035.44	TL	402699	395	129	1035.44	903.83	106875	310	0	1035.44	98.22	62880	245	0
2	10	4	0.95	0.9	15308.52	TL	530177	254	77	15308.53	633.94	112819	202	0	15308.55	74.14	64754	151	0
2	10	4	0.95	0.95	6568.42	TL	719797	323	96	6568.44	447.72	101886	259	0	6568.44	77.51	61461	198	0
2	10	4	0.95	0.99	1151.5	TL	2466961	398	83	1151.5	283.05	108027	314	0	1151.5	61.56	59944	246	0
2	10	4	0.99	0.9	16427.74	3368.19	4511574	261	0	16427.77	80.27	106377	206	0	16427.79	20.96	62378	155	0
2	10	4	0.99	0.95	7087.38	3217.48	4521393	329	0	7087.4	80.28	106997	262	0	7087.41	18.36	64030	200	0
2	10	4	0.99	0.99	1248.79	2916.42	4674505	394	0	1248.79	71.19	105746	317	0	1248.79	10.99	63231	247	0
3	10	4	0.9	0.9	7634.2	TL	1017170	405	117	7634.21	54.83	169307	317	0	7634.24	7.53	59996	425	0
3	10	4	0.9	0.95	2831.98	TL	4106398	618	94	2831.99	160.52	169405	473	0	2832.0	51.15	62368	647	0
3	10	4	0.9	0.99	426.98	TL	3943526	853	145	426.98	31.29	167671	677	0	426.99	6.15	60641	941	0
3	10	4	0.95	0.9	8261.66	TL	2140430	411	85	8261.7	50.83	164335	329	0	8261.71	16.56	60012	444	0
3	10	4	0.95	0.95	3101.52	TL	1900515	602	148	3101.52	91.34	169682	484	0	3101.54	24.84	59050	662	0
3	10	4	0.95	0.99	473.82	TL	1910358	870	232	473.82	132.23	167385	684	0	473.82	32.68	59213	946	0
3	10	4	0.99	0.9	8781.17	TL	1328184	414	108	8781.2	134.84	169687	339	0	8781.22	34.23	59813	458	0
3	10	4	0.99	0.95	3325.92	TL	1488764	602	183	3325.92	193.58	168284	493	0	3325.94	37.8	58848	674	0
3	10	4	0.99	0.99	513.04	TL	876457	878	288	513.04	193.01	164907	684	0	513.05	40.97	60543	949	0
4	10	4	0.9	0.9	7922.0	TL	778826	397	113	7922.02	67.61	113420	315	0	7922.04	8.98	61545	395	0
4	10	4	0.9	0.95	2949.84	3311.23	4366644	574	0	2949.85	393.58	162362	469	0	2949.86	67.57	61619	595	0
4	10	4	0.9	0.99	445.55	TL	416769	830	300	445.55	878.53	118281	664	0	445.55	112.35	59347	863	0
4	10	4	0.95	0.9	8576.83	TL	1096353	407	98	8576.86	248.37	119405	324	0	8576.88	60.82	62874	411	0
4	10	4	0.95	0.95	3231.13	TL	3098395	589	105	3231.14	109.59	112259	481	0	3231.15	42.64	60968	608	0
4	10	4	0.95	0.99	494.43	TL	2226964	836	163	494.43	87.86	114954	677	0	494.43	26.25	62700	868	0
4	10	4	0.99	0.9	9118.99	TL	1467230	415	98	9119.03	90.95	112155	336	0	9119.05	29.83	62191	423	0
4	10	4	0.99	0.95	3465.32	TL	1549051	584	141	3465.33	114.81	105600	484	0	3465.33	34.73	61795	620	0
4	10	4	0.99	0.99	535.36	TL	1339390	849	195	535.36	114.38	111113	674	0	535.37	38.12	59382	872	0
5	10	4	0.9	0.9	11391.0	TL	1165417	302	85	11391.03	66.84	115543	245	0	11391.03	6.04	60687	214	0
5	10	4	0.9	0.95	4651.31	TL	618238	412	132	4651.32	421.83	115223	321	0	4651.33	67.35	60559	296	0
5	10	4	0.9	0.99	776.84	TL	3732818	528	98	776.85	537.01	113300	421	0	776.85	97.51	62272	388	0
5	10	4	0.95	0.9	12436.95	TL	2855730	309	56	12436.96	86.85	115633	246	0	12436.98	25.66	61361	221	0
5	10	4	0.95	0.95	5124.17	TL	2424206	417	95	5124.19	89.36	115154	334	0	5124.19	26.35	61834	301	0
5	10	4	0.95	0.99	863.4	TL	1881621	533	121	863.4	120.94	113683	421	0	863.4	30.19	61091	390	0
5	10	4	0.99	0.9	13306.61	TL	1161970	322	83	13306.64	148.16	117859	254	0	13306.64	37.13	62305	227	0
5	10	4	0.99	0.95	5518.91	TL	1654105	486	109	5518.93	114.76	108189	333	0	5518.93	39.16	58890	305	0
5	10	4	0.99	0.99	935.93	TL	1692962	534	130	935.94	111.69	109256	420	0	935.94	34.86	62607	391	0

Table 4.13: Performance Comparison of the Formulations for $N = 12$

Instance					F^{3}_{MINLP}					F^{SYM}_{MINLP}					F^{EXT}_{MINLP}				
ID	N	L	Se	Sp	Obj	Runtime (s)	Nodes	Gap_r (%)	Gap (%)	Obj	Runtime (s)	Nodes	Gap_r (%)	Gap (%)	Obj	Runtime (s)	Nodes	Gap_r (%)	Gap (%)
1	12	3	0.9	0.9	6825.24	TL	148962	869	697	6826.09	TL	287175	721	184	6825.27	TL	20623803	657	464
1	12	3	0.9	0.95	2377.63	TL	148956	1378	1082	2377.63	TL	204127	1148	309	2377.64	TL	9733486	1063	884
1	12	3	0.9	0.99	334.82	TL	171034	2131	1693	334.82	TL	301602	1750	457	334.82	TL	10248519	1656	1255
1	12	3	0.95	0.9	7344.56	TL	164845	909	704	7344.54	TL	184568	752	204	7344.58	TL	10089616	689	565
1	12	3	0.95	0.95	2593.77	TL	380775	1416	640	2593.77	TL	307778	1175	290	2593.79	TL	27246422	1093	730
1	12	3	0.95	0.99	371.16	TL	154553	2134	1684	371.16	TL	318857	1782	465	371.16	TL	22368445	1666	1228
1	12	3	0.99	0.9	7771.95	TL	150275	942	712	7772.78	TL	311871	779	285	7771.98	TL	22488899	714	477
1	12	3	0.99	0.95	2773.43	TL	421912	1448	660	2773.42	TL	331875	1201	310	2773.45	TL	25084173	1115	810
1	12	3	0.99	0.99	401.58	TL	178455	2153	1712	401.58	TL	334482	1785	446	401.58	TL	25774101	1673	1106
1	12	4	0.9	0.9	10807.4	TL	509629	475	187	10805.62	TL	814922	410	92	10805.64	TL	3394362	331	248
1	12	4	0.9	0.95	4205.68	TL	624808	642	264	4205.69	TL	577818	583	133	4205.7	TL	3389710	481	357
1	12	4	0.9	0.99	669.72	TL	594745	918	359	670.19	TL	604700	797	180	669.72	TL	3006449	661	497
1	12	4	0.95	0.9	11744.13	TL	542061	468	193	11753.79	TL	543763	428	100	11744.15	TL	2686390	344	262
1	12	4	0.95	0.95	4620.08	TL	1083163	651	275	4622.87	TL	1186092	605	128	4620.09	TL	4593244	490	341
1	12	4	0.95	0.99	743.86	TL	659633	922	367	744.34	TL	760603	781	183	743.82	TL	3376358	664	511
1	12	4	0.99	0.9	12522.92	TL	654818	477	199	12522.92	TL	802118	437	110	12522.94	TL	4204092	354	268
1	12	4	0.99	0.95	4965.59	TL	760033	698	282	4965.58	TL	1152435	601	136	4965.59	TL	5484791	497	326
1	12	4	0.99	0.99	805.89	TL	740018	878	358	806.46	TL	1296804	792	174	805.9	TL	4622552	666	465
2	12	3	0.9	0.9	4230.03	TL	109285	1451	1218	4230.13	TL	294961	1216	684	4230.04	TL	22644605	1300	955
2	12	3	0.9	0.95	1217.55	TL	162909	2827	2381	1217.56	TL	227116	2351	720	1217.56	TL	10962208	2548	2063
2	12	3	0.9	0.99	130.47	TL	279468	5759	5219	130.47	TL	211019	4793	2757	130.47	TL	8612894	5211	4201
2	12	3	0.95	0.9	4480.39	TL	248863	1545	1399	4480.39	TL	182174	1284	834	4480.42	TL	8794783	1386	1168
2	12	3	0.95	0.95	1310.51	TL	143453	2941	2469	1310.51	TL	131458	2456	864	1310.52	TL	7720290	2654	2197
2	12	3	0.95	0.99	143.91	TL	1149877	5818	5167	143.91	TL	270098	4829	1724	143.92	TL	26317114	5270	3796
2	12	3	0.99	0.9	4685.3	TL	191730	1620	1334	4685.33	TL	290299	1355	469	4685.32	TL	22474463	1453	1036
2	12	3	0.99	0.95	1387.24	TL	186748	3026	2536	1387.24	TL	277325	2523	772	1387.25	TL	22910626	2735	1924
2	12	3	0.99	0.99	155.14	TL	1541961	5841	4797	155.14	TL	342853	4897	2466	155.15	TL	24507166	5313	4114
2	12	4	0.9	0.9	6341.72	TL	668983	847	323	6341.72	TL	1311816	732	168	6341.76	TL	3454986	750	568
2	12	4	0.9	0.95	2110.26	TL	527695	1440	608	2110.27	TL	636330	1236	335	2110.28	TL	3480909	1273	1038
2	12	4	0.9	0.99	279.06	TL	163732	2401	1554	279.06	TL	602493	2011	590	279.06	TL	2779580	2110	1750
2	12	4	0.95	0.9	6797.69	TL	391462	891	382	6797.7	TL	467309	758	234	6797.73	TL	2450349	790	601
2	12	4	0.95	0.95	2294.78	TL	338665	1493	616	2294.78	TL	431709	1254	372	2294.79	TL	2236424	1313	1116
2	12	4	0.95	0.99	309.01	TL	890311	2349	876	309.01	TL	1755900	2028	498	309.01	TL	8240603	2127	1267
2	12	4	0.99	0.9	7173.44	TL	357954	931	484	7173.45	TL	826922	802	250	7173.48	TL	4200257	821	621
2	12	4	0.99	0.95	2447.88	TL	1264300	1534	966	2447.87	TL	971004	1298	323	2447.9	TL	4076688	1343	989
2	12	4	0.99	0.99	334.06	TL	783972	2411	929	334.06	TL	1312159	2033	488	334.07	TL	7500278	2138	1440
3	12	3	0.9	0.9	5230.43	TL	185284	1149	907	5230.43	TL	356298	958	355	5230.45	TL	24675414	965	757
3	12	3	0.9	0.95	1642.97	TL	172449	2031	1619	1642.97	TL	153987	1711	493	1642.98	TL	13497053	1733	1427
3	12	3	0.9	0.99	200.96	TL	150826	3606	2890	200.96	TL	167583	3042	1684	200.96	TL	11488737	3104	2590
3	12	3	0.95	0.9	5579.32	TL	284777	1217	973	5579.32	TL	197564	1020	296	5579.34	TL	10328822	1022	823
3	12	3	0.95	0.95	1779.55	TL	120713	2115	1739	1779.56	TL	156148	1776	725	1779.57	TL	9896034	1794	1493
3	12	3	0.95	0.99	222.22	TL	169961	3674	2963	222.22	TL	324416	3075	845	222.23	TL	26186342	3134	2395
3	12	3	0.99	0.9	5866.11	TL	160173	1234	769	5866.1	TL	272481	1063	305	5866.22	TL	22531156	1065	811
3	12	3	0.99	0.95	1892.68	TL	203301	2152	1712	1892.68	TL	429660	1822	501	1892.69	TL	24171420	1840	1396
3	12	3	0.99	0.99	240.0	TL	161585	3691	2945	240.0	TL	200558	3081	880	240.01	TL	29302021	3154	2386
3	12	4	0.9	0.9	8080.09	TL	216166	647	450	8080.07	TL	1494937	570	141	8080.1	TL	5174766	521	370
3	12	4	0.9	0.95	2900.25	TL	315821	986	521	2900.24	TL	683838	875	247	2900.26	TL	3005978	819	660
3	12	4	0.9	0.99	421.27	TL	256698	1390	760	421.27	TL	607339	1319	340	421.27	TL	2995443	1236	1000
3	12	4	0.95	0.9	8718.26	TL	502918	666	284	8718.26	TL	582309	596	166	8718.28	TL	2820325	545	448
3	12	4	0.95	0.95	3169.66	TL	234877	1023	463	3169.66	TL	432298	896	302	3169.68	TL	2388162	840	665
3	12	4	0.95	0.99	467.21	TL	1146194	1524	1045	467.21	TL	929074	1336	342	467.21	TL	3719066	1243	1007
3	12	4	0.99	0.9	9245.89	TL	340331	709	433	9245.9	TL	825661	613	168	9245.93	TL	3802178	563	428
3	12	4	0.99	0.95	3393.75	TL	665243	1059	437	3393.75	TL	825305	918	254	3393.77	TL	3598137	856	681
3	12	4	0.99	0.99	505.67	TL	621949	1529	782	505.67	TL	1025552	1308	365	505.67	TL	4259389	1249	975
4	12	3	0.9	0.9	4728.73	TL	508449	1281	1063	4728.73	TL	175467	1065	315	4728.76	TL	24524202	1125	834
4	12	3	0.9	0.95	1449.55	TL	156186	2347	1924	1449.55	TL	259677	1950	504	1449.56	TL	13532963	2072	1719
4	12	3	0.9	0.99	173.31	TL	197350	4281	3466	173.31	TL	238689	3526	607	173.31	TL	10656984	3798	3061
4	12	3	0.95	0.9	5032.47	TL	245566	1362	1174	5032.47	TL	187139	1130	216	5032.49	TL	10183631	1194	1003
4	12	3	0.95	0.95	1567.82	TL	208940	2433	2154	1567.82	TL	217649	2018	1000	1567.83	TL	8919347	2147	1613
4	12	3	0.95	0.99	191.59	TL	1008773	4321	3530	191.59	TL	341474	3592	590	191.59	TL	29385042	3833	2857
4	12	3	0.99	0.9	5282.04	TL	392114	1420	522	5282.04	TL	396921	1178	255	5282.07	TL	23414654	1247	927
4	12	3	0.99	0.95	1665.73	TL	1930324	2496	2023	1665.72	TL	247190	2080	337	1665.74	TL	29620533	2205	1652
4	12	3	0.99	0.99	206.87	TL	350488	4349	1652	206.87	TL	375224	3608	652	206.87	TL	25612159	3858	2593
4	12	4	0.9	0.9	7189.53	TL	939239	755	251	7189.52	TL	1017880	520	119	7189.55	TL	4978638	636	471
4	12	4	0.9	0.95	2516.16	TL	620597	1186	456	2516.16	TL	552956	825	193	2516.17	TL	3147146	1026	775
4	12	4	0.9	0.99	356.35	TL	702029	1845	662	356.35	TL	578553	1257	305	356.35	TL	2777482	1588	1199
4	12	4	0.95	0.9	7738.81	TL	638181	777	313	7738.83	TL	518270	544	132	7738.85	TL	2900142	667	555
4	12	4	0.95	0.95	2745.74	TL	537201	1239	441	2745.75	TL	428523	842	205	2745.77	TL	2170463	1054	884
4	12	4	0.95	0.99	395.06	TL	729967	1853	888	395.06	TL	1248786	1265	284	395.06	TL	5736061	1598	1169
4	12	4	0.99	0.9	8192.63	TL	678650	807	318	8192.62	TL	739363	559	128	8192.66	TL	3418153	691	486
4	12	4	0.99	0.95	2936.61	TL	1075129	1230	487	2936.62	TL	1464252	868	175	2936.63	TL	6450596	1075	719
4	12	4	0.99	0.99	427.46	TL	652570	1875	715	427.46	TL	829476	1281	293	427.47	TL	4199828	1605	1188
5	12	3	0.9	0.9	7075.72	TL	206777	817	437	7075.55	TL	475022	673	444	7075.73	TL	26105697	624	461
5	12	3	0.9	0.95	2502.4	TL	379555	1276	557	2502.52	TL	338599	1055	715	2502.42	TL	11764701	996	827
5	12	3	0.9	0.99	359.59	TL	401235	1942	840	359.6	TL	288991	1587	288	359.6	TL	8947774	1520	1134
5	12	3	0.95	0.9	7623.14	TL	304592	855	443	7623.97	TL	401799	704	483	7623.08	TL	10778203	654	538
5	12	3	0.95	0.95	2732.77	TL	222892	1317	762	2732.89	TL	491604	1082	211	2732.9	TL	26914323	1023	769
5	12	3	0.95	0.99	398.76	TL	305612	1947	854	398.83	TL	404268	1601	284	398.76	TL	10531288	1529	1155
5	12	3	0.99	0.9	8074.71	TL	313329	871	366	8074.71	TL	934340	718	476	8074.72	TL	23557754	677	493
5	12	3	0.99	0.95	2924.34	TL	166345	1334	801	2924.36	TL	308566	1102	755	2924.36	TL	10269348	1043	843
5	12	3	0.99	0.99	431.54	TL	392929	1957	828	431.62	TL	465118	1608	291	431.55	TL	26157550	1535	1127
5	12	4	0.9	0.9	11231.48	TL	641592	453	170	11232.42	TL	556394	348	75	11231.5	TL	3755860	314	236
5	12	4	0.9	0.95	4419.9	TL	568636	611	237	4420.68	TL	563779	499	112	4419.91	TL	2770335	451	344
5	12	4	0.9	0.99	712.48	TL	540536	857	317	712.63	TL	571092	659	149	712.48	TL	3002432	613	494
5	12	4	0.95	0.9	12219.11	TL	478464	469	175	12220.92	TL	541668	366	80	12219.16	TL	2511265	326	255
5	12	4	0.95	0.95	4858.77	TL	722973	650	234	4858.78	TL	1048286	506	97	4858.78	TL	4764410	459	351
5	12	4	0.95	0.99	791.46	TL	716666	860	323	791.63	TL	697320	663	136	791.46	TL	3959173	615	449
5	12	4	0.99	0.9	13039.13	TL	748843	480	188	13041.09	TL	1067324	376	77	13039.16	TL	4491577	335	252
5	12	4	0.99	0.95	5224.81	TL	388882	659	251	5224.81	TL	522884	512	120	5224.82	TL	3009565	466	388
5	12	4	0.99	0.99	857.63	TL	781303	862	354	857.73	TL	1166046	662	131	857.64	TL	5367120	617	412

Table 4.14: Comparison of heuristics for N = 6, L = 3

Instance						GRADIENT		SPIRAL		LEAST		HIGHEST		BOTH	
ID	N	L	Se	Sp	Best Known	Obj	Time (s)	Obj	Time (s)	Obj	Time (s)	Obj	Time (s)	Obj	Time (s)
1	6	3	0.9	0.9	3893.84	-	-	-	-	3893.84	0.39	3895.95	0.55	-	-
1	6	3	0.9	0.95	1415.34	-	-	-	-	1415.34	0.37	1416.47	0.49	-	-
1	6	3	0.9	0.99	209.73	-	-	-	-	209.73	0.4	209.96	0.66	-	-
1	6	3	0.95	0.9	4205.28	-	-	-	-	4205.28	0.09	4207.65	0.15	-	-
1	6	3	0.95	0.95	1548.31	-	-	-	-	1548.31	0.09	1549.57	0.15	-	-
1	6	3	0.95	0.99	232.68	-	-	-	-	232.68	0.08	232.94	0.16	-	-
1	6	3	0.99	0.9	4463.01	-	-	-	-	4463.01	0.08	4465.6	0.14	-	-
1	6	3	0.99	0.95	1658.97	-	-	-	-	1658.97	0.08	1660.34	0.16	-	-
1	6	3	0.99	0.99	251.90	-	-	-	-	251.9	0.08	252.19	0.12	-	-
2	6	3	0.9	0.9	3433.36	-	-	-	-	3433.36	0.16	3435.41	0.1	-	-
2	6	3	0.9	0.95	1197.61	-	-	-	-	1197.61	0.09	1198.69	0.1	-	-
2	6	3	0.9	0.99	168.93	-	-	-	-	168.93	0.08	169.16	0.09	-	-
2	6	3	0.95	0.9	3694.60	-	-	-	-	3694.6	0.09	3696.9	0.1	-	-
2	6	3	0.95	0.95	1306.60	-	-	-	-	1306.6	0.08	1307.82	0.08	-	-
2	6	3	0.95	0.99	187.27	-	-	-	-	187.27	0.09	187.53	0.1	-	-
2	6	3	0.99	0.9	3910.40	-	-	-	-	3910.4	0.09	3912.9	0.1	-	-
2	6	3	0.99	0.95	1397.20	-	-	-	-	1397.2	0.08	1398.52	0.1	-	-
2	6	3	0.99	0.99	202.62	-	-	-	-	202.62	0.11	202.9	0.09	-	-
3	6	3	0.9	0.9	2788.27	-	-	-	-	2788.27	0.19	2788.56	0.16	-	-
3	6	3	0.9	0.95	911.43	-	-	-	-	911.43	0.16	911.58	0.16	-	-
3	6	3	0.9	0.99	118.98	-	-	-	-	118.98	0.14	119.01	0.12	-	-
3	6	3	0.95	0.9	2983.31	-	-	-	-	2983.31	0.14	2983.63	0.15	-	-
3	6	3	0.95	0.95	990.19	-	-	-	-	990.19	0.16	990.36	0.15	-	-
3	6	3	0.95	0.99	131.73	-	-	-	-	131.73	0.15	131.77	0.13	-	-
3	6	3	0.99	0.9	3144.01	-	-	-	-	3144.01	0.15	3144.36	0.14	-	-
3	6	3	0.99	0.95	1055.53	-	-	-	-	1055.53	0.15	1055.72	0.14	-	-
3	6	3	0.99	0.99	142.40	-	-	-	-	142.4	0.16	142.44	0.13	-	-
4	6	3	0.9	0.9	4252.19	-	-	-	-	4252.2	0.24	4268.17	0.15	-	-
4	6	3	0.9	0.95	1574.77	-	-	-	-	1574.78	0.18	1583.26	0.2	-	-
4	6	3	0.9	0.99	237.62	-	-	-	-	237.62	0.16	239.4	0.15	-	-
4	6	3	0.95	0.9	4600.53	-	-	-	-	4600.54	0.15	4618.45	0.15	-	-
4	6	3	0.95	0.95	1724.61	-	-	-	-	1724.61	0.18	1734.1	0.2	-	-
4	6	3	0.95	0.99	263.70	-	-	-	-	263.7	0.16	265.68	0.16	-	-
4	6	3	0.99	0.9	4888.97	-	-	-	-	4888.98	0.17	4908.53	0.18	-	-
4	6	3	0.99	0.95	1849.37	-	-	-	-	1849.37	0.15	1859.69	0.16	-	-
4	6	3	0.99	0.99	285.53	-	-	-	-	285.53	0.18	287.68	0.22	-	-
5	6	3	0.9	0.9	3501.57	-	-	-	-	3501.57	0.17	3510.71	0.17	-	-
5	6	3	0.9	0.95	1219.68	-	-	-	-	1219.68	0.18	1224.54	0.16	-	-
5	6	3	0.9	0.99	171.08	-	-	-	-	171.08	0.15	172.1	0.14	-	-
5	6	3	0.95	0.9	3768.03	-	-	-	-	3768.03	0.18	3778.28	0.16	-	-
5	6	3	0.95	0.95	1330.42	-	-	-	-	1330.42	0.16	1335.85	0.15	-	-
5	6	3	0.95	0.99	189.63	-	-	-	-	189.63	0.14	190.76	0.16	-	-
5	6	3	0.99	0.9	3988.06	-	-	-	-	3988.06	0.14	3999.25	0.17	-	-
5	6	3	0.99	0.95	1422.44	-	-	-	-	1422.44	0.15	1428.35	0.14	-	-
5	6	3	0.99	0.99	205.15	-	-	-	-	205.15	0.18	206.39	0.14	-	-

Table 4.15: Comparison of heuristics for N = 9, L = 3

Instance						GRADIENT		SPIRAL		LEAST		HIGHEST		BOTH	
ID	N	L	Se	Sp	Best Known	Obj	Time (s)	Obj	Time (s)	Obj	Time (s)	Obj	Time (s)	Obj	Time (s)
1	9	3	0.9	0.9	7179.75	7192.19	0.0	7285.62	0.0	7179.76	2.56	7192.19	2.43	7192.19	1.11
1	9	3	0.9	0.95	2747.80	2754.28	0.0	2803.17	0.0	2747.82	19.09	2754.28	15.5	2754.28	2.37
1	9	3	0.9	0.99	429.89	431.22	0.0	441.34	0.0	429.89	13.69	431.22	11.17	431.22	2.08
1	9	3	0.95	0.9	7791.14	7805.08	0.0	7909.7	0.0	7791.18	9.84	7805.08	8.69	7805.08	1.64
1	9	3	0.95	0.95	3015.44	3022.67	0.0	3077.27	0.0	3015.46	13.22	3022.67	12.41	3022.67	2.07
1	9	3	0.95	0.99	477.33	478.81	0.0	490.09	0.0	477.33	15.82	478.81	14.51	478.81	2.15
1	9	3	0.99	0.9	8298.16	8313.33	0.0	8427.35	0.0	8298.18	16.35	8313.33	15.6	8313.33	2.04
1	9	3	0.99	0.95	3238.49	3246.35	0.0	3305.74	0.0	3238.51	17.95	3246.35	16.19	3246.35	2.15
1	9	3	0.99	0.99	517.06	518.68	0.0	530.92	0.0	517.07	20.72	518.68	18.41	518.68	2.26
2	9	3	0.9	0.9	4540.93	4544.23	0.0	4621.48	0.0	4540.94	4.07	4544.23	3.89	4544.23	1.23
2	9	3	0.9	0.95	1519.01	1520.7	0.0	1561.0	0.0	1519.02	20.03	1520.7	18.91	1520.7	2.58
2	9	3	0.9	0.99	203.44	203.79	0.0	212.1	0.0	203.44	21.48	203.79	20.79	203.79	2.55
2	9	3	0.95	0.9	4868.71	4872.43	0.0	4958.9	0.0	4868.76	15.65	4872.43	14.15	4872.43	1.78
2	9	3	0.95	0.95	1652.66	1654.55	0.0	1699.55	0.0	1652.68	17.71	1654.55	16.5	1654.55	1.72
2	9	3	0.95	0.99	225.33	225.72	0.0	234.99	0.0	225.34	22.75	225.72	20.67	225.72	1.92
2	9	3	0.99	0.9	5139.03	5143.05	0.0	5237.28	0.0	5139.06	23.12	5143.05	22.88	5143.05	1.97
2	9	3	0.99	0.95	1763.61	1765.67	0.0	1814.61	0.0	1763.63	28.37	1765.67	26.38	1765.67	2.58
2	9	3	0.99	0.99	243.65	244.07	0.0	254.14	0.0	243.66	24.31	244.07	26.29	244.07	2.38
3	9	3	0.9	0.9	4022.33	4022.35	0.0	4156.07	0.0	4022.35	4.28	4022.35	3.89	4022.35	0.8
3	9	3	0.9	0.95	1269.75	1269.76	0.0	1339.57	0.0	1269.76	25.34	1269.76	26.13	1269.76	1.54
3	9	3	0.9	0.99	155.89	155.89	0.0	170.31	0.0	155.89	21.09	155.89	21.29	155.89	1.54
3	9	3	0.95	0.9	4292.77	4292.79	0.0	4442.49	0.0	4292.79	22.22	4292.79	21.11	4292.79	1.44
3	9	3	0.95	0.95	1375.68	1375.69	0.0	1453.65	0.0	1375.69	25.75	1375.69	27.32	1375.69	1.41
3	9	3	0.95	0.99	172.39	172.4	0.0	188.46	0.0	172.4	29.13	172.4	31.34	172.4	1.62
3	9	3	0.99	0.9	4515.09	4515.11	0.0	4678.23	0.0	4515.11	29.15	4515.11	30.62	4515.11	1.56
3	9	3	0.99	0.95	1463.41	1463.42	0.0	1548.21	0.0	1463.42	34.42	1463.42	34.37	1463.42	1.55
3	9	3	0.99	0.99	186.19	186.19	0.0	203.64	0.0	186.19	35.62	186.19	33.46	186.19	1.66
4	9	3	0.9	0.9	4298.11	4298.14	0.0	4387.85	0.0	4298.14	3.72	4298.14	3.44	4298.14	0.68
4	9	3	0.9	0.95	1400.97	1400.99	0.0	1447.82	0.0	1400.99	26.8	1400.99	21.88	1400.99	1.37
4	9	3	0.9	0.99	180.67	180.67	0.0	190.34	0.0	180.67	15.74	180.67	15.81	180.67	1.23
4	9	3	0.95	0.9	4598.77	4598.8	0.0	4699.23	0.0	4598.8	27.2	4598.8	23.66	4598.8	1.47
4	9	3	0.95	0.95	1521.41	1521.43	0.0	1573.72	0.0	1521.43	21.84	1521.43	21.81	1521.43	1.37
4	9	3	0.95	0.99	199.98	199.98	0.0	210.76	0.0	199.98	25.92	199.98	22.98	199.98	1.57
4	9	3	0.99	0.9	4846.34	4846.38	0.0	4955.82	0.0	4846.38	24.26	4846.38	24.03	4846.38	1.62
4	9	3	0.99	0.95	1621.29	1621.31	0.0	1678.19	0.0	1621.31	29.76	1621.31	25.53	1621.31	1.52
4	9	3	0.99	0.99	216.12	216.13	0.0	227.84	0.0	216.13	28.32	216.13	24.54	216.13	1.52
5	9	3	0.9	0.9	4125.75	4125.78	0.0	4305.15	0.0	4125.78	2.84	4125.78	2.82	4125.78	0.77
5	9	3	0.9	0.95	1316.93	1316.94	0.0	1410.59	0.0	1316.94	13.19	1316.94	12.89	1316.94	1.67
5	9	3	0.9	0.99	164.40	164.4	0.0	183.74	0.0	164.4	10.09	164.4	11.55	164.4	1.19
5	9	3	0.95	0.9	4407.09	4407.11	0.0	4607.92	0.0	4407.11	14.15	4407.11	13.88	4407.11	1.38
5	9	3	0.95	0.95	1427.94	1427.95	0.0	1532.52	0.0	1427.95	15.49	1427.95	14.66	1427.95	1.34
5	9	3	0.95	0.99	181.86	181.86	0.0	203.41	0.0	181.86	15.3	181.86	14.66	181.86	1.3
5	9	3	0.99	0.9	4638.48	4638.51	0.0	4857.33	0.0	4638.51	18.49	4638.51	18.36	4638.51	1.41
5	9	3	0.99	0.95	1519.90	1519.93	0.0	1633.67	0.0	1519.93	17.76	1519.93	16.47	1519.93	1.5
5	9	3	0.99	0.99	196.46	196.46	0.0	219.87	0.0	196.46	16.52	196.46	18.26	196.46	1.51

Table 4.16: Comparison of heuristics for N = 10, L = 4

Instance						GRADIENT		SPIRAL		LEAST		HIGHEST		BOTH	
ID	N	L	Se	Sp	Best Known	Obj	Time (s)	Obj	Time (s)	Obj	Time (s)	Obj	Time (s)	Obj	Time (s)
1	10	4	0.9	0.9	10642.81	-	-	-	-	10642.8	1.6	10783.8	2.32	-	-
1	10	4	0.9	0.95	4280.02	-	-	-	-	4280.03	3.25	4354.37	3.6	-	-
1	10	4	0.9	0.99	703.76	-	-	-	-	703.76	3.92	719.24	5.74	-	-
1	10	4	0.95	0.9	11603.44	-	-	-	-	11603.5	2.7	11761.4	2.66	-	-
1	10	4	0.95	0.95	4710.78	-	-	-	-	4710.81	1.8	4793.86	2.07	-	-
1	10	4	0.95	0.99	781.98	-	-	-	-	781.99	1.68	799.24	2.23	-	-
1	10	4	0.99	0.9	12401.63	-	-	-	-	12401.7	3.2	12573.9	2.76	-	-
1	10	4	0.99	0.95	5070.25	-	-	-	-	5070.27	1.51	5160.64	2.71	-	-
1	10	4	0.99	0.99	847.54	-	-	-	-	847.54	2.6	866.28	2.42	-	-
2	10	4	0.9	0.9	13964.95	-	-	-	-	13965.0	2.01	13997.4	1.89	-	-
2	10	4	0.9	0.95	5947.46	-	-	-	-	5947.48	4.06	5964.56	3.99	-	-
2	10	4	0.9	0.99	1035.44	-	-	-	-	1035.44	4.58	1039.0	5.59	-	-
2	10	4	0.95	0.9	15308.52	-	-	-	-	15308.6	3.68	15344.9	4.4	-	-
2	10	4	0.95	0.95	6568.42	-	-	-	-	6568.44	3.18	6587.53	3.78	-	-
2	10	4	0.95	0.99	1151.50	-	-	-	-	1151.5	3.0	1155.47	4.05	-	-
2	10	4	0.99	0.9	16427.74	-	-	-	-	16427.8	3.06	16467.4	2.14	-	-
2	10	4	0.99	0.95	7087.38	-	-	-	-	7087.41	2.08	7108.18	2.33	-	-
2	10	4	0.99	0.99	1248.79	-	-	-	-	1248.79	1.62	1253.1	1.84	-	-
3	10	4	0.9	0.9	7634.20	-	-	-	-	7634.24	1.11	7672.26	1.46	-	-
3	10	4	0.9	0.95	2831.98	-	-	-	-	2832.0	2.4	2852.13	2.43	-	-
3	10	4	0.9	0.99	426.98	-	-	-	-	426.99	1.2	431.19	1.19	-	-
3	10	4	0.95	0.9	8261.66	-	-	-	-	8261.71	1.19	8304.33	1.27	-	-
3	10	4	0.95	0.95	3101.52	-	-	-	-	3101.54	1.7	3124.03	1.69	-	-
3	10	4	0.95	0.99	473.82	-	-	-	-	473.82	1.93	478.51	1.72	-	-
3	10	4	0.99	0.9	8781.17	-	-	-	-	8781.22	1.31	8827.71	1.84	-	-
3	10	4	0.99	0.95	3325.92	-	-	-	-	3325.94	1.42	3350.42	1.77	-	-
3	10	4	0.99	0.99	513.04	-	-	-	-	513.05	1.47	518.14	2.01	-	-
4	10	4	0.9	0.9	7922.00	-	-	-	-	7922.04	2.54	8118.86	2.13	-	-
4	10	4	0.9	0.95	2949.84	-	-	-	-	2949.86	3.8	3053.81	4.44	-	-
4	10	4	0.9	0.99	445.55	-	-	-	-	445.55	3.92	467.22	4.15	-	-
4	10	4	0.95	0.9	8576.83	-	-	-	-	8576.88	3.84	8797.48	3.67	-	-
4	10	4	0.95	0.95	3231.13	-	-	-	-	3231.15	2.49	3347.29	2.69	-	-
4	10	4	0.95	0.99	494.43	-	-	-	-	494.43	3.0	518.58	2.45	-	-
4	10	4	0.99	0.9	9118.99	-	-	-	-	9119.05	3.38	9359.65	2.75	-	-
4	10	4	0.99	0.95	3465.32	-	-	-	-	3465.33	3.66	3591.72	2.59	-	-
4	10	4	0.99	0.99	535.36	-	-	-	-	535.36	2.34	561.6	2.64	-	-
5	10	4	0.9	0.9	11391.00	-	-	-	-	11391.0	1.78	11527.6	1.91	-	-
5	10	4	0.9	0.95	4651.31	-	-	-	-	4651.33	2.49	4723.35	3.67	-	-
5	10	4	0.9	0.99	776.84	-	-	-	-	776.85	2.9	791.84	4.06	-	-
5	10	4	0.95	0.9	12436.95	-	-	-	-	12437.0	1.79	12590.0	2.87	-	-
5	10	4	0.95	0.95	5124.17	-	-	-	-	5124.19	2.09	5204.66	2.5	-	-
5	10	4	0.95	0.99	863.40	-	-	-	-	863.4	1.6	880.12	2.87	-	-
5	10	4	0.99	0.9	13306.61	-	-	-	-	13306.6	1.75	13473.5	3.08	-	-
5	10	4	0.99	0.95	5518.91	-	-	-	-	5518.93	2.4	5606.49	2.58	-	-
5	10	4	0.99	0.99	935.93	-	-	-	-	935.94	1.63	954.1	2.28	-	-

Table 4.17: Comparison of heuristics for N = 12, L = 3

Instance						GRADIENT		SPIRAL		LEAST		HIGHEST		BOTH	
ID	N	L	Se	Sp	Best Known	Obj	Time (s)	Obj	Time (s)	Obj	Time (s)	Obj	Time (s)	Obj	Time (s)
1	12	3	0.9	0.9	6825.24	-	-	-	-	6826.12	302.83	6833.92	180.97	6826.12	122.04
1	12	3	0.9	0.95	2377.63	-	-	-	-	2377.64	183.21	2377.64	302.03	2377.64	128.96
1	12	3	0.9	0.99	334.82	-	-	-	-	334.82	318.56	335.12	180.76	334.82	123.61
1	12	3	0.95	0.9	7344.54	-	-	-	-	7346.03	241.64	7344.11	180.45	7344.58	127.54
1	12	3	0.95	0.95	2593.77	-	-	-	-	2593.79	181.06	2593.79	241.05	2593.79	130.19
1	12	3	0.95	0.99	371.16	-	-	-	-	371.31	251.07	371.16	187.74	371.16	132.1
1	12	3	0.99	0.9	7771.95	-	-	-	-	7773.59	319.5	7772.38	387.1	7772.81	115.31
1	12	3	0.99	0.95	2773.42	-	-	-	-	2773.93	271.44	2773.45	302.63	2773.45	126.46
1	12	3	0.99	0.99	401.58	-	-	-	-	401.74	206.92	403.58	180.42	401.58	104.17
2	12	3	0.9	0.9	4230.03	-	-	-	-	4230.15	242.58	4230.66	181.07	4230.15	120.41
2	12	3	0.9	0.95	1217.55	-	-	-	-	1217.56	310.13	1217.98	181.42	1217.56	124.83
2	12	3	0.9	0.99	130.47	-	-	-	-	130.89	316.61	130.5	183.25	130.47	178.81
2	12	3	0.95	0.9	4480.39	-	-	-	-	4480.42	244.04	4481.0	301.0	4480.42	126.95
2	12	3	0.95	0.95	1310.51	-	-	-	-	1310.52	247.56	1310.55	241.38	1310.52	156.15
2	12	3	0.95	0.99	143.91	-	-	-	-	143.92	368.77	144.05	185.76	143.92	130.12
2	12	3	0.99	0.9	4685.30	-	-	-	-	4685.36	424.33	4691.39	183.22	4685.36	111.23
2	12	3	0.99	0.95	1387.24	-	-	-	-	1387.25	278.83	1391.57	180.45	1387.25	160.28
2	12	3	0.99	0.99	155.14	-	-	-	-	155.66	246.97	155.15	361.8	155.15	91.12
3	12	3	0.9	0.9	5230.43	-	-	-	-	5230.45	302.76	5230.53	241.22	5230.45	239.77
3	12	3	0.9	0.95	1642.97	-	-	-	-	1643.0	304.36	1644.96	184.52	1642.98	160.51
3	12	3	0.9	0.99	200.96	-	-	-	-	200.98	192.31	200.98	244.82	200.96	126.36
3	12	3	0.95	0.9	5579.32	-	-	-	-	5579.34	304.08	5579.42	247.32	5579.34	201.8
3	12	3	0.95	0.95	1779.55	-	-	-	-	1779.57	264.68	1779.57	188.66	1779.57	175.47
3	12	3	0.95	0.99	222.22	-	-	-	-	222.23	306.62	222.23	122.07	222.23	150.99
3	12	3	0.99	0.9	5866.10	-	-	-	-	5866.22	252.78	5870.5	180.8	5866.14	188.85
3	12	3	0.99	0.95	1892.68	-	-	-	-	1892.72	259.89	1892.69	200.18	1892.69	182.42
3	12	3	0.99	0.99	240.00	-	-	-	-	240.02	181.18	240.65	180.38	240.0	174.95
4	12	3	0.9	0.9	4728.73	-	-	-	-	4728.76	302.68	4728.76	241.24	4728.76	165.12
4	12	3	0.9	0.95	1449.55	-	-	-	-	1449.56	271.7	1449.56	395.03	1449.56	160.39
4	12	3	0.9	0.99	173.31	-	-	-	-	173.52	190.92	173.43	270.97	173.31	181.7
4	12	3	0.95	0.9	5032.47	-	-	-	-	5032.49	383.92	5032.49	337.91	5032.49	183.46
4	12	3	0.95	0.95	1567.82	-	-	-	-	1568.58	247.24	1567.83	247.67	1567.83	163.46
4	12	3	0.95	0.99	191.59	-	-	-	-	191.59	186.65	191.59	310.45	191.59	173.2
4	12	3	0.99	0.9	5282.04	-	-	-	-	5282.07	367.56	5282.07	180.53	5282.07	162.02
4	12	3	0.99	0.95	1665.72	-	-	-	-	1665.74	193.35	1665.74	300.94	1665.74	144.24
4	12	3	0.99	0.99	206.87	-	-	-	-	206.87	241.47	206.87	181.04	206.87	93.29
5	12	3	0.9	0.9	7075.55	-	-	-	-	7076.69	242.11	7076.83	362.29	7076.83	178.76
5	12	3	0.9	0.95	2502.40	-	-	-	-	2502.42	270.91	2502.93	311.71	2502.93	158.63
5	12	3	0.9	0.99	359.59	-	-	-	-	359.66	182.56	359.78	186.92	359.66	157.25
5	12	3	0.95	0.9	7623.08	-	-	-	-	7624.6	211.74	7624.14	248.45	7624.06	172.66
5	12	3	0.95	0.95	2732.77	-	-	-	-	2733.38	211.72	2733.34	251.77	2733.34	186.34
5	12	3	0.95	0.99	398.76	-	-	-	-	398.8	182.74	398.84	321.9	398.83	152.64
5	12	3	0.99	0.9	8074.71	-	-	-	-	8077.22	257.21	8076.41	310.01	8076.41	183.21
5	12	3	0.99	0.95	2924.34	-	-	-	-	2926.92	208.86	2924.96	328.58	2924.96	180.41
5	12	3	0.99	0.99	431.54	-	-	-	-	431.55	240.77	431.62	300.46	431.62	129.98

Table 4.18: Comparison of heuristics for N = 12, L = 4

Instance						GRADIENT		SPIRAL		LEAST		HIGHEST		BOTH	
ID	N	L	Se	Sp	Best Known	Obj	Time (s)	Obj	Time (s)	Obj	Time (s)	Obj	Time (s)	Obj	Time (s)
1	12	4	0.9	0.9	10805.62	-	-	-	-	10814.3	88.0	10814.3	86.16	10814.3	17.89
1	12	4	0.9	0.95	4205.68	-	-	-	-	4210.03	63.99	4210.1	53.9	4210.1	71.31
1	12	4	0.9	0.99	669.72	-	-	-	-	670.55	69.52	670.58	39.97	670.58	50.93
1	12	4	0.95	0.9	11744.13	-	-	-	-	11753.8	81.45	11753.8	60.01	11753.8	48.83
1	12	4	0.95	0.95	4620.08	-	-	-	-	4624.91	60.94	4624.98	53.41	4624.98	9.14
1	12	4	0.95	0.99	743.82	-	-	-	-	744.74	85.92	744.78	58.39	744.78	33.7
1	12	4	0.99	0.9	12522.92	-	-	-	-	12533.5	81.09	12533.5	72.95	12533.5	22.62
1	12	4	0.99	0.95	4965.58	-	-	-	-	4970.82	60.17	4970.91	26.67	4970.91	34.28
1	12	4	0.99	0.99	805.89	-	-	-	-	806.9	76.94	806.94	44.63	806.94	27.06
2	12	4	0.9	0.9	6341.72	-	-	-	-	6344.27	80.1	6341.76	69.38	6344.27	37.84
2	12	4	0.9	0.95	2110.26	-	-	-	-	2112.12	67.13	2110.28	70.09	2112.12	22.3
2	12	4	0.9	0.99	279.06	-	-	-	-	279.53	48.24	279.06	71.81	279.53	16.38
2	12	4	0.95	0.9	6797.69	-	-	-	-	6800.69	61.09	6797.73	52.62	6800.69	17.12
2	12	4	0.95	0.95	2294.78	-	-	-	-	2296.88	56.6	2294.79	64.36	2296.88	40.0
2	12	4	0.95	0.99	309.01	-	-	-	-	309.53	64.23	309.01	66.42	309.53	32.01
2	12	4	0.99	0.9	7173.44	-	-	-	-	7176.8	42.21	7173.48	40.78	7176.8	20.12
2	12	4	0.99	0.95	2447.87	-	-	-	-	2450.19	48.0	2447.9	49.23	2450.19	12.14
2	12	4	0.99	0.99	334.06	-	-	-	-	334.64	32.77	334.07	23.28	334.64	12.3
3	12	4	0.9	0.9	8080.07	-	-	-	-	8080.1	49.81	8080.1	42.09	8080.1	42.99
3	12	4	0.9	0.95	2900.24	-	-	-	-	2900.26	71.66	2900.26	53.93	2900.26	34.15
3	12	4	0.9	0.99	421.27	-	-	-	-	421.27	42.12	421.27	51.56	421.27	55.51
3	12	4	0.95	0.9	8718.26	-	-	-	-	8718.28	69.7	8718.28	47.93	8718.28	24.05
3	12	4	0.95	0.95	3169.66	-	-	-	-	3169.68	60.68	3169.68	58.91	3169.68	33.2
3	12	4	0.95	0.99	467.21	-	-	-	-	467.21	48.57	467.21	62.15	467.21	21.34
3	12	4	0.99	0.9	9245.89	-	-	-	-	9245.93	56.27	9245.93	37.1	9245.93	31.73
3	12	4	0.99	0.95	3393.75	-	-	-	-	3393.77	57.11	3393.77	39.68	3393.77	18.13
3	12	4	0.99	0.99	505.67	-	-	-	-	505.67	51.47	505.67	49.0	505.67	32.87
4	12	4	0.9	0.9	7189.52	-	-	-	-	7189.55	88.77	7200.88	53.42	7200.88	24.03
4	12	4	0.9	0.95	2516.16	-	-	-	-	2516.17	84.61	2522.73	61.64	2522.73	31.52
4	12	4	0.9	0.99	356.35	-	-	-	-	356.35	72.76	357.81	62.92	357.81	51.99
4	12	4	0.95	0.9	7738.81	-	-	-	-	7738.85	84.64	7751.68	54.7	7751.68	25.18
4	12	4	0.95	0.95	2745.74	-	-	-	-	2745.77	68.9	2753.13	51.6	2753.13	27.74
4	12	4	0.95	0.99	395.06	-	-	-	-	395.06	78.48	396.69	63.5	396.69	53.74
4	12	4	0.99	0.9	8192.62	-	-	-	-	8192.66	95.75	8206.75	42.86	8206.75	22.17
4	12	4	0.99	0.95	2936.61	-	-	-	-	2936.63	53.18	2944.67	20.66	2944.67	14.57
4	12	4	0.99	0.99	427.46	-	-	-	-	427.47	26.66	429.24	17.11	429.24	5.25
5	12	4	0.9	0.9	11231.48	-	-	-	-	11233.1	67.75	11247.1	45.27	11247.1	28.74
5	12	4	0.9	0.95	4419.90	-	-	-	-	4420.69	73.08	4427.86	72.54	4427.86	45.87
5	12	4	0.9	0.99	712.48	-	-	-	-	712.63	75.51	714.09	96.91	714.09	38.17
5	12	4	0.95	0.9	12219.11	-	-	-	-	12220.9	64.63	12236.5	55.36	12236.5	55.38
5	12	4	0.95	0.95	4858.77	-	-	-	-	4859.64	60.67	4867.64	61.27	4867.64	37.64
5	12	4	0.95	0.99	791.46	-	-	-	-	791.63	60.85	793.26	92.88	793.26	42.06
5	12	4	0.99	0.9	13039.13	-	-	-	-	13041.1	97.05	13058.1	69.51	13058.1	53.3
5	12	4	0.99	0.95	5224.81	-	-	-	-	5225.75	63.68	5234.45	68.61	5234.45	49.05
5	12	4	0.99	0.99	857.63	-	-	-	-	857.81	15.32	859.58	12.04	859.58	3.62

Table 4.19: All possible groups of size $L = 3$ for $N = 6$ and their C_k, D_{kl} values, with $Se = Sp = 0.95$ and $\mathbf{p} = (0.01, 0.02, 0.03, 0.04, 0.05, 0.06)$.

Group	**Composition**	$\mathbf{C_k}$	$\mathbf{D_{kl}}$
G_1	$\{1,2,3\}$	-5992.98	$D_{1,8} = 3989.59$, $D_{1,9} = 3985.58$, $D_{1,10} = 3981.58$, $D_{1,14} = 3989.59$, $D_{1,15} = 3985.58$, $D_{1,16} = 3981.58$, $D_{1,17} = 3989.59$, $D_{1,18} = 3985.58$, $D_{1,19} = 3981.58$
G_2	$\{1,2,4\}$	-5982.45	$D_{2,6} = 3989.59$, $D_{2,7} = 3985.58$, $D_{2,10} = 3977.59$, $D_{2,12} = 3989.59$, $D_{2,13} = 3985.58$, $D_{2,16} = 3977.59$, $D_{2,17} = 3989.59$, $D_{2,18} = 3985.58$, $D_{2,20} = 3977.59$
G_3	$\{1,2,5\}$	-5971.92	$D_{3,5} = 3989.59$, $D_{3,7} = 3981.58$, $D_{3,9} = 3977.59$, $D_{3,11} = 3989.59$, $D_{3,13} = 3981.58$, $D_{3,15} = 3977.59$, $D_{3,17} = 3989.59$, $D_{3,19} = 3981.58$, $D_{3,20} = 3977.59$
G_4	$\{1,2,6\}$	-5961.39	$D_{4,5} = 3985.58$, $D_{4,6} = 3981.58$, $D_{4,8} = 3977.59$, $D_{4,11} = 3985.58$, $D_{4,12} = 3981.58$, $D_{4,14} = 3977.59$, $D_{4,18} = 3985.58$, $D_{4,19} = 3981.58$, $D_{4,20} = 3977.59$
G_5	$\{1,3,4\}$	-5971.94	$D_{5,10} = 3973.60$, $D_{5,12} = 3989.59$, $D_{5,13} = 3985.58$, $D_{5,14} = 3989.59$, $D_{5,15} = 3985.58$, $D_{5,19} = 3973.60$, $D_{5,20} = 3973.60$
G_6	$\{1,3,5\}$	-5961.43	$D_{6,9} = 3973.60$, $D_{6,11} = 3989.59$, $D_{6,13} = 3981.58$, $D_{6,14} = 3989.59$, $D_{6,16} = 3981.58$, $D_{6,18} = 3973.60$, $D_{6,20} = 3973.60$
G_7	$\{1,3,6\}$	-5950.91	$D_{7,8} = 3973.60$, $D_{7,11} = 3985.58$, $D_{7,12} = 3981.58$, $D_{7,15} = 3985.58$, $D_{7,16} = 3981.58$, $D_{7,17} = 3973.60$, $D_{7,20} = 3973.60$
G_8	$\{1,4,5\}$	-5950.93	$D_{8,11} = 3989.59$, $D_{8,12} = 3989.59$, $D_{8,15} = 3977.59$, $D_{8,16} = 3977.59$, $D_{8,18} = 3973.60$, $D_{8,19} = 3973.60$
G_9	$\{1,4,6\}$	-5940.43	$D_{9,11} = 3985.58$, $D_{9,13} = 3985.58$, $D_{9,14} = 3977.59$, $D_{9,16} = 3977.59$, $D_{9,17} = 3973.60$, $D_{9,19} = 3973.60$
G_{10}	$\{1,5,6\}$	-5929.95	$D_{10,12} = 3981.58$, $D_{10,13} = 3981.58$, $D_{10,14} = 3977.59$, $D_{10,15} = 3977.59$, $D_{10,17} = 3973.60$, $D_{10,18} = 3973.60$
G_{11}	$\{2,3,4\}$	-5961.46	$D_{11,16} = 3969.63$, $D_{11,19} = 3969.63$, $D_{11,20} = 3969.63$
G_{12}	$\{2,3,5\}$	-5950.96	$D_{12,15} = 3969.63$, $D_{12,18} = 3969.63$, $D_{12,20} = 3969.63$
G_{13}	$\{2,3,6\}$	-5940.45	$D_{13,14} = 3969.63$, $D_{13,17} = 3969.63$, $D_{13,20} = 3969.63$
G_{14}	$\{2,4,5\}$	-5940.48	$D_{14,18} = 3969.63$, $D_{14,19} = 3969.63$
G_{15}	$\{2,4,6\}$	-5929.99	$D_{15,17} = 3969.63$, $D_{15,19} = 3969.63$
G_{16}	$\{2,5,6\}$	-5919.52	$D_{16,17} = 3969.63$, $D_{16,18} = 3969.63$
G_{17}	$\{3,4,5\}$	-5930.03	
G_{18}	$\{3,4,6\}$	-5919.55	
G_{19}	$\{3,5,6\}$	-5909.09	
G_{20}	$\{4,5,6\}$	-5898.67	

Table 4.20: Comparison of Branching Rules for N=6, Instance ID = 1

L	Se	Sp	Configuration	LB	UB	Δ UB (%)	$\#y$	$\#x$	# nodes	Time$_r$ (s)	Total Time (s)	Gap$_r$ (%)	Gap (%)
3	0.9	0.9	BP-HFX	3893.84	3893.84	0.0001	18	73	1	0.02	0.02	0.00	0.00
3	0.9	0.9	BP-HFY	3893.84	3893.84	0.0001	18	73	1	0.02	0.02	0.00	0.00
3	0.9	0.9	BP-RF	3893.84	3893.84	0.0001	18	73	1	0.02	0.02	0.00	0.00
3	0.9	0.95	BP-HFX	1415.34	1415.34	0.0	20	90	1	0.02	0.03	0.00	0.00
3	0.9	0.95	BP-HFY	1415.34	1415.34	0.0	20	90	1	0.02	0.02	0.00	0.00
3	0.9	0.95	BP-RF	1415.34	1415.34	0.0	20	90	1	0.02	0.03	0.00	0.00
3	0.9	0.99	BP-HFX	209.73	209.73	0.0001	19	81	1	0.02	0.02	0.00	0.00
3	0.9	0.99	BP-HFY	209.73	209.73	0.0001	19	81	1	0.02	0.02	0.00	0.00
3	0.9	0.99	BP-RF	209.73	209.73	0.0001	19	81	1	0.02	0.02	0.00	0.00
3	0.95	0.9	BP-HFX	4205.28	4205.28	0.0	20	90	1	0.02	0.02	0.00	0.00
3	0.95	0.9	BP-HFY	4205.28	4205.28	0.0	20	90	1	0.02	0.03	0.00	0.00
3	0.95	0.9	BP-RF	4205.28	4205.28	0.0	20	90	1	0.01	0.02	0.00	0.00
3	0.95	0.95	BP-HFX	1548.31	1548.31	0.0	18	73	1	0.02	0.02	0.00	0.00
3	0.95	0.95	BP-HFY	1548.31	1548.31	0.0	18	73	1	0.02	0.02	0.00	0.00
3	0.95	0.95	BP-RF	1548.31	1548.31	0.0	18	73	1	0.02	0.02	0.00	0.00
3	0.95	0.99	BP-HFX	232.68	232.68	0.0	19	81	1	0.02	0.02	0.00	0.00
3	0.95	0.99	BP-HFY	232.68	232.68	0.0	19	81	1	0.02	0.02	0.00	0.00
3	0.95	0.99	BP-RF	232.68	232.68	0.0	19	81	1	0.02	0.02	0.00	0.00
3	0.99	0.9	BP-HFX	4463.01	4463.01	0.0	20	90	1	0.02	0.02	0.00	0.00
3	0.99	0.9	BP-HFY	4463.01	4463.01	0.0	20	90	1	0.01	0.02	0.00	0.00
3	0.99	0.9	BP-RF	4463.01	4463.01	0.0	20	90	1	0.02	0.02	0.00	0.00
3	0.99	0.95	BP-HFX	1658.97	1658.97	0.0	18	73	1	0.01	0.01	0.00	0.00
3	0.99	0.95	BP-HFY	1658.97	1658.97	0.0	18	73	1	0.01	0.01	0.00	0.00
3	0.99	0.95	BP-RF	1658.97	1658.97	0.0	18	73	1	0.01	0.01	0.00	0.00
3	0.99	0.99	BP-HFX	251.90	251.90	0.0	20	90	1	0.02	0.02	0.00	0.00
3	0.99	0.99	BP-HFY	251.90	251.90	0.0	20	90	1	0.01	0.02	0.00	0.00
3	0.99	0.99	BP-RF	251.90	251.90	0.0	20	90	1	0.02	0.02	0.00	0.00

Table 4.21: Comparison of Branching Rules for N=6, Instance ID = 2

L	Se	Sp	Configuration	LB	UB	Δ UB (%)	$\#y$	$\#x$	# nodes	Time$_r$ (s)	Total Time (s)	Gap$_r$ (%)	Gap (%)
3	0.9	0.9	BP-HFX	3433.36	3433.36	0.0	20	90	1	0.02	0.02	0.00	0.00
3	0.9	0.9	BP-HFY	3433.36	3433.36	0.0	20	90	1	0.02	0.03	0.00	0.00
3	0.9	0.9	BP-RF	3433.36	3433.36	0.0	20	90	1	0.02	0.03	0.00	0.00
3	0.9	0.95	BP-HFX	1197.61	1197.61	0.0002	19	81	1	0.02	0.02	0.00	0.00
3	0.9	0.95	BP-HFY	1197.61	1197.61	0.0002	19	81	1	0.02	0.03	0.00	0.00
3	0.9	0.95	BP-RF	1197.61	1197.61	0.0002	19	81	1	0.02	0.02	0.00	0.00
3	0.9	0.99	BP-HFX	168.93	168.93	0.0003	19	81	1	0.02	0.02	0.00	0.00
3	0.9	0.99	BP-HFY	168.93	168.93	0.0003	19	81	1	0.02	0.02	0.00	0.00
3	0.9	0.99	BP-RF	168.93	168.93	0.0003	19	81	1	0.02	0.03	0.00	0.00
3	0.95	0.9	BP-HFX	3694.60	3694.60	0.0	19	81	1	0.02	0.02	0.00	0.00
3	0.95	0.9	BP-HFY	3694.60	3694.60	0.0	19	81	1	0.02	0.02	0.00	0.00
3	0.95	0.9	BP-RF	3694.60	3694.60	0.0	19	81	1	0.01	0.01	0.00	0.00
3	0.95	0.95	BP-HFX	1306.60	1306.60	0.0	20	90	1	0.02	0.02	0.00	0.00
3	0.95	0.95	BP-HFY	1306.60	1306.60	0.0	20	90	1	0.02	0.03	0.00	0.00
3	0.95	0.95	BP-RF	1306.60	1306.60	0.0	20	90	1	0.02	0.03	0.00	0.00
3	0.95	0.99	BP-HFX	187.27	187.27	0.0001	19	81	1	0.01	0.02	0.00	0.00
3	0.95	0.99	BP-HFY	187.27	187.27	0.0001	19	81	1	0.02	0.02	0.00	0.00
3	0.95	0.99	BP-RF	187.27	187.27	0.0001	19	81	1	0.01	0.01	0.00	0.00
3	0.99	0.9	BP-HFX	3910.40	3910.40	0.0001	19	81	1	0.02	0.03	0.00	0.00
3	0.99	0.9	BP-HFY	3910.40	3910.40	0.0001	19	81	1	0.02	0.02	0.00	0.00
3	0.99	0.9	BP-RF	3910.40	3910.40	0.0001	19	81	1	0.02	0.02	0.00	0.00
3	0.99	0.95	BP-HFX	1397.20	1397.20	0.0	20	90	1	0.01	0.01	0.00	0.00
3	0.99	0.95	BP-HFY	1397.20	1397.20	0.0	20	90	1	0.02	0.03	0.00	0.00
3	0.99	0.95	BP-RF	1397.20	1397.20	0.0	20	90	1	0.02	0.03	0.00	0.00
3	0.99	0.99	BP-HFX	202.62	202.62	0.0	18	73	1	0.01	0.02	0.00	0.00
3	0.99	0.99	BP-HFY	202.62	202.62	0.0	18	73	1	0.01	0.01	0.00	0.00
3	0.99	0.99	BP-RF	202.62	202.62	0.0	18	73	1	0.01	0.01	0.00	0.00

Table 4.22: Comparison of Branching Rules for N=6, Instance ID = 3

L	Se	Sp	Configuration	LB	UB	Δ UB (%)	$\#y$	$\#x$	# nodes	Time$_r$ (s)	Total Time (s)	Gap$_r$ (%)	Gap (%)
3	0.9	0.9	BP-HFX	2788.27	2788.27	0.0	18	73	1	0.02	0.02	0.00	0.00
3	0.9	0.9	BP-HFY	2788.27	2788.27	0.0	18	73	1	0.01	0.02	0.00	0.00
3	0.9	0.9	BP-RF	2788.27	2788.27	0.0	18	73	1	0.02	0.02	0.00	0.00
3	0.9	0.95	BP-HFX	911.43	911.43	0.0	19	81	1	0.01	0.02	0.00	0.00
3	0.9	0.95	BP-HFY	911.43	911.43	0.0	19	81	1	0.02	0.02	0.00	0.00
3	0.9	0.95	BP-RF	911.43	911.43	0.0	19	81	1	0.02	0.02	0.00	0.00
3	0.9	0.99	BP-HFX	118.98	118.98	0.0001	20	90	1	0.02	0.02	0.00	0.00
3	0.9	0.99	BP-HFY	118.98	118.98	0.0001	20	90	1	0.01	0.02	0.00	0.00
3	0.9	0.99	BP-RF	118.98	118.98	0.0001	20	90	1	0.02	0.02	0.00	0.00
3	0.95	0.9	BP-HFX	2983.31	2983.31	0.0001	19	81	1	0.02	0.02	0.00	0.00
3	0.95	0.9	BP-HFY	2983.31	2983.31	0.0001	19	81	1	0.02	0.02	0.00	0.00
3	0.95	0.9	BP-RF	2983.31	2983.31	0.0001	19	81	1	0.01	0.02	0.00	0.00
3	0.95	0.95	BP-HFX	990.19	990.19	0.0	20	90	1	0.02	0.02	0.00	0.00
3	0.95	0.95	BP-HFY	990.19	990.19	0.0	20	90	1	0.02	0.02	0.00	0.00
3	0.95	0.95	BP-RF	990.19	990.19	0.0	20	90	1	0.02	0.02	0.00	0.00
3	0.95	0.99	BP-HFX	131.73	131.73	0.0001	17	65	1	0.01	0.01	0.00	0.00
3	0.95	0.99	BP-HFY	131.73	131.73	0.0001	17	65	1	0.00	0.01	0.00	0.00
3	0.95	0.99	BP-RF	131.73	131.73	0.0001	17	65	1	0.01	0.02	0.00	0.00
3	0.99	0.9	BP-HFX	3144.01	3144.01	0.0001	19	81	1	0.01	0.01	0.00	0.00
3	0.99	0.9	BP-HFY	3144.01	3144.01	0.0001	19	81	1	0.01	0.01	0.00	0.00
3	0.99	0.9	BP-RF	3144.01	3144.01	0.0001	19	81	1	0.01	0.01	0.00	0.00
3	0.99	0.95	BP-HFX	1055.53	1055.53	0.0	18	73	1	0.00	0.01	0.00	0.00
3	0.99	0.95	BP-HFY	1055.53	1055.53	0.0	18	73	1	0.01	0.01	0.00	0.00
3	0.99	0.95	BP-RF	1055.53	1055.53	0.0	18	73	1	0.01	0.01	0.00	0.00
3	0.99	0.99	BP-HFX	142.40	142.40	0.0003	18	73	1	0.01	0.01	0.00	0.00
3	0.99	0.99	BP-HFY	142.40	142.40	0.0003	18	73	1	0.01	0.01	0.00	0.00
3	0.99	0.99	BP-RF	142.40	142.40	0.0003	18	73	1	0.01	0.01	0.00	0.00

Table 4.23: Comparison of Branching Rules for N=6, Instance ID = 4

L	Se	Sp	Configuration	LB	UB	Δ UB (%)	$\#y$	$\#x$	# nodes	Time$_r$ (s)	Total Time (s)	Gap$_r$ (%)	Gap (%)
3	0.9	0.9	BP-HFX	4252.20	4252.20	0.0001	19	81	1	0.01	0.01	0.00	0.00
3	0.9	0.9	BP-HFY	4252.20	4252.20	0.0001	19	81	1	0.01	0.01	0.00	0.00
3	0.9	0.9	BP-RF	4252.20	4252.20	0.0001	19	81	1	0.01	0.01	0.00	0.00
3	0.9	0.95	BP-HFX	1574.78	1574.78	0.0003	20	90	1	0.01	0.01	0.00	0.00
3	0.9	0.95	BP-HFY	1574.78	1574.78	0.0003	20	90	1	0.01	0.01	0.00	0.00
3	0.9	0.95	BP-RF	1574.78	1574.78	0.0003	20	90	1	0.01	0.01	0.00	0.00
3	0.9	0.99	BP-HFX	237.62	237.62	0.0001	20	90	1	0.00	0.01	0.00	0.00
3	0.9	0.99	BP-HFY	237.62	237.62	0.0001	20	90	1	0.01	0.01	0.00	0.00
3	0.9	0.99	BP-RF	237.62	237.62	0.0001	20	90	1	0.01	0.01	0.00	0.00
3	0.95	0.9	BP-HFX	4600.54	4600.54	0.0001	17	64	1	0.00	0.01	0.00	0.00
3	0.95	0.9	BP-HFY	4600.54	4600.54	0.0001	17	64	1	0.00	0.01	0.00	0.00
3	0.95	0.9	BP-RF	4600.54	4600.54	0.0001	17	64	1	0.01	0.01	0.00	0.00
3	0.95	0.95	BP-HFX	1724.61	1724.61	0.0	20	90	1	0.01	0.01	0.00	0.00
3	0.95	0.95	BP-HFY	1724.61	1724.61	0.0	20	90	1	0.01	0.01	0.00	0.00
3	0.95	0.95	BP-RF	1724.61	1724.61	0.0	20	90	1	0.01	0.01	0.00	0.00
3	0.95	0.99	BP-HFX	263.70	263.70	0.0001	20	90	1	0.01	0.01	0.00	0.00
3	0.95	0.99	BP-HFY	263.70	263.70	0.0001	20	90	1	0.01	0.01	0.00	0.00
3	0.95	0.99	BP-RF	263.70	263.70	0.0001	20	90	1	0.01	0.01	0.00	0.00
3	0.99	0.9	BP-HFX	4888.98	4888.98	0.0001	20	90	1	0.01	0.01	0.00	0.00
3	0.99	0.9	BP-HFY	4888.98	4888.98	0.0001	20	90	1	0.01	0.01	0.00	0.00
3	0.99	0.9	BP-RF	4888.98	4888.98	0.0001	20	90	1	0.01	0.01	0.00	0.00
3	0.99	0.95	BP-HFX	1849.37	1849.37	0.0002	19	81	1	0.01	0.01	0.00	0.00
3	0.99	0.95	BP-HFY	1849.37	1849.37	0.0002	19	81	1	0.01	0.01	0.00	0.00
3	0.99	0.95	BP-RF	1849.37	1849.37	0.0002	19	81	1	0.01	0.01	0.00	0.00
3	0.99	0.99	BP-HFX	285.53	285.53	0.0001	20	90	1	0.01	0.01	0.00	0.00
3	0.99	0.99	BP-HFY	285.53	285.53	0.0001	20	90	1	0.01	0.01	0.00	0.00
3	0.99	0.99	BP-RF	285.53	285.53	0.0001	20	90	1	0.02	0.02	0.00	0.00

Table 4.24: Comparison of Branching Rules for N=6, Instance ID = 5

L	Se	Sp	Configuration	LB	UB	Δ UB (%)	$\#y$	$\#x$	# nodes	Time$_r$ (s)	Total Time (s)	Gap$_r$ (%)	Gap (%)
3	0.9	0.9	BP-HFX	3501.57	3501.57	0.0	18	73	1	0.01	0.01	0.00	0.00
3	0.9	0.9	BP-HFY	3501.57	3501.57	0.0	18	73	1	0.01	0.01	0.00	0.00
3	0.9	0.9	BP-RF	3501.57	3501.57	0.0	18	73	1	0.01	0.01	0.00	0.00
3	0.9	0.95	BP-HFX	1219.68	1219.68	0.0001	19	81	1	0.01	0.01	0.00	0.00
3	0.9	0.95	BP-HFY	1219.68	1219.68	0.0001	19	81	1	0.01	0.01	0.00	0.00
3	0.9	0.95	BP-RF	1219.68	1219.68	0.0001	19	81	1	0.01	0.01	0.00	0.00
3	0.9	0.99	BP-HFX	171.08	171.08	0.0002	17	66	1	0.01	0.01	0.00	0.00
3	0.9	0.99	BP-HFY	171.08	171.08	0.0002	17	66	1	0.01	0.01	0.00	0.00
3	0.9	0.99	BP-RF	171.08	171.08	0.0002	17	66	1	0.01	0.01	0.00	0.00
3	0.95	0.9	BP-HFX	3768.03	3768.03	0.0001	19	81	1	0.01	0.01	0.00	0.00
3	0.95	0.9	BP-HFY	3768.03	3768.03	0.0001	19	81	1	0.02	0.02	0.00	0.00
3	0.95	0.9	BP-RF	3768.03	3768.03	0.0001	19	81	1	0.01	0.01	0.00	0.00
3	0.95	0.95	BP-HFX	1330.42	1330.42	0.0003	19	81	1	0.01	0.01	0.00	0.00
3	0.95	0.95	BP-HFY	1330.42	1330.42	0.0003	19	81	1	0.01	0.01	0.00	0.00
3	0.95	0.95	BP-RF	1330.42	1330.42	0.0003	19	81	1	0.01	0.01	0.00	0.00
3	0.95	0.99	BP-HFX	189.63	189.63	0.0	18	73	1	0.01	0.01	0.00	0.00
3	0.95	0.99	BP-HFY	189.63	189.63	0.0	18	73	1	0.01	0.01	0.00	0.00
3	0.95	0.99	BP-RF	189.63	189.63	0.0	18	73	1	0.00	0.01	0.00	0.00
3	0.99	0.9	BP-HFX	3988.06	3988.06	0.0	19	81	1	0.01	0.01	0.00	0.00
3	0.99	0.9	BP-HFY	3988.06	3988.06	0.0	19	81	1	0.01	0.01	0.00	0.00
3	0.99	0.9	BP-RF	3988.06	3988.06	0.0	19	81	1	0.01	0.01	0.00	0.00
3	0.99	0.95	BP-HFX	1422.44	1422.44	0.0	19	81	1	0.01	0.01	0.00	0.00
3	0.99	0.95	BP-HFY	1422.44	1422.44	0.0	19	81	1	0.01	0.01	0.00	0.00
3	0.99	0.95	BP-RF	1422.44	1422.44	0.0	19	81	1	0.01	0.02	0.00	0.00
3	0.99	0.99	BP-HFX	205.15	205.15	0.0	20	90	1	0.01	0.01	0.00	0.00
3	0.99	0.99	BP-HFY	205.15	205.15	0.0	20	90	1	0.01	0.02	0.00	0.00
3	0.99	0.99	BP-RF	205.15	205.15	0.0	20	90	1	0.01	0.01	0.00	0.00

Table 4.25: Comparison of Branching Rules for N=9, Instance ID = 1

L	Se	Sp	Configuration	LB	UB	Δ UB (%)	$\#y$	$\#x$	# nodes	Time$_r$ (s)	Total Time (s)	Gap$_r$ (%)	Gap (%)
3	0.9	0.9	BP-HFX	7179.76	7179.76	0.0	56	827	1	0.04	0.06	0.00	0.00
3	0.9	0.9	BP-HFY	7179.76	7179.76	0.0	56	827	1	0.04	0.06	0.00	0.00
3	0.9	0.9	BP-RF	7179.76	7179.76	0.0	58	892	1	0.03	0.04	0.00	0.00
3	0.9	0.95	BP-HFX	2747.82	2747.82	0.0001	56	813	1	0.03	0.05	0.00	0.00
3	0.9	0.95	BP-HFY	2747.82	2747.82	0.0001	56	813	1	0.03	0.05	0.00	0.00
3	0.9	0.95	BP-RF	2747.82	2747.82	0.0001	56	813	1	0.03	0.05	0.00	0.00
3	0.9	0.99	BP-HFX	429.89	429.89	0.0001	38	374	1	0.02	0.03	0.00	0.00
3	0.9	0.99	BP-HFY	429.89	429.89	0.0001	38	374	1	0.02	0.03	0.00	0.00
3	0.9	0.99	BP-RF	429.89	429.89	0.0001	38	374	1	0.02	0.03	0.00	0.00
3	0.95	0.9	BP-HFX	7791.18	7791.18	0.0	56	831	1	0.03	0.05	0.00	0.00
3	0.95	0.9	BP-HFY	7791.18	7791.18	0.0	56	831	1	0.04	0.05	0.00	0.00
3	0.95	0.9	BP-RF	7791.18	7791.18	0.0	56	831	1	0.03	0.05	0.00	0.00
3	0.95	0.95	BP-HFX	3015.46	3015.46	0.0001	60	954	1	0.04	0.07	0.00	0.00
3	0.95	0.95	BP-HFY	3015.46	3015.46	0.0001	60	954	1	0.06	0.08	0.00	0.00
3	0.95	0.95	BP-RF	3015.46	3015.46	0.0001	60	954	1	0.04	0.07	0.00	0.00
3	0.95	0.99	BP-HFX	477.33	477.33	0.0	39	398	1	0.02	0.03	0.00	0.00
3	0.95	0.99	BP-HFY	477.33	477.33	0.0	39	398	1	0.02	0.02	0.00	0.00
3	0.95	0.99	BP-RF	477.33	477.33	0.0	39	398	1	0.02	0.02	0.00	0.00
3	0.99	0.9	BP-HFX	8298.18	8298.18	0.0	61	997	1	0.06	0.09	0.00	0.00
3	0.99	0.9	BP-HFY	8298.18	8298.18	0.0	61	997	1	0.06	0.09	0.00	0.00
3	0.99	0.9	BP-RF	8298.18	8298.18	0.0	61	997	1	0.05	0.09	0.00	0.00
3	0.99	0.95	BP-HFX	3238.51	3238.51	0.0001	56	833	1	0.04	0.05	0.00	0.00
3	0.99	0.95	BP-HFY	3238.51	3238.51	0.0001	56	833	1	0.03	0.05	0.00	0.00
3	0.99	0.95	BP-RF	3238.51	3238.51	0.0001	56	833	1	0.04	0.05	0.00	0.00
3	0.99	0.99	BP-HFX	517.07	517.07	0.0	45	531	1	0.02	0.03	0.00	0.00
3	0.99	0.99	BP-HFY	517.07	517.07	0.0	45	531	1	0.02	0.03	0.00	0.00
3	0.99	0.99	BP-RF	517.07	517.07	0.0	45	531	1	0.02	0.03	0.00	0.00

Table 4.26: Comparison of Branching Rules for N=9, Instance ID = 2

L	Se	Sp	Configuration	LB	UB	Δ UB (%)	$\#y$	$\#x$	# nodes	Time$_r$ (s)	Total Time (s)	Gap$_r$ (%)	Gap (%)
3	0.9	0.9	BP-HFX	4540.94	4540.94	0.0092	59	910	1	0.04	0.05	0.00	0.00
3	0.9	0.9	BP-HFY	4540.94	4540.94	0.0092	59	910	1	0.04	0.06	0.00	0.00
3	0.9	0.9	BP-RF	4540.94	4540.94	0.0092	59	910	1	0.04	0.05	0.00	0.00
3	0.9	0.95	BP-HFX	1519.02	1519.02	0.0141	56	823	1	0.04	0.05	0.00	0.00
3	0.9	0.95	BP-HFY	1519.02	1519.02	0.0141	56	823	1	0.04	0.05	0.00	0.00
3	0.9	0.95	BP-RF	1519.02	1519.02	0.0141	56	823	1	0.04	0.05	0.00	0.00
3	0.9	0.99	BP-HFX	203.49	203.49	0.0001	36	350	1	0.02	0.02	0.00	0.00
3	0.9	0.99	BP-HFY	203.49	203.49	0.0001	36	350	1	0.02	0.02	0.00	0.00
3	0.9	0.99	BP-RF	203.49	203.49	0.0001	36	350	1	0.02	0.02	0.00	0.00
3	0.95	0.9	BP-HFX	4868.76	4868.76	0.0095	57	863	1	0.04	0.07	0.00	0.00
3	0.95	0.9	BP-HFY	4868.76	4868.76	0.0095	57	863	1	0.05	0.08	0.00	0.00
3	0.95	0.9	BP-RF	4868.76	4868.76	0.0095	57	863	1	0.05	0.08	0.00	0.00
3	0.95	0.95	BP-HFX	1652.68	1652.68	0.0147	61	979	1	0.04	0.05	0.00	0.00
3	0.95	0.95	BP-HFY	1652.68	1652.68	0.0147	61	979	1	0.04	0.05	0.00	0.00
3	0.95	0.95	BP-RF	1652.68	1652.68	0.0147	61	979	1	0.04	0.05	0.00	0.00
3	0.95	0.99	BP-HFX	225.39	225.39	0.0001	36	345	1	0.02	0.03	0.00	0.00
3	0.95	0.99	BP-HFY	225.39	225.39	0.0001	36	345	1	0.02	0.02	0.00	0.00
3	0.95	0.99	BP-RF	225.39	225.39	0.0001	36	345	1	0.02	0.02	0.00	0.00
3	0.99	0.9	BP-HFX	5139.06	5139.06	0.0098	62	1009	1	0.06	0.08	0.00	0.00
3	0.99	0.9	BP-HFY	5139.06	5139.06	0.0098	62	1009	1	0.06	0.08	0.00	0.00
3	0.99	0.9	BP-RF	5139.06	5139.06	0.0098	62	1009	1	0.05	0.07	0.00	0.00
3	0.99	0.95	BP-HFX	1763.89	1763.89	0.0	55	808	1	0.04	0.06	0.00	0.00
3	0.99	0.95	BP-HFY	1763.89	1763.89	0.0	55	808	1	0.04	0.06	0.00	0.00
3	0.99	0.95	BP-RF	1763.89	1763.89	0.0	55	808	1	0.04	0.06	0.00	0.00
3	0.99	0.99	BP-HFX	243.71	243.71	0.0	30	236	1	0.01	0.01	0.00	0.00
3	0.99	0.99	BP-HFY	243.71	243.71	0.0	30	236	1	0.01	0.01	0.00	0.00
3	0.99	0.99	BP-RF	243.71	243.71	0.0	30	236	1	0.01	0.01	0.00	0.00

Table 4.27: Comparison of Branching Rules for N=9, Instance ID = 3

L	Se	Sp	Configuration	LB	UB	Δ UB (%)	$\#y$	$\#x$	# nodes	Time$_r$ (s)	Total Time (s)	Gap$_r$ (%)	Gap (%)
3	0.9	0.9	BP-HFX	4022.35	4022.35	0.0	68	1231	1	0.07	0.10	0.00	0.00
3	0.9	0.9	BP-HFY	4022.35	4022.35	0.0	68	1231	1	0.07	0.10	0.00	0.00
3	0.9	0.9	BP-RF	4022.35	4022.35	0.0	68	1231	1	0.07	0.11	0.00	0.00
3	0.9	0.95	BP-HFX	1269.76	1269.76	0.0	63	1056	1	0.06	0.08	0.00	0.00
3	0.9	0.95	BP-HFY	1269.76	1269.76	0.0	63	1056	1	0.06	0.08	0.00	0.00
3	0.9	0.95	BP-RF	1269.76	1269.76	0.0	63	1056	1	0.06	0.08	0.00	0.00
3	0.9	0.99	BP-HFX	155.89	155.89	0.0002	46	563	1	0.03	0.04	0.00	0.00
3	0.9	0.99	BP-HFY	155.89	155.89	0.0002	46	563	1	0.03	0.04	0.00	0.00
3	0.9	0.99	BP-RF	155.89	155.89	0.0002	46	563	1	0.03	0.04	0.00	0.00
3	0.95	0.9	BP-HFX	4292.79	4292.79	0.0	67	1190	1	0.04	0.06	0.00	0.00
3	0.95	0.9	BP-HFY	4292.79	4292.79	0.0	67	1190	1	0.05	0.06	0.00	0.00
3	0.95	0.9	BP-RF	4292.79	4292.79	0.0	67	1190	1	0.04	0.07	0.00	0.00
3	0.95	0.95	BP-HFX	1375.69	1375.69	0.0	65	1125	1	0.06	0.07	0.00	0.00
3	0.95	0.95	BP-HFY	1375.69	1375.69	0.0	65	1125	1	0.06	0.07	0.00	0.00
3	0.95	0.95	BP-RF	1375.69	1375.69	0.0	65	1125	1	0.06	0.08	0.00	0.00
3	0.95	0.99	BP-HFX	172.39	172.39	0.0002	45	545	1	0.03	0.04	0.00	0.00
3	0.95	0.99	BP-HFY	172.39	172.39	0.0002	45	545	1	0.03	0.04	0.00	0.00
3	0.95	0.99	BP-RF	172.39	172.39	0.0002	45	545	1	0.03	0.04	0.00	0.00
3	0.99	0.9	BP-HFX	4515.11	4515.11	0.0	68	1226	1	0.07	0.10	0.00	0.00
3	0.99	0.9	BP-HFY	4515.11	4515.11	0.0	68	1226	1	0.07	0.10	0.00	0.00
3	0.99	0.9	BP-RF	4515.11	4515.11	0.0	68	1226	1	0.07	0.11	0.00	0.00
3	0.99	0.95	BP-HFX	1463.42	1463.42	0.0	64	1089	1	0.05	0.06	0.00	0.00
3	0.99	0.95	BP-HFY	1463.42	1463.42	0.0	64	1089	1	0.05	0.06	0.00	0.00
3	0.99	0.95	BP-RF	1463.42	1463.42	0.0	64	1089	1	0.05	0.07	0.00	0.00
3	0.99	0.99	BP-HFX	186.19	186.19	0.0	49	632	1	0.03	0.04	0.00	0.00
3	0.99	0.99	BP-HFY	186.19	186.19	0.0	49	632	1	0.03	0.04	0.00	0.00
3	0.99	0.99	BP-RF	186.19	186.19	0.0	49	632	1	0.03	0.04	0.00	0.00

Table 4.28: Comparison of Branching Rules for N=9, Instance ID = 4

L	Se	Sp	Configuration	LB	UB	Δ UB (%)	$\#y$	$\#x$	# nodes	Time$_r$ (s)	Total Time (s)	Gap$_r$ (%)	Gap (%)
3	0.9	0.9	BP-HFX	4298.14	4298.14	0.0001	67	1193	3	0.06	0.12	0.01	0.00
3	0.9	0.9	BP-HFY	4298.14	4298.14	0.0001	67	1193	3	0.07	0.14	0.01	0.00
3	0.9	0.9	BP-RF	4298.14	4298.14	0.0001	72	1383	3	0.06	0.18	0.01	0.00
3	0.9	0.95	BP-HFX	1400.99	1400.99	0.0003	72	1378	13	0.05	0.32	0.03	0.00
3	0.9	0.95	BP-HFY	1400.99	1400.99	0.0003	70	1302	3	0.05	0.12	0.03	0.00
3	0.9	0.95	BP-RF	1400.99	1400.99	0.0003	77	1585	9	0.07	0.48	0.04	0.00
3	0.9	0.99	BP-HFX	180.67	180.67	0.0	53	725	9	0.03	0.16	0.02	0.00
3	0.9	0.99	BP-HFY	180.67	180.67	0.0	41	445	1	0.03	0.04	0.00	0.00
3	0.9	0.99	BP-RF	180.67	180.67	0.0	53	744	3	0.03	0.08	0.02	0.00
3	0.95	0.9	BP-HFX	4598.80	4598.80	0.0	61	984	3	0.04	0.09	0.00	0.00
3	0.95	0.9	BP-HFY	4598.80	4598.80	0.0	61	985	3	0.04	0.09	0.01	0.00
3	0.95	0.9	BP-RF	4598.80	4598.80	0.0	72	1379	7	0.03	0.31	0.00	0.00
3	0.95	0.95	BP-HFX	1521.43	1521.43	0.0001	67	1194	5	0.05	0.14	0.03	0.00
3	0.95	0.95	BP-HFY	1521.43	1521.43	0.0001	69	1268	3	0.05	0.11	0.04	0.00
3	0.95	0.95	BP-RF	1521.43	1521.43	0.0001	80	1711	11	0.04	0.53	0.02	0.00
3	0.95	0.99	BP-HFX	199.98	199.98	0.0002	47	572	1	0.03	0.04	0.00	0.00
3	0.95	0.99	BP-HFY	199.98	199.98	0.0002	39	410	1	0.02	0.03	0.00	0.00
3	0.95	0.99	BP-RF	199.98	199.98	0.0002	58	888	5	0.04	0.13	0.03	0.00
3	0.99	0.9	BP-HFX	4846.38	4846.38	0.0	61	989	3	0.04	0.11	0.44	0.00
3	0.99	0.9	BP-HFY	4846.38	4846.38	0.0	67	1197	3	0.04	0.10	0.01	0.00
3	0.99	0.9	BP-RF	4846.38	4846.38	0.0	76	1541	7	0.04	0.27	0.01	0.00
3	0.99	0.95	BP-HFX	1621.31	1621.31	0.0002	75	1502	13	0.04	0.30	0.05	0.00
3	0.99	0.95	BP-HFY	1621.31	1621.31	0.0002	67	1191	3	0.05	0.11	0.52	0.00
3	0.99	0.95	BP-RF	1621.31	1621.31	0.0002	75	1504	11	0.05	0.48	0.04	0.00
3	0.99	0.99	BP-HFX	216.13	216.13	0.0002	41	441	3	0.03	0.05	0.02	0.00
3	0.99	0.99	BP-HFY	216.13	216.13	0.0002	48	600	3	0.03	0.07	0.04	0.00
3	0.99	0.99	BP-RF	216.13	216.13	0.0002	65	1133	9	0.03	0.25	0.06	0.00

Table 4.29: Comparison of Branching Rules for N=9, Instance ID = 5

L	Se	Sp	Configuration	LB	UB	Δ UB (%)	$\#y$	$\#x$	# nodes	Time$_r$ (s)	Total Time (s)	Gap$_r$ (%)	Gap (%)
3	0.9	0.9	BP-HFX	4125.78	4125.78	0.0001	61	991	1	0.06	0.09	0.00	0.00
3	0.9	0.9	BP-HFY	4125.78	4125.78	0.0001	61	991	1	0.06	0.09	0.00	0.00
3	0.9	0.9	BP-RF	4125.78	4125.78	0.0001	61	991	1	0.06	0.10	0.00	0.00
3	0.9	0.95	BP-HFX	1316.94	1316.94	0.0002	65	1119	1	0.06	0.07	0.00	0.00
3	0.9	0.95	BP-HFY	1316.94	1316.94	0.0002	65	1119	1	0.06	0.07	0.00	0.00
3	0.9	0.95	BP-RF	1316.94	1316.94	0.0002	65	1119	1	0.07	0.09	0.00	0.00
3	0.9	0.99	BP-HFX	164.40	164.40	0.0	44	510	1	0.02	0.03	0.00	0.00
3	0.9	0.99	BP-HFY	164.40	164.40	0.0	44	510	1	0.02	0.03	0.00	0.00
3	0.9	0.99	BP-RF	164.40	164.40	0.0	44	510	1	0.03	0.03	0.00	0.00
3	0.95	0.9	BP-HFX	4407.11	4407.11	0.0	65	1125	1	0.05	0.09	0.00	0.00
3	0.95	0.9	BP-HFY	4407.11	4407.11	0.0	65	1125	1	0.06	0.07	0.00	0.00
3	0.95	0.9	BP-RF	4407.11	4407.11	0.0	65	1125	1	0.05	0.07	0.00	0.00
3	0.95	0.95	BP-HFX	1427.95	1427.95	0.0	59	924	1	0.04	0.05	0.00	0.00
3	0.95	0.95	BP-HFY	1427.95	1427.95	0.0	59	924	1	0.04	0.05	0.00	0.00
3	0.95	0.95	BP-RF	1427.95	1427.95	0.0	59	924	1	0.05	0.06	0.00	0.00
3	0.95	0.99	BP-HFX	181.86	181.86	0.0	43	493	1	0.03	0.04	0.00	0.00
3	0.95	0.99	BP-HFY	181.86	181.86	0.0	43	493	1	0.03	0.04	0.00	0.00
3	0.95	0.99	BP-RF	181.86	181.86	0.0	43	493	1	0.03	0.04	0.00	0.00
3	0.99	0.9	BP-HFX	4638.51	4638.51	0.0	67	1192	1	0.07	0.10	0.00	0.00
3	0.99	0.9	BP-HFY	4638.51	4638.51	0.0	67	1192	1	0.06	0.10	0.00	0.00
3	0.99	0.9	BP-RF	4638.51	4638.51	0.0	67	1192	1	0.06	0.10	0.00	0.00
3	0.99	0.95	BP-HFX	1519.93	1519.93	0.0002	59	929	1	0.04	0.05	0.00	0.00
3	0.99	0.95	BP-HFY	1519.93	1519.93	0.0002	59	929	1	0.04	0.05	0.00	0.00
3	0.99	0.95	BP-RF	1519.93	1519.93	0.0002	59	929	1	0.04	0.05	0.00	0.00
3	0.99	0.99	BP-HFX	196.46	196.46	0.0002	48	607	1	0.03	0.04	0.00	0.00
3	0.99	0.99	BP-HFY	196.46	196.46	0.0002	48	607	1	0.03	0.04	0.00	0.00
3	0.99	0.99	BP-RF	196.46	196.46	0.0002	48	607	1	0.03	0.04	0.00	0.00

Table 4.30: Comparison of Branching Rules for N=10, Instance ID = 1

L	Se	Sp	Configuration	LB	UB	Δ UB (%)	$\#y$	$\#x$	# nodes	Time$_r$ (s)	Total Time (s)	Gap$_r$ (%)	Gap (%)
4	0.9	0.9	BP-HFX	10642.84	10642.84	0.0034	130	3184	1	0.39	0.56	0.00	0.00
4	0.9	0.9	BP-HFY	10642.84	10642.84	0.0034	130	3184	1	0.43	0.63	0.00	0.00
4	0.9	0.9	BP-RF	10642.84	10642.84	0.0034	130	3184	1	0.45	0.68	0.00	0.00
4	0.9	0.95	BP-HFX	4280.03	4280.03	0.0044	132	3287	1	0.28	0.40	0.00	0.00
4	0.9	0.95	BP-HFY	4280.03	4280.03	0.0044	132	3287	1	0.29	0.41	0.00	0.00
4	0.9	0.95	BP-RF	4280.03	4280.03	0.0044	132	3287	1	0.31	0.45	0.00	0.00
4	0.9	0.99	BP-HFX	703.80	703.80	0.0	105	2083	1	0.19	0.24	0.00	0.00
4	0.9	0.99	BP-HFY	703.80	703.80	0.0	105	2083	1	0.17	0.22	0.00	0.00
4	0.9	0.99	BP-RF	703.80	703.80	0.0	105	2083	1	0.19	0.23	0.00	0.00
4	0.95	0.9	BP-HFX	11603.48	11603.48	0.0036	136	3481	1	0.40	0.62	0.00	0.00
4	0.95	0.9	BP-HFY	11603.48	11603.48	0.0036	136	3481	1	0.43	0.69	0.00	0.00
4	0.95	0.9	BP-RF	11603.48	11603.48	0.0036	136	3481	1	0.46	0.72	0.00	0.00
4	0.95	0.95	BP-HFX	4710.81	4710.81	0.0046	131	3264	1	0.32	0.44	0.00	0.00
4	0.95	0.95	BP-HFY	4710.81	4710.81	0.0046	131	3264	1	0.32	0.46	0.00	0.00
4	0.95	0.95	BP-RF	4710.81	4710.81	0.0046	131	3264	1	0.36	0.50	0.00	0.00
4	0.95	0.99	BP-HFX	782.03	782.03	0.0	109	2232	1	0.19	0.25	0.00	0.00
4	0.95	0.99	BP-HFY	782.03	782.03	0.0	109	2232	1	0.20	0.26	0.00	0.00
4	0.95	0.99	BP-RF	782.03	782.03	0.0	109	2232	1	0.21	0.27	0.00	0.00
4	0.99	0.9	BP-HFX	12401.66	12401.66	0.0035	145	3959	1	0.41	0.60	0.00	0.00
4	0.99	0.9	BP-HFY	12401.66	12401.66	0.0035	145	3959	1	0.44	0.65	0.00	0.00
4	0.99	0.9	BP-RF	12401.66	12401.66	0.0035	145	3959	1	0.49	0.73	0.00	0.00
4	0.99	0.95	BP-HFX	5070.27	5070.27	0.0047	139	3647	1	0.38	0.56	0.00	0.00
4	0.99	0.95	BP-HFY	5070.27	5070.27	0.0047	139	3647	1	0.43	0.62	0.00	0.00
4	0.99	0.95	BP-RF	5070.27	5070.27	0.0047	139	3647	1	0.48	0.69	0.00	0.00
4	0.99	0.99	BP-HFX	847.54	847.54	0.0058	113	2435	1	0.21	0.24	0.00	0.00
4	0.99	0.99	BP-HFY	847.54	847.54	0.0058	113	2435	1	0.22	0.25	0.00	0.00
4	0.99	0.99	BP-RF	847.54	847.54	0.0058	113	2435	1	0.23	0.27	0.00	0.00

Table 4.31: Comparison of Branching Rules for N=10, Instance ID = 2

L	Se	Sp	Configuration	LB	UB	Δ UB (%)	$\#y$	$\#x$	# nodes	Time$_r$ (s)	Total Time (s)	Gap$_r$ (%)	Gap (%)
4	0.9	0.9	BP-HFX	13964.98	13964.98	0.0001	100	1874	1	0.20	0.30	0.00	0.00
4	0.9	0.9	BP-HFY	13964.98	13964.98	0.0001	100	1874	1	0.21	0.32	0.00	0.00
4	0.9	0.9	BP-RF	13964.98	13964.98	0.0001	100	1874	1	0.30	0.45	0.00	0.00
4	0.9	0.95	BP-HFX	5947.48	5947.48	0.0001	98	1813	1	0.19	0.29	0.00	0.00
4	0.9	0.95	BP-HFY	5947.48	5947.48	0.0001	98	1813	1	0.20	0.32	0.00	0.00
4	0.9	0.95	BP-RF	5947.48	5947.48	0.0001	98	1813	1	0.24	0.40	0.00	0.00
4	0.9	0.99	BP-HFX	1035.44	1035.44	0.0	74	1031	1	0.09	0.11	0.00	0.00
4	0.9	0.99	BP-HFY	1035.44	1035.44	0.0	74	1031	1	0.09	0.11	0.00	0.00
4	0.9	0.99	BP-RF	1035.44	1035.44	0.0	74	1031	1	0.09	0.12	0.00	0.00
4	0.95	0.9	BP-HFX	15308.55	15308.55	0.0003	103	1998	1	0.23	0.38	0.00	0.00
4	0.95	0.9	BP-HFY	15308.55	15308.55	0.0003	103	1998	1	0.28	0.45	0.00	0.00
4	0.95	0.9	BP-RF	15308.55	15308.55	0.0003	103	1998	1	0.32	0.54	0.00	0.00
4	0.95	0.95	BP-HFX	6568.44	6568.44	0.0	106	2116	1	0.23	0.38	0.00	0.00
4	0.95	0.95	BP-HFY	6568.44	6568.44	0.0	106	2116	1	0.25	0.42	0.00	0.00
4	0.95	0.95	BP-RF	6568.44	6568.44	0.0	106	2116	1	0.27	0.48	0.00	0.00
4	0.95	0.99	BP-HFX	1151.50	1151.50	0.0	75	1081	1	0.11	0.14	0.00	0.00
4	0.95	0.99	BP-HFY	1151.50	1151.50	0.0	75	1081	1	0.11	0.14	0.00	0.00
4	0.95	0.99	BP-RF	1151.50	1151.50	0.0	75	1081	1	0.12	0.17	0.00	0.00
4	0.99	0.9	BP-HFX	16427.79	16427.79	0.0001	106	2121	1	0.19	0.30	0.00	0.00
4	0.99	0.9	BP-HFY	16427.79	16427.79	0.0001	106	2121	1	0.20	0.31	0.00	0.00
4	0.99	0.9	BP-RF	16427.79	16427.79	0.0001	106	2121	1	0.22	0.34	0.00	0.00
4	0.99	0.95	BP-HFX	7087.41	7087.41	0.0001	109	2263	1	0.25	0.41	0.00	0.00
4	0.99	0.95	BP-HFY	7087.41	7087.41	0.0001	109	2263	1	0.27	0.42	0.00	0.00
4	0.99	0.95	BP-RF	7087.41	7087.41	0.0001	109	2263	1	0.25	0.41	0.00	0.00
4	0.99	0.99	BP-HFX	1248.79	1248.79	0.0	89	1504	1	0.14	0.20	0.00	0.00
4	0.99	0.99	BP-HFY	1248.79	1248.79	0.0	89	1504	1	0.17	0.24	0.00	0.00
4	0.99	0.99	BP-RF	1248.79	1248.79	0.0	89	1504	1	0.15	0.24	0.00	0.00

Table 4.32: Comparison of Branching Rules for N=10, Instance ID = 3

L	Se	Sp	Configuration	LB	UB	Δ UB (%)	$\#y$	$\#x$	# nodes	Time$_r$ (s)	Total Time (s)	Gap$_r$ (%)	Gap (%)
4	0.9	0.9	BP-HFX	7634.24	7634.24	0.0	176	5868	15	0.26	2.53	0.40	0.00
4	0.9	0.9	BP-HFY	7634.24	7634.24	0.0	154	4459	3	0.27	0.84	0.40	0.00
4	0.9	0.9	BP-RF	7634.24	7634.24	0.0	181	6200	13	0.29	3.45	0.40	0.00
4	0.9	0.95	BP-HFX	2832.00	2832.00	0.0001	133	3315	1	0.39	0.56	0.00	0.00
4	0.9	0.95	BP-HFY	2832.00	2832.00	0.0001	127	3044	1	0.31	0.45	0.00	0.00
4	0.9	0.95	BP-RF	2832.00	2832.00	0.0001	131	3221	1	0.32	0.45	0.00	0.00
4	0.9	0.99	BP-HFX	426.99	426.99	0.0	107	2143	1	0.17	0.20	0.00	0.00
4	0.9	0.99	BP-HFY	426.99	426.99	0.0	114	2459	1	0.27	0.30	0.00	0.00
4	0.9	0.99	BP-RF	426.99	426.99	0.0	107	2143	1	0.17	0.21	0.00	0.00
4	0.95	0.9	BP-HFX	8261.71	8261.71	0.0	183	6345	35	0.23	5.27	0.61	0.00
4	0.95	0.9	BP-HFY	8261.71	8261.71	0.0	143	3855	3	0.23	0.74	0.30	0.00
4	0.95	0.9	BP-RF	8261.71	8261.71	0.0	180	6134	13	0.23	3.22	0.61	0.00
4	0.95	0.95	BP-HFX	3101.54	3101.54	0.0001	131	3221	1	0.34	0.54	0.00	0.00
4	0.95	0.95	BP-HFY	3101.54	3101.54	0.0001	141	3736	1	0.37	0.51	0.00	0.00
4	0.95	0.95	BP-RF	3101.54	3101.54	0.0001	131	3248	1	0.36	0.53	0.00	0.00
4	0.95	0.99	BP-HFX	473.82	473.82	0.0	113	2413	1	0.22	0.25	0.00	0.00
4	0.95	0.99	BP-HFY	473.82	473.82	0.0	121	2754	1	0.21	0.24	0.00	0.00
4	0.95	0.99	BP-RF	473.82	473.82	0.0	103	2015	1	0.21	0.23	0.00	0.00
4	0.99	0.9	BP-HFX	8781.22	8781.22	0.0	167	5267	13	0.18	2.19	0.65	0.00
4	0.99	0.9	BP-HFY	8781.22	8781.22	0.0	152	4350	5	0.17	1.20	0.54	0.00
4	0.99	0.9	BP-RF	8781.22	8781.22	0.0	174	5740	9	0.31	2.58	0.26	0.00
4	0.99	0.95	BP-HFX	3325.94	3325.94	0.0	129	3147	1	0.37	0.56	0.00	0.00
4	0.99	0.95	BP-HFY	3325.94	3325.94	0.0	139	3633	1	0.51	0.76	0.00	0.00
4	0.99	0.95	BP-RF	3325.94	3325.94	0.0	130	3164	1	0.36	0.50	0.00	0.00
4	0.99	0.99	BP-HFX	513.05	513.05	0.0001	102	1951	1	0.21	0.25	0.00	0.00
4	0.99	0.99	BP-HFY	513.05	513.05	0.0001	108	2209	1	0.21	0.25	0.00	0.00
4	0.99	0.99	BP-RF	513.05	513.05	0.0001	110	2254	1	0.20	0.24	0.00	0.00

Table 4.33: Comparison of Branching Rules for N=10, Instance ID = 4

L	Se	Sp	Configuration	LB	UB	Δ UB (%)	$\#y$	$\#x$	# nodes	Time$_r$ (s)	Total Time (s)	Gap$_r$ (%)	Gap (%)
4	0.9	0.9	BP-HFX	7922.04	7922.04	0.0	201	7684	121	0.26	40.35	0.76	0.00
4	0.9	0.9	BP-HFY	7922.04	7922.04	0.0	159	4752	3	0.25	1.00	0.76	0.00
4	0.9	0.9	BP-RF	7922.04	7922.04	0.0	196	7314	97	0.28	29.47	0.76	0.00
4	0.9	0.95	BP-HFX	2949.86	2949.86	0.0001	201	7683	119	0.21	39.88	0.90	0.00
4	0.9	0.95	BP-HFY	2949.86	2949.86	0.0001	146	4021	3	0.27	0.69	0.80	0.00
4	0.9	0.95	BP-RF	2949.86	2949.86	0.0001	192	7017	31	0.22	7.15	1.62	0.00
4	0.9	0.99	BP-HFX	445.55	445.55	0.0	184	6438	71	0.25	13.20	0.44	0.00
4	0.9	0.99	BP-HFY	445.55	445.55	0.0	127	3036	3	0.20	0.52	0.45	0.00
4	0.9	0.99	BP-RF	445.55	445.55	0.0	162	4972	19	0.25	3.71	0.46	0.00
4	0.95	0.9	BP-HFX	8576.88	8576.88	0.0001	206	8081	147	0.23	54.89	0.60	0.00
4	0.95	0.9	BP-HFY	8576.88	8576.88	0.0001	153	4422	3	0.26	0.64	0.75	0.00
4	0.95	0.9	BP-RF	8576.88	8576.88	0.0001	195	7238	45	0.23	12.10	0.89	0.00
4	0.95	0.95	BP-HFX	3231.15	3231.15	0.0	197	7376	93	0.32	26.56	0.51	0.00
4	0.95	0.95	BP-HFY	3231.15	3231.15	0.0	147	4067	3	0.31	0.65	0.52	0.00
4	0.95	0.95	BP-RF	3231.15	3231.15	0.0	185	6504	37	0.29	7.96	0.51	0.00
4	0.95	0.99	BP-HFX	494.43	494.43	0.0	176	5859	55	0.36	9.00	0.45	0.00
4	0.95	0.99	BP-HFY	494.43	494.43	0.0	138	3589	3	0.37	0.64	0.46	0.00
4	0.95	0.99	BP-RF	494.43	494.43	0.0	167	5294	21	0.30	4.46	0.47	0.00
4	0.99	0.9	BP-HFX	9119.05	9119.05	0.0	200	7605	111	0.31	34.70	0.66	0.00
4	0.99	0.9	BP-HFY	9119.05	9119.05	0.0	155	4559	3	0.25	0.70	1.63	0.00
4	0.99	0.9	BP-RF	9119.05	9119.05	0.0	202	7771	61	0.32	19.17	0.83	0.00
4	0.99	0.95	BP-HFX	3465.33	3465.33	0.0	201	7683	93	0.27	27.68	1.11	0.00
4	0.99	0.95	BP-HFY	3465.33	3465.33	0.0	140	3693	3	0.28	0.72	0.86	0.00
4	0.99	0.95	BP-RF	3465.33	3465.33	0.0	177	5937	49	0.26	10.64	0.82	0.00
4	0.99	0.99	BP-HFX	535.37	535.37	0.0	186	6570	81	0.28	17.49	0.46	0.00
4	0.99	0.99	BP-HFY	535.37	535.37	0.0	133	3317	3	0.28	0.58	0.46	0.00
4	0.99	0.99	BP-RF	535.37	535.37	0.0	164	5104	23	0.29	4.43	0.45	0.00

Table 4.34: Comparison of Branching Rules for N=10, Instance ID = 5

L	Se	Sp	Configuration	LB	UB	Δ UB (%)	$\#y$	$\#x$	# nodes	Time$_r$ (s)	Total Time (s)	Gap$_r$ (%)	Gap (%)
4	0.9	0.9	BP-HFX	11391.86	11391.86	0.0004	111	2328	1	0.23	0.34	0.00	0.00
4	0.9	0.9	BP-HFY	11391.86	11391.86	0.0004	111	2328	1	0.26	0.39	0.00	0.00
4	0.9	0.9	BP-RF	11391.86	11391.86	0.0004	111	2328	1	0.25	0.35	0.00	0.00
4	0.9	0.95	BP-HFX	4651.33	4651.33	0.0093	132	3273	1	0.33	0.54	0.00	0.00
4	0.9	0.95	BP-HFY	4651.33	4651.33	0.0093	132	3273	1	0.36	0.55	0.00	0.00
4	0.9	0.95	BP-RF	4651.33	4651.33	0.0093	132	3273	1	0.34	0.53	0.00	0.00
4	0.9	0.99	BP-HFX	776.94	776.94	0.0	114	2436	1	0.25	0.31	0.00	0.00
4	0.9	0.99	BP-HFY	776.94	776.94	0.0	114	2436	1	0.31	0.38	0.00	0.00
4	0.9	0.99	BP-RF	776.94	776.94	0.0	114	2436	1	0.25	0.32	0.00	0.00
4	0.95	0.9	BP-HFX	12436.98	12436.98	0.0074	144	3907	1	0.37	0.55	0.00	0.00
4	0.95	0.9	BP-HFY	12436.98	12436.98	0.0074	144	3907	1	0.49	0.69	0.00	0.00
4	0.95	0.9	BP-RF	12436.98	12436.98	0.0074	144	3907	1	0.39	0.58	0.00	0.00
4	0.95	0.95	BP-HFX	5124.19	5124.19	0.0094	139	3661	1	0.37	0.53	0.00	0.00
4	0.95	0.95	BP-HFY	5124.19	5124.19	0.0094	139	3661	1	0.47	0.68	0.00	0.00
4	0.95	0.95	BP-RF	5124.19	5124.19	0.0094	139	3661	1	0.38	0.55	0.00	0.00
4	0.95	0.99	BP-HFX	863.50	863.50	0.0	105	2076	1	0.21	0.25	0.00	0.00
4	0.95	0.99	BP-HFY	863.50	863.50	0.0	105	2076	1	0.22	0.27	0.00	0.00
4	0.95	0.99	BP-RF	863.50	863.50	0.0	105	2076	1	0.21	0.26	0.00	0.00
4	0.99	0.9	BP-HFX	13307.65	13307.60	0.0	132	3305	1	0.37	0.56	0.00	0.00
4	0.99	0.9	BP-HFY	13307.65	13307.60	0.0	132	3305	1	0.37	0.56	0.00	0.00
4	0.99	0.9	BP-RF	13307.65	13307.60	0.0	132	3305	1	0.38	0.58	0.00	0.00
4	0.99	0.95	BP-HFX	5519.46	5519.46	0.0	126	2986	1	0.25	0.38	0.00	0.00
4	0.99	0.95	BP-HFY	5519.46	5519.46	0.0	126	2986	1	0.26	0.37	0.00	0.00
4	0.99	0.95	BP-RF	5519.46	5519.46	0.0	126	2986	1	0.26	0.39	0.00	0.00
4	0.99	0.99	BP-HFX	936.04	936.04	0.0	108	2182	1	0.16	0.22	0.00	0.00
4	0.99	0.99	BP-HFY	936.04	936.04	0.0	108	2182	1	0.16	0.22	0.00	0.00
4	0.99	0.99	BP-RF	936.04	936.04	0.0	108	2182	1	0.17	0.23	0.00	0.00

Table 4.35: Comparison of Branching Rules for N=12, Instance ID = 1

L	Se	Sp	Configuration	LB	UB	Δ UB (%)	$\#y$	$\#x$	# nodes	Time$_r$ (s)	Total Time (s)	Gap$_r$ (%)	Gap (%)
3	0.9	0.9	BP-HFX	6825.27	6825.27	0.1012	206	10410	285	0.07	118.50	0.41	0.00
3	0.9	0.9	BP-HFY	6825.27	6825.27	0.1012	194	9236	131	0.07	22.68	0.41	0.00
3	0.9	0.9	BP-RF	6825.27	6825.27	0.1012	201	9914	313	0.06	81.63	0.41	0.00
3	0.9	0.95	BP-HFX	2377.64	2377.64	0.2079	203	10104	449	0.07	270.76	0.78	0.00
3	0.9	0.95	BP-HFY	2377.64	2377.64	0.2079	197	9522	165	0.08	37.45	0.37	0.00
3	0.9	0.95	BP-RF	2377.64	2377.64	0.2079	209	10713	1077	0.09	1261.13	0.36	0.00
3	0.9	0.99	BP-HFX	334.95	334.95	0.3565	192	9030	533	0.04	305.08	0.50	0.00
3	0.9	0.99	BP-HFY	334.82	334.82	0.3949	199	9692	1193	0.03	1276.36	0.48	0.00
3	0.9	0.99	BP-RF	334.29	334.95	0.3565	212	11025	1947	0.04	TL	0.56	0.20
3	0.95	0.9	BP-HFX	7343.73	7343.73	0.1092	200	9807	313	0.07	144.34	0.51	0.00
3	0.95	0.9	BP-HFY	7343.73	7343.73	0.1092	192	9042	103	0.06	17.90	0.46	0.00
3	0.95	0.9	BP-RF	7343.73	7343.73	0.1092	200	9828	261	0.06	86.74	0.42	0.00
3	0.95	0.95	BP-HFX	2593.79	2593.79	0.2496	203	10108	413	0.07	224.19	0.82	0.00
3	0.95	0.95	BP-HFY	2593.79	2593.79	0.2496	206	10405	761	0.09	594.81	0.89	0.00
3	0.95	0.95	BP-RF	2593.79	2593.79	0.2496	205	10312	565	0.08	320.79	0.80	0.00
3	0.95	0.99	BP-HFX	371.16	371.16	0.3984	202	10010	1047	0.04	1054.02	0.47	0.00
3	0.95	0.99	BP-HFY	371.16	371.16	0.3984	207	10514	1277	0.04	1489.66	0.55	0.00
3	0.95	0.99	BP-RF	371.16	371.16	0.3984	199	9715	463	0.03	190.66	0.50	0.00
3	0.99	0.9	BP-HFX	7771.98	7771.98	0.1155	199	9713	311	0.07	142.85	0.44	0.00
3	0.99	0.9	BP-HFY	7771.98	7771.98	0.1155	188	8675	145	0.08	30.87	0.49	0.00
3	0.99	0.9	BP-RF	7771.98	7771.98	0.1155	209	10708	261	0.07	111.07	0.60	0.00
3	0.99	0.95	BP-HFX	2773.45	2773.45	0.2236	203	10103	513	0.07	322.33	0.78	0.00
3	0.99	0.95	BP-HFY	2773.45	2773.45	0.2236	199	9718	313	0.11	117.16	0.39	0.00
3	0.99	0.95	BP-RF	2773.45	2773.45	0.2236	214	11236	1083	0.07	1344.45	0.99	0.00
3	0.99	0.99	BP-HFX	401.58	401.58	0.4007	207	10513	1107	0.06	1262.97	0.61	0.00
3	0.99	0.99	BP-HFY	401.58	401.58	0.4007	195	9313	881	0.04	676.61	0.57	0.00
3	0.99	0.99	BP-RF	401.14	402.13	0.2642	211	10920	1955	0.05	TL	0.51	0.25
4	0.9	0.9	BP-HFX	10805.64	10805.64	0.0801	208	9429	3	0.21	2.53	1.13	0.00
4	0.9	0.9	BP-HFY	10805.64	10805.64	0.0801	202	8934	5	0.25	2.41	0.33	0.00
4	0.9	0.9	BP-RF	10807.41	10807.41	0.0637	292	18825	17	0.18	10.16	0.85	0.00
4	0.9	0.95	BP-HFX	4205.70	4205.70	0.1046	316	21970	37	0.23	26.12	0.75	0.00
4	0.9	0.95	BP-HFY	4205.70	4205.70	0.1046	200	8788	9	0.29	2.68	0.35	0.00
4	0.9	0.95	BP-RF	4205.70	4205.70	0.1046	279	17162	13	0.25	13.07	0.52	0.00
4	0.9	0.99	BP-HFX	669.72	669.72	0.129	233	11998	34	0.28	10.46	0.09	0.00
4	0.9	0.99	BP-HFY	669.89	669.89	0.1033	186	7593	16	0.32	3.96	0.14	0.00
4	0.9	0.99	BP-RF	670.58	670.58	0.0001	249	13787	35	0.28	14.86	0.11	0.00
4	0.95	0.9	BP-HFX	11744.15	11744.15	0.0821	194	8277	1	1.12	1.90	0.00	0.00
4	0.95	0.9	BP-HFY	11744.15	11744.15	0.0821	165	5968	1	0.95	1.64	0.00	0.00
4	0.95	0.9	BP-RF	11744.15	11744.15	0.0821	273	16435	7	0.25	7.04	0.75	0.00
4	0.95	0.95	BP-HFX	4620.09	4620.09	0.1058	305	20396	39	0.21	23.27	0.64	0.00
4	0.95	0.95	BP-HFY	4620.09	4620.09	0.1058	222	10793	15	0.25	4.84	0.62	0.00
4	0.95	0.95	BP-RF	4621.09	4621.09	0.0841	300	19883	17	0.40	17.16	0.62	0.00
4	0.95	0.99	BP-HFX	743.82	743.82	0.1294	255	14356	58	0.26	26.92	0.12	0.00
4	0.95	0.99	BP-HFY	744.29	744.29	0.0661	167	6149	13	0.33	2.86	0.13	0.00
4	0.95	0.99	BP-RF	744.65	744.65	0.0173	254	14357	41	0.26	18.32	0.12	0.00
4	0.99	0.9	BP-HFX	12522.94	12522.94	0.0843	213	9924	3	0.23	2.30	0.43	0.00
4	0.99	0.9	BP-HFY	12522.94	12522.94	0.0843	220	10585	9	0.18	3.47	0.46	0.00
4	0.99	0.9	BP-RF	12525.52	12525.52	0.0637	284	17765	13	0.17	13.32	0.82	0.00
4	0.99	0.95	BP-HFX	4965.59	4965.59	0.107	330	23930	49	0.21	39.27	0.80	0.00
4	0.99	0.95	BP-HFY	4965.59	4965.59	0.107	237	12332	11	0.24	5.31	0.76	0.00
4	0.99	0.95	BP-RF	4965.93	4965.93	0.1001	310	21181	17	0.56	23.18	0.44	0.00
4	0.99	0.99	BP-HFX	805.90	805.90	0.1296	336	24883	185	0.27	211.65	0.13	0.00
4	0.99	0.99	BP-HFY	805.90	805.90	0.1296	177	6939	14	0.23	3.04	1.01	0.00
4	0.99	0.99	BP-RF	806.94	806.94	0.0007	282	17671	49	0.36	32.10	0.14	0.00

Table 4.36: Comparison of Branching Rules for N=12, Instance ID = 2

L	Se	Sp	Configuration	LB	UB	Δ UB (%)	$\#y$	$\#x$	# nodes	Time$_r$ (s)	Total Time (s)	Gap$_r$ (%)	Gap (%)
3	0.9	0.9	BP-HFX	4212.88	4230.04	0.0145	228	12756	1795	0.14	TL	1.14	0.41
3	0.9	0.9	BP-HFY	4202.10	4230.40	0.0061	223	12200	1877	0.11	TL	1.14	0.67
3	0.9	0.9	BP-RF	4183.03	4230.66	0.0001	212	11030	2060	0.10	TL	1.14	1.14
3	0.9	0.95	BP-HFX	1210.19	1217.56	0.0473	220	11880	1858	0.18	TL	1.49	0.61
3	0.9	0.95	BP-HFY	1217.56	1217.56	0.0473	214	11236	1475	0.17	2027.28	1.47	0.00
3	0.9	0.95	BP-RF	1200.24	1218.14	0.0003	211	10928	2023	0.16	TL	1.49	1.49
3	0.9	0.99	BP-HFX	126.90	130.58	1.2781	220	11880	2040	0.07	TL	4.23	2.90
3	0.9	0.99	BP-HFY	126.88	132.27	0.0	211	10924	2086	0.06	TL	4.25	4.25
3	0.9	0.99	BP-RF	126.93	131.50	0.5824	218	11664	2110	0.07	TL	4.21	3.60
3	0.95	0.9	BP-HFX	4480.35	4480.35	0.0146	219	11772	1119	0.17	1414.67	0.96	0.00
3	0.95	0.9	BP-HFY	4451.30	4481.00	0.0	219	11772	1896	0.09	TL	1.20	0.67
3	0.95	0.9	BP-RF	4426.73	4481.00	0.0	207	10519	2597	0.10	TL	1.23	1.23
3	0.95	0.95	BP-HFX	1305.54	1310.52	0.0502	219	11772	1881	0.20	TL	1.56	0.38
3	0.95	0.95	BP-HFY	1310.52	1310.52	0.0502	215	11345	939	0.24	901.80	1.57	0.00
3	0.95	0.95	BP-RF	1278.95	1310.55	0.0302	215	11340	2511	0.10	TL	2.50	2.47
3	0.95	0.99	BP-HFX	139.67	144.04	1.2959	220	11880	1992	0.08	TL	4.48	3.12
3	0.95	0.99	BP-HFY	143.92	143.92	1.3777	214	11239	3227	0.09	2864.89	4.35	0.00
3	0.95	0.99	BP-RF	139.82	143.92	1.3777	212	11027	1663	0.11	TL	4.37	2.93
3	0.99	0.9	BP-HFX	4685.32	4685.32	0.02	220	11880	1411	0.21	2313.00	1.08	0.00
3	0.99	0.9	BP-HFY	4685.32	4685.32	0.02	214	11237	1021	0.25	1155.14	1.06	0.00
3	0.99	0.9	BP-RF	4650.07	4685.60	0.0087	219	11772	2562	0.17	TL	0.78	0.76
3	0.99	0.95	BP-HFX	1387.25	1387.25	0.053	228	12756	3509	0.25	3568.82	1.60	0.00
3	0.99	0.95	BP-HFY	1387.25	1387.25	0.053	224	12312	1289	0.32	1661.88	2.41	0.00
3	0.99	0.95	BP-RF	1365.90	1387.25	0.053	199	9722	1598	0.23	TL	1.62	1.56
3	0.99	0.99	BP-HFX	150.63	155.15	1.3919	216	11450	1956	0.11	TL	4.45	3.00
3	0.99	0.99	BP-HFY	150.67	157.34	0.0	209	10719	2005	0.10	TL	4.42	4.42
3	0.99	0.99	BP-RF	150.53	155.15	1.3919	212	11022	1449	0.11	TL	4.52	3.06
4	0.9	0.9	BP-HFX	6337.14	6341.76	0.0396	486	53426	680	0.48	TL	1.18	0.07
4	0.9	0.9	BP-HFY	6341.76	6341.76	0.0396	428	41066	177	0.50	217.82	0.98	0.00
4	0.9	0.9	BP-RF	6341.76	6341.76	0.0396	460	47801	491	0.84	1436.68	0.94	0.00
4	0.9	0.95	BP-HFX	2100.29	2110.28	0.0867	488	53873	668	0.71	TL	1.86	0.48
4	0.9	0.95	BP-HFY	2110.28	2110.28	0.0867	459	47524	319	1.04	646.32	1.63	0.00
4	0.9	0.95	BP-RF	2078.99	2112.11	0.0	451	45845	924	0.56	TL	1.59	1.59
4	0.9	0.99	BP-HFX	276.21	279.06	0.1639	489	54100	920	0.47	TL	1.79	1.03
4	0.9	0.99	BP-HFY	279.06	279.06	0.1639	449	45421	591	0.35	1409.33	1.76	0.00
4	0.9	0.99	BP-RF	275.45	279.52	0.0	460	47818	1028	0.31	TL	1.82	1.48
4	0.95	0.9	BP-HFX	6785.79	6797.73	0.0436	478	51611	692	0.62	TL	2.01	0.18
4	0.95	0.9	BP-HFY	6797.73	6797.73	0.0436	438	43145	199	0.81	285.85	1.20	0.00
4	0.95	0.9	BP-RF	6798.45	6798.45	0.0329	433	42148	441	0.36	702.93	1.28	0.00
4	0.95	0.95	BP-HFX	2294.79	2294.79	0.0904	485	53204	687	0.81	TL	1.62	0.00
4	0.95	0.95	BP-HFY	2294.79	2294.79	0.0904	464	48582	395	1.17	906.34	1.66	0.00
4	0.95	0.95	BP-RF	2294.79	2294.79	0.0908	469	49709	1137	0.67	3195.66	1.52	0.00
4	0.95	0.99	BP-HFX	305.30	309.01	0.1654	486	53439	701	0.52	TL	1.77	1.22
4	0.95	0.99	BP-HFY	309.01	309.01	0.1654	449	45453	607	0.58	507.24	1.79	0.00
4	0.95	0.99	BP-RF	305.09	309.01	0.1654	423	40295	885	0.40	TL	1.72	1.29
4	0.99	0.9	BP-HFX	7167.01	7173.48	0.0462	486	53426	670	0.67	TL	1.37	0.09
4	0.99	0.9	BP-HFY	7173.48	7173.48	0.0462	441	43715	191	0.69	272.89	1.09	0.00
4	0.99	0.9	BP-RF	7173.48	7173.48	0.0463	437	43027	481	0.38	739.78	1.16	0.00
4	0.99	0.95	BP-HFX	2435.94	2447.90	0.0932	486	53427	689	1.29	TL	1.74	0.49
4	0.99	0.95	BP-HFY	2447.90	2447.90	0.0932	464	48577	361	1.07	796.78	1.73	0.00
4	0.99	0.95	BP-RF	2382.91	2447.90	0.0932	420	39664	778	1.52	TL	2.82	2.73
4	0.99	0.99	BP-HFX	329.88	334.07	0.1663	486	53430	712	0.73	TL	1.81	1.27
4	0.99	0.99	BP-HFY	334.14	334.14	0.1435	448	45259	535	0.91	1206.14	1.84	0.00
4	0.99	0.99	BP-RF	331.27	334.07	0.1663	418	39275	762	1.08	TL	1.79	0.84

Table 4.37: Comparison of Branching Rules for N=12, Instance ID = 3

L	Se	Sp	Configuration	LB	UB	Δ UB (%)	$\#y$	$\#x$	# nodes	Time$_r$ (s)	Total Time (s)	Gap$_r$ (%)	Gap (%)
3	0.9	0.9	BP-HFX	5230.45	5230.45	0.0	224	12312	1393	0.12	2167.82	0.77	0.00
3	0.9	0.9	BP-HFY	5230.45	5230.45	0.0	217	11557	481	0.12	238.19	0.77	0.00
3	0.9	0.9	BP-RF	5230.45	5230.45	0.0	226	12535	1241	0.12	1569.99	0.77	0.00
3	0.9	0.95	BP-HFX	1635.93	1642.98	0.0014	227	12645	1673	0.16	TL	1.34	0.43
3	0.9	0.95	BP-HFY	1642.98	1642.98	0.0014	226	12534	1139	0.13	1299.45	0.77	0.00
3	0.9	0.95	BP-RF	1630.61	1643.00	0.0001	227	12645	1899	0.11	TL	1.82	0.76
3	0.9	0.99	BP-HFX	200.16	200.98	0.0001	219	11772	1694	0.04	TL	1.23	0.41
3	0.9	0.99	BP-HFY	200.96	200.96	0.0076	224	12313	1685	0.06	2500.98	1.23	0.00
3	0.9	0.99	BP-RF	198.48	200.96	0.0076	218	11665	1938	0.06	TL	1.35	1.25
3	0.95	0.9	BP-HFX	5579.34	5579.34	0.0	220	11880	1091	0.16	1404.10	0.89	0.00
3	0.95	0.9	BP-HFY	5579.34	5579.34	0.0	208	10613	139	0.10	28.78	0.80	0.00
3	0.95	0.9	BP-RF	5579.34	5579.34	0.0	219	11772	1475	0.16	2446.30	0.71	0.00
3	0.95	0.95	BP-HFX	1772.44	1779.57	0.0016	227	12645	1779	0.14	TL	0.79	0.40
3	0.95	0.95	BP-HFY	1779.57	1779.57	0.0016	227	12645	1241	0.13	1563.92	0.81	0.00
3	0.95	0.95	BP-RF	1779.57	1779.57	0.0016	226	12534	1603	0.15	3081.25	1.39	0.00
3	0.95	0.99	BP-HFX	220.12	222.23	0.0079	220	11880	1890	0.10	TL	1.36	0.96
3	0.95	0.99	BP-HFY	222.24	222.24	0.0002	215	11343	2043	0.06	3436.45	1.18	0.00
3	0.95	0.99	BP-RF	219.52	222.24	0.0002	224	12312	1699	0.08	TL	1.24	1.24
3	0.99	0.9	BP-HFX	5866.14	5866.14	0.0	218	11664	995	0.17	1192.78	0.67	0.00
3	0.99	0.9	BP-HFY	5866.14	5866.14	0.0	216	11450	419	0.09	231.69	0.90	0.00
3	0.99	0.9	BP-RF	5866.14	5866.14	0.0	220	11880	1307	0.19	2605.49	0.77	0.00
3	0.99	0.95	BP-HFX	1892.69	1892.69	0.0016	219	11772	1507	0.24	2651.90	1.38	0.00
3	0.99	0.95	BP-HFY	1892.69	1892.69	0.0016	206	10411	107	0.18	28.61	1.47	0.00
3	0.99	0.95	BP-RF	1892.69	1892.69	0.0016	219	11772	1427	0.24	2641.85	1.59	0.00
3	0.99	0.99	BP-HFX	237.33	240.01	0.0078	220	11880	1676	0.09	TL	1.39	1.13
3	0.99	0.99	BP-HFY	240.02	240.02	0.0	203	10113	365	0.07	153.01	1.39	0.00
3	0.99	0.99	BP-RF	240.02	240.02	0.0	220	11880	1929	0.08	3403.58	1.37	0.00
4	0.9	0.9	BP-HFX	8080.10	8080.10	0.0	475	50994	727	0.35	TL	0.98	0.00
4	0.9	0.9	BP-HFY	8080.10	8080.10	0.0	368	30137	25	0.45	25.92	0.90	0.00
4	0.9	0.9	BP-RF	8080.10	8080.10	0.0	383	32812	101	0.34	103.93	1.10	0.00
4	0.9	0.95	BP-HFX	2900.26	2900.26	0.0	468	49415	631	0.80	TL	1.34	0.00
4	0.9	0.95	BP-HFY	2900.26	2900.26	0.0	375	31438	35	0.79	45.56	1.38	0.00
4	0.9	0.95	BP-RF	2900.26	2900.26	0.0	430	41625	271	0.72	468.55	1.03	0.00
4	0.9	0.99	BP-HFX	418.20	421.27	0.0	448	45236	717	0.55	TL	0.95	0.73
4	0.9	0.99	BP-HFY	421.27	421.27	0.0	307	20947	51	0.61	41.82	1.00	0.00
4	0.9	0.99	BP-RF	421.27	421.27	0.0	416	38985	269	0.60	539.22	0.97	0.00
4	0.95	0.9	BP-HFX	8718.28	8718.28	0.0	476	51193	681	0.66	TL	1.10	0.00
4	0.95	0.9	BP-HFY	8718.28	8718.28	0.0	346	26594	25	0.53	25.37	0.92	0.00
4	0.95	0.9	BP-RF	8718.28	8718.28	0.0	380	32211	171	1.05	244.11	0.94	0.00
4	0.95	0.95	BP-HFX	3161.40	3169.68	0.0001	483	52760	685	1.09	TL	1.15	0.26
4	0.95	0.95	BP-HFY	3169.68	3169.68	0.0001	364	29522	35	0.84	47.63	1.16	0.00
4	0.95	0.95	BP-RF	3169.68	3169.68	0.0001	394	34734	277	1.25	532.80	1.27	0.00
4	0.95	0.99	BP-HFX	463.91	467.21	0.0	463	48353	713	0.88	TL	1.01	0.71
4	0.95	0.99	BP-HFY	467.21	467.21	0.0	271	16130	37	0.50	28.02	1.01	0.00
4	0.95	0.99	BP-RF	467.21	467.21	0.0	394	34832	273	1.13	576.44	1.04	0.00
4	0.99	0.9	BP-HFX	9235.97	9245.93	0.0	474	50756	709	0.54	TL	1.19	0.11
4	0.99	0.9	BP-HFY	9245.93	9245.93	0.0	355	27958	27	0.43	30.28	1.10	0.00
4	0.99	0.9	BP-RF	9245.93	9245.93	0.0	387	33463	159	0.96	316.04	1.02	0.00
4	0.99	0.95	BP-HFX	3393.77	3393.77	0.0001	472	50271	657	1.49	TL	1.53	0.00
4	0.99	0.95	BP-HFY	3393.77	3393.77	0.0001	368	30188	33	0.74	48.67	1.40	0.00
4	0.99	0.95	BP-RF	3393.77	3393.77	0.0001	415	38630	517	2.63	1587.83	1.15	0.00
4	0.99	0.99	BP-HFX	501.50	505.67	0.0001	457	47110	640	1.12	TL	1.01	0.83
4	0.99	0.99	BP-HFY	505.67	505.67	0.0001	301	20122	39	0.75	36.74	1.01	0.00
4	0.99	0.99	BP-RF	505.67	505.67	0.0001	424	40544	251	0.73	453.13	1.05	0.00

Table 4.38: Comparison of Branching Rules for N=12, Instance ID = 4

L	Se	Sp	Configuration	LB	UB	Δ UB (%)	$\#y$	$\#x$	# nodes	Time$_r$ (s)	Total Time (s)	Gap$_r$ (%)	Gap (%)
3	0.9	0.9	BP-HFX	4728.85	4728.85	0.2	210	10824	191	0.04	57.69	0.59	0.00
3	0.9	0.9	BP-HFY	4728.85	4728.85	0.2	182	8121	143	0.04	19.66	0.59	0.00
3	0.9	0.9	BP-RF	4710.68	4728.76	0.202	211	10922	2077	0.04	TL	0.59	0.38
3	0.9	0.95	BP-HFX	1449.56	1449.56	0.0468	212	11026	241	0.08	80.21	0.36	0.00
3	0.9	0.95	BP-HFY	1449.62	1449.62	0.0427	175	7483	75	0.07	9.33	0.35	0.00
3	0.9	0.95	BP-RF	1450.24	1450.24	0.0	213	11124	1793	0.07	3037.61	0.36	0.00
3	0.9	0.99	BP-HFX	173.45	173.45	0.2755	163	6480	347	0.04	94.36	0.75	0.00
3	0.9	0.99	BP-HFY	173.44	173.44	0.2823	137	4609	99	0.04	8.69	0.85	0.00
3	0.9	0.99	BP-RF	172.63	173.31	0.357	211	10927	1849	0.06	TL	0.75	0.39
3	0.95	0.9	BP-HFX	5032.49	5032.49	0.2254	211	10925	201	0.05	66.84	0.83	0.00
3	0.95	0.9	BP-HFY	5032.60	5032.60	0.2233	176	7596	99	0.08	11.71	0.66	0.00
3	0.95	0.9	BP-RF	5032.49	5032.49	0.2254	210	10817	1487	0.06	2077.42	1.03	0.00
3	0.95	0.95	BP-HFX	1567.83	1567.83	0.0477	209	10715	227	0.07	69.38	0.38	0.00
3	0.95	0.95	BP-HFY	1567.83	1567.83	0.0477	156	5919	35	0.06	3.42	0.36	0.00
3	0.95	0.95	BP-RF	1568.02	1568.02	0.0356	209	10715	1477	0.15	2635.01	0.38	0.00
3	0.95	0.99	BP-HFX	191.81	191.81	0.244	177	7668	360	0.03	113.47	0.79	0.00
3	0.95	0.99	BP-HFY	191.95	191.95	0.1713	160	6236	171	0.04	24.24	0.90	0.00
3	0.95	0.99	BP-RF	190.50	191.59	0.3589	209	10722	1764	0.07	TL	0.93	0.57
3	0.99	0.9	BP-HFX	5282.07	5282.07	0.2439	209	10714	221	0.06	62.54	0.84	0.00
3	0.99	0.9	BP-HFY	5282.26	5282.26	0.2403	188	8659	49	0.05	6.45	0.99	0.00
3	0.99	0.9	BP-RF	5275.60	5283.89	0.2094	220	11880	1602	0.11	TL	0.72	0.16
3	0.99	0.95	BP-HFX	1665.74	1665.74	0.049	215	11346	289	0.07	114.12	0.40	0.00
3	0.99	0.95	BP-HFY	1665.74	1665.74	0.049	178	7787	55	0.10	7.35	0.95	0.00
3	0.99	0.95	BP-RF	1665.95	1665.95	0.0368	208	10612	1647	0.18	3335.68	0.39	0.00
3	0.99	0.99	BP-HFX	207.02	207.02	0.2891	183	8216	349	0.04	115.28	0.95	0.00
3	0.99	0.99	BP-HFY	207.19	207.19	0.2092	127	3943	89	0.06	7.94	0.91	0.00
3	0.99	0.99	BP-RF	205.93	206.87	0.3603	212	11028	1723	0.07	TL	0.82	0.46
4	0.9	0.9	BP-HFX	7189.55	7189.55	0.1573	431	41874	195	0.30	361.94	0.71	0.00
4	0.9	0.9	BP-HFY	7189.55	7189.55	0.1573	339	25520	53	0.27	30.28	0.60	0.00
4	0.9	0.9	BP-RF	7190.68	7190.68	0.1417	394	34801	83	0.22	123.69	0.87	0.00
4	0.9	0.95	BP-HFX	2516.17	2516.17	0.2599	420	39588	273	0.35	572.38	1.00	0.00
4	0.9	0.95	BP-HFY	2516.17	2516.17	0.2599	376	31586	105	0.41	89.82	1.07	0.00
4	0.9	0.95	BP-RF	2516.17	2516.17	0.2599	375	31439	209	0.39	262.09	1.00	0.00
4	0.9	0.99	BP-HFX	356.42	356.42	0.3904	398	35463	515	0.21	1098.52	0.79	0.00
4	0.9	0.99	BP-HFY	356.42	356.42	0.3905	333	24757	279	0.31	236.36	0.48	0.00
4	0.9	0.99	BP-RF	356.51	356.51	0.3639	450	45686	931	0.20	3163.67	0.70	0.00
4	0.95	0.9	BP-HFX	7738.85	7738.85	0.1655	426	40676	189	0.32	371.21	0.75	0.00
4	0.95	0.9	BP-HFY	7738.85	7738.85	0.1655	366	29979	43	0.30	31.54	0.83	0.00
4	0.95	0.9	BP-RF	7738.85	7738.85	0.1655	391	34203	175	0.65	321.44	0.79	0.00
4	0.95	0.95	BP-HFX	2745.77	2745.77	0.2673	442	43954	325	0.32	781.43	1.35	0.00
4	0.95	0.95	BP-HFY	2745.77	2745.77	0.2673	387	33437	105	0.35	91.09	1.21	0.00
4	0.95	0.95	BP-RF	2745.77	2745.77	0.2673	421	39857	351	0.67	918.33	1.13	0.00
4	0.95	0.99	BP-HFX	395.06	395.06	0.4117	401	36110	497	0.35	1048.94	0.84	0.00
4	0.95	0.99	BP-HFY	395.06	395.06	0.4117	319	22626	217	0.31	159.74	0.78	0.00
4	0.95	0.99	BP-RF	395.23	395.23	0.37	414	38582	615	0.47	1949.08	0.80	0.00
4	0.99	0.9	BP-HFX	8192.66	8192.66	0.1717	430	41485	205	0.33	412.50	0.81	0.00
4	0.99	0.9	BP-HFY	8192.66	8192.66	0.1717	361	29045	63	0.27	42.75	0.82	0.00
4	0.99	0.9	BP-RF	8193.97	8193.97	0.1557	394	34669	139	0.75	311.24	0.60	0.00
4	0.99	0.95	BP-HFX	2936.63	2936.63	0.2731	424	40324	301	0.43	668.41	1.25	0.00
4	0.99	0.95	BP-HFY	2936.63	2936.63	0.2731	379	32057	87	0.48	73.99	1.29	0.00
4	0.99	0.95	BP-RF	2936.63	2936.63	0.2731	409	37553	341	1.42	796.11	1.08	0.00
4	0.99	0.99	BP-HFX	427.47	427.47	0.4136	403	36438	499	0.38	1088.07	0.82	0.00
4	0.99	0.99	BP-HFY	427.55	427.55	0.3948	313	21811	171	0.29	104.36	0.76	0.00
4	0.99	0.99	BP-RF	427.87	427.87	0.3189	385	33290	426	1.01	1094.77	0.78	0.00

Table 4.39: Comparison of Branching Rules for N=12, Instance ID = 5

L	Se	Sp	Configuration	LB	UB	Δ UB (%)	$\#y$	$\#x$	# nodes	Time$_r$ (s)	Total Time (s)	Gap$_r$ (%)	Gap (%)
3	0.9	0.9	BP-HFX	7075.36	7075.36	0.044	191	8953	503	0.04	208.05	0.52	0.00
3	0.9	0.9	BP-HFY	7075.35	7075.35	0.044	195	9322	761	0.05	462.75	0.52	0.00
3	0.9	0.9	BP-RF	7076.24	7076.24	0.0316	203	10107	651	0.04	399.67	0.52	0.00
3	0.9	0.95	BP-HFX	2502.42	2502.42	0.0565	195	9327	743	0.05	451.55	0.72	0.00
3	0.9	0.95	BP-HFY	2502.42	2502.42	0.0565	196	9422	725	0.05	433.87	0.16	0.00
3	0.9	0.95	BP-RF	2502.42	2502.42	0.0565	195	9339	453	0.05	176.66	0.17	0.00
3	0.9	0.99	BP-HFX	359.61	359.61	0.0146	183	8196	753	0.02	429.01	0.07	0.00
3	0.9	0.99	BP-HFY	359.65	359.65	0.0056	143	4995	205	0.04	32.25	0.13	0.00
3	0.9	0.99	BP-RF	359.62	359.62	0.0135	167	6889	575	0.04	229.38	0.11	0.00
3	0.95	0.9	BP-HFX	7622.46	7622.46	0.0452	193	9147	487	0.06	212.63	0.34	0.00
3	0.95	0.9	BP-HFY	7622.46	7622.46	0.0452	192	9036	505	0.06	263.95	0.32	0.00
3	0.95	0.9	BP-RF	7622.48	7622.48	0.045	205	10313	433	0.06	184.32	0.29	0.00
3	0.95	0.95	BP-HFX	2732.78	2732.78	0.0573	198	9615	713	0.06	450.23	0.18	0.00
3	0.95	0.95	BP-HFY	2732.78	2732.78	0.0573	193	9132	647	0.06	410.19	0.62	0.00
3	0.95	0.95	BP-RF	2732.78	2732.78	0.0573	205	10309	903	0.05	767.43	0.69	0.00
3	0.95	0.99	BP-HFX	398.76	398.76	0.0194	179	7851	785	0.04	472.23	0.06	0.00
3	0.95	0.99	BP-HFY	398.84	398.84	0.0	177	7665	603	0.03	305.30	0.11	0.00
3	0.95	0.99	BP-RF	398.84	398.84	0.0	157	6029	283	0.05	64.84	0.13	0.00
3	0.99	0.9	BP-HFX	8074.72	8074.72	0.0461	190	8853	461	0.06	193.91	0.41	0.00
3	0.99	0.9	BP-HFY	8074.72	8074.72	0.0461	192	9044	619	0.06	400.27	0.32	0.00
3	0.99	0.9	BP-RF	8074.72	8074.72	0.0461	201	9933	553	0.06	324.36	0.27	0.00
3	0.99	0.95	BP-HFX	2924.42	2924.42	0.0197	205	10311	775	0.07	554.91	0.14	0.00
3	0.99	0.95	BP-HFY	2924.36	2924.36	0.0219	197	9513	681	0.12	465.78	0.16	0.00
3	0.99	0.95	BP-RF	2924.36	2924.36	0.0219	201	9924	805	0.06	659.86	0.53	0.00
3	0.99	0.99	BP-HFX	431.61	431.61	0.0054	181	8039	711	0.05	393.01	0.13	0.00
3	0.99	0.99	BP-HFY	431.57	431.57	0.0134	174	7404	565	0.03	269.52	0.09	0.00
3	0.99	0.99	BP-RF	431.63	431.63	0.0001	203	10109	1449	0.05	1876.45	0.07	0.00
4	0.9	0.9	BP-HFX	11231.50	11231.50	0.0756	392	34116	259	0.09	460.21	0.64	0.00
4	0.9	0.9	BP-HFY	11231.50	11231.50	0.0756	308	20871	57	0.17	30.75	0.69	0.00
4	0.9	0.9	BP-RF	11233.21	11233.21	0.0604	321	22846	75	0.20	45.26	0.52	0.00
4	0.9	0.95	BP-HFX	4419.91	4419.91	0.0964	400	35611	401	0.15	990.37	0.65	0.00
4	0.9	0.95	BP-HFY	4419.91	4419.91	0.0964	307	20700	97	0.16	57.97	0.49	0.00
4	0.9	0.95	BP-RF	4420.95	4420.95	0.073	334	24777	103	0.15	78.66	0.64	0.00
4	0.9	0.99	BP-HFX	712.55	712.55	0.1088	371	30600	591	0.11	1590.38	0.14	0.00
4	0.9	0.99	BP-HFY	712.48	712.48	0.1189	270	15972	167	0.14	93.39	1.18	0.00
4	0.9	0.99	BP-RF	712.67	712.67	0.0925	275	16819	113	0.15	43.68	0.17	0.00
4	0.95	0.9	BP-HFX	12219.16	12219.16	0.0781	379	31769	233	0.22	381.55	0.46	0.00
4	0.95	0.9	BP-HFY	12219.16	12219.16	0.0781	267	15642	35	0.15	14.49	0.31	0.00
4	0.95	0.9	BP-RF	12219.68	12219.68	0.0737	337	25282	69	0.22	64.37	0.42	0.00
4	0.95	0.95	BP-HFX	4858.78	4858.78	0.0976	400	35632	415	0.19	1048.97	0.57	0.00
4	0.95	0.95	BP-HFY	4858.78	4858.78	0.0976	350	27063	139	0.14	125.78	0.70	0.00
4	0.95	0.95	BP-RF	4858.93	4858.93	0.0947	324	23287	71	0.12	55.30	0.73	0.00
4	0.95	0.99	BP-HFX	791.50	791.50	0.1139	366	29666	621	0.16	1554.45	0.17	0.00
4	0.95	0.99	BP-HFY	791.49	791.49	0.1156	248	13482	150	0.18	77.27	0.17	0.00
4	0.95	0.99	BP-RF	792.41	792.41	0.0	373	31216	251	0.14	349.82	0.12	0.00
4	0.99	0.9	BP-HFX	13039.16	13039.16	0.0792	391	33966	277	0.11	537.85	0.42	0.00
4	0.99	0.9	BP-HFY	13039.16	13039.16	0.0792	305	20431	45	0.13	29.42	0.63	0.00
4	0.99	0.9	BP-RF	13042.42	13042.42	0.0542	330	24164	73	0.28	61.77	0.50	0.00
4	0.99	0.95	BP-HFX	5224.82	5224.82	0.0985	395	34640	433	0.18	1145.01	0.71	0.00
4	0.99	0.95	BP-HFY	5224.82	5224.82	0.0985	330	23932	107	0.18	87.20	0.68	0.00
4	0.99	0.95	BP-RF	5224.82	5224.82	0.0985	348	27014	163	0.14	154.55	0.74	0.00
4	0.99	0.99	BP-HFX	857.64	857.64	0.1194	375	31192	604	0.15	1581.25	0.17	0.00
4	0.99	0.99	BP-HFY	857.68	857.68	0.1141	243	12961	130	0.19	64.30	0.18	0.00
4	0.99	0.99	BP-RF	857.71	857.71	0.1103	253	14175	67	0.22	36.29	0.18	0.00

Table 4.40: Comparison of Branching Rules for N=16, Instance ID = 1

L	Se	Sp	Configuration	LB	UB	Δ UB (%)	$\#y$	$\#x$	# nodes	Time$_r$ (s)	Total Time (s)	Gap$_r$ (%)	Gap (%)
4	0.9	0.9	BP-HFX	15502.60	15502.60	0.0123	1043	260629	399	0.49	TL	0.70	0.00
4	0.9	0.9	BP-HFY	15396.23	15504.45	0.0003	754	136515	666	0.48	TL	0.70	0.70
4	0.9	0.9	BP-RF	15396.23	15504.28	0.0014	930	206772	244	0.50	TL	0.70	0.70
4	0.9	0.95	BP-HFX	6085.40	6112.78	0.0	1027	252350	128	0.47	TL	0.90	0.45
4	0.9	0.95	BP-HFY	6112.28	6112.28	0.0082	893	189977	99	0.47	1867.84	0.92	0.00
4	0.9	0.95	BP-RF	6047.11	6112.78	0.0	848	172067	239	0.53	TL	1.09	1.09
4	0.9	0.99	BP-HFX	979.28	985.16	0.0	885	187591	249	0.71	TL	0.60	0.60
4	0.9	0.99	BP-HFY	979.38	985.16	0.0	693	114897	566	0.49	TL	0.59	0.59
4	0.9	0.99	BP-RF	979.36	985.16	0.0	874	183305	283	0.53	TL	0.59	0.59
4	0.95	0.9	BP-HFX	16817.56	16870.78	0.012	1098	289305	245	0.54	TL	0.93	0.32
4	0.95	0.9	BP-HFY	16746.07	16872.80	0.0	792	150726	667	0.45	TL	0.76	0.76
4	0.95	0.9	BP-RF	16735.28	16872.80	0.0	902	194694	189	0.45	TL	0.82	0.82
4	0.95	0.95	BP-HFX	6689.40	6720.07	0.0	1044	261801	88	0.66	TL	1.56	0.46
4	0.95	0.95	BP-HFY	6719.49	6719.49	0.0087	941	211459	113	0.64	2409.64	0.89	0.00
4	0.95	0.95	BP-RF	6662.12	6720.07	0.0	885	187116	195	0.54	TL	0.87	0.87
4	0.95	0.99	BP-HFX	1087.55	1094.35	0.0	828	164062	276	0.44	TL	1.62	0.63
4	0.95	0.99	BP-HFY	1094.35	1094.35	0.0	549	71078	61	0.66	241.92	0.61	0.00
4	0.95	0.99	BP-RF	1087.78	1094.35	0.0	851	172805	217	0.49	TL	0.60	0.60
4	0.99	0.9	BP-HFX	17948.12	18006.62	0.0143	1125	304047	170	0.40	TL	0.96	0.33
4	0.99	0.9	BP-HFY	17803.73	18008.80	0.0022	783	147510	611	0.39	TL	1.15	1.15
4	0.99	0.9	BP-RF	18001.01	18001.01	0.0455	898	193073	202	0.53	2523.30	0.69	0.00
4	0.99	0.95	BP-HFX	7192.82	7226.57	0.0	1056	267709	108	0.55	TL	0.97	0.47
4	0.99	0.95	BP-HFY	7225.67	7225.67	0.0124	1001	239832	191	0.67	TL	0.93	0.00
4	0.99	0.95	BP-RF	7154.52	7210.26	0.2257	948	215543	187	0.55	TL	1.01	0.78
4	0.99	0.99	BP-HFX	1185.83	1185.83	0.0	874	183205	275	0.52	TL	1.52	0.00
4	0.99	0.99	BP-HFY	1185.83	1185.83	0.0	806	155518	427	0.69	TL	1.54	0.00
4	0.99	0.99	BP-RF	1169.13	1185.83	0.0	832	165281	269	0.68	TL	1.43	1.43

Table 4.41: Comparison of Branching Rules for N=16, Instance ID = 2

L	Se	Sp	Configuration	LB	UB	Δ UB (%)	$\#y$	$\#x$	# nodes	Time$_r$ (s)	Total Time (s)	Gap$_r$ (%)	Gap (%)
4	0.9	0.9	BP-HFX	10513.78	10513.78	0.0078	1144	314284	71	0.51	TL	0.87	0.00
4	0.9	0.9	BP-HFY	10493.90	10512.79	0.0172	1159	322493	228	0.51	TL	0.87	0.18
4	0.9	0.9	BP-RF	10423.73	10514.60	0.0	947	215633	128	0.49	TL	0.87	0.87
4	0.9	0.95	BP-HFX	3719.52	3736.50	0.0	1072	275537	66	0.85	TL	1.07	0.46
4	0.9	0.95	BP-HFY	3720.37	3735.84	0.0177	1051	264261	168	0.86	TL	0.95	0.42
4	0.9	0.95	BP-RF	3698.39	3736.31	0.0051	876	184269	157	0.90	TL	1.03	1.03
4	0.9	0.99	BP-HFX	531.55	535.38	0.0	974	227388	349	0.49	TL	0.72	0.72
4	0.9	0.99	BP-HFY	531.17	535.38	0.0	867	180079	438	0.71	TL	0.79	0.79
4	0.9	0.99	BP-RF	531.33	535.38	0.0	819	160588	283	0.43	TL	0.76	0.76
4	0.95	0.9	BP-HFX	11308.57	11335.47	0.0012	1089	284597	56	0.80	TL	0.63	0.24
4	0.95	0.9	BP-HFY	11311.81	11333.53	0.0183	1143	313153	168	0.53	TL	0.64	0.19
4	0.95	0.9	BP-RF	11245.47	11335.57	0.0002	957	219865	117	0.59	TL	0.80	0.80
4	0.95	0.95	BP-HFX	4061.30	4080.80	0.0001	1052	264993	74	0.76	TL	1.30	0.48
4	0.95	0.95	BP-HFY	4061.99	4079.60	0.0293	1177	332584	204	0.83	TL	1.05	0.43
4	0.95	0.95	BP-RF	4036.47	4080.80	0.0001	913	200082	177	0.80	TL	1.10	1.10
4	0.95	0.99	BP-HFX	589.12	593.62	0.0	940	212333	136	0.55	TL	0.76	0.76
4	0.95	0.99	BP-HFY	589.08	593.62	0.0	899	193314	407	0.54	TL	0.77	0.77
4	0.95	0.99	BP-RF	588.91	593.62	0.0	784	147545	339	0.57	TL	0.80	0.80
4	0.99	0.9	BP-HFX	11983.99	12012.95	0.0088	1119	300529	86	0.55	TL	0.76	0.24
4	0.99	0.9	BP-HFY	11985.80	12011.75	0.0187	1174	331425	271	0.60	TL	0.74	0.22
4	0.99	0.9	BP-RF	11899.13	12014.00	0.0	908	197737	124	0.58	TL	0.97	0.97
4	0.99	0.95	BP-HFX	4367.05	4367.05	0.0	1049	263669	77	0.89	TL	1.21	0.00
4	0.99	0.95	BP-HFY	4346.30	4366.20	0.0195	1093	286052	161	1.23	TL	1.03	0.46
4	0.99	0.95	BP-RF	4328.15	4365.47	0.0361	1168	328543	121	1.07	TL	0.90	0.86
4	0.99	0.99	BP-HFX	642.38	642.38	0.0	1004	242737	211	0.73	TL	0.82	0.00
4	0.99	0.99	BP-HFY	642.38	642.38	0.0	913	199746	391	0.92	TL	0.80	0.00
4	0.99	0.99	BP-RF	637.21	642.33	0.0087	804	154894	178	0.99	TL	0.81	0.80

Table 4.42: Comparison of Branching Rules for N=16, Instance ID = 3

L	Se	Sp	Configuration	LB	UB	Δ UB (%)	$\#y$	$\#x$	# nodes	Time$_r$ (s)	Total Time (s)	Gap$_r$ (%)	Gap (%)
4	0.9	0.9	BP-HFX	15339.92	15340.70	0.0964	884	185911	128	0.52	TL	0.47	0.01
4	0.9	0.9	BP-HFY	15340.70	15340.70	0.0964	721	122894	59	0.53	345.13	0.47	0.00
4	0.9	0.9	BP-RF	15283.90	15340.70	0.0964	828	163901	304	0.55	TL	0.47	0.37
4	0.9	0.95	BP-HFX	6048.72	6048.72	0.1253	626	92570	51	0.65	424.56	0.53	0.00
4	0.9	0.95	BP-HFY	6048.88	6048.88	0.1226	510	61020	34	0.60	77.45	0.63	0.00
4	0.9	0.95	BP-RF	6020.39	6053.80	0.0414	790	149369	327	0.56	TL	0.60	0.55
4	0.9	0.99	BP-HFX	975.90	975.90	0.0	270	16869	19	0.47	16.67	0.02	0.00
4	0.9	0.99	BP-HFY	975.90	975.90	0.0	136	4299	3	0.36	0.87	0.00	0.00
4	0.9	0.99	BP-RF	975.90	975.90	0.0	291	19989	27	0.54	22.70	0.01	0.00
4	0.95	0.9	BP-HFX	16694.06	16694.06	0.0972	868	178892	123	0.44	TL	0.63	0.00
4	0.95	0.9	BP-HFY	16693.67	16693.67	0.0995	838	166643	103	0.46	679.97	0.62	0.00
4	0.95	0.9	BP-RF	16606.80	16699.04	0.0674	891	189931	290	0.51	TL	0.62	0.56
4	0.95	0.95	BP-HFX	6649.94	6649.94	0.1721	628	93053	55	0.69	510.45	1.03	0.00
4	0.95	0.95	BP-HFY	6649.83	6649.83	0.1737	589	81486	29	0.48	131.32	0.93	0.00
4	0.95	0.95	BP-RF	6650.00	6650.00	0.1711	695	114921	55	0.59	814.67	0.72	0.00
4	0.95	0.99	BP-HFX	1084.08	1084.08	0.0	187	7926	7	0.48	2.69	0.03	0.00
4	0.95	0.99	BP-HFY	1084.08	1084.08	0.0	221	11160	9	0.48	5.21	0.03	0.00
4	0.95	0.99	BP-RF	1083.93	1083.93	0.0142	343	27632	31	0.39	41.35	0.85	0.00
4	0.99	0.9	BP-HFX	17816.70	17816.96	0.1012	879	183575	116	0.53	TL	0.75	0.00
4	0.99	0.9	BP-HFY	17816.96	17816.96	0.1012	839	167175	73	0.56	673.21	0.73	0.00
4	0.99	0.9	BP-RF	17731.36	17816.96	0.1012	913	199207	204	0.53	TL	0.58	0.48
4	0.99	0.95	BP-HFX	7151.39	7151.39	0.1029	777	143357	93	0.57	1358.05	0.84	0.00
4	0.99	0.95	BP-HFY	7151.17	7151.17	0.1059	619	90420	37	0.37	164.21	0.74	0.00
4	0.99	0.95	BP-RF	7151.17	7151.17	0.1059	855	175203	123	0.34	3354.35	0.62	0.00
4	0.99	0.99	BP-HFX	1174.72	1174.72	0.0002	137	4266	3	0.41	0.85	0.86	0.00
4	0.99	0.99	BP-HFY	1174.72	1174.72	0.0002	190	8235	5	0.45	2.70	0.94	0.00
4	0.99	0.99	BP-RF	1174.72	1174.72	0.0002	360	30210	23	0.50	49.42	0.03	0.00

Table 4.43: Comparison of Branching Rules for N=16, Instance ID = 4

L	Se	Sp	Configuration	LB	UB	Δ UB (%)	$\#y$	$\#x$	# nodes	Time$_r$ (s)	Total Time (s)	Gap$_r$ (%)	Gap (%)
4	0.9	0.9	BP-HFX	11093.57	11093.57	0.0003	997	238252	65	0.45	TL	0.65	0.00
4	0.9	0.9	BP-HFY	11092.67	11092.67	0.0083	1085	281976	135	0.51	TL	0.65	0.00
4	0.9	0.9	BP-RF	11022.39	11093.57	0.0003	861	178301	138	0.51	TL	0.65	0.65
4	0.9	0.95	BP-HFX	3997.28	4014.02	0.0001	1024	251380	88	0.50	TL	0.96	0.42
4	0.9	0.95	BP-HFY	3999.21	4013.31	0.0176	1010	244063	336	0.87	TL	0.90	0.35
4	0.9	0.95	BP-RF	3982.88	4013.64	0.0094	883	187699	194	0.74	TL	0.78	0.77
4	0.9	0.99	BP-HFX	583.97	588.34	0.0	1035	256955	247	0.54	TL	0.75	0.75
4	0.9	0.99	BP-HFY	583.99	588.33	0.0012	880	185355	405	0.34	TL	0.74	0.74
4	0.9	0.99	BP-RF	584.07	588.31	0.0041	813	158663	366	0.47	TL	0.73	0.73
4	0.95	0.9	BP-HFX	11978.29	11978.29	0.0001	1131	307270	81	0.54	TL	0.62	0.00
4	0.95	0.9	BP-HFY	11967.10	11977.49	0.0068	1084	281282	140	0.68	TL	0.63	0.09
4	0.95	0.9	BP-RF	11897.02	11978.29	0.0001	883	187378	130	0.49	TL	0.68	0.68
4	0.95	0.95	BP-HFX	4389.12	4389.12	0.0	1102	291493	81	0.54	TL	1.13	0.00
4	0.95	0.95	BP-HFY	4371.99	4388.34	0.0177	1057	267802	175	0.60	TL	1.05	0.37
4	0.95	0.95	BP-RF	4349.29	4388.70	0.0095	839	168557	270	1.09	TL	0.92	0.91
4	0.95	0.99	BP-HFX	647.74	652.58	0.0	918	200838	176	0.45	TL	0.75	0.75
4	0.95	0.99	BP-HFY	648.09	652.58	0.0	881	185015	440	0.49	TL	0.73	0.69
4	0.95	0.99	BP-RF	647.79	652.56	0.0042	849	173417	333	0.66	TL	0.74	0.74
4	0.99	0.9	BP-HFX	12710.00	12710.00	0.0	1151	318225	61	0.55	TL	0.65	0.00
4	0.99	0.9	BP-HFY	12708.99	12708.99	0.0079	1091	285004	131	0.64	TL	0.57	0.00
4	0.99	0.9	BP-RF	12613.86	12710.00	0.0	865	180040	201	0.56	TL	0.76	0.76
4	0.99	0.95	BP-HFX	4680.13	4701.19	0.0	1097	289091	102	0.72	TL	0.91	0.45
4	0.99	0.95	BP-HFY	4682.22	4700.35	0.018	1060	269319	216	0.83	TL	1.03	0.39
4	0.99	0.95	BP-RF	4656.36	4700.73	0.0098	869	181704	272	0.81	TL	0.96	0.95
4	0.99	0.99	BP-HFX	701.01	706.37	0.0013	878	184018	296	0.53	TL	0.77	0.76
4	0.99	0.99	BP-HFY	701.21	706.29	0.0118	895	191916	462	0.58	TL	0.77	0.72
4	0.99	0.99	BP-RF	701.08	706.35	0.0042	815	159244	451	0.60	TL	0.76	0.75

Table 4.44: Comparison of Branching Rules for N=16, Instance ID = 5

L	Se	Sp	Configuration	LB	UB	Δ UB (%)	$\#y$	$\#x$	# nodes	Time$_r$ (s)	Total Time (s)	Gap$_r$ (%)	Gap (%)
4	0.9	0.9	BP-HFX	13092.36	13097.89	0.0001	1068	272830	82	0.51	TL	0.36	0.04
4	0.9	0.9	BP-HFY	13097.89	13097.89	0.0001	849	171333	47	0.51	561.46	0.36	0.00
4	0.9	0.9	BP-RF	13097.89	13097.89	0.0001	967	225098	63	0.49	TL	0.36	0.00
4	0.9	0.95	BP-HFX	4956.62	4962.33	0.0001	967	222782	92	0.73	TL	0.57	0.12
4	0.9	0.95	BP-HFY	4962.33	4962.33	0.0001	761	137154	31	0.55	368.50	0.75	0.00
4	0.9	0.95	BP-RF	4936.29	4962.33	0.0001	879	185964	96	0.68	TL	0.53	0.53
4	0.9	0.99	BP-HFX	765.27	766.67	0.0	722	123487	254	0.60	TL	0.18	0.18
4	0.9	0.99	BP-HFY	766.67	766.67	0.0	427	42758	23	0.64	63.59	0.21	0.00
4	0.9	0.99	BP-RF	766.67	766.67	0.0	526	65916	79	0.69	371.16	0.19	0.00
4	0.95	0.9	BP-HFX	14201.00	14201.00	0.0	1058	267547	71	0.51	TL	0.48	0.00
4	0.95	0.9	BP-HFY	14201.00	14201.00	0.0	902	193415	53	0.45	656.07	0.34	0.00
4	0.95	0.9	BP-RF	14185.39	14201.00	0.0	957	220162	49	0.51	TL	0.38	0.11
4	0.95	0.95	BP-HFX	5435.48	5441.98	0.0	967	223164	88	0.57	TL	0.82	0.12
4	0.95	0.95	BP-HFY	5441.98	5441.98	0.0	784	145865	29	0.87	417.94	0.57	0.00
4	0.95	0.95	BP-RF	5412.57	5441.98	0.0	939	212140	173	0.71	TL	0.54	0.54
4	0.95	0.99	BP-HFX	851.10	851.10	0.0	763	138114	223	0.57	TL	0.20	0.00
4	0.95	0.99	BP-HFY	851.10	851.10	0.0	434	43843	27	0.55	77.07	0.20	0.00
4	0.95	0.99	BP-RF	849.43	851.10	0.0	807	156823	346	0.50	TL	0.20	0.20
4	0.99	0.9	BP-HFX	15108.01	15115.25	0.0003	1072	274535	94	0.46	TL	0.56	0.05
4	0.99	0.9	BP-HFY	15115.25	15115.25	0.0003	901	193386	43	0.39	573.68	0.51	0.00
4	0.99	0.9	BP-RF	15115.25	15115.25	0.0003	987	234439	49	0.59	TL	0.51	0.00
4	0.99	0.95	BP-HFX	5834.16	5841.58	0.0	969	224094	84	0.82	TL	0.60	0.13
4	0.99	0.95	BP-HFY	5841.58	5841.58	0.0	820	159832	31	1.16	550.83	0.53	0.00
4	0.99	0.95	BP-RF	5803.38	5841.58	0.0	894	192741	136	0.77	TL	0.66	0.66
4	0.99	0.99	BP-HFX	921.81	921.81	0.0	694	113479	283	0.58	TL	0.19	0.00
4	0.99	0.99	BP-HFY	921.81	921.81	0.0	472	51851	29	0.74	98.52	0.19	0.00
4	0.99	0.99	BP-RF	919.76	921.81	0.0	755	136901	222	0.88	TL	0.22	0.22

Table 4.45: Comparison of Branching Rules for N=25, Instance ID = 1

L	Se	Sp	Configuration	LB	UB	Δ UB (%)	$\#y$	$\#x$	# nodes	Time$_r$ (s)	Total Time (s)	Gap$_r$ (%)	Gap (%)
5	0.9	0.9	BP-HFX	35425.53	35601.40	0.0	1591	514918	44	3.72	TL	0.50	0.50
5	0.9	0.9	BP-HFY	35425.53	35599.95	0.0041	1465	436658	66	3.69	TL	0.50	0.49
5	0.9	0.9	BP-RF	35425.53	35601.40	0.0	1355	402129	64	3.69	TL	0.50	0.50
5	0.9	0.95	BP-HFX	14996.59	15089.88	0.0214	1365	392474	87	5.79	TL	0.64	0.62
5	0.9	0.95	BP-HFY	15014.54	15087.07	0.0399	1375	401447	112	4.71	TL	0.52	0.48
5	0.9	0.95	BP-RF	15011.90	15093.10	0.0	1113	268272	54	3.88	TL	0.54	0.54
5	0.9	0.99	BP-HFX	2613.09	2614.50	0.0192	1187	294540	57	5.21	TL	0.72	0.05
5	0.9	0.99	BP-HFY	2599.80	2614.45	0.021	1134	278571	103	7.29	TL	0.58	0.56
5	0.9	0.99	BP-RF	2594.07	2615.00	0.0001	1041	241552	57	5.01	TL	0.81	0.81
5	0.95	0.9	BP-HFX	38833.46	39012.07	0.0001	1673	597628	65	6.14	TL	0.46	0.46
5	0.95	0.9	BP-HFY	38794.33	39012.07	0.0001	1492	461733	72	6.29	TL	0.56	0.56
5	0.95	0.9	BP-RF	38754.12	39012.07	0.0001	1192	310499	44	6.30	TL	0.67	0.67
5	0.95	0.95	BP-HFX	16587.65	16658.63	0.001	1468	438907	45	11.26	TL	0.43	0.43
5	0.95	0.95	BP-HFY	16582.50	16658.46	0.002	1452	441917	113	9.43	TL	0.46	0.46
5	0.95	0.95	BP-RF	16584.07	16658.76	0.0002	1136	282261	36	10.40	TL	0.45	0.45
5	0.95	0.99	BP-HFX	2905.98	2907.18	0.0247	1246	331681	40	4.50	TL	0.72	0.04
5	0.95	0.99	BP-HFY	2883.60	2907.38	0.0179	1183	299243	61	5.39	TL	0.84	0.82
5	0.95	0.99	BP-RF	2886.14	2907.90	0.0	1070	253542	63	4.02	TL	0.75	0.75
5	0.99	0.9	BP-HFX	41537.45	41852.69	0.0	1686	598911	33	2.85	TL	0.76	0.76
5	0.99	0.9	BP-HFY	41570.07	41845.01	0.0184	1420	409805	92	4.95	TL	0.68	0.66
5	0.99	0.9	BP-RF	41649.96	41834.73	0.0429	1267	350698	44	4.43	TL	0.49	0.44
5	0.99	0.95	BP-HFX	17864.47	17972.11	0.0283	1554	503062	84	5.44	TL	0.63	0.60
5	0.99	0.95	BP-HFY	17879.08	17970.28	0.0385	1409	418629	89	5.02	TL	0.55	0.51
5	0.99	0.95	BP-RF	17882.70	17977.16	0.0002	1162	292406	34	6.01	TL	0.53	0.53
5	0.99	0.99	BP-HFX	3129.42	3153.42	0.0	1302	350450	37	4.52	TL	0.77	0.77
5	0.99	0.99	BP-HFY	3128.84	3152.96	0.0146	1047	234756	102	4.99	TL	0.79	0.77
5	0.99	0.99	BP-RF	3134.83	3153.42	0.0	1091	259518	47	4.25	TL	0.59	0.59

Table 4.46: Comparison of Branching Rules for N=25, Instance ID = 2

L	Se	Sp	Configuration	LB	UB	Δ UB (%)	$\#y$	$\#x$	# nodes	Time$_r$ (s)	Total Time (s)	Gap$_r$ (%)	Gap (%)
5	0.9	0.9	BP-HFX	28859.43	29041.70	0.0	1623	555452	37	5.99	TL	0.63	0.63
5	0.9	0.9	BP-HFY	28859.43	29041.70	0.0	1503	470234	60	5.97	TL	0.63	0.63
5	0.9	0.9	BP-RF	28859.43	29041.70	0.0	1196	317364	27	6.03	TL	0.63	0.63
5	0.9	0.95	BP-HFX	11724.20	11833.69	0.0018	1432	427910	61	4.83	TL	0.94	0.93
5	0.9	0.95	BP-HFY	11744.47	11833.85	0.0004	1494	469890	54	4.56	TL	0.76	0.76
5	0.9	0.95	BP-RF	11757.01	11833.85	0.0004	1164	292675	29	6.00	TL	0.65	0.65
5	0.9	0.99	BP-HFX	1953.82	1973.10	0.0	1547	514084	65	6.97	TL	0.99	0.99
5	0.9	0.99	BP-HFY	1956.19	1973.03	0.0036	1090	247752	124	6.89	TL	0.86	0.86
5	0.9	0.99	BP-RF	1951.14	1973.10	0.0	1056	246443	56	7.08	TL	1.13	1.13
5	0.95	0.9	BP-HFX	31493.77	31702.80	0.0	1569	531517	60	5.34	TL	0.66	0.66
5	0.95	0.9	BP-HFY	31522.19	31698.79	0.0127	1481	472936	67	7.08	TL	0.57	0.56
5	0.95	0.9	BP-RF	31479.47	31702.80	0.0	1223	327996	22	4.96	TL	0.71	0.71
5	0.95	0.95	BP-HFX	12924.39	13035.39	0.0001	1576	527040	42	4.89	TL	0.86	0.86
5	0.95	0.95	BP-HFY	12931.23	13035.39	0.0001	1401	416095	58	4.77	TL	0.81	0.81
5	0.95	0.95	BP-RF	12933.07	13035.39	0.0001	1077	257746	24	8.59	TL	0.79	0.79
5	0.95	0.99	BP-HFX	2172.15	2192.88	0.0	1775	670369	21	7.04	TL	0.95	0.95
5	0.95	0.99	BP-HFY	2169.24	2192.25	0.0289	1316	349690	106	4.46	TL	1.09	1.06
5	0.95	0.99	BP-RF	2172.63	2192.88	0.0	1355	402259	64	6.00	TL	0.93	0.93
5	0.99	0.9	BP-HFX	33700.88	33915.30	0.0	1680	601080	29	7.03	TL	0.64	0.64
5	0.99	0.9	BP-HFY	33687.49	33915.30	0.0	1458	441675	60	5.93	TL	0.68	0.68
5	0.99	0.9	BP-RF	33695.66	33915.30	0.0	1250	342719	23	4.90	TL	0.65	0.65
5	0.99	0.95	BP-HFX	13943.50	14038.38	0.0001	1617	539029	27	6.73	TL	0.68	0.68
5	0.99	0.95	BP-HFY	13898.99	14038.38	0.0001	1340	369335	84	6.35	TL	1.00	1.00
5	0.99	0.95	BP-RF	13948.63	14038.38	0.0001	1093	263127	22	8.00	TL	0.64	0.64
5	0.99	0.99	BP-HFX	2354.35	2378.47	0.0	1426	429026	97	7.35	TL	1.02	1.02
5	0.99	0.99	BP-HFY	2353.79	2377.83	0.0269	1211	308281	110	5.40	TL	1.05	1.02
5	0.99	0.99	BP-RF	2354.55	2374.45	0.1691	1145	286341	58	6.59	TL	1.02	0.85

Table 4.47: Comparison of Branching Rules for N=25, Instance ID = 3

L	Se	Sp	Configuration	LB	UB	Δ UB (%)	$\#y$	$\#x$	# nodes	Time$_r$ (s)	Total Time (s)	Gap$_r$ (%)	Gap (%)
5	0.9	0.9	BP-HFX	31351.32	31546.02	0.0088	1604	544266	71	4.30	TL	0.63	0.62
5	0.9	0.9	BP-HFY	31351.32	31548.78	0.0001	1281	331462	141	4.55	TL	0.63	0.63
5	0.9	0.9	BP-RF	31351.32	31548.78	0.0001	1401	421874	54	4.42	TL	0.63	0.63
5	0.9	0.95	BP-HFX	12956.69	13078.90	0.0	1699	608620	36	3.19	TL	0.94	0.94
5	0.9	0.95	BP-HFY	13000.41	13078.90	0.0	1540	494840	43	6.00	TL	0.60	0.60
5	0.9	0.95	BP-RF	13002.78	13078.90	0.0	1262	343178	50	5.70	TL	0.59	0.59
5	0.9	0.99	BP-HFX	2201.58	2218.49	0.0	1391	399624	85	5.33	TL	0.77	0.77
5	0.9	0.99	BP-HFY	2202.75	2218.49	0.0	1285	336617	81	6.29	TL	0.71	0.71
5	0.9	0.99	BP-RF	2201.04	2218.49	0.0	1177	298319	84	5.30	TL	0.79	0.79
5	0.95	0.9	BP-HFX	34214.49	34495.40	0.0	1642	568987	92	3.20	TL	0.82	0.82
5	0.95	0.9	BP-HFY	34312.14	34495.40	0.0	1257	313348	148	6.62	TL	0.53	0.53
5	0.95	0.9	BP-RF	34330.86	34495.40	0.0	1197	307634	36	3.42	TL	0.48	0.48
5	0.95	0.95	BP-HFX	14329.38	14421.78	0.0001	1750	641639	23	3.91	TL	0.64	0.64
5	0.95	0.95	BP-HFY	14332.57	14421.78	0.0001	1466	425842	48	8.43	TL	0.62	0.62
5	0.95	0.95	BP-RF	14327.90	14421.78	0.0001	1224	326055	57	7.32	TL	0.66	0.66
5	0.95	0.99	BP-HFX	2437.87	2466.24	0.0001	1408	397879	43	4.98	TL	1.16	1.16
5	0.95	0.99	BP-HFY	2447.23	2466.24	0.0001	1285	322299	80	7.01	TL	0.78	0.78
5	0.95	0.99	BP-RF	2449.26	2466.24	0.0001	1124	276252	88	5.67	TL	0.69	0.69
5	0.99	0.9	BP-HFX	36668.73	36947.10	0.0	1552	492843	92	4.93	TL	0.76	0.76
5	0.99	0.9	BP-HFY	36707.50	36935.45	0.0315	1511	471161	47	5.99	TL	0.65	0.62
5	0.99	0.9	BP-RF	36694.08	36947.10	0.0	1118	273784	35	6.34	TL	0.69	0.69
5	0.99	0.95	BP-HFX	15373.55	15543.28	0.0001	1562	503042	96	3.74	TL	1.10	1.10
5	0.99	0.95	BP-HFY	15438.89	15543.28	0.0001	1322	374209	89	6.24	TL	0.68	0.68
5	0.99	0.95	BP-RF	15432.33	15543.28	0.0001	1090	249909	32	4.84	TL	0.72	0.72
5	0.99	0.99	BP-HFX	2641.62	2673.87	0.0	1342	374944	81	6.46	TL	1.22	1.22
5	0.99	0.99	BP-HFY	2652.37	2673.87	0.0	1295	327620	81	4.24	TL	0.81	0.81
5	0.99	0.99	BP-RF	2645.49	2673.87	0.0	1098	261261	60	4.65	TL	1.07	1.07

Table 4.48: Comparison of Branching Rules for N=25, Instance ID = 4

L	Se	Sp	Configuration	LB	UB	Δ UB (%)	$\#y$	$\#x$	# nodes	Time$_r$ (s)	Total Time (s)	Gap$_r$ (%)	Gap (%)
5	0.9	0.9	BP-HFX	36707.55	36918.08	0.0079	1850	721278	41	4.10	TL	0.58	0.57
5	0.9	0.9	BP-HFY	36707.55	36910.40	0.0287	1470	447293	98	3.78	TL	0.58	0.55
5	0.9	0.9	BP-RF	36707.55	36921.00	0.0	1125	278002	33	3.96	TL	0.58	0.58
5	0.9	0.95	BP-HFX	15666.80	15746.00	0.0159	1436	415707	80	3.55	TL	0.52	0.51
5	0.9	0.95	BP-HFY	15666.80	15745.17	0.0212	1362	389045	107	3.71	TL	0.52	0.50
5	0.9	0.95	BP-RF	15664.16	15748.50	0.0	1199	316320	35	5.78	TL	0.54	0.54
5	0.9	0.99	BP-HFX	2729.54	2744.69	0.0	1301	351612	41	4.63	TL	0.55	0.55
5	0.9	0.99	BP-HFY	2729.09	2744.69	0.0	1025	221344	148	5.27	TL	0.57	0.57
5	0.9	0.99	BP-RF	2725.64	2744.69	0.0	1061	248520	61	4.49	TL	0.70	0.70
5	0.95	0.9	BP-HFX	40150.87	40467.53	0.0328	1696	604713	46	3.49	TL	0.82	0.79
5	0.95	0.9	BP-HFY	40208.87	40471.23	0.0236	1389	389229	121	4.13	TL	0.68	0.65
5	0.95	0.9	BP-RF	40292.63	40480.80	0.0	1303	371434	43	5.49	TL	0.47	0.47
5	0.95	0.95	BP-HFX	17248.97	17394.10	0.0	1835	732125	33	3.50	TL	0.84	0.84
5	0.95	0.95	BP-HFY	17270.28	17390.38	0.0214	1284	341972	123	3.92	TL	0.72	0.70
5	0.95	0.95	BP-RF	17288.14	17394.10	0.0	1256	346954	37	3.72	TL	0.61	0.61
5	0.95	0.99	BP-HFX	3033.20	3051.78	0.0197	1092	256051	64	3.66	TL	0.63	0.61
5	0.95	0.99	BP-HFY	3029.26	3052.38	0.0	1067	245356	147	4.46	TL	0.76	0.76
5	0.95	0.99	BP-RF	3031.91	3052.38	0.0	1174	303787	56	5.08	TL	0.68	0.68
5	0.99	0.9	BP-HFX	43046.05	43446.40	0.0	1761	645819	30	3.30	TL	0.93	0.93
5	0.99	0.9	BP-HFY	43177.67	43431.51	0.0343	1343	379993	77	5.04	TL	0.62	0.59
5	0.99	0.9	BP-RF	43236.05	43446.40	0.0	1273	354932	40	4.90	TL	0.49	0.49
5	0.99	0.95	BP-HFX	18670.15	18769.32	0.0004	1372	396707	140	5.38	TL	0.53	0.53
5	0.99	0.95	BP-HFY	18659.72	18769.32	0.0004	1355	392017	126	7.01	TL	0.59	0.59
5	0.99	0.95	BP-RF	18623.83	18769.40	0.0	1251	337119	68	4.09	TL	0.78	0.78
5	0.99	0.99	BP-HFX	3289.06	3310.30	0.0	1205	304609	83	4.64	TL	0.65	0.65
5	0.99	0.99	BP-HFY	3286.57	3309.54	0.0231	1119	267784	107	5.15	TL	0.72	0.70
5	0.99	0.99	BP-RF	3289.23	3310.30	0.0	1055	243901	57	5.29	TL	0.64	0.64

Table 4.49: Comparison of Branching Rules for N=25, Instance ID = 5

L	Se	Sp	Configuration	LB	UB	Δ UB (%)	$\#y$	$\#x$	# nodes	Time$_r$ (s)	Total Time (s)	Gap$_r$ (%)	Gap (%)
5	0.9	0.9	BP-HFX	33120.80	33267.90	0.0003	1618	554948	86	7.13	TL	0.44	0.44
5	0.9	0.9	BP-HFY	33120.80	33268.00	0.0	1510	480737	100	7.40	TL	0.44	0.44
5	0.9	0.9	BP-RF	33120.80	33268.00	0.0	1101	265167	29	7.48	TL	0.44	0.44
5	0.9	0.95	BP-HFX	13811.87	13920.61	0.005	1529	508623	118	4.62	TL	0.79	0.79
5	0.9	0.95	BP-HFY	13813.03	13918.90	0.0173	1486	477826	93	7.71	TL	0.78	0.77
5	0.9	0.95	BP-RF	13850.16	13921.30	0.0	1076	254613	33	7.14	TL	0.51	0.51
5	0.9	0.99	BP-HFX	2363.04	2381.75	0.0	1384	399073	43	8.04	TL	0.79	0.79
5	0.9	0.99	BP-HFY	2364.07	2381.75	0.0	1273	345285	125	8.33	TL	0.75	0.75
5	0.9	0.99	BP-RF	2363.91	2381.75	0.0	1140	282065	87	9.04	TL	0.75	0.75
5	0.95	0.9	BP-HFX	36195.87	36401.31	0.0302	1565	517720	83	7.24	TL	0.60	0.57
5	0.95	0.9	BP-HFY	36189.00	36402.95	0.0257	1530	494066	101	6.33	TL	0.62	0.59
5	0.95	0.9	BP-RF	36220.41	36412.30	0.0	1107	270171	23	6.15	TL	0.53	0.53
5	0.95	0.95	BP-HFX	15224.60	15356.68	0.0131	1616	557621	66	7.42	TL	0.88	0.87
5	0.95	0.95	BP-HFY	15261.75	15358.00	0.0045	1467	453366	92	7.02	TL	0.64	0.63
5	0.95	0.95	BP-RF	15244.05	15358.70	0.0	1135	279535	32	7.28	TL	0.75	0.75
5	0.95	0.99	BP-HFX	2623.49	2648.05	0.0001	1355	385588	43	7.66	TL	0.94	0.94
5	0.95	0.99	BP-HFY	2623.45	2648.05	0.0001	1148	278486	101	8.68	TL	0.94	0.94
5	0.95	0.99	BP-RF	2631.08	2648.05	0.0001	1103	268649	74	12.03	TL	0.64	0.64
5	0.99	0.9	BP-HFX	38815.47	39015.70	0.0264	1479	451031	90	6.56	TL	0.54	0.52
5	0.99	0.9	BP-HFY	38752.74	39022.42	0.0092	1605	560076	114	7.51	TL	0.71	0.70
5	0.99	0.9	BP-RF	38752.84	39025.99	0.0	1140	287642	27	6.18	TL	0.70	0.70
5	0.99	0.95	BP-HFX	16454.96	16559.40	0.0	1729	641806	34	10.91	TL	0.63	0.63
5	0.99	0.95	BP-HFY	16462.69	16556.49	0.0176	1619	563045	73	7.25	TL	0.59	0.57
5	0.99	0.95	BP-RF	16442.61	16559.40	0.0	1137	280411	31	6.34	TL	0.71	0.71
5	0.99	0.99	BP-HFX	2849.70	2871.24	0.0	1301	360303	49	9.13	TL	0.76	0.76
5	0.99	0.99	BP-HFY	2849.57	2871.21	0.001	1329	365790	79	7.39	TL	0.76	0.76
5	0.99	0.99	BP-RF	2849.01	2871.24	0.0	1206	317063	76	10.85	TL	0.78	0.78

Table 4.65: Comparison of Branching Rules for N=64, Instance ID = 1

L	Se	Sp	Configuration	LB	UB	Δ UB (%)	$\#y$	$\#x$	# nodes	Time$_r$ (s)	Total Time (s)	Gap$_r$ (%)	Gap (%)
4	0.9	0.9	BP-HFX	55463.13	55727.18	0.0	1897	406420	12	61.93	TL	0.48	0.48
4	0.9	0.9	BP-HFY	55463.13	55727.18	0.0	1737	336398	14	61.43	TL	0.48	0.48
4	0.9	0.9	BP-RF	55463.13	55727.18	0.0	1463	229474	15	62.36	TL	0.48	0.48
4	0.9	0.95	BP-HFX	21331.80	21445.10	0.0	1509	256395	12	68.15	TL	0.53	0.53
4	0.9	0.95	BP-HFY	21329.38	21445.10	0.0	1467	237822	12	41.05	TL	0.54	0.54
4	0.9	0.95	BP-RF	21322.44	21445.10	0.0	1178	148961	15	75.42	TL	0.58	0.58
4	0.9	0.99	BP-HFX	3366.66	3366.66	0.0	372	14417	1	56.28	56.90	0.00	0.00
4	0.9	0.99	BP-HFY	3366.66	3366.66	0.0	366	14047	1	57.14	57.89	0.00	0.00
4	0.9	0.99	BP-RF	3366.66	3366.66	0.0	377	14742	1	65.61	66.26	0.00	0.00
4	0.95	0.9	BP-HFX	60198.04	60506.76	0.0001	1857	402527	12	72.51	TL	0.51	0.51
4	0.95	0.9	BP-HFY	60293.80	60506.76	0.0001	1829	372554	12	84.30	TL	0.35	0.35
4	0.95	0.9	BP-RF	60271.60	60506.76	0.0001	1522	248721	13	81.46	TL	0.39	0.39
4	0.95	0.95	BP-HFX	23419.26	23535.40	0.0	1528	257344	11	54.30	TL	0.50	0.50
4	0.95	0.95	BP-HFY	23407.79	23535.40	0.0	1554	265182	12	47.31	TL	0.55	0.55
4	0.95	0.95	BP-RF	23454.87	23535.40	0.0	1242	164722	18	56.43	TL	0.34	0.34
4	0.95	0.99	BP-HFX	3738.31	3738.31	0.0001	424	18859	3	74.56	151.82	0.00	0.00
4	0.95	0.99	BP-HFY	3738.31	3738.31	0.0001	400	16782	1	60.79	76.56	0.00	0.00
4	0.95	0.99	BP-RF	3738.04	3738.31	0.0001	820	72476	41	56.73	TL	0.01	0.01
4	0.99	0.9	BP-HFX	64190.95	64467.30	0.0	1843	390817	11	71.66	TL	0.43	0.43
4	0.99	0.9	BP-HFY	64199.42	64467.30	0.0	1869	397193	11	124.65	TL	0.42	0.42
4	0.99	0.9	BP-RF	64228.73	64467.30	0.0	1488	239278	13	81.51	TL	0.37	0.37
4	0.99	0.95	BP-HFX	25160.56	25284.20	0.0	1568	276328	12	84.93	TL	0.49	0.49
4	0.99	0.95	BP-HFY	25169.65	25284.20	0.0	1534	257894	11	55.41	TL	0.46	0.46
4	0.99	0.95	BP-RF	25177.74	25284.20	0.0	1244	164513	17	50.22	TL	0.42	0.42
4	0.99	0.99	BP-HFX	4049.50	4049.63	0.0001	1056	126463	33	37.76	TL	0.00	0.00
4	0.99	0.99	BP-HFY	4049.45	4049.63	0.0001	846	76156	43	40.70	TL	0.00	0.00
4	0.99	0.99	BP-RF	4049.31	4049.63	0.0001	780	65286	46	30.64	TL	0.01	0.01

Table 4.66: Comparison of Branching Rules for N=64, Instance ID = 2

L	Se	Sp	Configuration	LB	UB	Δ UB (%)	$\#y$	$\#x$	# nodes	Time$_r$ (s)	Total Time (s)	Gap$_r$ (%)	Gap (%)
4	0.9	0.9	BP-HFX	54022.75	54243.60	0.0	1837	389994	14	51.50	TL	0.41	0.41
4	0.9	0.9	BP-HFY	54022.75	54243.60	0.0	1825	381102	14	51.58	TL	0.41	0.41
4	0.9	0.9	BP-RF	54022.75	54243.60	0.0	1506	245748	15	53.87	TL	0.41	0.41
4	0.9	0.95	BP-HFX	20627.86	20755.09	0.0001	1547	270970	13	43.29	TL	0.62	0.62
4	0.9	0.95	BP-HFY	20654.96	20755.09	0.0001	1459	236600	15	42.69	TL	0.48	0.48
4	0.9	0.95	BP-RF	20640.30	20755.09	0.0001	1290	178587	16	43.30	TL	0.56	0.56
4	0.9	0.99	BP-HFX	3241.36	3242.63	0.0	1185	178401	32	27.63	TL	0.04	0.04
4	0.9	0.99	BP-HFY	3241.46	3242.63	0.0	1135	162069	30	43.48	TL	0.04	0.04
4	0.9	0.99	BP-RF	3241.22	3242.63	0.0	916	93018	41	62.47	TL	0.04	0.04
4	0.95	0.9	BP-HFX	58630.50	58867.80	0.0	1890	412213	13	65.68	TL	0.40	0.40
4	0.95	0.9	BP-HFY	58672.53	58867.80	0.0	1797	365479	15	57.04	TL	0.33	0.33
4	0.95	0.9	BP-RF	58609.82	58867.80	0.0	1497	242269	16	51.79	TL	0.44	0.44
4	0.95	0.95	BP-HFX	22680.77	22775.70	0.0	1548	270841	13	42.17	TL	0.42	0.42
4	0.95	0.95	BP-HFY	22669.61	22775.70	0.0	1505	252224	11	52.05	TL	0.47	0.47
4	0.95	0.95	BP-RF	22584.66	22775.70	0.0	1216	159647	18	40.68	TL	0.85	0.85
4	0.95	0.99	BP-HFX	3599.16	3600.34	0.0001	1249	197196	26	31.25	TL	0.03	0.03
4	0.95	0.99	BP-HFY	3598.50	3600.34	0.0001	1221	182292	30	46.33	TL	0.05	0.05
4	0.95	0.99	BP-RF	3598.71	3600.34	0.0001	870	85930	40	45.57	TL	0.05	0.05
4	0.99	0.9	BP-HFX	62507.96	62689.99	0.0	1883	409857	13	64.83	TL	0.29	0.29
4	0.99	0.9	BP-HFY	62359.12	62689.99	0.0	1835	391053	14	52.70	TL	0.53	0.53
4	0.99	0.9	BP-RF	62480.85	62689.99	0.0	1530	253222	14	61.46	TL	0.33	0.33
4	0.99	0.95	BP-HFX	24346.31	24459.60	0.0	1595	290196	12	47.46	TL	0.47	0.47
4	0.99	0.95	BP-HFY	24314.02	24459.60	0.0	1590	279371	13	50.68	TL	0.60	0.60
4	0.99	0.95	BP-RF	24342.90	24459.60	0.0	1241	166998	17	49.12	TL	0.48	0.48
4	0.99	0.99	BP-HFX	3897.76	3899.97	0.0001	1274	202051	26	48.21	TL	0.06	0.06
4	0.99	0.99	BP-HFY	3855.41	3899.97	0.0001	1252	197815	27	34.19	TL	1.16	1.16
4	0.99	0.99	BP-RF	3858.52	3899.97	0.0001	867	84482	42	24.43	TL	1.07	1.07

Table 4.67: Comparison of Branching Rules for N=64, Instance ID = 3

L	Se	Sp	Configuration	LB	UB	Δ UB (%)	$\#y$	$\#x$	# nodes	Time$_r$ (s)	Total Time (s)	Gap$_r$ (%)	Gap (%)
4	0.9	0.9	BP-HFX	49301.48	49473.00	0.0	1907	408117	10	94.33	TL	0.35	0.35
4	0.9	0.9	BP-HFY	49301.48	49473.00	0.0	1812	364063	11	92.76	TL	0.35	0.35
4	0.9	0.9	BP-RF	49301.48	49473.00	0.0	1617	278741	12	85.16	TL	0.35	0.35
4	0.9	0.95	BP-HFX	18295.15	18423.26	0.0002	1526	260184	11	50.15	TL	0.70	0.70
4	0.9	0.95	BP-HFY	18348.30	18423.26	0.0002	1552	265594	11	63.94	TL	0.41	0.41
4	0.9	0.95	BP-RF	18336.34	18423.26	0.0002	1280	174847	17	49.14	TL	0.47	0.47
4	0.9	0.99	BP-HFX	2788.57	2789.01	0.0	1177	162953	28	47.12	TL	0.02	0.02
4	0.9	0.99	BP-HFY	2788.76	2789.01	0.0	1030	124457	29	44.66	TL	0.01	0.01
4	0.9	0.99	BP-RF	2788.42	2789.01	0.0	1017	116914	37	62.25	TL	0.02	0.02
4	0.95	0.9	BP-HFX	53310.08	53561.38	0.0	1826	375478	11	87.33	TL	0.47	0.47
4	0.95	0.9	BP-HFY	53324.33	53561.38	0.0	1829	375135	11	145.87	TL	0.44	0.44
4	0.95	0.9	BP-RF	53359.40	53561.38	0.0	1572	262987	13	81.59	TL	0.38	0.38
4	0.95	0.95	BP-HFX	20098.83	20185.60	0.0	1553	267030	11	64.08	TL	0.43	0.43
4	0.95	0.95	BP-HFY	20072.54	20185.60	0.0	1537	259107	10	63.92	TL	0.56	0.56
4	0.95	0.95	BP-RF	20088.86	20185.60	0.0	1349	195192	13	57.11	TL	0.48	0.48
4	0.95	0.99	BP-HFX	3094.36	3095.11	0.0	1138	154632	26	104.26	TL	0.02	0.02
4	0.95	0.99	BP-HFY	3094.21	3095.11	0.0	1157	157577	26	65.16	TL	0.03	0.03
4	0.95	0.99	BP-RF	3094.60	3095.11	0.0	992	109392	35	65.55	TL	0.02	0.02
4	0.99	0.9	BP-HFX	56717.68	56962.30	0.0	1894	414399	11	95.57	TL	0.43	0.43
4	0.99	0.9	BP-HFY	56729.34	56962.30	0.0	1912	412379	10	101.28	TL	0.41	0.41
4	0.99	0.9	BP-RF	56713.63	56962.30	0.0	1641	289638	12	91.40	TL	0.44	0.44
4	0.99	0.95	BP-HFX	21571.71	21649.30	0.0	1560	268907	9	71.67	TL	0.36	0.36
4	0.99	0.95	BP-HFY	21553.96	21649.30	0.0	1620	288374	10	65.76	TL	0.44	0.44
4	0.99	0.95	BP-RF	21568.02	21649.30	0.0	1323	187617	13	66.86	TL	0.38	0.38
4	0.99	0.99	BP-HFX	3350.66	3351.46	0.0	1326	214992	24	73.80	TL	0.02	0.02
4	0.99	0.99	BP-HFY	3350.63	3351.46	0.0	1252	186924	24	85.55	TL	0.02	0.02
4	0.99	0.99	BP-RF	3350.70	3351.46	0.0	995	109277	33	67.38	TL	0.02	0.02

Table 4.68: Comparison of Branching Rules for N=64, Instance ID = 4

L	Se	Sp	Configuration	LB	UB	Δ UB (%)	$\#y$	$\#x$	# nodes	Time$_r$ (s)	Total Time (s)	Gap$_r$ (%)	Gap (%)
4	0.9	0.9	BP-HFX	55169.70	55386.36	0.0001	1834	391289	13	54.79	TL	0.39	0.39
4	0.9	0.9	BP-HFY	55169.70	55386.36	0.0001	1814	369976	14	54.45	TL	0.39	0.39
4	0.9	0.9	BP-RF	55169.70	55386.36	0.0001	1559	259733	14	53.63	TL	0.39	0.39
4	0.9	0.95	BP-HFX	21207.28	21297.30	0.0	1536	269872	15	40.60	TL	0.42	0.42
4	0.9	0.95	BP-HFY	21174.55	21297.30	0.0	1483	244046	13	39.34	TL	0.58	0.58
4	0.9	0.95	BP-RF	21117.74	21297.30	0.0	1183	150116	19	39.28	TL	0.85	0.85
4	0.9	0.99	BP-HFX	3343.22	3344.06	0.0	1185	167547	32	62.33	TL	0.03	0.03
4	0.9	0.99	BP-HFY	3343.29	3344.06	0.0	1122	156209	35	37.03	TL	0.02	0.02
4	0.9	0.99	BP-RF	3343.17	3344.06	0.0	916	95964	43	50.45	TL	0.03	0.03
4	0.95	0.9	BP-HFX	59896.26	60137.40	0.0	1919	422470	12	52.74	TL	0.40	0.40
4	0.95	0.9	BP-HFY	59900.75	60137.40	0.0	1896	406074	13	69.56	TL	0.40	0.40
4	0.95	0.9	BP-RF	59903.72	60137.40	0.0	1525	249651	15	59.42	TL	0.39	0.39
4	0.95	0.95	BP-HFX	23251.69	23378.70	0.0	1532	268371	14	41.86	TL	0.55	0.55
4	0.95	0.95	BP-HFY	23273.38	23378.70	0.0	1500	252984	13	42.51	TL	0.45	0.45
4	0.95	0.95	BP-RF	23229.38	23378.70	0.0	1286	177200	16	48.68	TL	0.64	0.64
4	0.95	0.99	BP-HFX	3711.82	3713.21	0.0	1203	180493	27	66.43	TL	0.04	0.04
4	0.95	0.99	BP-HFY	3712.05	3713.21	0.0	1153	167926	33	56.88	TL	0.03	0.03
4	0.95	0.99	BP-RF	3711.98	3713.21	0.0	892	89334	41	64.41	TL	0.03	0.03
4	0.99	0.9	BP-HFX	63802.82	64068.95	0.0001	1911	413601	12	63.39	TL	0.42	0.42
4	0.99	0.9	BP-HFY	63836.31	64068.95	0.0001	1877	401901	14	63.06	TL	0.36	0.36
4	0.99	0.9	BP-RF	63835.49	64068.95	0.0001	1503	242401	14	70.90	TL	0.37	0.37
4	0.99	0.95	BP-HFX	25017.18	25111.10	0.0	1580	282423	12	44.78	TL	0.38	0.38
4	0.99	0.95	BP-HFY	24984.22	25111.10	0.0	1572	275880	12	43.65	TL	0.51	0.51
4	0.99	0.95	BP-RF	25015.33	25111.10	0.0	1254	168432	16	68.06	TL	0.38	0.38
4	0.99	0.99	BP-HFX	3982.74	4022.44	0.0	1242	194654	25	25.04	TL	1.00	1.00
4	0.99	0.99	BP-HFY	3983.20	4022.44	0.0	1093	142836	31	48.00	TL	0.99	0.99
4	0.99	0.99	BP-RF	4021.09	4022.44	0.0	836	76743	36	29.22	TL	0.03	0.03

Table 4.69: Comparison of Branching Rules for N=64, Instance ID = 5

L	Se	Sp	Configuration	LB	UB	Δ UB (%)	$\#y$	$\#x$	# nodes	Time$_r$ (s)	Total Time (s)	Gap$_r$ (%)	Gap (%)
4	0.9	0.9	BP-HFX	50755.09	50952.76	0.0001	1749	350806	13	65.95	TL	0.39	0.39
4	0.9	0.9	BP-HFY	50755.09	50952.76	0.0001	1796	363040	13	64.58	TL	0.39	0.39
4	0.9	0.9	BP-RF	50755.09	50952.76	0.0001	1590	271406	14	59.73	TL	0.39	0.39
4	0.9	0.95	BP-HFX	19082.93	19165.68	0.0001	1530	259328	12	69.92	TL	0.43	0.43
4	0.9	0.95	BP-HFY	19096.52	19165.68	0.0001	1485	244399	12	54.26	TL	0.36	0.36
4	0.9	0.95	BP-RF	19079.68	19165.68	0.0001	1221	160769	19	44.64	TL	0.45	0.45
4	0.9	0.99	BP-HFX	2936.48	2937.51	0.0	1126	154377	27	71.12	TL	0.04	0.04
4	0.9	0.99	BP-HFY	2936.68	2937.51	0.0	1106	147502	31	43.90	TL	0.03	0.03
4	0.9	0.99	BP-RF	2936.51	2937.51	0.0	899	90150	42	83.44	TL	0.03	0.03
4	0.95	0.9	BP-HFX	54998.36	55205.00	0.0	1878	402651	12	68.50	TL	0.38	0.38
4	0.95	0.9	BP-HFY	54758.66	55205.00	0.0	1865	392386	13	67.15	TL	0.82	0.82
4	0.95	0.9	BP-RF	54870.86	55205.00	0.0	1517	247055	15	57.46	TL	0.61	0.61
4	0.95	0.95	BP-HFX	20907.83	21008.37	0.0002	1570	275724	12	48.70	TL	0.48	0.48
4	0.95	0.95	BP-HFY	20919.60	21008.37	0.0002	1479	240513	11	48.99	TL	0.42	0.42
4	0.95	0.95	BP-RF	20891.70	21008.37	0.0002	1232	163023	17	39.93	TL	0.56	0.56
4	0.95	0.99	BP-HFX	3259.05	3260.54	0.0	1245	190171	26	99.82	TL	0.05	0.05
4	0.95	0.99	BP-HFY	3259.44	3260.54	0.0	1196	178056	28	50.25	TL	0.03	0.03
4	0.95	0.99	BP-RF	3259.15	3260.54	0.0	898	89148	38	52.91	TL	0.04	0.04
4	0.99	0.9	BP-HFX	58515.59	58730.66	0.0001	1915	422573	11	77.61	TL	0.37	0.37
4	0.99	0.9	BP-HFY	58537.42	58730.66	0.0001	1913	412764	12	77.25	TL	0.33	0.33
4	0.99	0.9	BP-RF	58492.16	58730.66	0.0001	1579	268208	13	67.80	TL	0.41	0.41
4	0.99	0.95	BP-HFX	22426.73	22543.10	0.0	1594	285164	11	54.06	TL	0.52	0.52
4	0.99	0.95	BP-HFY	22440.43	22543.10	0.0	1569	268361	11	57.84	TL	0.46	0.46
4	0.99	0.95	BP-RF	22444.01	22543.10	0.0	1287	178532	15	49.76	TL	0.44	0.44
4	0.99	0.99	BP-HFX	3493.26	3531.09	0.0001	1199	172463	24	57.21	TL	1.08	1.08
4	0.99	0.99	BP-HFY	3529.46	3531.09	0.0001	1306	206438	26	47.09	TL	0.05	0.05
4	0.99	0.99	BP-RF	3529.33	3531.09	0.0001	890	89632	40	64.59	TL	0.05	0.05

Table 4.80: Performance Comparison of the Formulations for $N = 6$

Instance					F^{EXT}_{RLT}					F^{EXT}_{MINLP}				
ID	N	L	Se	Sp	Obj	Runtime (s)	Nodes	Gap_r (%)	Gap (%)	Obj	Runtime (s)	Nodes	Gap_r (%)	Gap (%)
1	6	3	0.9	0.9	3893.84	0.02	1	0.0	0.0	3893.84	0.33	1	0.0	0.0
1	6	3	0.9	0.95	1415.34	0.02	1	0.0	0.0	1415.34	0.3	1	0.0	0.0
1	6	3	0.9	0.99	209.73	0.02	1	0.0	0.0	209.73	0.34	1	0.0	0.0
1	6	3	0.95	0.9	4205.28	0.02	1	0.0	0.0	4205.28	0.08	1	0.0	0.0
1	6	3	0.95	0.95	1548.31	0.02	1	0.0	0.0	1548.31	0.07	1	0.0	0.0
1	6	3	0.95	0.99	232.68	0.02	1	0.0	0.0	232.68	0.07	1	0.0	0.0
1	6	3	0.99	0.9	4463.01	0.02	1	0.0	0.0	4463.01	0.08	1	0.0	0.0
1	6	3	0.99	0.95	1658.97	0.02	1	0.0	0.0	1658.97	0.07	1	0.0	0.0
1	6	3	0.99	0.99	251.9	0.02	1	0.0	0.0	251.9	0.07	1	0.0	0.0
2	6	3	0.9	0.9	3433.36	0.02	1	0.0	0.0	3433.36	0.08	1	0.0	0.0
2	6	3	0.9	0.95	1197.61	0.02	1	0.0	0.0	1197.61	0.08	1	0.0	0.0
2	6	3	0.9	0.99	168.93	0.02	1	0.0	0.0	168.93	0.08	1	0.0	0.0
2	6	3	0.95	0.9	3694.6	0.02	1	0.0	0.0	3694.6	0.08	1	0.0	0.0
2	6	3	0.95	0.95	1306.6	0.02	1	0.0	0.0	1306.6	0.08	1	0.0	0.0
2	6	3	0.95	0.99	187.27	0.02	1	0.0	0.0	187.27	0.08	1	0.0	0.0
2	6	3	0.99	0.9	3910.4	0.02	1	0.0	0.0	3910.4	0.08	1	0.0	0.0
2	6	3	0.99	0.95	1397.2	0.02	1	0.0	0.0	1397.2	0.07	1	0.0	0.0
2	6	3	0.99	0.99	202.62	0.02	1	0.0	0.0	202.62	0.08	1	0.0	0.0
3	6	3	0.9	0.9	2788.27	0.02	1	0.0	0.0	2788.27	0.08	1	0.0	0.0
3	6	3	0.9	0.95	911.43	0.02	1	0.0	0.0	911.43	0.09	1	0.0	0.0
3	6	3	0.9	0.99	118.98	0.03	1	0.0	0.0	118.98	0.07	1	0.0	0.0
3	6	3	0.95	0.9	2983.31	0.02	1	0.0	0.0	2983.31	0.07	1	0.0	0.0
3	6	3	0.95	0.95	990.19	0.02	1	0.0	0.0	990.19	0.07	1	0.0	0.0
3	6	3	0.95	0.99	131.73	0.02	1	0.0	0.0	131.73	0.08	1	0.0	0.0
3	6	3	0.99	0.9	3144.01	0.02	1	0.0	0.0	3144.01	0.08	1	0.0	0.0
3	6	3	0.99	0.95	1055.53	0.02	1	0.0	0.0	1055.53	0.07	1	0.0	0.0
3	6	3	0.99	0.99	142.4	0.01	1	0.0	0.0	142.4	0.07	1	0.0	0.0
4	6	3	0.9	0.9	4252.2	0.02	1	0.0	0.0	4252.2	0.12	16	170.0	0.0
4	6	3	0.9	0.95	1574.78	0.01	1	0.0	0.0	1574.78	0.11	11	276.0	0.0
4	6	3	0.9	0.99	237.62	0.01	1	0.0	0.0	237.62	0.08	1	0.0	0.0
4	6	3	0.95	0.9	4600.54	0.01	1	0.0	0.0	4600.54	0.08	1	0.0	0.0
4	6	3	0.95	0.95	1724.61	0.01	1	0.0	0.0	1724.61	0.07	1	0.0	0.0
4	6	3	0.95	0.99	263.7	0.01	1	0.0	0.0	263.7	0.08	1	0.0	0.0
4	6	3	0.99	0.9	4888.98	0.01	1	0.0	0.0	4888.98	0.09	1	0.0	0.0
4	6	3	0.99	0.95	1849.37	0.01	1	0.0	0.0	1849.37	0.11	16	287.0	0.0
4	6	3	0.99	0.99	285.53	0.01	1	0.0	0.0	285.53	0.11	14	397.0	0.0
5	6	3	0.9	0.9	3501.57	0.02	1	0.0	0.0	3501.57	0.08	1	0.0	0.0
5	6	3	0.9	0.95	1219.68	0.01	1	0.0	0.0	1219.68	0.07	1	0.0	0.0
5	6	3	0.9	0.99	171.08	0.01	1	0.0	0.0	171.08	0.07	1	0.0	0.0
5	6	3	0.95	0.9	3768.03	0.01	1	0.0	0.0	3768.03	0.07	1	0.0	0.0
5	6	3	0.95	0.95	1330.42	0.01	1	0.0	0.0	1330.42	0.07	1	0.0	0.0
5	6	3	0.95	0.99	189.63	0.01	1	0.0	0.0	189.63	0.07	1	0.0	0.0
5	6	3	0.99	0.9	3988.06	0.01	1	0.0	0.0	3988.06	0.07	1	0.0	0.0
5	6	3	0.99	0.95	1422.44	0.01	1	0.0	0.0	1422.44	0.05	1	0.0	0.0
5	6	3	0.99	0.99	205.15	0.01	1	0.0	0.0	205.15	0.06	1	0.0	0.0

Table 4.81: Performance Comparison of the Formulations for $N = 9$

Instance					F^{EXT}_{RLT}					F^{EXT}_{MINLP}				
ID	N	L	Se	Sp	Obj	Runtime (s)	Nodes	Gap_r (%)	Gap (%)	Obj	Runtime (s)	Nodes	Gap_r (%)	Gap (%)
1	9	3	0.9	0.9	7179.76	0.04	1	0.0	0.0	7179.76	2.76	2651	97.7	0.0
1	9	3	0.9	0.95	2747.82	0.04	1	0.0	0.0	2747.82	5.4	986	113.0	0.0
1	9	3	0.9	0.99	429.89	0.05	1	0.0	0.0	429.89	3.47	1384	212.0	0.0
1	9	3	0.95	0.9	7791.18	0.08	1	0.0	0.0	7791.18	0.75	1	0.0	0.0
1	9	3	0.95	0.95	3015.46	0.05	1	0.0	0.0	3015.46	0.84	1	0.0	0.0
1	9	3	0.95	0.99	477.33	0.04	1	0.0	0.0	477.33	1.78	22	77.4	0.0
1	9	3	0.99	0.9	8298.18	0.05	1	0.0	0.0	8298.18	1.02	1	0.0	0.0
1	9	3	0.99	0.95	3238.51	0.04	1	0.0	0.0	3238.51	7.21	1092	119.0	0.0
1	9	3	0.99	0.99	517.07	0.08	1	0.0	0.0	517.07	2.38	20	77.6	0.0
2	9	3	0.9	0.9	4541.36	0.05	1	0.0	0.0	4540.94	18.54	34601	691.0	0.0
2	9	3	0.9	0.95	1519.02	0.06	1	0.0	0.0	1519.02	3.68	1124	319.0	0.0
2	9	3	0.9	0.99	203.45	0.06	1	0.0	0.0	203.45	2.38	325	306.0	0.0
2	9	3	0.95	0.9	4869.22	0.04	1	0.0	0.0	4868.76	1.8	272	135.0	0.0
2	9	3	0.95	0.95	1652.68	0.07	1	0.0	0.0	1652.68	2.58	941	316.0	0.0
2	9	3	0.95	0.99	225.34	0.09	1	0.0	0.0	225.34	2.96	466	311.0	0.0
2	9	3	0.99	0.9	5139.56	0.05	1	0.0	0.0	5139.06	2.75	329	143.0	0.0
2	9	3	0.99	0.95	1763.63	0.06	1	0.0	0.0	1763.63	3.89	866	336.0	0.0
2	9	3	0.99	0.99	243.66	0.07	1	0.0	0.0	243.66	4.4	584	308.0	0.0
3	9	3	0.9	0.9	4022.35	0.04	1	0.0	0.0	4022.35	14.68	31413	801.0	0.0
3	9	3	0.9	0.95	1269.76	0.04	1	0.0	0.0	1269.76	118.96	32947	1434.0	0.0
3	9	3	0.9	0.99	155.89	0.06	1	0.0	0.0	155.89	86.4	34223	2565.0	0.0
3	9	3	0.95	0.9	4292.79	0.06	1	0.0	0.0	4292.79	106.45	33450	847.0	0.0
3	9	3	0.95	0.95	1375.69	0.04	1	0.0	0.0	1375.69	156.35	32423	1484.0	0.0
3	9	3	0.95	0.99	172.39	0.05	1	0.0	0.0	172.39	194.91	33323	2587.0	0.0
3	9	3	0.99	0.9	4515.11	0.04	1	0.0	0.0	4515.11	212.56	31754	883.0	0.0
3	9	3	0.99	0.95	1463.42	0.04	1	0.0	0.0	1463.42	220.83	32361	1522.0	0.0
3	9	3	0.99	0.99	186.19	0.06	1	0.0	0.0	186.19	221.13	32945	2602.0	0.0
4	9	3	0.9	0.9	4298.14	0.09	1	0.0	0.0	4298.14	17.79	28383	737.0	0.0
4	9	3	0.9	0.95	1400.99	0.09	1	0.0	0.0	1400.99	19.81	30512	1278.0	0.0
4	9	3	0.9	0.99	180.67	0.18	1	0.0	0.0	180.67	37.26	29695	2175.0	0.0
4	9	3	0.95	0.9	4598.8	0.06	1	0.0	0.0	4598.8	70.59	28725	778.0	0.0
4	9	3	0.95	0.95	1521.43	0.12	1	0.0	0.0	1521.43	61.04	30511	1320.0	0.0
4	9	3	0.95	0.99	199.98	0.17	1	0.0	0.0	199.98	61.99	30052	2192.0	0.0
4	9	3	0.99	0.9	4846.38	0.06	1	0.0	0.0	4846.38	61.11	28904	809.0	0.0
4	9	3	0.99	0.95	1621.31	0.1	1	0.0	0.0	1621.31	85.71	30740	1351.0	0.0
4	9	3	0.99	0.99	216.13	0.18	1	0.0	0.0	216.13	154.71	42611	2205.0	0.0
5	9	3	0.9	0.9	4125.78	0.04	1	0.0	0.0	4125.78	1.88	562	132.0	0.0
5	9	3	0.9	0.95	1316.94	0.04	1	0.0	0.0	1316.94	1.51	90	236.0	0.0
5	9	3	0.9	0.99	164.4	0.05	1	0.0	0.0	164.4	2.1	347	128.0	0.0
5	9	3	0.95	0.9	4407.11	0.05	1	0.0	0.0	4407.11	1.92	192	147.0	0.0
5	9	3	0.95	0.95	1427.95	0.04	1	0.0	0.0	1427.95	16.98	6427	507.0	0.0
5	9	3	0.95	0.99	181.86	0.04	1	0.0	0.0	181.86	3.57	751	582.0	0.0
5	9	3	0.99	0.9	4638.51	0.07	1	0.0	0.0	4638.51	1.47	46	133.0	0.0
5	9	3	0.99	0.95	1519.93	0.04	1	0.0	0.0	1519.93	12.96	5475	519.0	0.0
5	9	3	0.99	0.99	196.46	0.04	1	0.0	0.0	196.46	2.39	288	130.0	0.0

Table 4.82: Performance Comparison of the Formulations for $N = 10$

Instance					F^{EXT}_{RLT}					F^{EXT}_{MINLP}				
ID	N	L	Se	Sp	Obj	Runtime (s)	Nodes	Gap_r (%)	Gap (%)	Obj	Runtime (s)	Nodes	Gap_r (%)	Gap (%)
1	10	4	0.9	0.9	10643.21	0.5	1	0.0	0.0	10642.84	6.07	59585	242.0	0.0
1	10	4	0.9	0.95	4280.22	0.36	1	0.0	0.0	4280.03	59.73	61424	339.0	0.0
1	10	4	0.9	0.99	703.8	0.36	1	0.0	0.0	703.76	98.15	59994	451.0	0.0
1	10	4	0.95	0.9	11603.89	0.54	1	0.0	0.0	11603.48	41.6	62182	249.0	0.0
1	10	4	0.95	0.95	4711.03	0.4	1	0.0	0.0	4710.81	7.76	62632	346.0	0.0
1	10	4	0.95	0.99	782.03	0.48	1	0.0	0.0	781.99	30.21	57460	454.0	0.0
1	10	4	0.99	0.9	12402.11	0.51	1	0.0	0.0	12401.66	25.55	60116	257.0	0.0
1	10	4	0.99	0.95	5070.51	0.42	1	0.0	0.0	5070.27	20.97	62857	349.0	0.0
1	10	4	0.99	0.99	847.59	0.39	1	0.0	0.0	847.54	21.62	62711	455.0	0.0
2	10	4	0.9	0.9	13964.98	0.42	1	0.0	0.0	13964.98	5.83	63609	147.0	0.0
2	10	4	0.9	0.95	5947.48	0.35	1	0.0	0.0	5947.48	70.95	63681	195.0	0.0
2	10	4	0.9	0.99	1035.44	0.25	1	0.0	0.0	1035.44	98.22	62880	245.0	0.0
2	10	4	0.95	0.9	15308.55	0.41	1	0.0	0.0	15308.55	74.14	64754	151.0	0.0
2	10	4	0.95	0.95	6568.44	0.29	1	0.0	0.0	6568.44	77.51	61461	198.0	0.0
2	10	4	0.95	0.99	1151.5	0.23	1	0.0	0.0	1151.5	61.56	59944	246.0	0.0
2	10	4	0.99	0.9	16427.79	0.43	1	0.0	0.0	16427.79	20.96	62378	155.0	0.0
2	10	4	0.99	0.95	7087.41	0.3	1	0.0	0.0	7087.41	18.36	64030	200.0	0.0
2	10	4	0.99	0.99	1248.79	0.31	1	0.0	0.0	1248.79	10.99	63231	247.0	0.0
3	10	4	0.9	0.9	7634.24	1.21	5	0.0	0.0	7634.24	7.53	59996	425.0	0.0
3	10	4	0.9	0.95	2832.0	0.51	1	0.0	0.0	2832.0	51.15	62368	647.0	0.0
3	10	4	0.9	0.99	426.99	0.52	1	0.0	0.0	426.99	6.15	60641	941.0	0.0
3	10	4	0.95	0.9	8261.71	1.24	3	0.0	0.0	8261.71	16.56	60012	444.0	0.0
3	10	4	0.95	0.95	3101.54	0.46	1	0.0	0.0	3101.54	24.84	59050	662.0	0.0
3	10	4	0.95	0.99	473.82	0.41	1	0.0	0.0	473.82	32.68	59213	946.0	0.0
3	10	4	0.99	0.9	8781.22	0.94	1	0.0	0.0	8781.22	34.23	59813	458.0	0.0
3	10	4	0.99	0.95	3325.94	0.47	1	0.0	0.0	3325.94	37.8	58848	674.0	0.0
3	10	4	0.99	0.99	513.05	0.59	1	0.0	0.0	513.05	40.97	60543	949.0	0.0
4	10	4	0.9	0.9	7922.04	1.01	3	0.01	0.0	7922.04	8.98	61545	395.0	0.0
4	10	4	0.9	0.95	2949.86	1.13	3	0.0	0.0	2949.86	67.57	61619	595.0	0.0
4	10	4	0.9	0.99	445.55	0.77	3	0.0	0.0	445.55	112.35	59347	863.0	0.0
4	10	4	0.95	0.9	8576.88	1.1	3	0.01	0.0	8576.88	60.82	62874	411.0	0.0
4	10	4	0.95	0.95	3231.15	1.06	3	0.0	0.0	3231.15	42.64	60968	608.0	0.0
4	10	4	0.95	0.99	494.43	0.95	3	0.0	0.0	494.43	26.25	62700	868.0	0.0
4	10	4	0.99	0.9	9119.05	1.06	3	0.01	0.0	9119.05	29.83	62191	423.0	0.0
4	10	4	0.99	0.95	3465.33	1.07	3	0.0	0.0	3465.33	34.73	61795	620.0	0.0
4	10	4	0.99	0.99	535.37	0.96	3	0.0	0.0	535.37	38.12	59382	872.0	0.0
5	10	4	0.9	0.9	11391.86	0.5	1	0.0	0.0	11391.03	6.04	60687	214.0	0.0
5	10	4	0.9	0.95	4651.76	0.43	1	0.0	0.0	4651.33	67.35	60559	296.0	0.0
5	10	4	0.9	0.99	776.85	0.5	1	0.0	0.0	776.85	97.51	62272	388.0	0.0
5	10	4	0.95	0.9	12437.9	0.48	1	0.0	0.0	12436.98	25.66	61361	221.0	0.0
5	10	4	0.95	0.95	5124.67	0.37	1	0.0	0.0	5124.19	26.35	61834	301.0	0.0
5	10	4	0.95	0.99	863.4	0.39	1	0.0	0.0	863.4	30.19	61091	390.0	0.0
5	10	4	0.99	0.9	13307.65	0.39	1	0.0	0.0	13306.64	37.13	62305	227.0	0.0
5	10	4	0.99	0.95	5519.46	0.38	1	0.0	0.0	5518.93	39.16	58890	305.0	0.0
5	10	4	0.99	0.99	935.94	0.47	1	0.0	0.0	935.94	34.86	62607	391.0	0.0

Table 4.83: Performance Comparison of the Formulations for $N = 12, L = 3$

Instance					F^{EXT}_{RLT}					F^{EXT}_{MINLP}				
ID	N	L	Se	Sp	Obj	Runtime (s)	Nodes	Gap_r (%)	Gap (%)	Obj	Runtime (s)	Nodes	Gap_r (%)	Gap (%)
1	12	3	0.9	0.9	6825.27	6.33	249	0.0	0.0	6825.27	TL	20623803	657.0	464.0
1	12	3	0.9	0.95	2377.64	6.48	372	0.0	0.0	2377.64	TL	9733486	1063.0	884.0
1	12	3	0.9	0.99	334.82	5.81	471	0.01	0.0	334.82	TL	10248519	1656.0	1255.0
1	12	3	0.95	0.9	7343.73	6.02	446	0.0	0.0	7344.58	TL	10089616	689.0	565.0
1	12	3	0.95	0.95	2593.79	4.48	325	0.0	0.0	2593.79	TL	27246422	1093.0	730.0
1	12	3	0.95	0.99	371.16	8.97	1239	0.01	0.0	371.16	TL	22368445	1666.0	1228.0
1	12	3	0.99	0.9	7771.98	4.04	183	0.0	0.0	7771.98	TL	22488899	714.0	477.0
1	12	3	0.99	0.95	2773.45	4.87	335	0.0	0.0	2773.45	TL	25084173	1115.0	810.0
1	12	3	0.99	0.99	401.58	8.55	1660	0.01	0.0	401.58	TL	25774101	1673.0	1106.0
2	12	3	0.9	0.9	4230.04	7.03	1101	0.01	0.0	4230.04	TL	22644605	1300.0	955.0
2	12	3	0.9	0.95	1217.56	13.83	5037	0.02	0.0	1217.56	TL	10962208	2548.0	2063.0
2	12	3	0.9	0.99	130.47	15.14	6053	0.05	0.0	130.47	TL	8612894	5211.0	4201.0
2	12	3	0.95	0.9	4480.35	8.65	2408	0.01	0.0	4480.42	TL	8794783	1386.0	1168.0
2	12	3	0.95	0.95	1310.52	12.61	3981	0.02	0.0	1310.52	TL	7720290	2654.0	2197.0
2	12	3	0.95	0.99	143.92	14.25	4125	0.05	0.0	143.92	TL	26317114	5270.0	3796.0
2	12	3	0.99	0.9	4685.32	11.0	3192	0.01	0.0	4685.32	TL	22474463	1453.0	1036.0
2	12	3	0.99	0.95	1387.25	16.45	5957	0.02	0.0	1387.25	TL	22910626	2735.0	1924.0
2	12	3	0.99	0.99	155.15	18.46	7715	0.05	0.0	155.15	TL	24507166	5313.0	4114.0
3	12	3	0.9	0.9	5230.45	9.01	710	0.0	0.0	5230.45	TL	24675414	965.0	757.0
3	12	3	0.9	0.95	1642.98	7.59	1129	0.01	0.0	1642.98	TL	13497053	1733.0	1427.0
3	12	3	0.9	0.99	200.96	10.1	1547	0.02	0.0	200.96	TL	11488737	3104.0	2590.0
3	12	3	0.95	0.9	5579.34	8.01	902	0.0	0.0	5579.34	TL	10328822	1022.0	823.0
3	12	3	0.95	0.95	1779.57	5.35	537	0.01	0.0	1779.57	TL	9896034	1794.0	1493.0
3	12	3	0.95	0.99	222.23	8.57	1539	0.02	0.0	222.23	TL	26186342	3134.0	2395.0
3	12	3	0.99	0.9	5866.14	7.7	1154	0.0	0.0	5866.22	TL	22531156	1065.0	811.0
3	12	3	0.99	0.95	1892.69	9.26	1416	0.01	0.0	1892.69	TL	24171420	1840.0	1396.0
3	12	3	0.99	0.99	240.01	7.48	687	0.02	0.0	240.01	TL	29302021	3154.0	2386.0
4	12	3	0.9	0.9	4728.76	2.11	24	0.0	0.0	4728.76	TL	24524202	1125.0	834.0
4	12	3	0.9	0.95	1449.56	2.25	25	0.0	0.0	1449.56	TL	13532963	2072.0	1719.0
4	12	3	0.9	0.99	173.31	7.61	937	0.01	0.0	173.31	TL	10656984	3798.0	3061.0
4	12	3	0.95	0.9	5032.49	1.99	28	0.0	0.0	5032.49	TL	10183631	1194.0	1003.0
4	12	3	0.95	0.95	1567.83	1.93	23	0.0	0.0	1567.83	TL	8919347	2147.0	1613.0
4	12	3	0.95	0.99	191.59	5.55	464	0.01	0.0	191.59	TL	29385042	3833.0	2857.0
4	12	3	0.99	0.9	5282.07	2.19	33	0.0	0.0	5282.07	TL	23414654	1247.0	927.0
4	12	3	0.99	0.95	1665.74	1.84	25	0.0	0.0	1665.74	TL	29620533	2205.0	1652.0
4	12	3	0.99	0.99	206.87	8.67	1144	0.01	0.0	206.87	TL	25612159	3858.0	2593.0
5	12	3	0.9	0.9	7075.35	6.07	728	0.0	0.0	7075.73	TL	26105697	624.0	461.0
5	12	3	0.9	0.95	2502.42	7.09	807	0.0	0.0	2502.42	TL	11764701	996.0	827.0
5	12	3	0.9	0.99	359.6	5.67	951	0.0	0.0	359.6	TL	8947774	1520.0	1134.0
5	12	3	0.95	0.9	7622.46	4.76	512	0.0	0.0	7623.08	TL	10778203	654.0	538.0
5	12	3	0.95	0.95	2732.78	6.4	879	0.0	0.0	2732.9	TL	26914323	1023.0	769.0
5	12	3	0.95	0.99	398.76	6.79	952	0.0	0.0	398.76	TL	10531288	1529.0	1155.0
5	12	3	0.99	0.9	8074.72	4.33	402	0.0	0.0	8074.72	TL	23557754	677.0	493.0
5	12	3	0.99	0.95	2924.36	5.5	572	0.0	0.0	2924.36	TL	10269348	1043.0	843.0
5	12	3	0.99	0.99	431.55	6.03	760	0.0	0.0	431.55	TL	26157550	1535.0	1127.0

Table 4.84: Performance Comparison of the Formulations for $N = 12, L = 4$

Instance					F^{EXT}_{RLT}					F^{EXT}_{MINLP}				
ID	N	L	Se	Sp	Obj	Runtime (s)	Nodes	Gap_r (%)	Gap (%)	Obj	Runtime (s)	Nodes	Gap_r (%)	Gap (%)
1	12	4	0.9	0.9	10805.64	7.86	1	0.0	0.0	10805.64	TL	3394362	331.0	248.0
1	12	4	0.9	0.95	4205.7	15.31	5	0.0	0.0	4205.7	TL	3389710	481.0	357.0
1	12	4	0.9	0.99	669.72	54.92	105	0.0	0.0	669.72	TL	3006449	661.0	497.0
1	12	4	0.95	0.9	11744.15	5.75	1	0.0	0.0	11744.15	TL	2686390	344.0	262.0
1	12	4	0.95	0.95	4620.09	18.03	7	0.0	0.0	4620.09	TL	4593244	490.0	341.0
1	12	4	0.95	0.99	743.82	46.44	83	0.0	0.0	743.82	TL	3376358	664.0	511.0
1	12	4	0.99	0.9	12522.94	6.46	1	0.0	0.0	12522.94	TL	4204092	354.0	268.0
1	12	4	0.99	0.95	4965.59	20.07	10	0.0	0.0	4965.59	TL	5484791	497.0	326.0
1	12	4	0.99	0.99	805.9	41.73	75	0.0	0.0	805.9	TL	4622552	666.0	465.0
2	12	4	0.9	0.9	6341.76	64.3	191	0.01	0.0	6341.76	TL	3454986	750.0	568.0
2	12	4	0.9	0.95	2110.28	131.23	313	0.01	0.0	2110.28	TL	3480909	1273.0	1038.0
2	12	4	0.9	0.99	279.06	126.09	269	0.02	0.0	279.06	TL	2779580	2110.0	1750.0
2	12	4	0.95	0.9	6797.73	64.77	197	0.01	0.0	6797.73	TL	2450349	790.0	601.0
2	12	4	0.95	0.95	2294.79	147.88	399	0.01	0.0	2294.79	TL	2236424	1313.0	1116.0
2	12	4	0.95	0.99	309.01	144.93	627	0.02	0.0	309.01	TL	8240603	2127.0	1267.0
2	12	4	0.99	0.9	7173.48	110.37	350	0.01	0.0	7173.48	TL	4200257	821.0	621.0
2	12	4	0.99	0.95	2447.9	173.02	951	0.01	0.0	2447.9	TL	4076688	1343.0	989.0
2	12	4	0.99	0.99	334.07	150.5	514	0.02	0.0	334.07	TL	7500278	2138.0	1440.0
3	12	4	0.9	0.9	8080.1	88.84	154	0.0	0.0	8080.1	TL	5174766	521.0	370.0
3	12	4	0.9	0.95	2900.26	69.63	109	0.01	0.0	2900.26	TL	3005978	819.0	660.0
3	12	4	0.9	0.99	421.27	171.31	343	0.01	0.0	421.27	TL	2995443	1236.0	1000.0
3	12	4	0.95	0.9	8718.28	75.4	132	0.0	0.0	8718.28	TL	2820325	545.0	448.0
3	12	4	0.95	0.95	3169.68	208.76	448	0.01	0.0	3169.68	TL	2388162	840.0	665.0
3	12	4	0.95	0.99	467.21	175.65	337	0.01	0.0	467.21	TL	3719066	1243.0	1007.0
3	12	4	0.99	0.9	9245.93	88.25	175	0.0	0.0	9245.93	TL	3802178	563.0	428.0
3	12	4	0.99	0.95	3393.77	138.28	336	0.01	0.0	3393.77	TL	3598137	856.0	681.0
3	12	4	0.99	0.99	505.67	157.83	238	0.01	0.0	505.67	TL	4259389	1249.0	975.0
4	12	4	0.9	0.9	7189.55	39.58	158	0.0	0.0	7189.55	TL	4978638	636.0	471.0
4	12	4	0.9	0.95	2516.17	42.02	214	0.01	0.0	2516.17	TL	3147146	1026.0	775.0
4	12	4	0.9	0.99	356.35	93.74	477	0.01	0.0	356.35	TL	2777482	1588.0	1199.0
4	12	4	0.95	0.9	7738.85	37.57	121	0.0	0.0	7738.85	TL	2900142	667.0	555.0
4	12	4	0.95	0.95	2745.77	43.52	165	0.01	0.0	2745.77	TL	2170463	1054.0	884.0
4	12	4	0.95	0.99	395.06	89.53	270	0.01	0.0	395.06	TL	5736061	1598.0	1169.0
4	12	4	0.99	0.9	8192.66	33.31	85	0.0	0.0	8192.66	TL	3418153	691.0	486.0
4	12	4	0.99	0.95	2936.63	70.12	426	0.01	0.0	2936.63	TL	6450596	1075.0	719.0
4	12	4	0.99	0.99	427.47	61.59	335	0.01	0.0	427.47	TL	4199828	1605.0	1188.0
5	12	4	0.9	0.9	11231.5	25.22	21	0.0	0.0	11231.5	TL	3755860	314.0	236.0
5	12	4	0.9	0.95	4419.91	65.71	118	0.0	0.0	4419.91	TL	2770335	451.0	344.0
5	12	4	0.9	0.99	712.48	68.93	209	0.0	0.0	712.48	TL	3002432	613.0	494.0
5	12	4	0.95	0.9	12219.16	59.64	98	0.0	0.0	12219.16	TL	2511265	326.0	255.0
5	12	4	0.95	0.95	4858.78	91.23	209	0.0	0.0	4858.78	TL	4764410	459.0	351.0
5	12	4	0.95	0.99	791.46	62.2	178	0.0	0.0	791.46	TL	3959173	615.0	449.0
5	12	4	0.99	0.9	13039.16	43.97	61	0.0	0.0	13039.16	TL	4491577	335.0	252.0
5	12	4	0.99	0.95	5224.82	57.88	107	0.0	0.0	5224.82	TL	3009565	466.0	388.0
5	12	4	0.99	0.99	857.64	59.37	248	0.0	0.0	857.64	TL	5367120	617.0	412.0

Résumé étendu en français

Le dépistage par tests groupés (*group testing*), introduit par Dorfman en 1943, vise à dépister efficacement une population de grande taille lorsque la prévalence est faible. Le principe est de regrouper plusieurs prélèvements et de réaliser un test unique sur le mélange : un résultat négatif déclare tous les individus du groupe négatifs, tandis qu'un résultat positif déclenche des tests additionnels permettant d'identifier les individus positifs. Cette approche permet de réduire le nombre total de tests et d'augmenter la capacité quotidienne de dépistage à ressources constantes. La question centrale des tests groupés est alors la conception des mélanges : quels échantillons mélanger ensemble, et donc comment former les groupes, afin d'obtenir le meilleur compromis entre économie de tests et fiabilité de la solution (faux positifs et faux négatifs).

Cette mise en œuvre optimale est délicate dès que l'on s'éloigne des hypothèses idéalisées. En pratique, les tests sont imparfaits (sensibilité et spécificité non égales à 100%), la population est hétérogène (les individus n'ont pas tous le même risque d'être positifs), et des contraintes opérationnelles telles que l'effet de dilution (risque de na as détecter un échantillion positif lorsque mélangé dans un grand groupe d'échantillons négatifs) imposent de limiter la taille des groupes. Ces éléments, pourtant déterminants pour la fiabilité et le coût du dépistage, rendent la conception de solutions de tests groupés nettement plus complexe que dans le cadre théorique classique.

Cette thèse se concentre sur un schéma bidimensionnel non adaptatif (c'est-à-dire conçu entièrement à l'avance, sans dépendre des résultats intermédiaires) dans lequel chaque individu est affecté exactement à deux groupes de taille égale. Un individu n'est re-testé individuellement que si et seulement si les deux groupes auxquels il appartient sont déclarés positifs (schéma de type AND). Cette stratégie est particulièrement attractive pour des dépistages massifs, car elle permet une exécution parallèle des tests de groupe, tout en ciblant les re-tests individuels sur un sous-ensemble réduit d'individus « suspects ». Elle s'inscrit dans la lignée des tests en « matrice/grille » (*array testing*), mais la thèse montre que la représentation en matrice n'est pas une contrainte fondamentale : ce qui compte est la structure combinatoire des recouvrements entre groupes. Dans les travaux existants, la plupart des méthodes pour ce schéma bidimensionnel restent heuristiques et reposent souvent sur des hypothèses simplificatrices (tests parfaits, population homogène), alors que l'enjeu applicatif exige de maîtriser simultanément la fiabilité de la solution (faux positifs et faux négatifs) et l'effort expérimental (nombre de tests).

L'objectif général de la thèse est donc de proposer des modèles et des algorithmes permettant de concevoir des solutions bidimensionnelles optimales ou de haute qualité, intégrant l'hétérogénéité des risques, l'imperfectibilité des tests et l'effet de dilution, tout en apportant des garanties lorsque cela est possible, et des heuristiques efficaces lorsque les tailles de population deviennent trop grandes.

Comme première contribution, le manuscrit montre d'abord que l'on peut aller au-delà de la conception historiquement *matricielle* dite « en grille ». Cette représentation, initialement motivée par des considérations pratiques (notamment l'organisation en plateaux des machines de test), constitue en réalité une restriction parmi toutes les manières possibles de concevoir un schéma bidimensionnel non adaptatif à groupes de taille égale. La thèse propose ainsi un cadre combinatoire plus général, dans lequel la structure essentielle est celle des recouvrements entre groupes, indépendamment d'une représentation en matrice.

Dans ce cadre, le manuscrit caractérise ensuite les *tailles de groupes admissibles* : pour une même taille de population à dépister, il peut exister plusieurs tailles L permettant de construire une solution où chaque individu apparaît dans exactement deux groupes, chaque groupe contient exactement L individus, et deux groupes se recoupent au plus en un individu. Cette caractérisation n'est pas seulement théorique : sa preuve est constructive et fournit des procédures explicites de construction de solutions réalisables. Cette généralisation constitue le fondement du problème d'optimisation étudié dans toute la thèse et fournit un point de départ généralisé pour les développements algorithmiques proposés.

Sur le plan statistique, la thèse établit ensuite des expressions opérationnelles des mesures de performance adaptées aux populations hétérogènes et aux tests imparfaits : espérances de faux positifs, de faux négatifs, et du nombre de tests. Un point important mis en évidence est le lien structurel entre le nombre attendu de tests et le nombre attendu de faux positifs, ce qui permet de se concentrer sur un objectif principal tout en contrôlant implicitement l'autre. À partir de ces mesures, la thèse propose plusieurs formulations d'optimisation. Une formulation mathématique compacte en variables d'affectation traduit naturellement le problème sous forme non linéaire non convexe, puis elle est reformulée pour aboutir à un programme quadratique en variables mixtes traitable par un solveur standard. Une formulation renforcée ajoute des contraintes de brisure de symétrie pour réduire drastiquement l'espace de recherche, un effet confirmé par l'étude expérimentale.

En complément des approches exactes, la thèse développe des heuristiques dédiées, indispensables pour traiter des tailles de population pertinentes en pratique. La première est constructive et s'appuie sur la preuve d'existence mentionnée ci-dessus ; elle est ensuite combinée à des stratégies d'amélioration par recherche locale. Deux familles de recherche locale sont proposées : une approche par échanges (*swap*) et une approche plus originale fondée sur des cycles d'éjection, formulés et résolus à l'aide d'un modèle de pro-

grammation mathématique à chaque itération. Cette approche matheuristique exploite la structure du problème pour proposer des mouvements d'amélioration plus puissants qu'un simple voisinage local. Des comparaisons empiriques sur des instances générées aléatoirement montrent l'intérêt de ces heuristiques et de la brisure de symétrie, et dégagent des propriétés structurelles des solutions de bonne qualité, en particulier l'intérêt de regrouper certains individus à faible risque afin de réduire les faux positifs attendus.

La deuxième contribution majeure est le développement d'une approche exacte de type *Branch-and-Price* basée sur une formulation étendue. L'idée est de raisonner non plus en affectations élémentaires, mais en sélection de groupes admissibles, ce qui conduit à un modèle avec un nombre potentiellement exponentiel de variables. Pour rendre ce cadre exploitable, la thèse établit une reformulation plus serrée (de type RLT) et met en place une génération simultanée de colonnes (groupes) et de lignes (contraintes), ce qui est nécessaire car la structure du maître induit l'apparition de contraintes pertinentes au fil des itérations. Le cœur algorithmique repose sur un sous-problème non linéaire en variables binaires avec un très grand défi étant l'estimation correcte des variables duales manquantes qui a été maîtrisé dans cette thèse. Ta thèse propose deux procédures exactes pour résoudre ce sous-problème, l'une via la résolution de sa formulation mathématique via un solveur commercial, l'autre via un algorithme de labellisation spécifique inspiré des méthodes de plus court chemin contraint et des heuristiques s'inspirant de ce dernier. Afin de disposer d'un certificat de qualité malgré les difficultés de convergence de la génération simultanée des colonnes et des lignes, une borne inférieure lagrangienne est intégrée au processus. Les règles de branchement utilisées sont inspirées de la littérature. Le Branch-and-Price est enrichit une heuristique primale ad hoc destinée à produire des solutions réalisables de bonne qualité. Les expériences montrent que l'essentiel de l'amélioration se produit au nœud racine : sur des instances synthétiques allant jusqu'à 100 individus, l'écart d'optimalité au nœud racine est en moyenne inférieur à 1,85%, ce qui fournit des garanties de performance dans des temps compatibles avec un usage opérationnel pour des tailles intermédiaires, tandis que l'exploration de l'arbre réduit souvent marginalement cet écart.

Enfin, la thèse propose une application réelle en collaboration avec le CHU de Lille, dans un contexte de dépistage multi-maladies auto-immunes via des tests multiplex d'anticorps antinucléaires (ANA). Dans ce cadre, chaque individu est associé non pas à un seul risque, mais à un vecteur de risques (un par biomarqueur), et la positivité est définie par la présence d'au moins un biomarqueur positif. La contribution méthodologique est de montrer que le cadre développé pour une maladie unique s'adapte naturellement à ce contexte multi-risque : les fonctions de coût et les objectifs sont ajustés pour intégrer la probabilité d'être positif à au moins un biomarqueur et la logique du test multiplex, tout en conservant la structure combinatoire du schéma bidimensionnel. Les résultats expérimentaux sur des populations de 50 à 200 individus issues d'études réelles montrent des économies substantielles par rapport au dépistage individuel, avec des réductions at-

tendues du nombre de tests allant typiquement de 27% à 56% selon les configurations, et, dans plusieurs cas, des économies supérieures à la moitié des tests nécessaires en dépistage individuel. Ces gains sont obtenus tout en conservant une erreur de classification très faible, et des écarts d'optimalité reportés allant de 0,04% à 3,53% sur les cas où une garantie de performance est accessible. Au-delà de la réduction de charge expérimentale, ces résultats suggèrent un impact économique direct dans des laboratoires à haut débit, où l'effort d'analyse et les coûts induits augmentent fortement avec le nombre de tests et les confirmations nécessaires.

En synthèse, cette thèse adopte une démarche intégrée de bout en bout : elle part de la définition et de la généralisation d'un schéma bidimensionnel non adaptatif à groupes de taille égale, dans un cadre réaliste (hétérogénéité des risques, tests imparfaits et effet de dilution), propose pour la première fois une modélisation d'optimisation dédiée (formulation MINLP puis renforcement par brisure de symétries), développe une formulation étendue et sa version renforcée de type RLT (avec résultats de comparaison théorique), conçoit des algorithmes de construction et d'amélioration de solutions, puis introduit une résolution exacte de référence via une approche *Branch-and-Price* avec génération simultanée de colonnes et de contraintes, borne lagrangienne et heuristiques primales. Enfin, la pertinence de l'ensemble est démontrée sur une application réelle en milieu hospitalier, ouvrant la voie à des déploiements dans des campagnes de dépistage à grande échelle.

Les perspectives principales portent sur l'amélioration des bornes inférieures et des techniques de renforcement (inégalités valides, reformulations plus serrées), sur l'augmentation de l'évolutivité des algorithmes de sous-problème (dominances, bornes de complétion), ainsi que sur l'exploration de méthodes hybrides et métaheuristiques capables de traiter des tailles de population très grandes tout en respectant des contraintes de faisabilité strictes. Enfin, au-delà de l'optimisation de la conception des groupes, l'implémentation pratique soulève une question opérationnelle importante : l'automatisation du pipetage et l'optimisation des séquences de préparation des mélanges, qui constituent un prolongement naturel de ce travail vers une intégration complète dans le flux de laboratoire.

Advanced Optimization Algorithms for Group Testing

Abstract: Group testing is a screening strategy that aims to identify infected individuals within a population using fewer tests than individual testing, particularly effective in low-prevalence contexts. In this thesis, we study a risk-based non-adaptive two-dimensional group testing problem, where each individual belongs to exactly two overlapping groups of equal size, and tests may be imperfect. We formulate an optimization problem that seeks to minimize a convex combination of the expected number of tests, false positives, and false negatives, while accounting for heterogeneous individual risk levels. We provide theoretical foundations to generalize two-dimensional designs beyond conventional matrix layouts and characterize the group sizes for which such designs are feasible. To generate feasible solutions, we develop several constructive algorithms and local search heuristics tailored to risk-based grouping. To solve the problem exactly, we propose multiple mathematical formulations: a compact nonlinear formulation and a stronger extended formulation based on group enumeration. For scalability, we introduce a tighter Reformulation-Linearization Technique (RLT)-based extended model. This is solved using a Branch-and-Price algorithm built on Simultaneous Column-and-Row Generation, with exact pricing solved via a dedicated labeling algorithm and Lagrangian bounding to guide the search. Synthetic instances up to 100 individuals with small group sizes are solved up to 1.85% in average of optimality gap in the root node. We then extend our framework to a multi-disease screening scenario using multiplex assays, which detect multiple biomarkers in a single test. This extension models the probability of an individual being positive for at least one biomarker and adapts the cost functions accordingly. We validate our approach on real clinical data for antinuclear antibody (ANA) screening in collaboration with Lille University Hospital. Our results show significant savings ranging from 27% to 55% in the expected number of tests, with minimal classification error on real-world based data from 50 to 200 individuals. This work offers the first exact optimization framework for realistic two-dimensional group testing and highlights its applicability in large-scale health screening programs.

Keywords: Two-dimensional Group Testing, Mathematical Programming, Branch-and-Price, Simultaneous Column-and-Row Generation, Multiplex Assays, Healthcare Screening, Combinatorial Optimization.

Algorithmes d'Optimisation Avancés pour les Tests Groupés

Résumé : Les tests groupés sont une stratégie de dépistage visant à identifier les individus infectés au sein d'une population tout en réduisant le nombre de tests nécessaires par rapport au dépistage individuel, notamment en contexte de faible prévalence. Cette thèse étudie le problème des tests groupés bidimensionnels non adaptatifs, dans lequels chaque individu appartient exactement à deux groupes qui se recoupent, de taille égale, et où la population à tester est hétérogène et où les tests peuvent être imparfaits. Nous formulons le problème d'optimisation cherchant à minimiser une combinaison convexe du nombre attendu de tests, de faux positifs et de faux négatifs, en tenant compte de l'hétérogénéité du risque individuel. Nous établissons des fondements théoriques permettant de généraliser les conceptions bidimensionnelles au-delà des grilles classiques, et caractérisons les tailles de groupe pour lesquelles ces conceptions sont réalisables. Plusieurs algorithmes constructifs et heuristiques de recherche locale sont développés pour générer des solutions faisables fondées sur le risque. Pour une résolution exacte, nous proposons plusieurs formulations mathématiques, dont une formulation compacte non linéaire et une formulation étendue plus forte basée sur l'énumération des groupes. Pour assurer l'évolutivité, nous introduisons un modèle étendu plus serré, basé sur la technique de reformulation et linéarisation (RLT), résolu par un algorithme de Branch-and-Price s'appuyant sur la génération simultanée de colonnes et de lignes. Le sous-problème exact est assuré par un algorithme de labellisation dédié, et une borne Lagrangienne guide la recherche. Des instances synthétiques allant jusqu'à 100 individus sont résolues avec un écart d'optimalité moyen inférieur à 1.85% au nœud racine. Nous étendons ensuite le cadre au dépistage multi-maladies à l'aide de tests multiplex, capables de détecter plusieurs biomarqueurs simultanément. Cette extension modélise la probabilité d'être positif à au moins un biomarqueur, avec adaptation des fonctions de coût. Une validation sur des données réelles de dépistage des anticorps antinucléaires (ANA) en collaboration avec le CHU de Lille montre des économies significatives allant de 27 % à 55 % par rapport à un dépistage individuel, avec des erreurs de classification très faibles pour des populations de 50 à 200 individus.

Mots-clés : Tests Groupés Bidimensionnels, Programmation Mathématique, Branch-and-Price, Génération Simultanée de Colonnes et de Lignes, Tests Multiplex, Dépistage en Santé, Optimisation Combinatoire.